Development of novel PBI-blended membranes for SO$_2$ electrolysis

R Peach

iD orcid.org 0000-0001-7697-0781

Thesis submitted in fulfilment of the requirements for the degree *Doctor of Philosophy in Chemistry* at the North-West University

Promoter: Prof HM Krieg

Co-promoter: Dr AJ Krüger

Co-promoter: Dr DG Bessarabov

Co-promoter: Dr JA Kerres

Graduation May 2019

21640904

DECLARATION

I, Retha Peach, declare that the thesis entitled: "Development of novel PBI-blended membranes for SO_2 electrolysis", submitted in fulfillment with the requirements for the degree *Philosophiae Doctor* in Chemistry, is my own work, except where acknowledged in the text, and has not been submitted in part to any other tertiary institution.

Signed at North-West University (Potchefstroom Campus)

18/02/2019

R Peach   Date

ACKNOWLEDGEMENTS

I herein express my sincerest gratitude towards:

- ❖ My Heavenly Farther for providing me with the strength, ability, determination and support of academic rolemodels, friends and loved ones throughout this study. May this work be unto His glory.

- ❖ My parents for all their support, unconditional love and words of encouragement especially during the challenging times of my research. When in doubt I could always rely on your reassurance that I would be able to finish what I started.

- ❖ Professor Henning M. Krieg, Membrane Technology, for his support and encouragement during the course of my studies in the group. I have learned and grown a great deal under your guidance and the opportunities that came with this research project.

- ❖ Dr. Jochen A. Kerres, Institute of Chemical Process Engineering, University of Stuttgart, for hosting me in Germany at the ICVT during research visits and never hesitating to provide input on my work.

- ❖ Dr. Andries J. Krüger and Dr. Dmitri Bessarabov from the DST-HySA Infrastructure. I valued the time and effort you put aside to listen and assist when needed.

- ❖ Mrs Hestelle Stoppel, financial administrator at the Chemical Research Beneficiation, for her efforts in the handling of our inquiries and always taking a personal interest in our work and well being.

- ❖ Chemical Research Beneficiation, North-West University, Potchefstroom Campus for the use of their laboratories and support provided during the course of my studies.

- ❖ Dr. L. Tiedt and Dr. A. Jordaan at the Laboratory of Electron Microscopy, North-West University, for their assistance with the SEM and TEM analysis.

- ❖ The DFG for their financial assistance within our collaboration with Dr. Kerres (DFG project number KE 673/11-1).

- ❖ The German Academic Exchange Service for the funding towards a long term research visit which allowed for extended collaboration with the ICVT project partners in Stuttgart, Germany.

- ❖ Colleageus at the Institute of Chemical Process Engineering, University of Stuttgart, for their assistance at the Institute, being part of my German experience and the friendships that now stretch across continents.

- ❖ The National Research Foundation of South-Africa for their financial support of my Ph.D. studies.

❖ Lastly, but not least, my brother and dear friends for providing me with the needed distractions and motivation during the course of my studies. It made the difficult times so much more bearable with you there.

ABSTRACT

In light of the increased applicability of hydrogen as a clean alternative fuel source, the demand for hydrogen and the subsequent production thereof is expected to grow significantly in the near future. From the hydrogen production technologies investigated thus far, the Hybrid Sulfur (HyS) thermo-chemical cycle, using a proton exchange membrane- based (PEM) electrolyser, has shown potential at larger scale. During the HyS process, H_2SO_4 is decomposed in a high temperature step to produce SO_2, O_2 and H_2O, of which the SO_2 is then electrochemically oxidised to produce H_2SO_4 and H_2 in the presence of water during SO_2 electrolysis. For the electrolysis, a membrane is required that possesses outstanding thermal and chemical (H_2SO_4) stability while maintaining high proton conductivities in limited humidification. Since optimum electrolysis performance was predicted at temperatures above 120 °C, Nafion would not be suitable, whereas initial studies on PBI-based membranes seem promising. It was hence the purpose of this study to develop and evaluate novel PBI-based membranes in terms of membrane composition (polymer, cross-linking and ratio), H_2SO_4 stability (ex situ) and SO_2 electrolyser performance (in situ) to identify suitable PEMs for future SO_2 electrolyser applications above 100 °C.

For this purpose, partially fluorinated and non-fluorinated bromo-methylated polymers (BrPAE-1 and BrPAE -2, respectively) were successfully synthesised and functionalised to be included as blend components with SFS and F_6PBI. The H_2SO_4 stability (80 wt% H_2SO_4 at 100 °C for 5 days) of specifically the fluorinated polybenzimidazole (F_6PBI) was excellent at effectively resisting sulfonation. The presence of partial sulfonation and dissolution (% wt changes) after H_2SO_4 treatment of the SFS, BrPAE-1 and -2 polymers, however, confirmed the need for further stabilisation by cross-linking. To study this, various combinations of polymers were combined. While this improved the stability somewhat, the introduction of ionic cross-links between, for example SFS and BrPAE-1/2 alone was not sufficient, requiring the addition of the highly stable F_6PBI. Subsequently, ionic- and covalent cross-linking were combined to yield a 4-component PBI-based blend membrane. Twelve different 4-component combinations were prepared with varying acid-base ratios (A-, B-, and C_{i-iv}). The 4-component PBI-blend membranes containing only partially fluorinated acidic (SFS) and basic (F_6PBI, BrPAE-1) polymers, again displayed the highest H_2SO_4 stability. The highest proton conductivity was measured for the blend membrane $1A_i$ (48 mS/cm at 120 °C). Three additional 4-component blend A type membranes (included sPPSU and PBIOO) were included, where blend $1A_i$ again displayed the highest H_2SO_4 stability (%wt change < 2 %; IEC_{Direct} change < 12 %, TGA degradation > 275 °C).

The SO_2 electrolysis performance (at 80 °C and 95 °C) of specifically the $1A_i$ blend surpassed that of the benchmark Nafion®115. At 120 °C, a significant decrease in cell voltage (up to 150 mV or nearly 50 %) was obtained for $1A_i$ when reaching the maximum current density of 1.0 A/cm². When

testing 1A$_i$ MEAs with varying thicknesses and catalyst loadings At 120 °C, a trade-off was found to exist between the concentration of H$_2$SO$_4$ produced and the performance attainable (cell voltages at maximum current densities). Steady state measurements at 0.3 A/cm^2 for 10 hours revealed an improvement in cell voltages (decrease of 60-175 mV). When comparing the voltage stepping at 80 °C and at 120 °C, a small current density increase (0.05 - 0.14 A/cm^2) was noted at 120 °C. Post treatment characterisation (SEM and TGA-FTIR) confirmed that both the1A$_i$ membrane and the hot-pressed catalyst remained stable during the electrolyser operations investiagted at 120 °C.

It was concluded from the study that the combined fluorinated nature of acidic (SFS) and basic (F$_6$PBI, BrPAE-1) polymers in the 4-component membrane 1A$_i$ contributed to a more compatible blend with improved H$_2$SO$_4$ stability and sufficient conductivity at temperatures below and above 100 °C. This was found to be in agreement with the improved SO$_2$ electrolyser performance noted at 80 °C and at 120 °C. This concludes that the aim set for developing a novel PBI-based blend membrane suitable for SO$_2$ electrolyser application, both at 80 and 120 °C, was achieved.

TABLE OF CONTENTS

Chapter 3 : Effect of ionic or covalent cross-linking on membrane stability 41

Chapter 4 : Effect of component composition on the stability of ionic-covalently cross-linked membranes 55

Chapter 6 : Influence of membrane composition and thickness, water flow rate, and catalyst loading on SO$_2$ electrolysis (120 °C) 106

ABBREVIATIONS

BPO   benzoyl peroxide

BrPAE   Brominated poly(aryl ether)

CEM   Cation exchange membrane

DFBP   Decafluorbiphenyl

DFDPS   4,4´-difluorodiphenylsulfone

DMAc   N,N-Dimethylacetamide

EMIm   2-Ethyl-1-methyl-imidazole

F_6PBI Fluorinated polybenzimidazole

GDE   Gas diffusion electrode

H_2SO_4 Sulfuric acid

HT   High temperature

HyS   Hybrid sulfur

IEC   Ion exchange capacity

iTMBP   4,4´-isopropylidenebis(2,6-dimethylphenol)

K_2CO_3 Sodium carbonate

MEA   Membrane electrode assembly

NaOH   Sodiumhydroxide

NBS   N-bromosuccinimide

NMP   N-methyl-2-pyrrolidone

PARSA   Polymeric aromatic sulfonic acid polymer

PBI   Polybenzimidazole

PEM   Proton exchange membrane

PFSA   Perfluorosulfonic acid polymer

SEM-EDX   Scanning electron microscopy coupled elemental analysis

SFS   Partially fluorinated sulfonated arylene main-chain polymer

SO$_2$	Sulfur dioxide
sPPSU	Sulfonated poly(phenyl sulfone)
TEM	Transmission electron microscopy
TMBP	Tertramethyl-bisphenol
TGA	Thermo gravimetric analysis

OUTPUTS FROM THE STUDY

Publications Related to Study:

Peach R, H.M. Krieg, A.J. Krüger, Jacobus J.C. Rossouw, D. Bessarabov, J.Kerres. Novel cross-linked partially fluorinated and non-fluorinated polyaromatic PBI-containing blend membranes for SO_2 electrolysis. International Journal of Hydrogen Energy 41 (2016) 11868-11883; DOI: 10.1016/j.ijhydene.2016.05.246

Peach R, Krieg HM, Krüger AJ, Bessarabov D, Kerres J. Novel cross-linked PBI-blended membranes evaluated for high temperature fuel cell application and SO_2 electrolysis. Materials Today: Proceedings. 2018;5:10524-32.

Peach R, Krieg HM, Krüger AJ, Bessarabov D, Kerres JA. PBI-Blended Membrane Evaluated in High Temperature SO_2 Electrolyzer. ECS Transactions. 2018;85:21-8.

Conference Poster and Presentations:

Peach R, Krieg HM, Krüger AJ, Bessarabov D, Kerres J. Novel cross-linked partially fluorinated and non-fluorinated polyaromatic PBI-containing blend membranes for SO_2 electrolysis. (Oral presentation), 1st Africa Energy Materials (AEM) conference, 28-31 March 2017, Pretoria.

Peach R, Krieg HM, Krüger AJ, Bessarabov D, Kerres J. Novel cross-linked PBI-blended membranes evaluated for high temperature fuel cell application and SO_2 electrolysis. (Poster), 1st AEM, 28-31 March 2017, Pretoria.

Peach R, Krieg HM, Krüger AJ, Bessarabov D, Kerres J. PBI-blended membrane evaluated in high temperature SO_2 electrolyser. (Oral presentation), 233rd ECS Meeting, 13-17 May 2018, Seattle.

CHAPTER 1 : INTRODUCTION (LITERATURE OVERVIEW AND OUTLINE)

1.1 Background

The demand for cleaner, more environmentally friendly energy sources, as alternatives to the traditionally known carbon based fuels is growing. Contenders include hydrogen, solar energy and bio fuels [1]. In light of the increased interest in hydrogen as a clean alternative fuel source and the continuous research on the development and commercialisation of alternative power systems for hydrogen production, the demand for hydrogen is expected to grow [2, 3].

With the potential of producing clean hydrogen at efficiencies and quantities considered economically and environmentally promising, the Hybrid Sulfur (HyS) thermo-chemical cycle, using a proton exchange membrane (PEM) electrolyser, has received increased attention over the past years [3-10]. Westinghouse Electric Corporation first presented the HyS process in the 1970s. As shown in Figure 1.1, the HyS cycle begins with a high temperature step (>800 °C) where H_2SO_4 is decomposed to produce SO_2, O_2 and H_2O [11, 12]. Subsequently, the SO_2 is fed to the anode of the lower temperature process step (SO_2 electrolyser), where it is electrochemically oxidised to produce H_2SO_4 at the anode and H_2 at the cathode in the presence of water [13, 14].
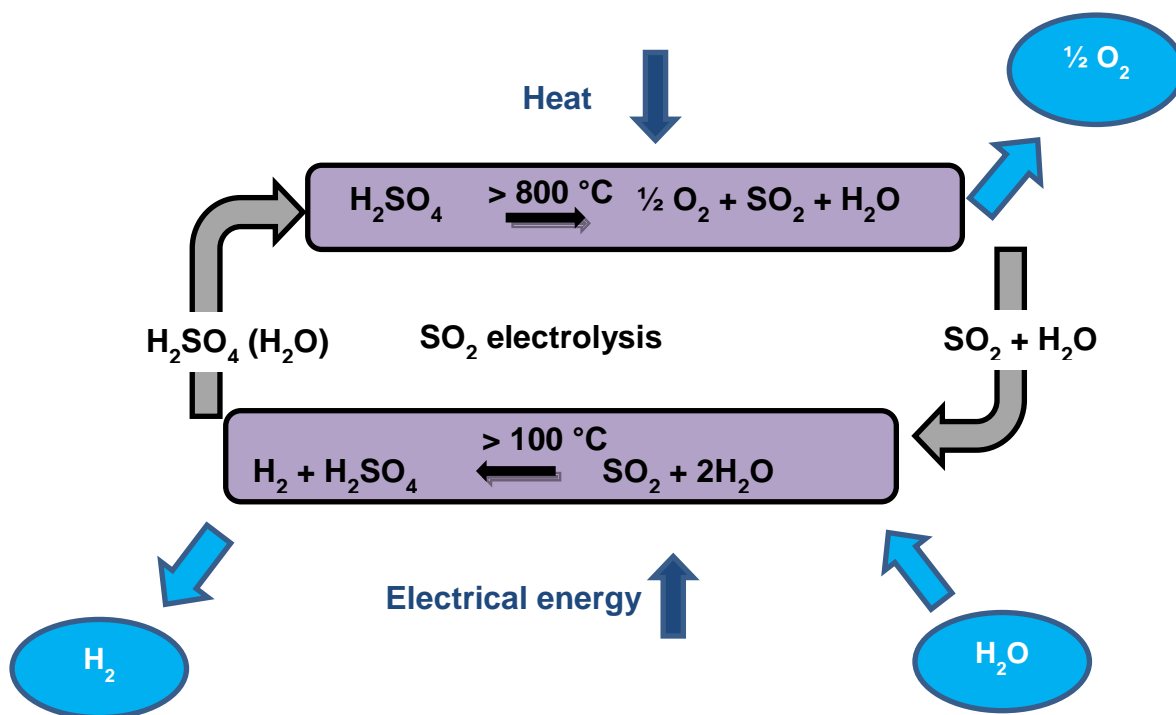
Figure 1.1: Schematic diagram of the two-step Hybrid Sulfur (HyS) cycle.

The overall reaction for the SO_2 electrolyser can be presented as:

$$SO_2 + 2\,H_2O \rightarrow H_2SO_4 + H_2 \qquad\qquad E° = 0.158 \text{ V vs. SHE} \qquad [1\text{-}1]$$

The theoretical voltage of 0.158 V needed for the electrolysis reaction [1-1] testifies to the advantage held by the thermochemical HyS cycle over normal water electrolysis, which requires 1.23 V [3]. Accordingly, a decreased practical voltage of below 1 V [14] has been reported for the SO_2 electrolyser in comparison to the 1.5 - 2 V required for water electrolysis [15].

While the HyS process can potentially produce clean hydrogen at efficiencies higher than water electrolysis, a further advantage includes the possibility to operate at elevated temperatures (>100 °C) [4, 13, 15], holding the potential benefit of faster electrode kinetics and simplified water management, thereby overcoming technical challenges typically encountered when operating below 100 °C [16-18]. As illustrated in Figure 1.2, the proton exchange membrane (PEM), which is part of the membrane electrode assembly (MEA), forms an integral part of the electrolyser system.
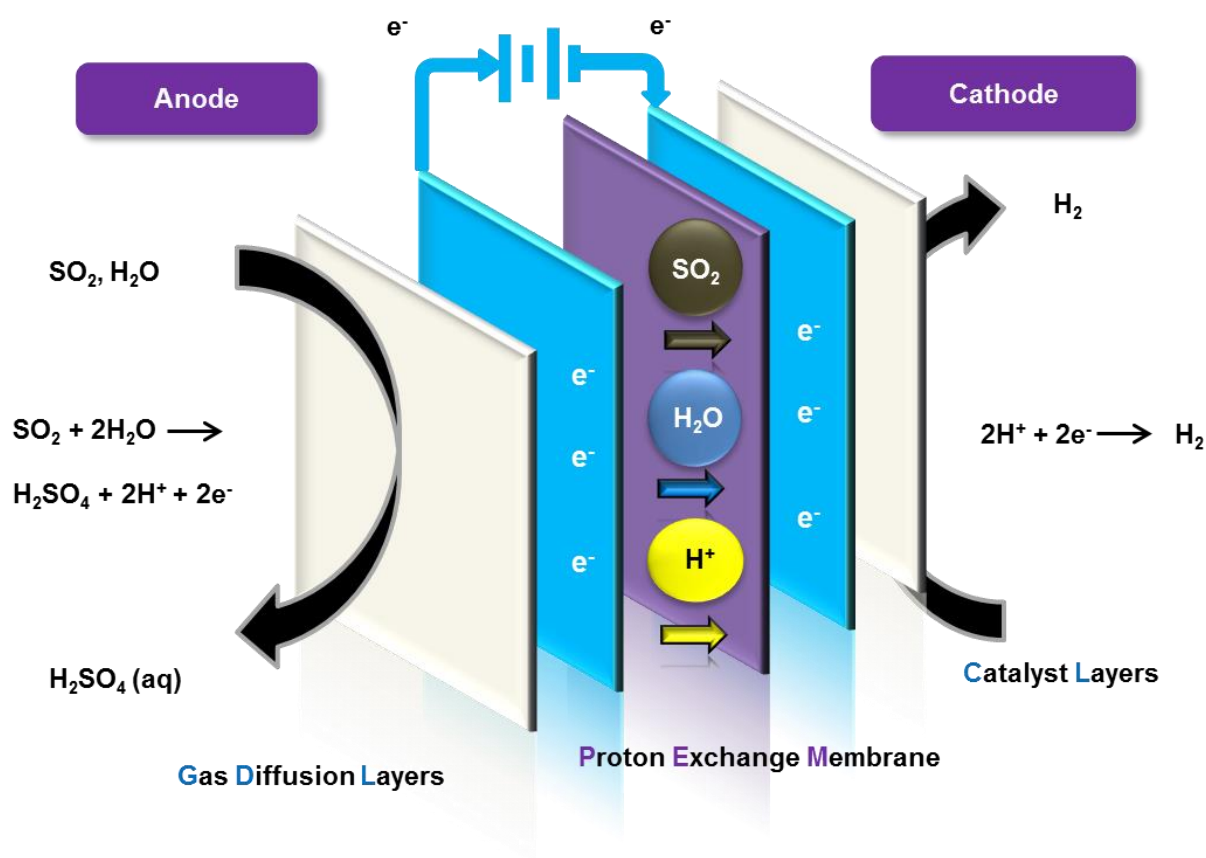
Figure 1.2: Membrane electrode assembly (MEA) for SO$_2$ electrolyser (>100 °C).

Under elevated temperature operating conditions (>100 °C), the PEM must be able to maintain both a high proton conductivity as well as acid (> 50 wt% H$_2$SO$_4$) and temperature stability. It is clear, in view of the advantages of operating at higher temperatures [19, 20] within the SO$_2$ electrolyser, that future membranes must possess sufficient thermal stability while maintaining high proton conductivities in spite of the decreased humidification at these temperatures. Furthermore the membrane also serves as a barrier to prohibit SO$_2$ cross-over to the cathode which could lead to the forming of unwanted sulfur-products and subsequent poisoning of the cathode catalyst.

It is in view of the humidification decrease (restricted water availability) that the use of the well-known perfluorosulfonic DuPont's Nafion® material becomes restricted [13]. This has led to the search for new and more suitable polymers [21-23] from which to manufacture membranes, thereby overcoming the problems associated with operating at elevated temperatures [17, 20, 24-26]. Of the many materials tested to date, polybenzimidazole (PBI) membranes are promising candidates due to the high ionic conductivity and heat resistance in the both oxidising and acidic environments [27-29]. The development of PBI-type

membranes has focussed on maintaining stability whilst ensuring sufficient ion conductivities, for example by ionically cross-linking suitable acidic and basic polymers [30-32].

Using cross-linking, suitable acidic and basic polymers (with corresponding acidic and basic groups) can be combined to obtain the properties required for a membrane to be used for SO_2 electrolysis. This method of developing and combining specific polymers for PEM manufacture allows for a more precise control over the properties such blended membranes would need, which was successfully demonstrated for both low and high temperature fuel cell applications [30, 33, 34].

Using this approach, it was found that acidic polymers such as sulfonated arylene main-chain ionomers blended with basic polybenzimidazole-based (PBI) polymers, produced membrane blends suitable for application in SO_2 electrolysis [35-37]. These novel blended membranes, when tested at 80 °C, yielded an improvement at the current density of 0.3 A.cm^{-2} when compared to the performance recorded for Nafion® under identical conditions [36]. However, while progress was made, further improvement of these acid-base blend membranes' long term stability and the compatibility of polymer components would be needed, especially when considering temperatures above 100 °C [35, 38, 39].

In more recent work [40, 41], the acid-base blend membrane concept was applied to anion-exchange membranes, where a molar excess of a halo-methylated polymer solution was mixed with a minor amount of a sulfonated polymer solution and added to a polybenzimidazole solution [40, 41]. Inclusion of an anion-exchange group by means of a halo-methylated polymer (BrPAE) to the PEM matrix was investigated, where an alkylated imidazole (e. g. 1-ethyl-2-methylimidazole) was added to ensure the formation of an anion-exchange groups by reacting with the halo-methyl groups.

Specific characterisation techniques (chemical and physical) have been developed to evaluate the sulfuric acid stability and suitability for SO_2 electrolysis of proposed blend membranes [36, 42]. The acid stability was determined by submerging the membranes in an 80 wt% sulfuric acid solution at 80 °C for 120 h, where after membranes were characterised by comparing weight and thickness changes, water uptake, ion exchange capacity (IEC), Scanning Electron Microscopy (SEM) coupled EDX (elemental analysis) and Thermo Gravimetric Analysis (TGA) measurements coupled with FTIR before and after treatment. More recently, in-situ characterisation of the MEA during operation in an SO_2 electrolyser included electrochemical impedance spectroscopy (EIS) in addition to the recording of polarisation curves (i-V) and voltage stability measurements [43].

During earlier SO_2 electrolysis studies at 80 °C, where Nafion® and simple acid-base cross-linked PEMs were used, dry SO_2 was fed to the anode and H_2O to the cathode which then diffused across the membrane during electrolysis [44]. Furthermore, it was demonstrated by Staser *et al.* [45] that by increasing the differential pressure across the membrane (thickness of 25 µm, NR-211) current density could be increased from 0.4 A/cm^2 to 1.0 A/cm^2. Subsequently the hydrogen production capacity also significantly improved with increased current density, at the cost of producing a more diluted sulfuric acid due to permeation of the water from the cathode to the anode.

Recently the SO_2-depolarised electrolyser (SDE) was further improved allowing operating temperatures of 110 °C when using a sulfonated PBI membrane [9, 10]. In this case, the H_2O was fed jointly with the SO_2, either through humidification or by directly injecting the H_2O at the anode of the cell at the required flow rates (water stoichiometry). The proposed SO_2 experimental set-up is shown in Figure 1.3. For operation above 100 °C, heated H_2O (steam) is to be supplied directly to the anode together with the SO_2, (3). For operation below 100 °C, dry SO_2 will be fed at the anode (5) and H_2O will be supplied at the cathode (4).
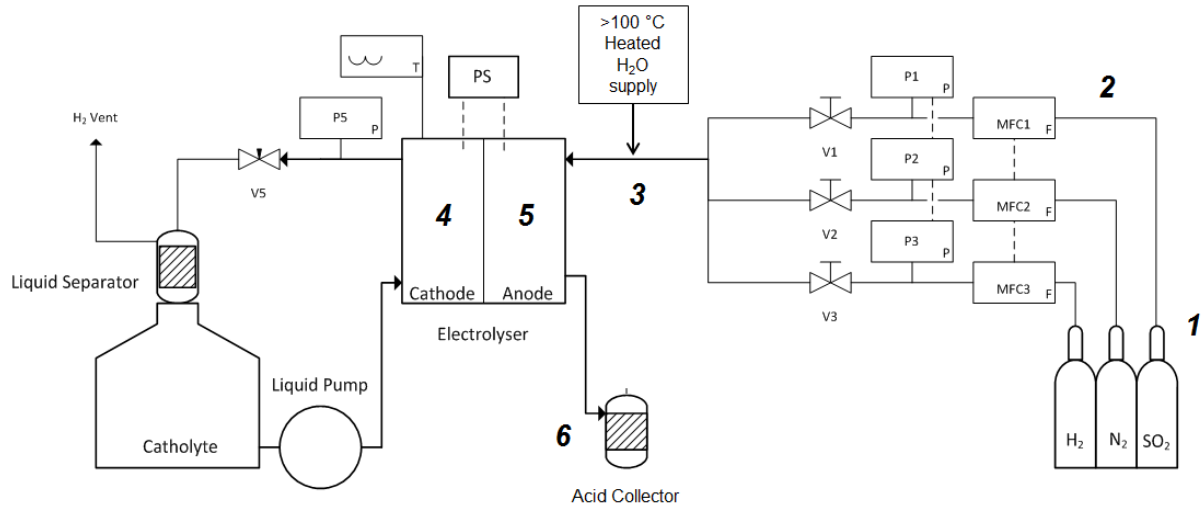
Figure 1.3: Schematic diagram of the experimental SO_2 electrolysis set-up for operations below and above 100 °C (modified from [46]). Consisting of a liquid cathode and a dry or humidified SO_2 anode feed with (1) – SO_2 supply, (2) – SO_2 flow meter, (3) – heated H_2O supply, (4) – Cathode, (5) – Anode and (6) – Glass acid collector.

In an earlier comparison study for the proposed liquid anode feed operating at 80 °C it was found that the s-PBI membrane yielded a better in comparison to the Nafion® (N212) [13]. Similar SO_2 electrolyser studies above 100 °C have however not been investigated for PBI-based blend membranes.

1.2 Problem statement

In view of the above, it would be of interest to evaluate the suitability and performance of novel cross-linked polymer systems (blend membranes) both below and above 100 °C in the SO_2 electrolyser. Although past characterisation studies have identified promising acid-base blend membranes for application in SO_2 electrolysis at 80 °C, further improvement with regards to stability of the blend membrane types at elevated temperatures (>100 °C) will need to be demonstrated. An H_2SO_4 acid stability assessment of individual acidic and basic polymer components to assess their contribution (improvement or deterioration) with regards to the stability and conductivity of the blend membrane as a unit has also not been completed. This elucidates the need to evaluate the effect of the cross-linking type and strength between polymer components and the influence thereof on the H_2SO_4, as well as oxidative and solvent extraction stability. In addition to evaluating the novel cross-linking concept of acid-base PBI-blended membranes, the influence of partially fluorinated blend components on the stability of the blend membranes within an H_2SO_4 environment have also not been established. It should be determined whether the best membrane properties are obtained when only partially fluorinated and non-fluorinated polymer components are blended with each other, or when non-fluorinated and partially fluorinated polymer components are blended together.

In order to further increase SO_2 electrolysis performances, such novel cross-linked polymer systems should be evaluated and compared both below and above 100 °C. Insight could further be gained through a more in-depth study on the influence of proposed blend membrane compositions (polymer, cross-linking and ratio) on SO_2 electrolyser performance, for example by linking results obtained from characterisation techniques performed ex situ on the blend membranes (H_2SO_4 stability) with the performance observed in situ through recording of polarisation curves and EIS measurements. Ultimately, a combined evaluation with respect to membrane composition (polymer, cross-linking and ratio), H_2SO_4 stability characterisation techniques (ex situ) and SO_2 electrolyser performance (in situ) is currently lacking. Lastly, an evaluation of membrane thickness, water flow rate and the effect of catalyst loading on SO_2 electrolysis performance and on product volumes and concentrations produced (H_2SO_4 and H_2) at temperatures above 100 °C has yet to be determined.

1.3 Aim and objectives of study
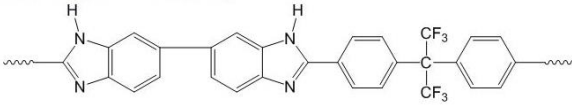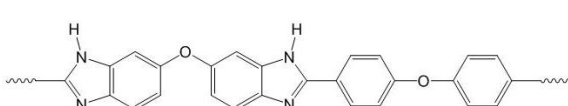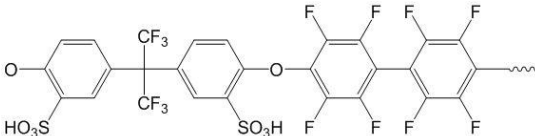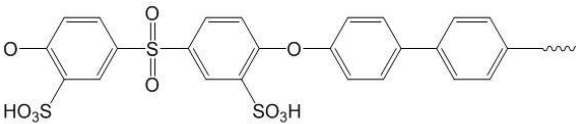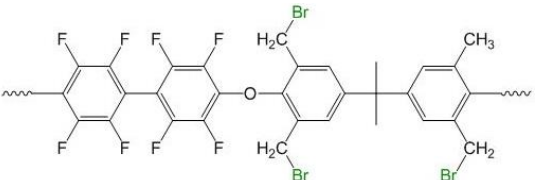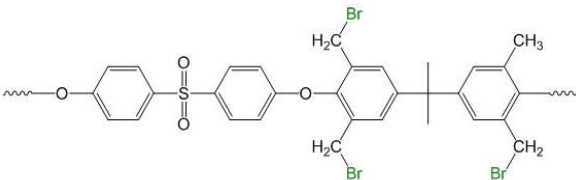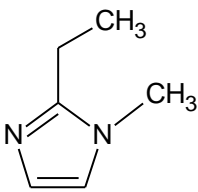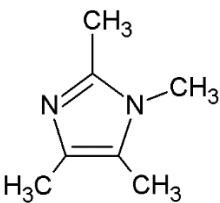
In view of the above, the aim of the study was to develop and characterise novel PBI-blended membranes and determine their SO_2 electrolyser performance below and above 100 °C.

To attain this, the following objectives were established:

- To manufacture halo-methylated (BrPAE) polymers and characterise SFS, F_6PBI and BrPAE in terms of H_2SO_4 stability.
- To determine the effect of cross-linking (type and strength) on membrane stability.
- To evaluate the effect of the composition of ionic-covalently cross-linked blend membranes on H_2SO_4, oxidative, and solvent extraction stability.
- To determine the effect of the type of acid and base used on the performance during SO_2 electrolysis at 80 °C and at 95 °C.
- To conclude by determining the influence of membrane type and thickness, water flow rate, and catalyst loading on the SO_2 electrolysis performance at 120°C.

In summary, a comparative study was conducted whereby different acidic, basic and halo-methylated (BrPAE) polymers were blended and the subsequent cross-linking possibilities and their influence on compatibility and stability of the blended membranes were investigated. The polymer structures of the blend components included in the study are presented in Table 1.1 Two electrolysis designs were used. At 80 °C and 95 °C, the water that was fed to the cathode had to diffuse across the membrane to facilitate the electrolysis at the anode. At 120 °C, the design was changed by feeding both the water and the SO_2 (g) directly to the anode (see Figure 1.3).

Table 1.1: Polymer components of the PBI-blended membranes.

Base component	
F$_6$PBI	**PBIOO**
Acid component	
SFS	**sPPSU**
BrPAE	
BrPAE-1	**BrPAE-2**
Imidazole	
EMIm	**TMIm**

F$_6$PBI = fluorinated polybenzimidazole; PBIOO = polybenzimidazole; SFS = partially fluorinated sulfonated arylene main-chain polymer; sPPSU = sulfonated poly(phenyl sulfone); BrPAE = bromo-methylated polymer (fluorinated and non-fluorinated); EMIm = 2-ethyl,1-methyl-imidazole and TMIm = 1,2,4,5-tetramethyl-imidazole.

For an overview of the nomenclature for the different acid-base blended membranes synthesised and discussed in the experimental chapters (Chapters 3-6), Table 1.2 was compiled. Accordingly, the numerical values (1-4) in the beginning of the membrane name, e.g. *1*A_i, refer to the specific acid and base blend components, e.g. SFS and F_6PBI, while the alphabetical capital letters (A-C), e.g. 1*A*$_i$, refer to the difference in acid-base ratios of the blend membranes, and the roman numbering (i-iv), e.g. 1A*$_i$*, at the end of the membrane name refers to the type of BrPAE and imidazole (BrPAE 1 or 2, EMIm or TMIm) used in the blend membrane.

Table 1.2: Nomenclature of acid-base blended membranes used in this study.

Membrane name	Membrane variables				
	Type of acid	Type of base	Acid-base ratio (wt %)	Type of BrPAE	Type of imidazole
1-4					
1A$_i$	**SFS**	**F$_6$PBI**	5.7:1	BrPAE-1	EMIm
2A$_i$	**sPPSU**	**PBIOO**	5.7:1	BrPAE-1	EMIm
3A$_i$	**SFS**	**PBIOO**	5.7:1	BrPAE-1	EMIm
4A$_i$	**sPPSU**	**F$_6$PBI**	5.7:1	BrPAE-1	EMIm
A-D					
1**A**$_i$	SFS	F$_6$PBI	**5.7:1**	BrPAE-1	EMIm
1**B**$_i$	SFS	F$_6$PBI	**1:4.7**	BrPAE-1	EMIm
1**C**$_i$	SFS	F$_6$PBI	**1:6.3**	BrPAE-1	EMIm
1**D**$_i$	SFS	F$_6$PBI	**1:1**	BrPAE-1	EMIm
i-iv					
1A$_i$	SFS	F$_6$PBI	5.7:1	**BrPAE-1**	**EMIm**
1A$_{ii}$	SFS	F$_6$PBI	5.7:1	**BrPAE-2**	**EMIm**
1A$_{iii}$	SFS	F$_6$PBI	5.7:1	**BrPAE-1**	**TMIm**
1A$_{iv}$	SFS	F$_6$PBI	5.7:1	**BrPAE-2**	**TMIm**

1.4 Outline of thesis

Chapter 1 gives a brief discussion on the potential and challenges arising for SO_2 electrolysis operated at elevated temperatures focussing on the H_2SO_4 stability of both individual polymer components and cross-linked blend membranes. Furthermore includes an overview of the relevant literature on polymer and membrane materials suited for application in SO_2 electrolysis at temperatures above 100 °C. The background was concluded with a problem statement, aim and objectives as well as an outline of the thesis.

Chapters 2 to 6 are the experimental chapters dealing both with polymer (Chapter 2) and membrane (Chapters 3-6) studies as shown in the flow diagram (Figure 1.4).

Polymer synthesis

(Chapter 2)

↓

Membrane synthesis (Effect of ionic or covalent cross-linking)

(Chapter 3)

↓

Membrane synthesis (Effect of component composition)

(Chapter 4)

↓   ↓

SO_2 electrolysis (80 °C and 95 °C)   **SO_2 electrolysis (120 °C)**
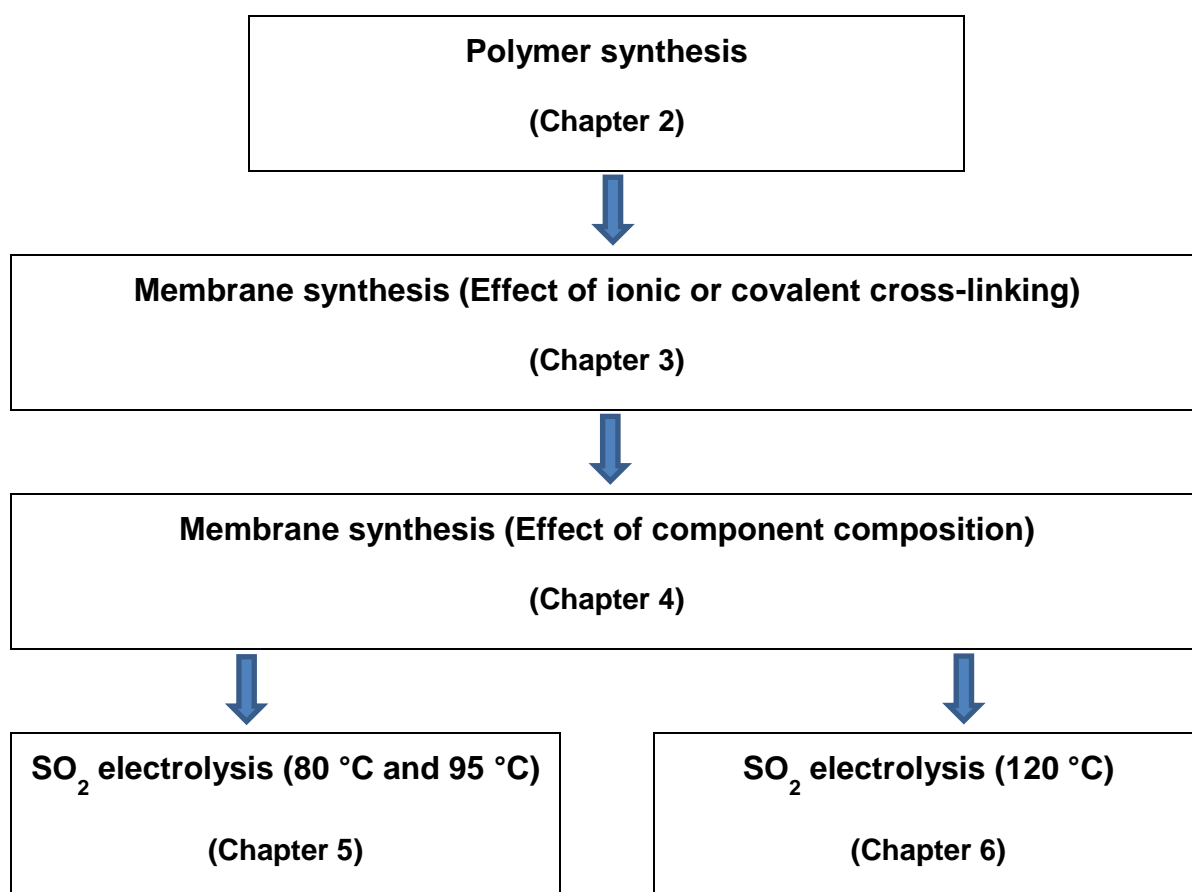
(Chapter 5)   **(Chapter 6)**

Figure 1.4: Flow diagram of the experimental Chapters 2-6.

Chapter 2 includes the polymer synthesis and H_2SO_4 stability assessment conducted on individual polymer components. In addition, it describes the characterisation techniques used (ex situ evaluation) in the rest of the study (Chapters 2-5).

In the results chapters (Chapters 3-6), the preparation and evaluation of various membrane combinations are described. Table 1.3 provides an overview of the types of membranes investigated and the chapters these are discussed in.

Table 1.3: Types of acid-base blended membranes used in the experimental chapters (Chapters 3-6).

Chapter	Membranes	Comment
3	1D & 1D$_{i-vi}$	Properties of ionic and covalent cross-linked SFS:F$_6$PBI containing blends
4	1A-C$_{i-iv}$	Properties of membranes with varying component compositions (SFS:F$_6$PBI ratios and type of BrPAE and imidazole)
5	1A$_i$, 2A$_{ii}$, 3A$_i$ & 4A$_i$	Influence of acid base types on the SO$_2$ performance at 80 °C and 95 °C. Acid and base ratios were the same as for blend membranes A in Chapter 4
6	1A$_i$, 1B$_i$ & 1C$_i$	Influence of SFS:F$_6$PBI ratios on the SO$_2$ electrolyser performance at 120 °C

In ***Chapter 3,*** various combinations of SFS/F$_6$PBI with BrPAE1/2 and TMIm/EMIm were prepared to determine the effect of ionic or covalent cross-linking on the stability of the blend membrane mixtures. This included an assessment on the organic solvent and H_2SO_4 stability of the membranes with relevant characterisation techniques.

In ***Chapter 4***, SFS/F$_6$PBI blends with varying SFS/F$_6$PBI ratios (1**A** to 1**C**) were prepared with various combinations of BrPAE1/2 and TMIm/EMIm (1A$_{i-iv}$ to 1C$_{i-iv}$) to determine the H_2SO_4, oxidative and organic solvent stability of these 12 membranes.

In ***Chapter 5***, four membranes with four combinations of acids (SFS or sPPSU) and bases (F_6PBI or PBIOO), ***1-4***A_i, were prepared. Subsequently their suitability for SO_2 electrolysis at 80 °C and 95 °C was investigated. Nafion® was included as reference material during SO_2 electrolysis.

In ***Chapter 6***, the most promising membranes from Chapters 5 & 6 ($1A_i$, $-B_i$ and $-C_i$) were prepared and used for SO_2 electrolysis at 120 °C. Furthermore the influence of membrane thickness, water flow rate and catalyst loading was determined for the best performing membrane ($1A_i$).

In ***Chapter 7*** the research presented throughout the study is reviewed, identifying the main methods used, and includes a summarised evaluation thereof. This chapter also includes recommendations for future studies.

Additional or background data not provided in Chapters 1-7, are given in three appendices (A, B and C) relating to Chapters 2, 4 and 6, respectively.

1.5 References

[1] Rosen MA, Scott DS. Comparative efficiency assessments for a range of hydrogen production processes. International Journal of Hydrogen Energy. 1998;23:653-9.

[2] Brey JJ, Brey R, Contreras I, Carazo AF. Roll-out of hydrogen fueling stations in Spain through a procedure based on data envelopment analysis. International Journal of Hydrogen Energy. 2014;39:4116-22.

[3] Gorensek MB, Summers WA. Hybrid sulfur flowsheets using PEM electrolysis and a bayonet decomposition reactor. International Journal of Hydrogen Energy. 2009;34:4097-114.

[4] Colón-Mercado HR, Hobbs DT. Catalyst evaluation for a sulfur dioxide-depolarized electrolyzer. Electrochemistry Communications. 2007;9:2649-53.

[5] Colón-Mercado H, Elvington MC, Hobbs DT. FY08 Membrane Characterization Report for the hybrid Sulfur Electrolyzer. 2008.

[6] Elvington MC, Colón-Mercado H, McCatty S, Stone SG, Hobbs DT. Evaluation of proton-conducting membranes for use in a sulfur dioxide depolarized electrolyzer. Journal of Power Sources. 2010;195:2823-9.

[7] Lokkiluoto A, Taskinen PA, Gasik M, Kojo IV, Peltola H, Barker MH, et al. Novel process concept for the production of H_2 and H_2SO_4 by SO_2-depolarized electrolysis. Environment, Development and Sustainability. 2012;14:529-40.

[8] Corgnale C, Shimpalee S, Gorensek MB, Satjaritanun P, Weidner JW, Summers WA. Numerical modeling of a bayonet heat exchanger-based reactor for sulfuric acid decomposition in thermochemical hydrogen production processes. International Journal of Hydrogen Energy. 2017;42:20463-72.

[9] T. R. Garrick, C. H. Wilkins, A. T. Pingitore, J. Mehlhoff, A. Gulledge, B. C. Benicewicz, et al. Characterizing Voltage Losses in an SO2 Depolarized Electrolyzer Using Sulfonated Polybenzimidazole Membranes. Journal of the Electrochemical Society. 2017;164:F1591-F5.

[10] Weidner JW. Electrolyzer performance for producing hydrogen via a solar-driven hybrid-sulfur process. Journal of Applied Electrochemistry. 2016:1-11.

[11] Sivasubramanian P, Ramasamy RP, Freire FJ, Holland CE, Weidner JW. Electrochemical hydrogen production from thermochemical cycles using a proton exchange membrane electrolyzer. International Journal of Hydrogen Energy. 2007;32:463-8.

[12] Brecher LE, Spewock S, Warde CJ. The Westinghouse Sulfur Cycle for the thermochemical decomposition of water. International Journal of Hydrogen Energy. 1977;2:7-15.

[13] Jayakumar JV, Gulledge A, Staser JA, Kim C-H, Benicewicz BC, Weidner JW. Polybenzimidazole Membranes for Hydrogen and Sulfuric acid Production in the Hybrid Sulfur Electrolyzer. ECS Electrochemistry Letters. 2012;1:F44-F8.

[14] Gorensek MB, Staser JA, Stanford TG, Weidner JW. A thermodynamic analysis of the SO_2/H_2SO_4 system in SO_2-depolarized electrolysis. International Journal of Hydrogen Energy. 2009;34:6089-95.

[15] Staser JA, Gorensek MB, Weidner JW. Quantifying Individual Potential Contributions of the Hybrid Sulfur Electrolyzer. Journal of The Electrochemical Society. 2010;157:B952-B8.

[16] Zeis R. Materials and characterization techniques for high-temperature polymer electrolyte membrane fuel cells. Beilstein Journal of Nanotechnology. 2015;6:68-83.

[17] Li Q, Jensen JO, Savinell RF, Bjerrum NJ. High temperature proton exchange membranes based on polybenzimidazoles for fuel cells. Progress in Polymer Science. 2009;34:449-77.

[18] Zhang J, Xie Z, Zhang J, Tang Y, Song C, Navessin T, et al. High temperature PEM fuel cells. Journal of Power Sources. 2006;160:872-91.

[19] Asensio JA, Sanchez EM, Gomez-Romero P. Proton-conducting membranes based on benzimidazole polymers for high-temperature PEM fuel cells. A chemical quest. Chemical Society Reviews. 2010;39:3210-39.

[20] Chandan A, Hattenberger M, El-kharouf A, Du S, Dhir A, Self V, et al. High temperature (HT) polymer electrolyte membrane fuel cells (PEMFC) – A review. Journal of Power Sources. 2013;231:264-78.

[21] Jouanneau J, Mercier R, Gonon L, Gebel G. Synthesis of Sulfonated Polybenzimidazoles from Functionalized Monomers: Preparation of Ionic Conducting Membranes. Macromolecules. 2007;40:983-90.

[22] Vogel H, Marvel CS. Polybenzimidazole, new thermally stable polymers. Journal of Polymer Science. 1961;50:511–39.

[23] Glipa X, Bonnet B, Mula B, Jones DJ, Roziere J. Investigation of the conduction properties of phosphoric and sulfuric acid doped polybenzimidazole. Journal of Materials Chemistry. 1999;9:3045-9.

[24] Yang C, Costamagna P, Srinivasan S, Benziger J, Bocarsly AB. Approaches and technical challenges to high temperature operation of proton exchange membrane fuel cells. Journal of Power Sources. 2001;103:1-9.

[25] Kondratenko MS, Gallyamov MO, Khokhlov AR. Performance of high temperature fuel cells with different types of PBI membranes as analysed by impedance spectroscopy. International Journal of Hydrogen Energy. 2012;37:2596-602.

[26] Bose S, Kuila T, Nguyen TXH, Kim NH, Lau K-t, Lee JH. Polymer membranes for high temperature proton exchange membrane fuel cell: Recent advances and challenges. Progress in Polymer Science. 2011;36:813-43.

[27] Savinell R, Yeager E, Tryk D, Landau U, Wainright J, Weng D, et al. A Polymer Electrolyte for Operation at Temperatures up to 200°C. Journal of The Electrochemical Society. 1994;141:L46-8.

[28] Seland F, Berning T, Børresen B, Tunold R. Improving the performance of high-temperature PEM fuel cells based on PBI electrolyte. Journal of Power Sources. 2006;160:27-36.

[29] Lobato J, Cañizares P, Rodrigo MA, Linares JJ, Pinar FJ. Study of the influence of the amount of $PBI–H_3PO_4$ in the catalytic layer of a high temperature PEMFC. International Journal of Hydrogen Energy. 2010;35:1347-55.

[30] Kerres JA. Blended and Cross-Linked Ionomer Membranes for Application in Membrane Fuel Cells. Fuel Cells. 2005;5:230-47.

[31] Peighambardoust SJ, Rowshanzamir S, Amjadi M. Review of the proton exchange membranes for fuel cell applications. International Journal of Hydrogen Energy. 2010;35:9349-84.

[32] Zuo Z, Fu Y, Manthiram A. Novel Blend Membranes Based on Acid-Base Interactions for Fuel Cells. Polymers. 2012;4:1627-44.

[33] Chromik A, Kerres JA. Degradation studies on acid–base blends for both LT and intermediate T fuel cells. Solid State Ionics. 2013;252:140-51.

[34] Schönberger F, Chromik A, Kerres J. Partially fluorinated poly(arylene ether)s: Investigation of the dependence of monomeric structures on polymerisability and degradation during sulfonation. Polymer. 2010;51:4299-313.

[35] Schoeman H, Krieg HM, Kruger AJ, Chromik A, Krajinovic K, Kerres J. H_2SO_4 stability of PBI-blend membranes for SO_2 electrolysis. International Journal of Hydrogen Energy. 2012;37:603-14.

[36] Peach R, Krieg HM, Krüger AJ, van der Westhuizen D, Bessarabov D, Kerres J. Comparison of ionically and ionical-covalently cross-linked polyaromatic membranes for SO_2 electrolysis. International Journal of Hydrogen Energy. 2014;39:28-40.

[37] Krüger AJ, Kerres J, Bessarabov D, Krieg HM. Evaluation of covalently and ionically cross-linked PBI-excess blends for application in SO_2 electrolysis. International Journal of Hydrogen Energy. 2015;40:8788-96.

[38] Peach R. Characterisation of proton exchange membranes in an H_2SO_4 environment. North-West University, Potchefstroom 2520, South Africa: North-West University, Potchefstroom campus; 2014.

[39] Krüger AJ, Cichon P, Kerres J, Bessarabov D, Krieg HM. Characterisation of a polyaromatic PBI blend membrane for SO_2 electrolysis. International Journal of Hydrogen Energy. 2015.

[40] Morandi CG, Peach R, Krieg HM, Kerres J. Novel morpholinium-functionalized anion-exchange PBI-polymer blends. Journal of Materials Chemistry A. 2015;3:1110-20.

[41] Morandi CG, Peach R, Krieg HM, Kerres J. Novel imidazolium-functionalized anion-exchange polymer PBI blend membranes. Journal of Membrane Science. 2015;476:256-63.

[42] Peach R. Characterisation of PEMs in an H_2SO_4 environment: North-West University, Potchefstroom Campus, South Africa; 2014.

[43] Kruger AJ, Krieg HM, van der Merwe J, Bessarabov D. Evalauation of MEA manufacturing parameters using EIS for SO_2 electrolysis. International Journal of Hydrogen Energy. 2014;39:18173-81.

[44] Staser JA, Ramasamy RP, Sivasubramanian P, Weidner JW. Effect of water on the electrochemical oxidation of gas-phase SO_2 in a PEM electrolyzer for H_2 production. Electrochemical and Soild-state Letters. 2007;10:E17-9.

[45] Staser JA, Weidner JW. Effect of Water Transport on the Production of Hydrogen and Sulfuric Acid in a PEM Electrolyzer. Journal of The Electrochemical Society. 2009;156:B16-B21.

[46] Krüger AJ, Krieg HM, Grigoriev SA, Bessarabov D. Various operating methods and parameters for SO_2 electrolysis. Energy Science & Engineering. 2015;3:468-80.

CHAPTER 2 : POLYMER SYNTHESIS, CHARACTERISATION AND H$_2$SO$_4$ STABILITY

Chapter Overview

For the possible inclusion in a membrane to be used in an SO$_2$ electrolyser, individual polymer components were identified in terms of their H$_2$SO$_4$ stability. From earlier SO$_2$ electrolysis studies, the partially fluorinated arylene main-chain polymer (SFS) and polybenzimidazole (F$_6$PBI) were identified as promising acidic and basic polymer components, to which brominated poly(aryl ether) polymers (both partially and non-fluorinated, BrPAE-1 and 2) could possibly be added as blend components. In this chapter, the synthesis and functionalisation of the mentioned BrPAE-1 and -2 polymers, which included polymer characterisation techniques such as GPC, NMR and elemental analysis is presented. After describing the synthesis (with adequate bromination degrees) of BrPAE-1 and -2, the polymers SFS and F$_6$PBI were included to determine the H$_2$SO$_4$ stability. For this, individual membrane films of the polymers SFS, F$_6$PBI, as well as the novel synthesised BrPAE-1 and 2 were exposed to 80 wt% H$_2$SO$_4$ at 100 °C for 5 days. Subsequently, the materials were characterised and compared to the characterisation data of said polymers before H$_2$SO$_4$ exposure. The characterisation entailed a comparison of % weight changes, IECs and TGA-FTIR data.

2.1 Introduction

Presently, commercial state-of-the-art membrane-based separation processes applied in energy storage, which are primarily focussed on charged membranes, have been found to be highly beneficial for electro-driven applications such as electrolysers [1]. As a result, ion-exchange membranes, with a generally high permselectivity, low electrical resistance and high mechanical stability, have received growing attention over the past years [2, 3]. To date, the commercial operation of most fuel cells, electrolysers and redox flow battery systems have relied on perfluorosulfonic acid (PFSA) ionomers such as Nafion® due to their excellent durability [4].

However, a shortcoming of the PFSA type materials includes the complex production processes associated with toxic intermediates being formed leading to challenges relating to the safe disposal and recycling of materials after use which has contributed to the high cost of PFSA materials. This has led to a growing interest in the development of alternative ionomer materials, with the focus specifically on arylene main-chain ionomers and the optimisation achievable through cross-linking of various suitable (co)polymers that have proven to be chemically and mechanically most suitable [4]. For the more recently developed membrane-based application of SO_2 electrolysis, it was shown that operating conditions above 100 °C would yield a potential benefit of faster electrode kinetics, simplified water management and the proposed reduction in catalyst usage [5-7]. This has given an additional impetus, apart from the high Nafion® cost, to develop more robust and possibly cheaper materials for this application.

When developing proton exchange membranes (PEMs) for the HyS electrolysis step, where SO_2 and H_2O are converted to H_2 and H_2SO_4, it is clear that such membranes should have both a high proton conductivity and H_2SO_4 stability. Various polymers have been investigated as possible building blocks for novel membranes with tailored properties specifically focussing on high chemical and mechanical stabilities with sufficient H^+ conductivities. These monomers have included, amongst others, the development of novel sulfonated arylene main-chain ionomers and their inclusion possibilities in acid-base blends [8, 9].

For these type of ionomers, Kerres et al. [10, 11] identified electron-deficient partially fluorinated sulfone (-SO_3H) group-containing arylene main-chain ionomers that are both chemically stable and conductive. Simultaneously, poly-arylenes (characterised by the aryl or hetero-aryl ring present in the main chain polymer) have been developed that are rigid high temperature polymers [12] with the ability to improve the thermal, mechanical and oxidative stability of polystyrene-based membrane materials [13]. Examples of main chain poly-arylenes that have been considered include sulfonated poly (ether ether ketone) (sPEEK), poly(ether sulfones) (PSU), poly(arylene ethers), polyesters and polyamides (PI) [14]. Although sPEEK has shown high thermal and mechanical stability along with adequate conductivity in proton exchange membrane fuel cell

(PEMFC) applications [15, 16], the proton conductivity and chemical durability of sPEEK reported at low relative humidity (RH) operation could be improved [16]. In addition, has been determined in earlier H_2SO_4 stability evaluation tests that significant dissolution of membrane fragments associated with the sPEEK blend component occurs in H_2SO_4 [17]. Similarly, dissolution of membrane fragments was also noted for the sulfonated polyethersulfone (sPSU) blends and could be ascribed to the sulfonation at the *ortho*-position of the ether bridge within the sPSU polymer in the presence of H_2SO_4 [18, 19].

In an attempt to develop suitable PEM systems, combining stability and efficient proton transfer, the blending of two or more polymers has been proposed [20]. Chromik and Kerres, for example, developed acid-base blended membranes that showed an improvement in conductivity and mechanical integrity reporting decreased water uptake and subsequent swelling of the membranes [21]. Acid-base polymer blends provide the possibility of using covalent cross-linking, ionical cross-linking and hydrogen bonding bridges separately or in combination, which has resulted in a substantial reduction in membrane swelling while improving mechanical and thermal stabilities [20, 22]. Accordingly, different acid-base complexes and blends have since been confirmed as promising alternatives to the commercially available PEMs such as PFSA. With specific reference to higher temperature applications as was the case in this study, the aromatic polybenzimidazole (PBI) type polymers are highly suitable due to their excellent thermal and mechanical properties [23]. These heterocyclic polymers are inexpensive with proven chemical resistance in different environments, and considered the ideal basic polymer component to contribute towards the stability in blends by adding a more proton conductive acidic polymer to the PBI [24].

To further improve the proton conductivity of PBI-based blends, Mader and Benicewicz have demonstrated the sulfonation of a PBI-based polymer (s-PBI), while maintaining excellent mechanical strength [25], further improving on the suitability of PBI-based membranes for high temperature applications (up to 200 °C). In addition to the modification of the PBI, different acidic-, basic- and cross-linking components have been blended and their suitability as PEMs for SO_2 electrolysis investigated [17, 26, 27]. These studies laid the basis for showing the possible suitability of such novel PBI-containing and non PBI-containing membrane types. Subsequently, it was established that blends containing partially fluorinated blend components such as the sulfonated arylene main-chain polymers (SFS) and partially fluorinated PBI (F_6PBI) provide further stability in an H_2SO_4 environment, which was expected considering the C-F bonds within the F_6PBI structure [28].

Although the mentioned studies provided insight into the effect of different blend components (membrane composition) and the cross-linking (interaction) between the blend components, an evaluation of the individual H_2SO_4 stabilities of the polymers has not yet been conducted. Therefore, in this study of developing novel PBI-based membranes for SO_2 electrolysis, the

previously identified polymer components will be evaluated separately polymers as cast polymer films.

In more recent studies it was shown that the inclusion of a halo-methylated aromatic component to a PBI and a sulfonated polymer, yielded macroscopically homogeneous, as well as mechanically and chemically stable membranes for a variety of possible applications [29, 30]. Accordingly, it was decided to include both the partially- and non-fluorinated bromo-methylated blend components, BrPAE-1 and 2 (see Chapter 1, Table 1.2), in the H_2SO_4 polymer stability assessment of this chapter. Earlier work by Katzfuss focussed on the development of better suited bromo-methylated polymers for anion exchange membrane applications, while attempting to use less toxic starting chemicals [31]. In this study, these optimised synthesis routes were used, followed by a complete characterisation of PAE-1 and 2 and their brominated polymer components BrPAE-1 and 2, which included analyses by gel permeation chromatography (GPC), nuclear magnetic resonance (NMR) and elemental analysis. The selected SFS and F_6PBI polymer components included in this section, and throughout the study (Chapters 2-6), were both used as provided by the group of Dr Kerres and obtained from Yanjin Technologies, respectively. After synthesis and characterisation, BrPAE-1 and 2 along with the provided SFS and F_6PBI polymers were cast as films and subjected to an H_2SO_4 stability assessment, which included a comparison of % weight changes, IECs and TGA-FTIR measurements before and after H_2SO_4 treatment.

2.2 Experimental

The polymers PAE-1 and -2 were first synthesised and functionalised (brominated) to produce polymers BrPAE-1 and -2 (Section 2.2.2) [30, 31]. After synthesis and funtionalisation of PAE-1 and -2 as well as BrPAE-1 and 2, the polymers were characterised using GPC, NMR and elemental analysis (Section 2.2.3). After the satisfactory synthesis and characterisation of both BrPAE-1 and -2 polymers, the H_2SO_4 stability (Section 2.2.4) of these, and the SFS and F_6PBI polymers, was determined. Characterisations of the polymer films before and after H_2SO_4 treatment (Section 2.2.5) entailed % weight changes, IECs and TGA-FTIR curve data before and after acid treatment.

2.2.1 Materials

The monomers 4,4´-difluorodiphenylsulfone (DFDPS) and 4,4´-isopropylidenebis(2,6-dimethylphenol) (iTMBP), along with the anhydrous N-methyl-2-pyrrolidone (NMP), potassium carbonate (K_2CO_3), N-bromosuccinimide (NBS), benzoyl peroxide (BPO), N,N-dimethylacetamide (DMAc, 99.5% purity), chloroform and methanol were purchased from Sigma-Aldrich and used without further purification. Decafluorbiphenyl (DFBP) was obtained from Alfa Aesar. F_6PBI and tertramethyl-bisphenol A (TMBP - 4,4´-(propane-2,2-diyl)bis(2,6-dimethylphenol)) were obtained from Yanjin Technologies. SFS was obtained from the group of Dr Kerres [32]. The 80 wt% H_2SO_4

used for the membrane treatment was prepared by diluting a 96 wt% H_2SO_4 (Merck) with DI water (18 MOhm, Milli-Q). For the IEC titrations, NaOH (ACE) and HCl (0.1 M, Titrosol®) solutions were prepared using Bromothymol blue as indicator (Merck). The lithium bromide and toluene standard used during GPC analysis was obtained from Sigma-Aldrich as analytical standards.

2.2.2 Polymer synthesis and functionalisation

Both a partially fluorinated (BrPAE-1) and a non-fluorinated (BrPAE-2) poly(aryl ether) polymer were prepared by means of nucleophilic aromatic polycondensation. These polymers served as bromo-methylated components for the blend membranes discussed in Chapters 3-5. As mentioned previously, the synthesis and bromination of BrPAE polymers was performed as described in earlier works [29-31], and characterised using GPC, NMR and elemental analysis to determine the successful synthesis and bromination degree of the BrPAE polymers. In Sections 2.2.2.1 – 2.2.2.4, the synthesis and subsequent bromination of PAE-1 and PAE-2 including the NMR data confirming the syntheses are presented.

2.2.2.1 Synthesis of PAE-1

To synthesise the partially fluorinated BrPAE-1, tertramethyl-bisphenol A (TMBP) was reacted with decafluorobiphenyl (DFBP) in a first step to yield PAE-1 as illustrated in Figure 2.1

578.5 g/mol
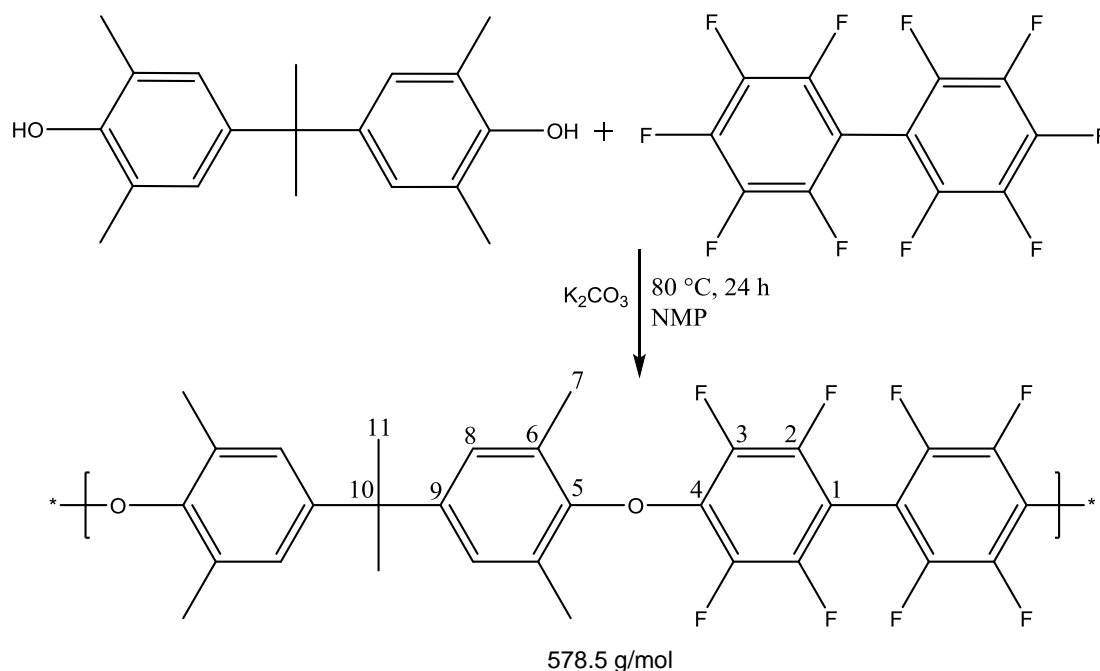
Figure 2.1: Synthesis of partially fluorinated PAE-1.

^{1}H-NMR (700 MHz, Chloroform-*d*) δ ppm : 6.81 (H-8), 2.13 (H-7), 1.56 (H-11); ^{13}C NMR(176 MHz, Chloroform-*d*) δ ppm: 151.29 (C-5); 147.70 (C-9); 145.50 (d, *J* = 245.4 Hz, C-2); 140.44 (d, *J* = 253.04 Hz, C-3); 137.75 (C-4); 128.65 (C-6); 127.49 (C-8), 99.4 (C-1); 42.06 (C-10); 30.94 (C-11); 16.55 (C-7); ^{19}F-NMR (376 MHz, Chloroform-*d*) δ ppm: -157.76 (F-2); -139.3 (F-3).

The method used was in accordance with the approach used by the group of Kerres for the synthesis of the BrPAE-1 [29, 31]. Accordingly, a 500 ml three-necked flask (equipped with a KPG stirrer) was set-up accommodating an argon inlet and reflux condenser, whereby 26.9 g (80.6 mmol) of decafluorobiphenyl (DFBP) and 22.8 g (80 mmol) of tetramethyl-bisphenol A (TMBP) was added under an argon atmosphere and dissolved in 320 ml of anhydrous N-methyl-2-pyrrolidone (NMP) at room temperature. After complete dissolution of the monomers, 66.3 g (480 mmol) of potassium carbonate was added and rinsed with an additional 40 ml of NMP while heating the solution to 80 °C. The heated solution was stirred for 24 hours. In this period, the solution turned from orange/red to a milky green and finally a milky yellow solution, which marked the completion of the polycondensation reaction. Thereafter the mixture was cooled to room temperature and gently poured into 1.5 L of water while stirring during the precipitation of the polymer. Finally, a light yellow polymer was obtained after filtering, which was washed several times in heated water to remove the remaining potassium carbonate and fluoride before drying overnight at 90 °C.

Yield: 41.5 g (71.7 mmol, 89.7%).

For ^{1}H, ^{13}C and ^{19}F NMR assignments see Figures A-1 to 3 (Appendix A).

2.2.2.2 Bromination of PAE-1 to BrPAE-1

The methyl groups of the PAE-1 polymer side chains were brominated in a subsequent reaction with NBS and BPO before the polymer was used further as blend component for the synthesis of the polymer films (Figure 2.2). The bromination reaction functionalises the polymer for the subsequent quaternisations with selected imidazoles (see Chapters 3 and 4).
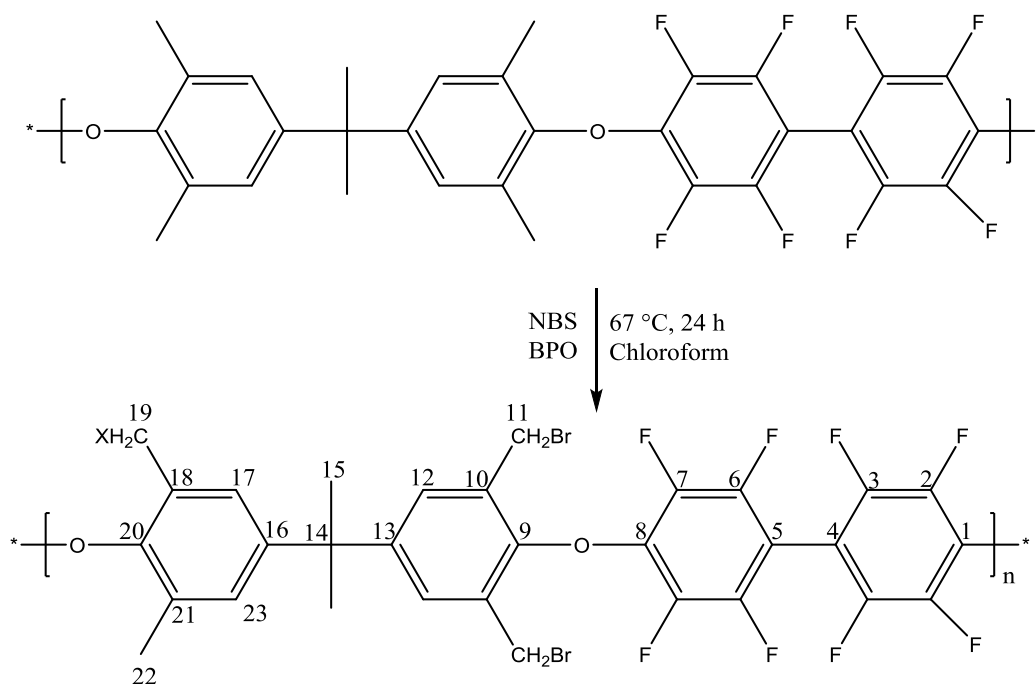
Figure 2.2: Bromination of BrPAE-1 with NBS to obtain the partially fluorinated BrPAE-1.

^{1}H-NMR (700 MHz, Chloroform-*d*) δ ppm: = 7,19 (H-12); 7,05 (H-17); 6,91 (H-23, X=Br); 6,86 (H-23, X=H); 4,42 (s, H-19); 4,37 (s, H-11); 2,12 (d, *J* = 37.4 Hz, H-22); 2,07 (d, *J* = 21,94 Hz, H-22); 1,69-1,63 (m, H-14); ^{13}C NMR(176 MHz, Chloroform-*d*) δ ppm: 150.30 (C-9); 148.93 (C-20, X= H); 148.34 (C-20, X = Br); 147.42 (C-2); 146.14 (C-16); 145.75 (C-13); 145.75-144.22 (C-3 + C-6); 140.64 (d, *J* = 30.52 Hz, C-7); 139.26 (C-8); 130.66 (C-12); 130.19 (C-18, X= H); 129.99 (C-18, X =Br); 129.29 (C-10); 129.25 (C-17 + C-23); 127.55 (C-21); 100.89 (C-4, C-5); 42,78 (C-15, X=Br); 42,59 (C-15, X=H); 30.958 (C-14, X=Br); 30.65 (C-14, X=H); 26.71 (C-19, X=Br); 26.62 (C-11); 16.54 (C-22); ^{19}F-NMR (235 MHz, Chloroform-*d*) δ ppm: -138.50 (F-3 + F-6)-156.87 (F-2 + F-7).

The bromination of PAE-1 entailed the dissolution of 7.0 g (12.1 mmol) PAE-1 in 100 mL of chloroform at room temperature. After complete dissolution was observed, 17.2 g (96.8 mmol) of NBS and 0.023 g (0.1 mmol) of BPO (radical initiator, for generation of Br radicals) were added with a further 20 mL of chloroform to the reaction solution, which subsequently turned yellow. The solution was then heated to 67 °C and stirred for 24 hours. Finally, the reaction mixture was cooled to room temperature and the brominated polymer BrPAE-1 was slowly precipitated into 1 L of methanol while gently stirring. The precipitated polymer was filtered and washed several times using hot methanol, before drying overnight at 90 °C.

Yield: 9.54 g (11.43 mmol, 97.8%); *Substitution*: 81 %.

For the ^{1}H spectrum see Figure 2.6 and Figures A-4 to A-6 (Appendix A) for the ^{13}C and ^{19}F NMR assignments. Molecular mass (g/mol) was determined as 834.1 g/mol after establishing the bromination degree for the BrPAE-1 (see Section 2.3.1).

It should be mentioned that during the course of the bromination reactions (see also Section 2.2.2.4), that possible bromine liberated during the reaction that was not condensed by the reflux condenser connected to the three-necked flask, was bubbled through a sodium thiosulfate solution which was then returned to the reaction flask.

2.2.2.3 Synthesis of PAE-2

The non-fluorinated BrPAE-2 was synthesised by the reaction of 4,4´-difluorodiphenylsulfone (DFDPS) with 4,4´-isopropylidenebis(2,6-dimethylphenol) (iTMBP) and tertramethyl-bisphenol A (TMBP) as illustrated in Figure 2.3.

498.6 g/mol
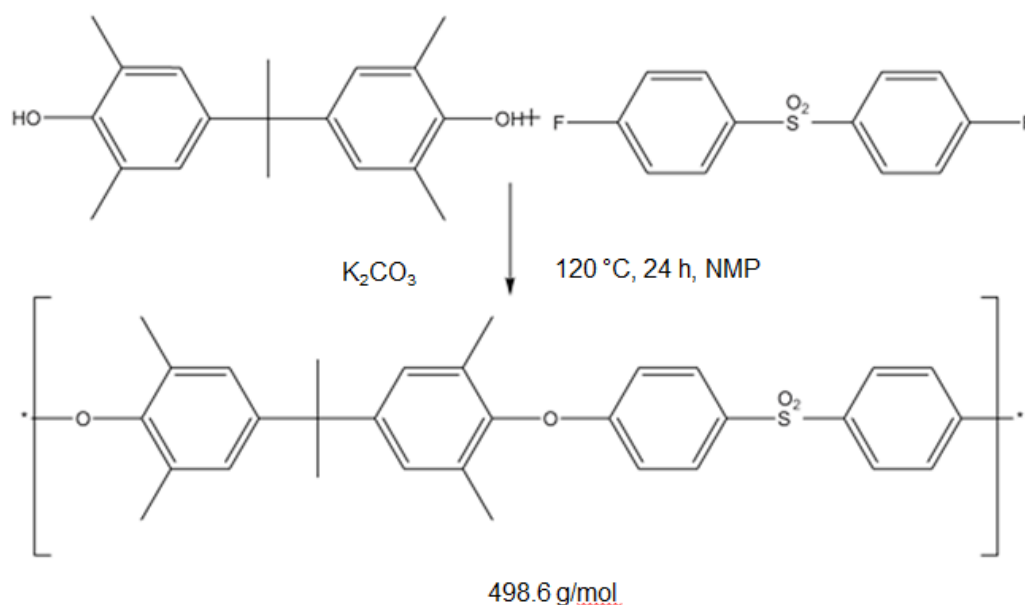
Figure 2.3: Synthesis of the non-fluorinated PAE-2.

^{1}H-NMR (700 MHz, Chloroform-*d*) δ ppm : 7,74 (d, J=9.03 Hz, H-2); 6.87 (s, H-8); 6.75 (d, J=8.82 Hz, H-3); 1.96 (s, H-7); 1.56-1.56 (m, H-11); ^{13}C NMR(176 MHz, Chloroform-*d*) δ ppm: 161.59 (C-4); 148.17 (C-5); 147.97 (C-9); 134.51 (C-1); 130.14 (C-2); 129.85 (C-6); 127.58 (C-8); 115.25 (C-3); 41.89 (C-10); 31.17 (C-11); 16.54 (C-7).

As shown in Figure 2.3, 12.7 g (50 mmol) DFDPS and 14.2 g (50 mmol) iTMBP were added to a 500 mL three-necked flask and mixed with 200 mL anhydrous NMP. After complete dissolution, 20.73 g (75 mmol) potassium carbonate was added with an additional 60 mL of NMP. Thereafter the solution was heated for 24 h at 120 °C, turning from the initial green to a dark brown colour. The reaction solution was carefully poured into 1 L of water and a beige precipitate (PAE-2) was obtained. The polymer was washed multiple times with hot water to ensure the excess potassium carbonate and potassium fluoride, which might have formed during the reaction, was removed.

Yield: 23.0 g (46.1 mmol, 92.3 %).

For ^{1}H and ^{13}C NMR assignments see Figures A-7 and 8 (Appendix A).

2.2.2.4 Bromination of PAE-2 to BrPAE-2

As illustrated in Figure 2.4 the polymer PAE-2 was brominated in the presence of NBS and BPO, in the same way as for BrPAE-1 (Figure 2.2), to yield BrPAE-2.
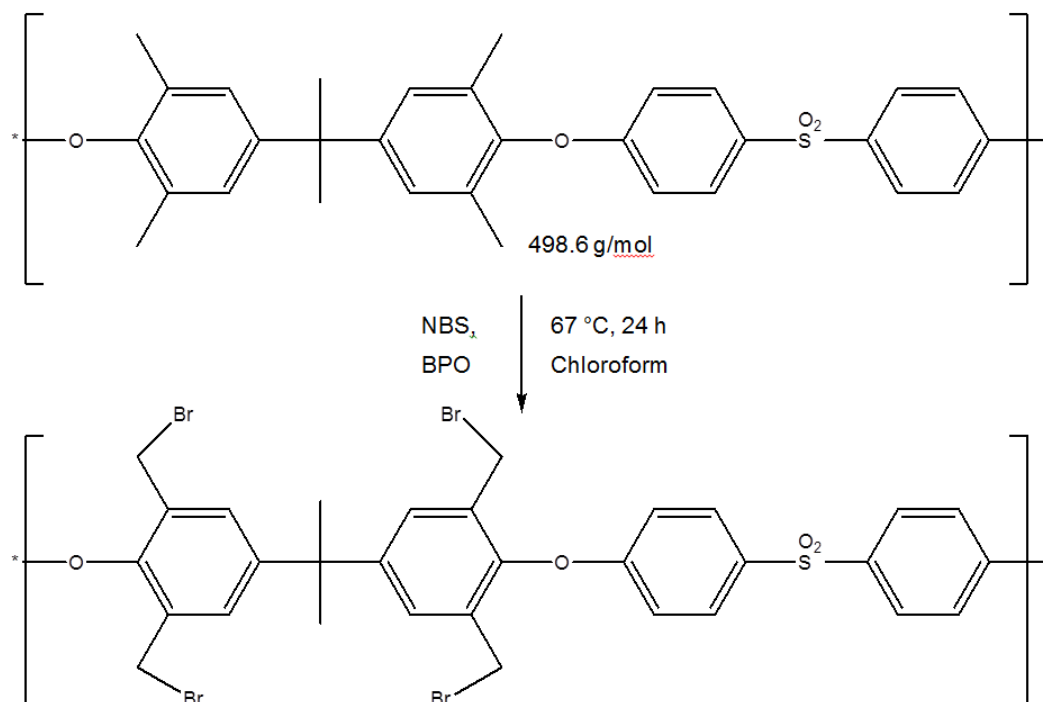
Figure 2.4: Bromination of PAE-2 to obtain BrPAE-2.

^{1}H-NMR (700 MHz, Chloroform-*d*) δ ppm: 7.80-7.74 (m, H-3 + H-6); 7.24 (H-17, X=H); 7.10 (H-17, X=Br); 7.00 (H-23); 6.89-6.86 (H-7); 6. 86 (s, H-12); 6.82 (d, H-2, X=Br); 6.77 (d, H-2, X=H); 4.23 (s, H-19), 4.18 (s, H-11); 2.10 (s, H-22, X=H); 1.95 (H-22, X=Br); 1.63 (m, H-14); ^{13}C NMR(176 MHz, Chloroform-*d*) δ ppm: 161.34 (tr, C-1, X=Br); 161.19 (C-1, X=H, C-8); 149.07 (C-9); 148.72 (C-20, X=H); 148.30 (C-20, X=Br); 148.15 (C-16, X=H); 148.03 (C-16, X=Br); 147.64 (C-13, X=H); 147.58 (C-13, X=Br); 135,11 (C-4 + C-5); 131.41 (C-12); 131.22 (C-10); 130.90 (C-18, X=H); 130.82 (C-18, X=Br); 130. 61 (C-21); 130.51 (C-17); 129.91 (C-3 + C-6); 127.79 (C-23); 127.60 (C-17); 116.09 (C-7); 115.72 (C-2, X=H); 115.28 (C-2, X=Br); 42.50 (d, C-15); 30.83 (q, C-14); 27.82 (d, C-19); 27.01 (d, C-11); 16.70 (C-22, X=H); 16.56 (C-22, X= Br).

For the bromination of the PAE-2 (Figure 2.4), 7.00 g (14.1 mmol) of PAE-2 was dissolved in 180 mL of chloroform at room temperature. After complete dissolution, 15.1 g (84.2 mmol) of NBS and 0.016 g (0.01 mmol) of BPO were added with a further 30 mL of chloroform to the reaction solution

before the solution turned yellow. Subsequently, the solution was heated to 67 °C and held constant for 24 hours while stirring during which the solution turned red. The reaction mixture was then cooled to room temperature and the brominated polymer BrPAE-2 was carefully precipitated into 1 L of methanol while gently stirring to obtain a polymer of light yellowish flocks. Thereafter BrPAE-2 was filtered and washed several times with hot methanol, before drying overnight at 90 °C.

Yield: 8.56 g (12.4 mmol, 88.6 %); *Substitution:* 60 %.

For ^{1}H and ^{13}C NMR assignments (without and with magnifications) see Figures A-9 to A-13 (Appendix A). Molecular mass (g/mol) was determined at 744.8 g/mol after establishing the bromination degree for BrPAE-2 (see Section 2.3.1).

2.2.3 Polymer characterisation

As mentioned earlier, the synthesised PAE-1, -2 and brominated BrPAE-1, -2 polymers were characterised using GPC, NMR and elemental analysis.

2.2.3.1 GPC

Gel permeation chromatography (GPC) was used to determine the average molar mass and the molar mass distribution of the synthesised polymers (BrPAE-1 and -2 and SFS was included). Both the number average $(\bar{M}_n)$ and weight average $(\bar{M}_w)$ molecular weights is considered important characterising parameters of the polymer [33]. The polydispersity index (PDI, [2-1]), also known as the molecular weight distribution, is the ratio of the weight average molecular weights $(\bar{M}_w)$ to the number average molecular weight $(\bar{M}_n)$ (see equation [2-1]), and was used to determine the distribution of polymer chain molecular weights in a given polymer. In an ideal case, a PDI = 1 indicates a monodisperse polymer chain (polymer chains of identical $\bar{M}_n$ and $\bar{M}_w$), while a PDI > 1 implies an increased heterogeneity and a more random arrangement regarding cross-linking, network formation, chain length and branching of the synthesised polymers.

$$PDI = \frac{\bar{M}_w}{\bar{M}_n} \qquad\qquad [2\text{-}1]$$

PDI: polydispersity index; $\bar{M}_w$: weight average molecular weight; $\bar{M}_n$: number average molecular weight.

In contrast to NMR measurements, the GPC measurement is not an absolute measurement and calibration with a universal standard is required (toluene was used in this study – see Section 2.3.1). For GPC analysis, the samples were dissolved in an eluent comprising dimethylacetamide (DMAc) and lithium bromide. The lithium bromide served to suppress intramolecular interactions that may occur within the polymer or even between the polymer and the solvent or stationary

phase (column material) as mentioned in earlier characterisation studies of the bromo-methylated polymers [31]. The GPC measurements were performed at a flow rate of 1 mL/min under a constant temperature of 60 °C on an Agilent Technologies GPC system (series 1200). An RI detector covering the relevant molecular weight ranges for the polymers under evaluation was used. Separating columns from Polymer Standards Service GmbH (PSS) sufficed as the stationary phase. The column system comprised a pre-column (PSS GRAM, 10 µm, 30 Å) and three other columns of various porosities (PSS GRAM, 10 µm, 100 Å, PSS GRAM, 10 µm, 3000 Å).

2.2.3.2 Nuclear magnetic resonance

In this study ^{1}H, ^{13}C and ^{19}F-NMR spectra were used to confirm the structures of the synthesised polymers PAE-1, -2 and BrPAE-1, -2. In addition, the bromination degree (BD) of BrPAE-1 and 2 with NBS was determined using the ^{1}H-NMR spectrum as described in Sections 2.3.1 (Figure 2.6).

PAE-1 and -2 were brominated on the side chains with NBS to introduce bromo-methylene groups (H-CH$_2$Br) onto the polymer structure later to be substituted with the imidazole groups (EMIm and TMIm) to form quaternary imidazolium compounds, CH$_2$-N$^+$(C)(CH)-Br$^-$ (see Chapter 3, Figure 3.1). The bromine content determined by the ^{1}H NMR spectrum was confirmed with the corresponding elemental analysis (see Appendix A-5, Table A-1). From the NMR spectra, the different peaks were integrated and placed in relation to each other. By means of Eq. [2-2], it was possible to determine the number of methyl groups successfully converted to brominated methylene groups through a radical substitution reaction.

$$BD\ [\%] = \frac{3 \cdot I(H-CH_2Br)}{3 \cdot I(H-CH_2Br) + 2 \cdot I(H-CH_3)} \cdot 100\ \%$$

$$[2\text{-}2]$$

BD: Bromination degree; I (H–CH$_2$Br) = Intensity of H-signals in the relevant bromo-methylene groups; I (H–CH$_3$) = Intensity of H-signals in the methyl group.

The average chain length of the synthesised BrPAE-1 and -2 polymers was determined using both GPC and NMR data by means of Eq. [2-3]. n was calculated using the number average molecular weight ($\bar{M}_n$) of the polymer chain determined by GPC and the average molecular weight ($\bar{M}_{WE}$) of the repeating unit of the polymer determined from the ^{1}H-NMR spectroscopy.

$$n = \frac{\bar{M}_n}{\bar{M}_{WE}}$$

$$[2\text{-}3]$$

n: chain length; $\bar{M}_n$: number average molecular weight; $\bar{M}_{WE}$: average molecular weight of the repeating polymer unit.

2.2.3.3 Elemental analysis

Quantitative elemental analysis is a technique known in the field of combustion analysis for the quantitative determination (in percentages) of the elements present within the analysed sample [34]. Carbon, hydrogen and nitrogen are respectively converted to CO_2, water and N_2/NO_x through combustion with oxygen, where any NO_x is catalytically reduced to N_2. The three gases are absorbed, then subsequently desorbed and quantified by a thermal conductivity detector. The oxygen content cannot be determined experimentally, but is rather estimated from the difference between 100% and the sum of the other elements present in the sample.

For this chapter, the elemental analysis was used in conjunction with the NMR spectra to verify the bromination degree of the polymers BrPAE-1 and 2.

2.2.4 H_2SO_4 stability of individual polymer components

As a pre-screening, the selected polymer components were subjected to an H_2SO_4 treatment to evaluate their H_2SO_4 stability at a temperature of 100 °C and to assess the need for further development with regards to cross-linking of polymer components (Chapter 3).

Firstly, the polymer films of the individual polymer components (SFS, F_6PBI, BrPAE-1 and -2) were prepared as described for the blend membranes (comprehensively discussed in both Chapters 3 and 4, see for example Section 4.2.2). Thereafter the dried polymer films were submerged in an 80 wt% H_2SO_4 solution for 5 days at 100 °C. After the acid treatment, the polymer films were repeatedly rinsed in deionised water and dried. Subsequently, the percentage weight change, ion exchange capacity (IEC) and TGA-FTIR measurements of the four polymers were compared before and after H_2SO_4 treatment as described in Section 2.2.5.

2.2.5 H_2SO_4 stability characterisation

2.2.5.1 Weight change

Dried weight changes were determined for each membrane sample before and after treatment on an Adams balance (PW analytical grade 0.0001 g). The weight changes were reported as a % of the dry weight before treatment.

2.2.5.2 Ion exchange capacity (IEC)

Experimentally, the IEC was determined through acid-base titrations [11, 35]. To attain this, the membrane samples were stirred in a saturated NaCl solution for 24 h before being titrated with 0.1 M NaOH from which the H^+ ions (acid) released and hence the direct IEC was determined.

$$IEC_{direct} = V*0.1/m \qquad\qquad [2\text{-}4]$$

where V is the volume of titration solution used (L) and m is the mass of the membrane (g).

2.2.5.3 TGA-FTIR

Thermogravimetry (TGA, Netzsch, Model STA 449C) was used to evaluate the thermal stability of polymers and blend membranes (Chapters 3-6) with a heating rate of 20 °C/min under an oxygen enriched atmosphere (65-70 % O_2, 35-30 % N_2). Coupling with FTIR allowed for analysis of the released gaseous products from the TGA with the FTIR spectrometer (Nicolet Nexus). The onset splitting-off of functional groups (e.g. –SO_3H as S-O stretch vibration at 13520-1380 cm^{-1} and C-O stretch vibration around 2200 cm^{-1}) was determined as described in [26, 36].

2.3 Results and discussion

Section 2.3.1 describes the polymer characterisation results and discussion for the synthesised PAE-1, -2 and BrPAE-1, -2, while Section 2.3.2 elaborates on the H_2SO_4 stability of the selected polymers, which included the synthesised BrPAE-1 and BrPAE-2, as well as the obtained SFS and F_6PBI polymers.

2.3.1 Polymer characterisation

The bromo-methylated polymers, BrPAE-1 and 2, were synthesised and successfully functionalised (brominated) as described in Section 2.2.2. In this section, the relevant GPC results ($\overline{M_n}$, $\overline{M_w}$ and calculated PDI and n), NMR spectras (Appendix. A, Figures A-1 to A-13) and elemental analysis (%Br content) will be discussed. The thermal stability of the PAE polymers was included in Section 2.3.2 when discussing the acid stabilities of the various polymers.

The change observed in the molecular weight distribution for polymers PAE-1 before and after bromination (BrPAE-1) is shown in Figure 2.5. A complete summary of the variables obtainable and calculable from the GPC and NMR data, including the weight average molecular weight ($\overline{M_w}$), and the number average molecular weight ($\overline{M_{n,}}$), for the PAE-1/2 and BrPAE-1/2 polymers is presented in Table 2.1.
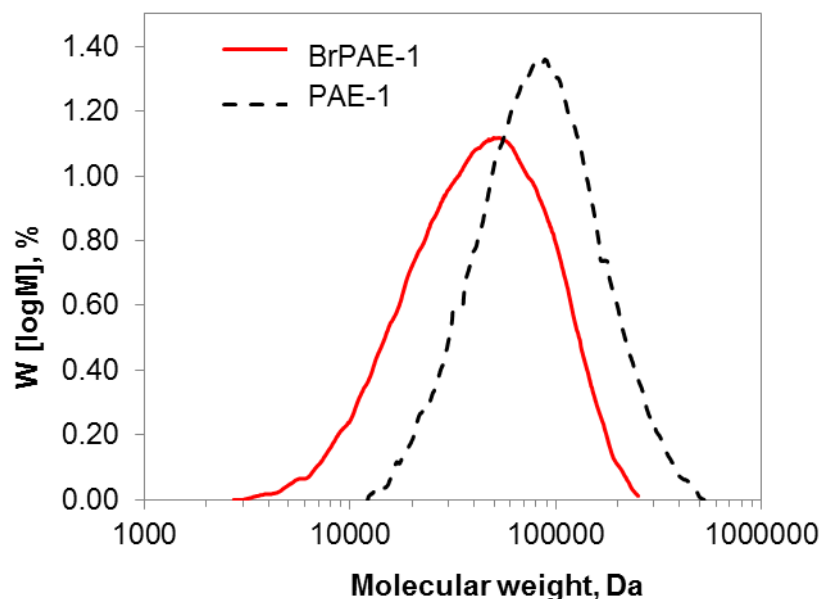
Figure 2.5: GPC- molecular weight distribution curve of PAE-1 and BrPAE-1.

Table 2.1: Summary of PAE polymer properties as determined from GPC and NMR analysis.

Polymers	M_{WE} (g/mol)	BD (%)	WE (Br$_{groups}$)	$\bar{M}_w$ * (kDa)	$\bar{M}_n$ * (kDa)	PDI	n
PAE-1	578.5	x	x	50.2	30.2	1.7	52.2
BrPAE-1	834.1	81.0	3.3	77.4	38.3	2.0	45.9
PAE-2	498.6	x	x	46.0	31.0	1.5	62.2
BrPAE-2	744.8	78.0	3.1	119.0	40.0	3.0	53.7

$\bar{M}_{WE}$ = molar mass of polymer, BD = bromination degree; WE = -CH$_2$Br group per repeating polymer unit; $\bar{M}_W$ and $\bar{M}_n$ = weight average molecular weight and number average molecular weightof the repeating polymer unit: * = Molecular mass distribution of RI-detectors.; PDI = polydispersity index; n = chain length, x = n.a. for non-brominated PEAs.

The significant broadening of the BrPAE-1 signal (solid red line), seen in Figure 2.5, corresponds to the noted increase in molecular weight ($\bar{M}_{WE}$, Table 2.1) due to successful bromination of PAE-1 (dashed line, Figure 2.5). Supported by analysis of the NMR spectra, the BD was determined as 81 % (see Figure 2.6) amounting to 3.3 Br$_{groups}$ per repeating unit (Eq. [2-2]) of the PAE-1 polymer. This corresponds to the noted increase in weight average molecular weight ($\bar{M}_w$) to 77.4 kDa of

BrPAE-1 from 50.2 kDa for PAE-1. Subsequently, the number average ($\bar{M}_n$, 26.8 %) and PDI (Eq. [2-1]) also increased due to the high BD (functionalised PAE-1). The increase of the PDI (from 1.7 to 2.0) was accompanied by the broadening of the molecular weight distribution of the brominated polymer (Figure 2.5). The noted decrease in chain length (see Eq. [2-3]) for BrPAE-1 could be ascribed to partial degradation of the polymer chain due to the presence of the bromide radical. However, the molecular weight of the BrPAE-1 was large enough to provide good film (membrane) forming properties without sacrificing mechanical stability.

Similarly, the bromination of PAE-2 showed an increase in molecular weight ($\bar{M}_{WE}$), while the BD was determined at 78%, amounting to 3.1 Br$_{groups}$ per repeating unit for BrPAE-2 (Table 2.1). The large increase noted for $\bar{M}_w$ (159%) and $\bar{M}_n$ (29%) with a subsequent high PDI might suggest some cross-linking occurring within the polymer during the bromination reaction. In comparison to BrPAE-1, the increased PDI of BrPAE-2 indicates the more heterogeneous nature of the cross-linking taking place in a more random arrangement. However, the determined molecular weight, and subsequent film forming properties of BrPAE-2 were sufficient for the purpose of this chapter as well as further use as a blend component (Chapters 3-5). It could be added that these results obtained in this section correlated well with earlier synthesis and bromination results of the PAE-1 and 2 polymers [31].

Figure 2.6 shows the ^{1}H-NMR spectrum of BrPAE-1. The intensity ratio between the H signals H-7, H-8 and H-11 (see also Figure A-1) confirms the successful co-polymerisation of the monomers TMBP and DFBP. The comparison of the NMR spectra of BrPAE-1 with the un-brominated polymer PAE-1 (Figure A-1), the peak detected at 4.38 ppm for BrPAE-1 as shown in Figure 2.6, confirms the successful bromination of PAE-1. The signals H-19 and H-22 in relation to one another account for the determined bromination degree of 81% for BrPAE-1 (3.25 –CH$_2$Br groups per repeat unit for the polymer, $\bar{M}_{WE}$: 834.1 g/mol).
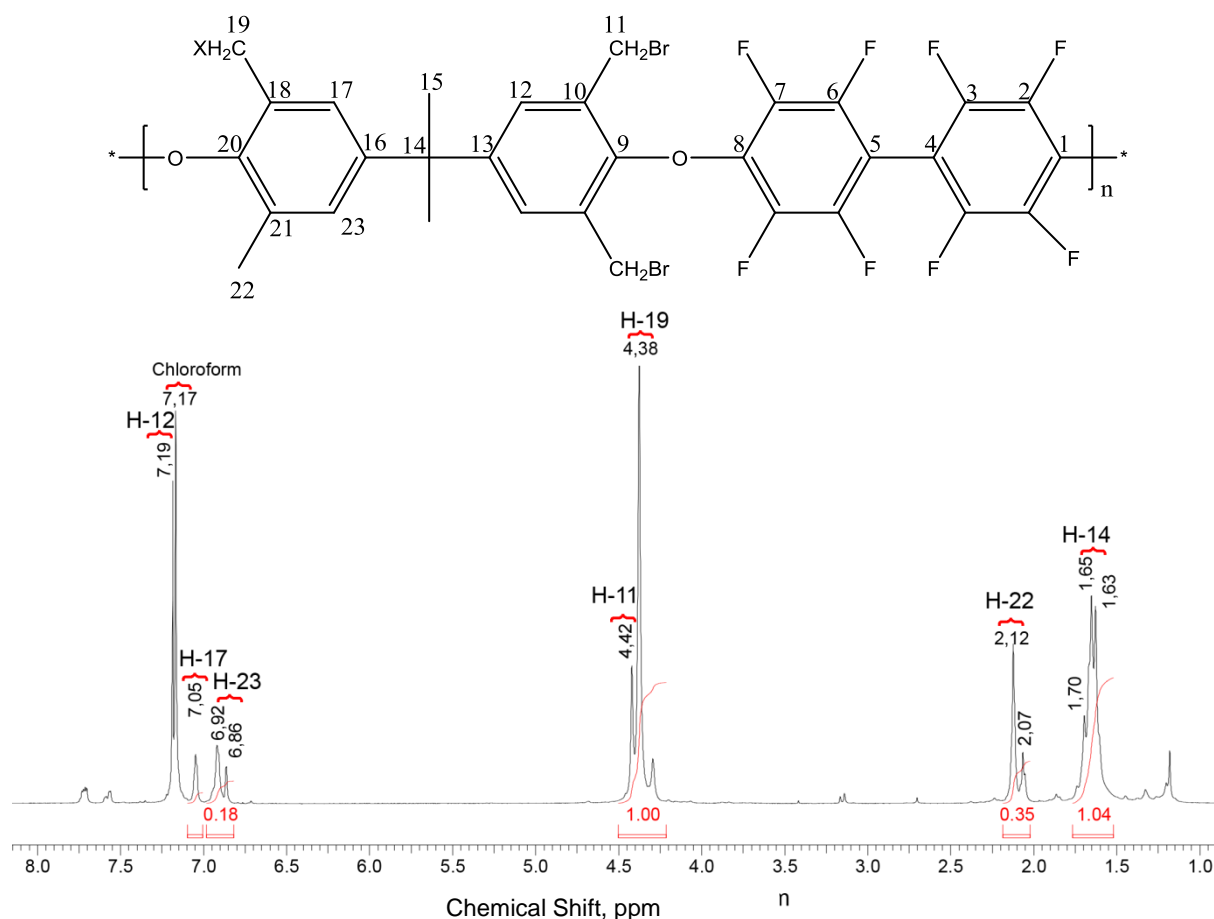
Figure 2.6: ^{1}H-NMR spectrum of BrPAE-1 in d-Chloroform.

^{1}H-NMR (700 MHz, Chloroform-*d*) δ ppm: = 7,19 (H-12); 7,05 (H-17); 6,92 (H-23, X=Br); 6,86 (H-23, X=H); 4,42 (s, H-19); 4,38 (s, H-11); 2,12 (d, *J* = 37.4 Hz, H-22); 2,07 (d, *J* = 21,94 Hz, H-22); 1,70-1,63 (m, H-14).

The same principal was applied to evaluate PAE-2 (Figures A-7 and A-9, Appendix A) where the bromination degree for BrPAE-2 was determined as 78 % (3.1 –CH$_2$Br groups per repeat unit for the polymer, $\bar{M}_{WE}$: 744.8 g/mol).

Lastly, the bromination degree, determined from the NMR spectra (3.3 and 3.1 Br$_{groups}$ per repeating unit BrPAE-1 and 2), was used to estimate the theoretical % elemental bromine (Calc.) present within the respective BrPAE-1 and -2 polymer samples analysed (Exp.) for comparison. The weight % of the remaining elements (C, H, O and S) in the BrPAE-1 and -2 samples was also calculated for comparison with the experimentally measured weight % (see Appendix A-5, Table A-1). Percentage differences (% diff) were found to range between -8.3 and 8.5 % for the measured elements (C, H, O, S and Br) and considered acceptable in support of the GPC and NMR data gathered on the BrPAE-1 and -2 polymers.

2.3.2 H_2SO_4 stability and characterisation of blend components

Four polymer film samples made from SFS, F_6PBI, BrPAE-1 and BrPAE-2, were rinsed and dried before and after the H_2SO_4 treatment followed by the characterisation of the polymers before and after acid treatment. The characterisation entailed measuring the % weight change, IEC, T_{onset} and T_{SO_2} (from TGA-FTIR measurements where applicable) before and after treatment. It should be mentioned that the IEC for SFS was only measureable after treatment, as the associated $–SO_3H$ groups were either absent (F_6PBI) or only present in quantities too low to accurately measure with acid-base titrations (Section 4.2.4.2). The IEC of SFS before treatment was experimentally determined as 2.14 meq/g in comparison to the 2.40 meq/g (12.2 % increase) measured afterwards, indicating a negligible degree of sulfonation of the SFS polymer structure with accompanying loss of low molecular fragments, without significantly impacting the mechanical integrity of the polymer film. Table 2.2 provides a summary of the H_2SO_4 stability data obtained for the treated polymer samples, excluding the IEC data of the SFS discussed above.

Table 2.2: Characterisation data of the H_2SO_4 treated polymer samples

Polymer	% wt change (%)	Before				After			
		T_{Onset} (°C)	res. wt (%)	T_{SO_2} (°C)	res. wt (%)	T_{Onset} (°C)	res. wt (%)	T_{SO_2} (°C)	res. wt (%)
SFS	-13.6	416.5	73.3	383.8	80.4	476.1	66.0	340.5	78.0
F_6PBI	-0.4	520.5	92.6	-	-	506.3	92.0	-	-
BrPAE-1	20.6	265.0	91.0	-	-	313.8	95.8	321.7	94.3
BrPAE-2	6.6	293.0	94.0	355.0	77.2	277.7	92.3	265.3	96.1

SO_2 peaks not detected for relevant polymers (F_6PBI and BrPAE-1) due to absence of sulfone groups in the structure of these polymers; res wt % = residual weight %; T_{Onset} and T_{SO2} was obtained from Appendix A-6

In past studies, the weight losses reported after similar (temperatures 80 and 100 °C) H_2SO_4 treatments of blended membranes containing a large SFS polymer content (>50%), were ascribed to the loss of low molecular fractions (such as oligomers) of the sulfonated SFS polymer [10, 26, 37]. As seen in Table 2.2, weight losses of 13.6 % were measured for the individual SFS polymer film after treatment in comparison to the negligible loss of 0.4 % noted for F_6PBI, confirming the stability of the F_6PBI [26, 27]. The weight loss obtained for SFS confirms the weight losses noted for SFS-containing blend membranes tested in earlier studies [17, 26]. From the TGA-FTIR data

(see Appendix A-6, Figures A-14), the T_{Onset} and T_{SO_2} values with accompanying residual weight % (res. wt %) before and after acid treatment were obtained. According to the T_{SO_2} in Table 2.2 (5th and 9th column), a decrease of 40 °C before and after treatment was obtained for SFS, confirming the loss of the low molecular fractions that simultaneously also increased the T_{Onset} temperature (with 60 °C) noted after treatment (Table 2.2, 3rd and 7th column). The T_{Onset} of F_6PBI (Appendix A, Figure A-15) decreased only slightly after acid treatment (2.7 %) and was considered negligible (likely associated with analytical error).

Simultaneously, respective weight increases of 20.6 and 6.6 % were reported for the partially fluorinated BrPAE-1 and non-fluorinated BrPAE-2 respectively, due to sulfonation, which was supported by the TGA-FTIR data presented in Table 2.2. It could be possible that the more hydrophobic BrPAE-1 (partially fluorinated) had a more separated nanomorphology than the BrPAE-2 (non-fluorinated), which led to a better accessibility of the more hydrophilic moieties of BrPAE-1 to the sulfuric acid, resulting in the higher sulfonation obtained at 100 °C. The proposed sulfonation of BrPAE-1 after the 80 wt% H_2SO_4 treatment at 100 °C is presented in Figure 2.7.

Figure 2.7: Proposed sulfonation reaction of the BrPAE-1 polymer due to 80 wt% H_2SO_4 treatment at 100 °C.
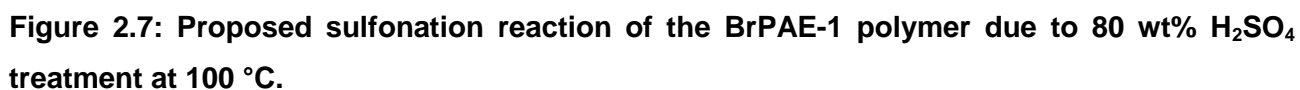
The TGA data of BrPAE-1 and BrPAE-2 is presented in Figure 2.8 and Appendix A-6 (Figures A-16) respectively. According to Figure 2.8, BrPAE-1 (partially fluorinated with an ether linkage) had a T_{onset} of 265 °C which was lower than the 293 °C noted for BrPAE-2 with the addition of a T_{SO_2} at 355 °C associated with the polyethersulfone (SO_2-detection) present in the polymer backbone. The % weight increase (21%) measured for BrPAE-1, and suspected sulfonation was confirmed by the TGA data obtained after acid treatment (Figure 2.8). A prominent SO_2 band was identified which is associated with the weight loss at 322 °C, stabilising the polymer backbone and resulting in an increased T_{onset} of 314 °C compared to the 265 °C before acid treatment.

It could be added that the outstanding thermal stability of F_6PBI (reported T_{onset} = 520 °C) serves to support its further inclusion as basic blend component, with the expected benefit of improved stability of blended materials containing SFS as acidic blend component which measured a T_{SO_2} and T_{onset} at 384 and 417 °C, respectively. In conclusion, the H_2SO_4 stability of the separate polymer components SFS, BrPAE-1 and -2 were acceptable but would require an improvement of stability to be able to withstand the possible sulfonation during SO_2 electrolyser operations at increased temperatures. Therefore it is suggested to further investigate the relevant cross-linking possibilities and accompanying strengths between blend components to assist in the design of a blend membrane with adequate chemical, mechanical and thermal stability that is suitable as a PEM in SO_2 electrolysis.
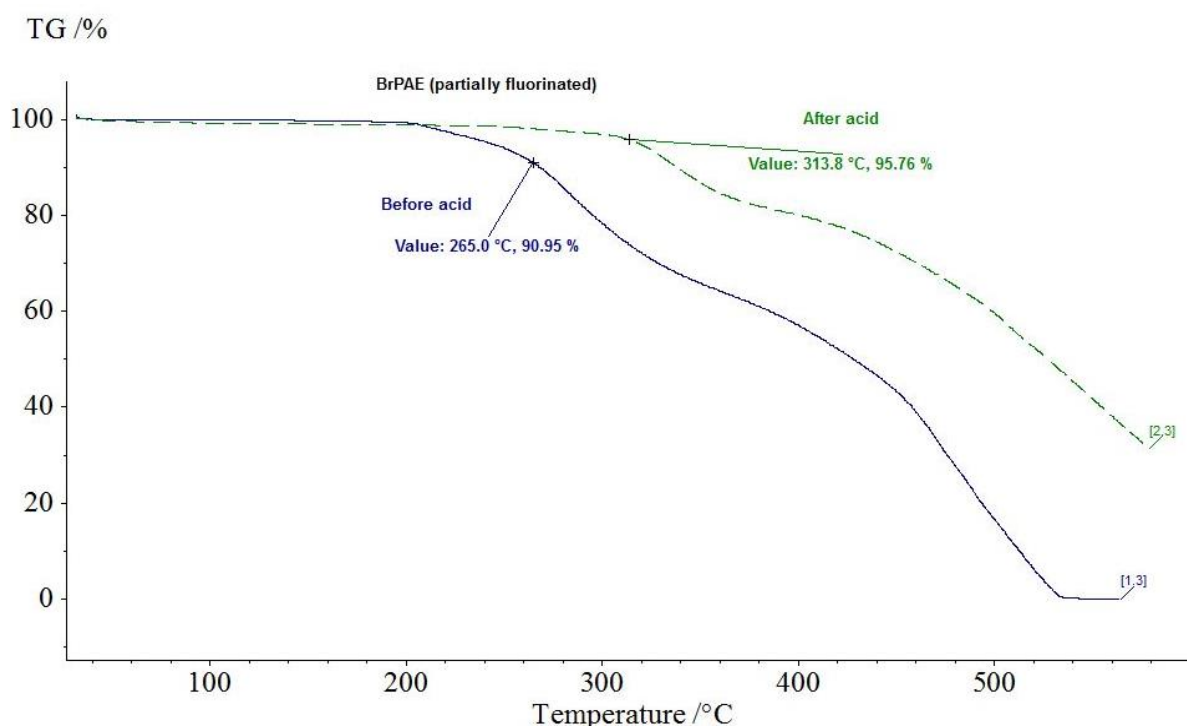
Figure 2.8: TGA curves recorded for polymer BrPAE-1 before and after acid treatment.

2.4 Conclusion

The suggested bromo-methylated polymers, BrPAE-1 and -2, were successfully synthesised and functionalised (brominated) for further application as blend components. The polymer characterisations of the PAE polymers confirmed the synthesis providing films suitable for further H_2SO_4 stability investigations where SFS and F_6PBI were included as acidic and basic blend components. The fluorinated polybenzimidazole (F_6PBI) proved exceptionally stable in the H_2SO_4 treatment conditions investigated, withstanding sulfonation unlike the sulfonation confirmed for the BrPAE-1 and -2 polymers in terms of the weight increases (6-21%) and the SFS polymer where a weight loss was noted (13%). This confirms that the polymers SFS, BrPAE-1 and -2 could be suitable as blend components, but would require further stabilisation by determining which type and strength of the possible cross-links (Chapter 3) between blend components would assist in the final design of a blend membrane (Chapter 4) with adequate chemical, mechanical and thermal stability for a suitable application as a PEM in SO_2 electrolysis (Chapters 5 and 6).

2.5 References

[1] Vogel C, Meier-Haack J. Preparation of ion-exchange materials and membranes. Desalination. 2014;342:156-74.

[2] Xu T. Review: Ion exchange membranes: State of their development and perspective. Journal of Membrane Science. 2005;263:1-29.

[3] Nagarale RK, Gohil GS, Shahi VK. Recent developments on ion-exchange membranes and electro-membrane processes. Advances in Colloid and Interface Science. 2006;119:97-130.

[4] Kerres JA. Design Concepts for Aromatic Ionomers and Ionomer Membranes to be Applied to Fuel Cells and Electrolysis. Polymer Reviews. 2015;55:273-306.

[5] Zeis R. Materials and characterization techniques for high-temperature polymer electrolyte membrane fuel cells. Beilstein Journal of Nanotechnology. 2015;6:68-83.

[6] Li Q, Jensen JO, Savinell RF, Bjerrum NJ. High temperature proton exchange membranes based on polybenzimidazoles for fuel cells. Progress in Polymer Science. 2009;34:449-77.

[7] Zhang J, Xie Z, Zhang J, Tang Y, Song C, Navessin T, et al. High temperature PEM fuel cells. Journal of Power Sources. 2006;160:872-91.

[8] Hartnig C, Jörissen L, Kerres J, Lehnert W, Scholta J. Materials for fuel cells 1st ed. . Boca Raton, New York, Boston, Washington DC: CRC Press & Cambridge: Woodhead Publishing Ltd.; 2008.

[9] Kerres J, Schönberger F. Chapter III: Proton exchange membranes and fuel cells: Nova Science Publishers, Inc.

[10] Kerres J, Schönberger F, Chromik A, Häring T, Li Q, Jensen JO, et al. Partially Fluorinated Arylene Polyethers and Their Ternary Blend Membranes with PBI and H3PO4. Part I. Synthesis and Characterisation of Polymers and Binary Blend Membranes. Fuel Cells. 2008;8:175-87.

[11] Kerres JA, Xing D, Schönberger F. Comparative investigation of novel PBI blend ionomer membranes from nonfluorinated and partially fluorinated poly arylene ethers. Journal of Polymer Science Part B: Polymer Physics. 2006;44:2311-26.

[12] Soczka-Guth Tea. International Patent WO99/29763. International Patent WO99/29763. 1999.

[13] Kerres JA. Development of ionomer membranes for fuel cells. Journal of Membrane Science. 2001;185:3-27.

[14] Smitha B, Sridhar S, Khan AA. Solid polymer electrolyte membranes for fuel cell applications- a review. Journal of Membrane Science. 2005;259:10-26.

[15] Rikukawa M, Sanui K. Proton-conducting polymer electrolyte membranes based on hydrocarbon polymers. Prog Polym Sci. 2000;25:1463-502.

[16] Trogadas P, Ramani V. Membrane and MEA Development in Polymer Electrolyte Fuel Cells. New York: Springer; 2009.

[17] Peach R. Characterisation of proton exchange membranes in an H_2SO_4 environment. North-West University, Potchefstroom 2520, South Africa: North-West University, Potchefstroom campus; 2014.

[18] Noshay A, Robenson LM. Sulphonated polysulphone. Journal Of Applied Polymer Science. 1976;20:1885-903.

[19] Xing D KJ. Improved performance of sulphonated polyarylene ethers for proton exchange membrane fuel cells. . Polymers For Advanced Technologies. 2006:591-7.

[20] Kerres JA. Blended and Cross-Linked Ionimer Membrane for Appliction in Membrane Fuel Cells. Fuel Cells. 2005;2:230-47.

[21] Chromik A, Kerres JA. Degradation studies on acid–base blends for both LT and intermediate T fuel cells. Solid State Ionics. 2013;252:140-51.

[22] Peighambardoust SJ, Rowshanzamir S, Amjadi M. Review of the proton exchange membranes for fuel cell applications. International Journal of Hydrogen Energy. 2010;35:9349-84.

[23] Mader JA, Benicewicz BC. Synthesis and Properties of Random Copolymers of Functionalised Polybenzimidazoles for High Temperature Fuel Cells. Fuel Cells. 2011;11:212-21.

[24] Krishnan NN, Lee H-J, Kim H-J, Kim J-Y, Hwang I, Jang JH, et al. Sulfonated poly(ether sulfone)/sulfonated polybenzimidazole blend membrane for fuel cell applications. European Polymer Journal. 2010;46:1633-41.

[25] Mader JA, Benicewicz BC. Sulfonated Polybenzimidazoles for High Temperature PEM Fuel Cells. Macromolecules. 2010;43:6706-15.

[26] Peach R, Krieg HM, Krüger AJ, van der Westhuizen D, Bessarabov D, Kerres J. Comparison of ionically and ionical-covalently cross-linked polyaromatic membranes for SO_2 electrolysis. International Journal of Hydrogen Energy. 2014;39:28-40.

[27] Schoeman H, Krieg HM, Kruger AJ, Chromik A, Krajinovic K, Kerres J. H_2SO_4 stability of PBI-blend membranes for SO_2 electrolysis. International Journal of Hydrogen Energy. 2012;37:603-14.

[28] Peach R, Krieg HM, Krüger AJ, Rossouw JJC, Bessarabov D, Kerres J. Novel cross-linked partially fluorinated and non-fluorinated polyaromatic PBI-containing blend membranes for SO_2 electrolysis. International Journal of Hydrogen Energy. 2016;41:11868-83.

[29] Morandi CG, Peach R, Krieg HM, Kerres J. Novel morpholinium-functionalized anion-exchange PBI-polymer blends. Journal of Materials Chemistry A. 2015;3:1110-20.

[30] Morandi CG, Peach R, Krieg HM, Kerres J. Novel imidazolium-functionalized anion-exchange polymer PBI blend membranes. Journal of Membrane Science. 2015;476:256-63.

[31] Katzfuss A. Synthese und Charakterisierung von kovalent vernetzten Anionenaustauschermembranen und deren Einsatz in Direkt-Methanol-Brennstoffzellen, sowie ESR spektroskopische Messungen zur Identifikation der Radikalbildung in der Membran. . Universitaet Stuttgart2013.

[32] Schönberger F, Chromik A, Kerres J. Partially fluorinated poly(arylene ether)s: Investigation of the dependence of monomeric structures on polymerisability and degradation during sulfonation. Polymer. 2010;51:4299-313.

[33] Ghosh P. Polymer science and technology : plastics, rubbers, blends and composites: New York, N.Y. : McGraw-Hill Education LLC., [2011]

3rd ed.; 2011.

[34] Chapter 8 - Quantitative elemental analysis. In: MÁZor L, editor. Comprehensive Analytical Chemistry: Elsevier; 1983. p. 275-411.

[35] Kerres J, Zhang W, Jörissen L, Gogel V. Application of Different Types of Polyaryl-Blend-Membranes in DMFC. Journal of New Materials for Electrochemical Systems. 2002;5:97-107.

[36] Kerres J, Ullrich A, Hein M, Gogel V, Friedrich KA, Jörissen L. Cross-Linked Polyaryl Blend Membranes for Polymer Electrolyte Fuel Cells. Fuel Cells. 2004;4:105-12.

[37] Krüger AJ, Kerres J, Bessarabov D, Krieg HM. Evaluation of covalently and ionically cross-linked PBI-excess blends for application in SO_2 electrolysis. International Journal of Hydrogen Energy. 2015;40:8788-96.

CHAPTER 3 : EFFECT OF IONIC OR COVALENT CROSS-LINKING ON MEMBRANE STABILITY

Chapter Overview

It was shown in Chapter 2 that the polymers SFS, F_6PBI, BrPAE-1 and -2 were suitable as blend components to be included in further cross-linking studies for SO_2 electrolyser applications. In this chapter the different types of cross-linking possibilities between the various polymer components were investigated. Seven 2-component blend membranes were prepared by combining two polymers (for example SFS:F_6PBI) in a 1:1 molar ratio. When preparing SFS:BrPAE membranes, the BrPAE was quaternised beforehand using either TMIm or EMIm. The compatibility and strength for each of the the seven cross-linked 2-component membranes (1D and 1D$_{i\text{-}vi}$) were evaluated by determining their water uptake as well as their solvent extraction stability in DMAc (90 °C for 4 days) and H_2SO_4 (80 wt% H_2SO_4 at 100 °C for 5 days – similar to what was described in Chapters 2, 4 & 5). The % weight changes and TGA-FTIR data obtained were compared before and after the H_2SO_4 treatment for an insight on the membrane optimisation required for the intended application in an SO_2 electrolyser at elevated temperatures (>100 °C). It was shown that the stability of the membranes decreased in the order 1D>1D$_v$>1D$_{vi}$> 1D$_{i,iii}$> 1D$_{ii,iv}$, showing that the strongest cross-linking was obtained when combining SFS/BrPAE-1 withF_6PBI, implying that ionic and covalent cross-linking in the presence of F_6PBI as blend component was most effective. It became clear that more than one type of cross-linking would be required for the harsh conditions experienced in a SO_2 electrolyser.

3.1 Introduction

In addition to developing suitable polymers, the required membrane properties and stabilities for an intended application could also be attained by cross-linking various (co)polymers. This provides additional flexibility for the optimisation of membrane properties by simply mixing polymer components to obtain blend membranes with both a high chemical stability and sufficient proton conductivity [1].

It has been determined that, for the purpose of obtaining macroscopically homogeneous blend membranes, polymers with similar structures, which allow for sufficient interactions between polymer components, are required [2]. The different types of interactions present within and between polymers can include Van der Waals forces, dipole-dipole forces, electrostatic interactions (ionic cross-linking), hydrogen bridges, and covalent cross-linking. The increasing strength of these interactions follows the order of: Van der Waals < dipole-dipole < hydrogen bridge < electrostatic interactions (ionic cross-linking) < covalent cross-linking [3].

In an attempt to develop novel ionomer membranes, Kerres *et al.* [4] concluded that Van der Waals- and dipole-dipole forces were too weak to ensure blend compatibility on their own. It was also found that blends solely relying on hydrogen-bridge interaction forces showed signs of incompatibility, with reported increases in swelling at elevated temperatures followed by the dissolution of the membrane at temperatures exceeding 90 ^{0}C [3]. Accordingly, it was shown that acid-base polymer blends containing interactions such as ionic- and covalent cross-linking with hydrogen bonding bridges, separately and in combination, displayed considerably reduced membrane swelling with improved mechanical- and thermal stabilities [5].

In acid-base blends, ionic interactions are typically found when a proton is transferred from an acidic group to a lone electron pair of, for example, an N-basic group, as is schematically illustrated in Figure 3.1. Covalent cross-links can form when the CH_2Hal group of a halomethylated polymer reacts with the imidazole-N-H group of polybenzimidazole within a membrane matrix [6, 7]. (see Chapter 4, Figure 4.1).
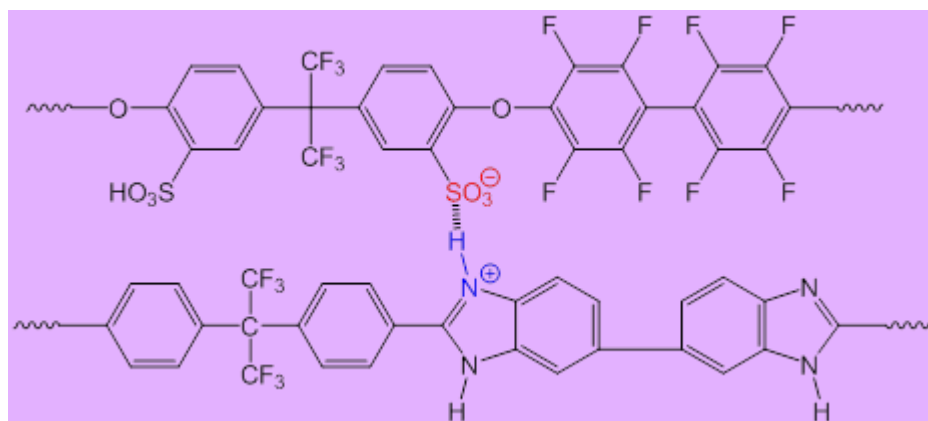
Figure 3.1: An example of ionic cross-linking between an acidic (SFS) and basic (PBI) polymer by protonation of the basic N-groups [1].

As mentioned in Section 2.1, and understandably so in view of the potential cross-linking found when mixing these two polymers, various studies have indicated the potential of the selected SFS- and F_6PBI polymers in blend membranes for SO_2 electrolysis [8-10]. In terms of the partially and non-fluorinated bromo-methylated polymers (BrPAE-1 and -2), it was shown in Chapter 2 that they underwent some degree of sulfonation during the H_2SO_4 treatment, showing weight increases between 6 and 21 %.

It was therefore the purpose of this chapter to investigate the types of cross-linking possibilities between the polymer components: SFS, F_6PBI, BrPAE-1 and BrPAE-2. To determine the effect of each type of cross-linking, 2-component blend membranes were prepared, combining the four polymers in question in a 1:1 molar ratio. This led to the synthesis of 7 cross-linked membranes (Section 3.2.2). The compatibility of these 7 membranes was evaluated (macroscopically) in Section 3.2.3 through film inspection of the casted membranes. This was followed by a solvent extraction experiment (DMAc) of the cross-linked membranes, including water uptake measurements at 25 °C and 90 °C. Lastly, the cross-linked membranes were subjected to a H_2SO_4 treatment. To determine the H_2SO_4 stability before characterisation (Section 3.2.4), the % weight changes and TGA-FTIR measurements before and after H_2SO_4 treatment were compared.

3.2 Experimental

3.2.1 Materials

The BrPAE polymers 1 and 2 were synthesised as described in Section 2.2.1, while SFS and F_6PBI were obtained from the group of Dr Kerres [11] and YANJIN Technology, respectively. The alkylated imidazoles, 1-ethyl-2-methylimidazole (EMIm) and tetramethylamine (TMIm) were purchased from Ionic Liquids Technologies GmbH and TCI, respectively. The DMAc and H_2SO_4 used in synthesis and characterisation studies were obtained from Sigma-Aldrich and Merck, respectively.

3.2.2 Membrane synthesis and post-treatment

The four selected polymer components (SFS, F_6PBI, BrPAE-1 and -2) were individually dissolved in DMAc to obtain solutions of 10 wt% (SFS and BrPAE) and 5 wt% (F_6PBI), respectively. For each membrane, two polymer solutions were mixed in a 1:1 molar ratio to yield 7 cross-linked membranes as shown in Table 3.1. The SFS polymeric solution was first neutralised with n-propylamine before mixing with F_6PBI to prevent precipitation of the poly-electrolyte complex. To ensure the cross-linking of BrPAE with specifically the SFS blend component (see also Section 4.2.2), the -CH_2Br groups of the BrPAE were quaternised using one of two imidazoles (TMIm or EMIm – see Chapter 1, Table 1.1 for their structure), which was added in a fourfold molar excess prior to the addition of the BrPAE to the SFS. The quaternisation was done according to the method described in earlier studies for the synthesis of AEMs [12, 13]. An example of the quaternisation reaction of BrPAE-1 and EMIm is shown in Figure 3.2 [13, 14].

Table 3.1: Cross-linked membrane types for the seven membranes.

Membrane	Components [a]	Cross-linking type [b]
1D	SFS:F_6PBI	Ionic
1D$_i$	SFS:BrPAE-1 EMIm	Ionic
1D$_{ii}$	SFS:BrPAE-2 EMIm	Ionic
1D$_{iii}$	SFS:BrPAE-1 TMIm	Ionic
1D$_{iv}$	SFS:BrPAE-2 TMIm	Ionic
1D$_v$	F_6PBI:BrPAE-1	Covalent
1D$_{vi}$	F_6PBI:BrPAE-2	Covalent

[a] Molar masses: SFS (779.3 g/mol), F_6PBI (534 g/mol), BrPAE-1 (815.2 g/mol) and BrPAE-2 (735.3 g/mol), [b] as determined in earlier studies. [9, 13].

As listed in Table 3.1, five ionic cross-linked membranes (1D and 1D$_{i\text{-}iv}$) were obtained by blending SFS with F$_6$PBI and the respective BrPAE-1 and -2 and an imidazole (EMIm or TMIm). Two covalent cross-linked membranes were produced by mixing F$_6$PBI with BrPAE-1 and -2.
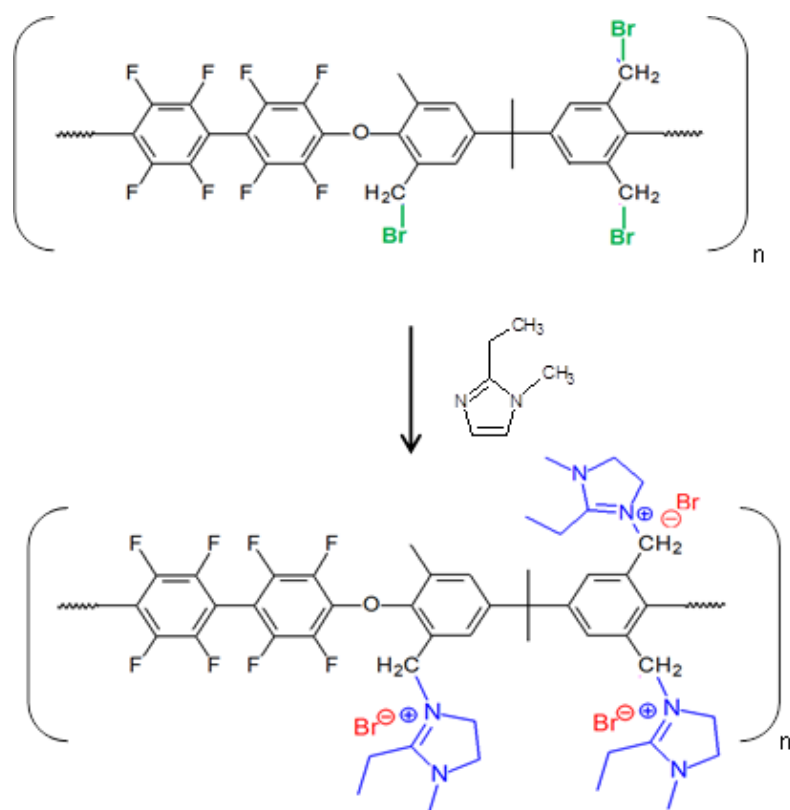
Figure 3.2: Quaternisation of a bromo-methylated polymer (BrPAE-1) with 1-ethyl-2-methylimidazole (EMIm).

The homogeneously mixed polymer solutions were then casted in petri dishes and placed in a convection oven at 80 °C for 2 hours before increasing the temperature to 130 °C for another 6 hours. After cooling, the membranes were removed and post-treated in a 10% HCl solution at 90 C for 48 h, followed by a H$_2$O post-treatment at 60 °C for another 48 h. The membrane samples were thereafter dried and weighed before continuing with treatment and characterisation studies.

3.2.3 Solvent extraction stability (DMAc) and water uptake

The membranes were macroscopically (physically) inspected to determine whether homogenous cross-linked blends were obtained pertaining to the compatibility of chosen polymer components for the intended PBI-blend membranes (Chapters 4-6). A solvent extraction experiment with DMAc was included to preliminarily establish the degree of cross-linking for the blends before continuing with H$_2$SO$_4$ stability determination and characterisation. This entailed placing the membranes in DMAc for 96 h (4 days) at 90 °C, whereafter the residual weight of the membrane fractions was

determined (expressed as a % weight loss, see also Section 4.2.3.3) [15]. In addition, the water uptake of the cross-linked membranes was determined at both room temperature (25 °C) and 90 °C and reported as wt% increases.

3.2.4 H$_2$SO$_4$ stability

Similarly to what had been described in Sections 2.2.4 and 2.2.5, the dried membrane samples were subjected to a H$_2$SO$_4$ treatment (80 wt% H$_2$SO$_4$ for 5 days at 100 °C) to determine weight changes (see Section 2.2.5.1), while TGA-FTIR measurements (see Section 2.2.5.3) were done before and after H$_2$SO$_4$ treatment. It should be added that no IEC values could be reported for the 1:1 cross-linked membranes as the residual number of free –SO$_3$H groups (not involved in cross-linking) was too low to accurately measure (see also Section 4.3.1.2).

3.3 Results and discussion

The rationale was to inspect to which degree the determined H$_2$SO$_4$ stability of selected polymers could be improved upon (where needed) by combining polymer components and the subsequent inclusion of ionic and covalent cross-links, respectively. Consequently, 7 cross-linking combinations from the selected polymers were identified for further separate evaluations regarding solvent extraction and H$_2$SO$_4$ stability.

Before subjecting the membranes to any treatment, they were visually inspected after synthesis. All 7 cross-linked membranes were macroscopically homogeneous and mechanically stable. As shown in Figure 3.3 (a), translucent, slightly yellow-coloured membranes were obtained for the cross-linked SFS and F$_6$PBI blend 1D. The BrPAE-containing blend membranes (1D$_{i-vi}$) yielded a more yellowish-brown membrane, as shown for 1D$_{iii}$ in Figure 3.3(b).
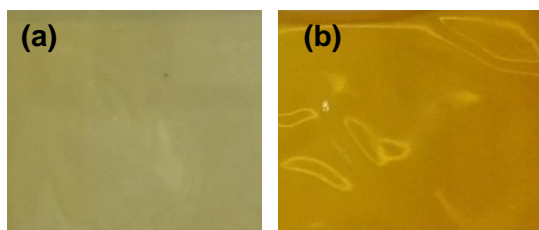

Figure 3.3: Photos of the cross-linked membranes (a) 1D and (b) 1D$_{iii}$.

3.3.1 Solvent extraction stability (DMAc) and water uptake

After confirming the structural cohesion of the membranes, they were subjected to the solvent extraction experiment with DMAc and the water uptake studies. The results are presented in Table 3.2. The negligibly small weight losses (1 to 4 %) when treated in DMAc, reported for the respective membranes in Table 3.2, confirmed the successful 1:1 cross-linking of the polymer components for all the membranes in the 1D series. This further served to confirm the success of the synthesis procedure both in terms of the oven temperature and the time allowed for cross-linking during solvent evaporation in the oven.

Table 3.2: Weight changes reported for the cross-linked membranes after DMAc extraction and with water uptake (25 °C and 90 °C).

Membrane	DMAc extraction	Water Uptake	
	% weight change	% at 25 °C	% at 90 °C
1D	-1.8	8.2	14
$1D_i$	-2.6	37	40
$1D_{ii}$	-2.8	28	30
$1D_{iii}$	-4.4	33	34
$1D_{iv}$	-1.1	29	33
$1D_v$	-3.4	8.4	14
$1D_{vi}$	-1.4	11	14

From Table 3.2 it was further noted that the covalent cross-linked membranes, $1D_v$ and $1D_{vi}$, showed smaller water uptakes (8-14%) in comparison to the ionic cross-linked $1D_{i-iv}$ membranes (28-40%), most likely due to the presence of the stronger covalent cross-links compared to the ionic crosslinks found in $1D_{i-iv}$. In contrast, the small weight increase noted for the ionic cross-linked SFS-F_6PBI membrane 1D could be associated with the close packing of polymer structures/chains during cross-linking (Figure 3.1) in contrast to the more bulky BrPAE-SFS ionic cross-link (see Figure 3.4), which could allow for better accessibility of the water molecules.

During the water uptake studies, only slight increases (1-6%) were observed between measurements at 25 °C and 90 °C, confirming the improvement of mechanical properties achieved through the cross-linking of polymer components when compared to the results presented in Chapter 2.
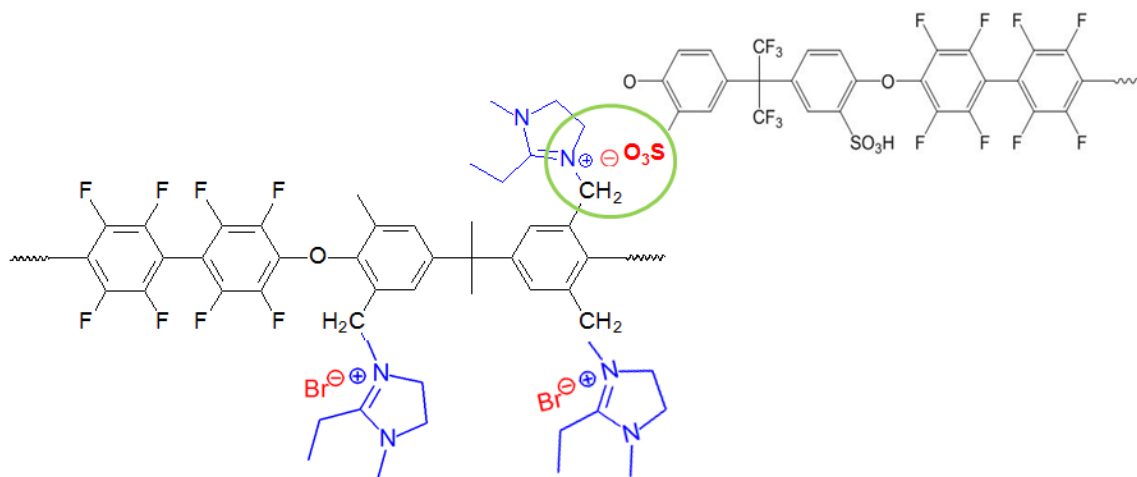
Figure 3.4: Ionic cross-linking between the quaternised BrPAE-1 and SFS.

3.3.2 H_2SO_4 stability

The possible improvement of the H_2SO_4 stability for the individual polymers (Chapter 2) through cross-linking was evaluated by comparing the % wt changes determined for the cross-linked membranes after H_2SO_4 treatment. Both the % wt changes and TGA-FTIR comparisons after H_2SO_4 treatment for the cross-linked membranes are shown in Table 3.3.

Table 3.3: % Weight and TGA-FTIR (T_{onset} and T_{SO2}) changes obtained for the cross-linked membranes due to H_2SO_4 treatment.

Membrane	Weight change (%)	T_{onset} [°C] Before	% Change After	T_{SO_2} [°C] Before	% Change After
1D	-3.40	391	8.8	398	8.00
1D$_i$	-35.9	357	6.80	378	-14.4
1D$_{ii}$	-40.4	372	5.60	379	-16.8
1D$_{iii}$	-32.3	368	-0.50	403	-16.8
1D$_{iv}$	-43.1	384	-3.10	378	-22.3
1D$_v$	-2.60	308	5.70	-	-
1D$_{vi}$	12.3	345	3.00	-	-

(-) = no peak detected for SO_2 association (below detection limit).

According to Chapter 2 (see Table 2.2), SFS only had a weight change of -13.6 %. This decreased to only -3.4 % after ionic cross-linking with F_6PBI (Table 3.3). This is in agreement with the outstanding chemical stability of only F_6PBI during H_2SO_4 treatment, as determined earlier (Chapter 2, Section 2.3.2). Furthermore, the partially fluorinated nature of both blend-forming polymers has been reported to contribute to blend compatibility and improved stability in the presence of the stronger C-F bonds with a higher binding energy [16, 17]. The improved compatibility also serves to limit the access of H_2SO_4 to the macromolecular chains and prohibits sulfonation and dissolution of polymer fragments as noted earlier for SFS (Table 2.2) [18].

From the data in Table 3.1 it is known that ionic cross-links are formed between SFS and BrPAE-1/2 in blends 1D$_i$-1D$_{iv}$ when having quaternised the -CH$_2$Br groups with imidazoles (EMIm or TMIm) (see Figure 3.2). With reference to Figure 3.4, it becomes evident that the membrane network formed by the sulfonated SFS and bromo-methylated polymer (BrPAE-1/2) is more bulky, which allows for better accessibility by the sulfuric acid to the polymer chains. Subsequently, sulfonation can occur (see Figure 2.7) with the accompanying dissolution of polymer fragments during the post-treatment of the materials (rinsing and drying). This accounts for the large weight losses observed (32-42%) for 1D$_{i-iv}$. It could be added that the non-fluorinated BrPAE-2 and SFS

(1D$_{ii}$ and 1D$_{iv}$) showed a higher % weight change, indicating a lower compatibility or more bulky orientation compared to both the partially fluorinated SFS and BrPAE-1 blend components (1D$_i$ and 1D$_{iii}$). Lastly, it should be noted that the respective imidazoles were added in excess during the synthesis of the cross-linked membranes and could account for some of the weight loss noted after treatment (washing from membrane).

It is also clear from Table 3.3 that the F$_6$PBI and BrPAE-1/2 containing membranes, 1D$_v$ and 1D$_{vi}$, had a smaller weight change (-2.6 to 12.3%) in comparison to the weight changes of the individual polymers (6.6 to 20.6 %) reported in Section 2.3.2 (Table 2.2). This is due to the covalent cross-linking with F$_6$PBI. Again, the improved compatibility of both partially fluorinated blend components in 1D$_v$ led to a smaller weight change (-2.6 %) than that of the non-fluorinated 1D$_{vi}$ (6.3 %) cross-linked with the partially fluorinated F$_6$PBI.

When discussing the TGA data, the results before acid treatment are discussed prior to discussing the effect of acid treatment. As can be seen from Figure 3.5, the thermal stability (TGA) of the individual polymer components SFS, BrPAE-1 and BrPAE-2 (solid colour lines) was significantly improved by the addition of the ionic cross-links (1D$_{i-iv}$) to the membrane network. The start of degradation, with corresponding residual weight %, for the respective polymers and cross-linked membranes is also reported in Figure 3.5. This was found to be in agreement with the increased T$_{onset}$ values summarised in Table 3.3 for the cross-linked membranes (1D$_{i-iv}$), which increased between 60 and 80 °C for the respective cross-linked membranes, 1D$_{i-iv}$ (see Chapter 2, Table 2.2).
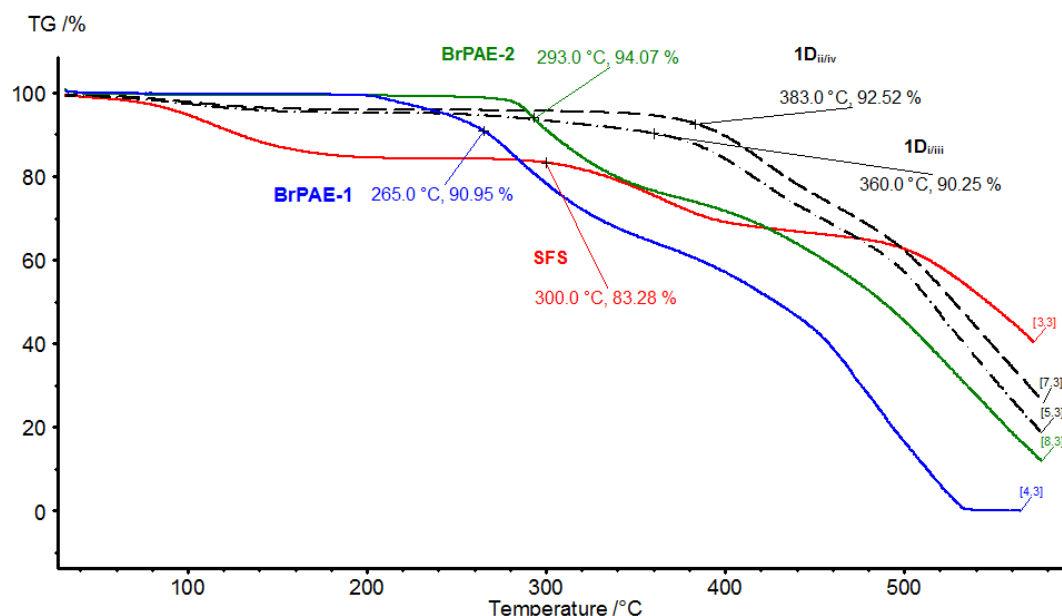
Figure 3.5: TGA curves recorded for the individual polymers SFS, BrPAE-1 and BrPAE-2, and ionic cross-linked membranes containing both SFS and BrPAE (1D$_{i-iv}$).

50

Similarly, the stable F_6PBI significantly increased the thermal stability of cross-linked membranes 1D, $1D_v$ and $1D_{vi}$ in the presence of SFS, BrPAE-1 or BrPAE-2, as is shown in Figure 3.6 for 1D and in Figure 3.7 for $1D_{v-vi}$. This is in agreement with the T_{onset} values (Table 3.3) that improved by 43 to 52 °C for the membranes $1D_v$ and $1D_{vi}$ containing BrPAE-1 and -2.
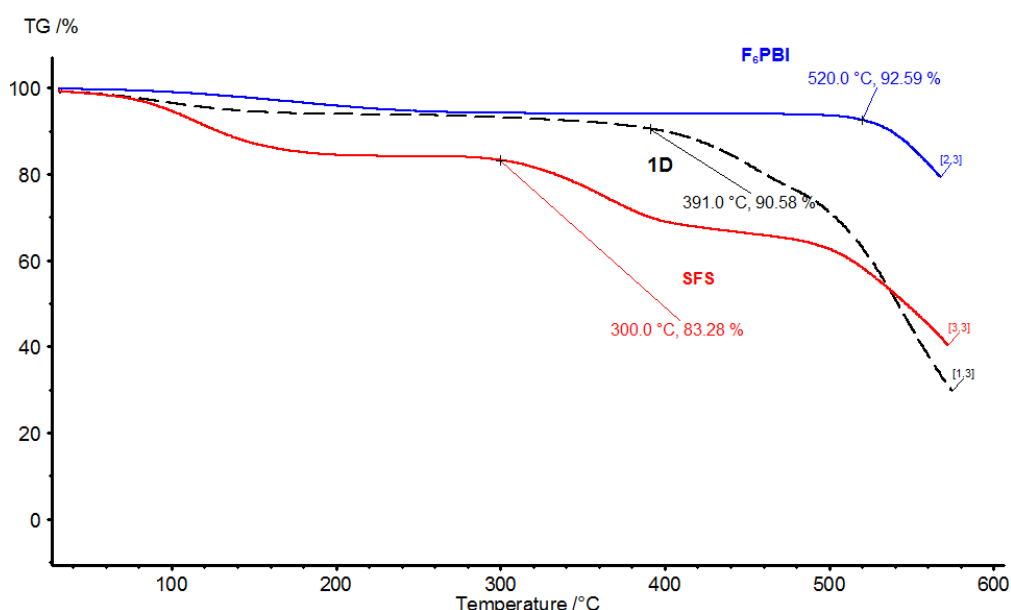
Figure 3.6: TGA curve of ionic cross-linked membrane 1D and blend components SFS and F_6PBI.
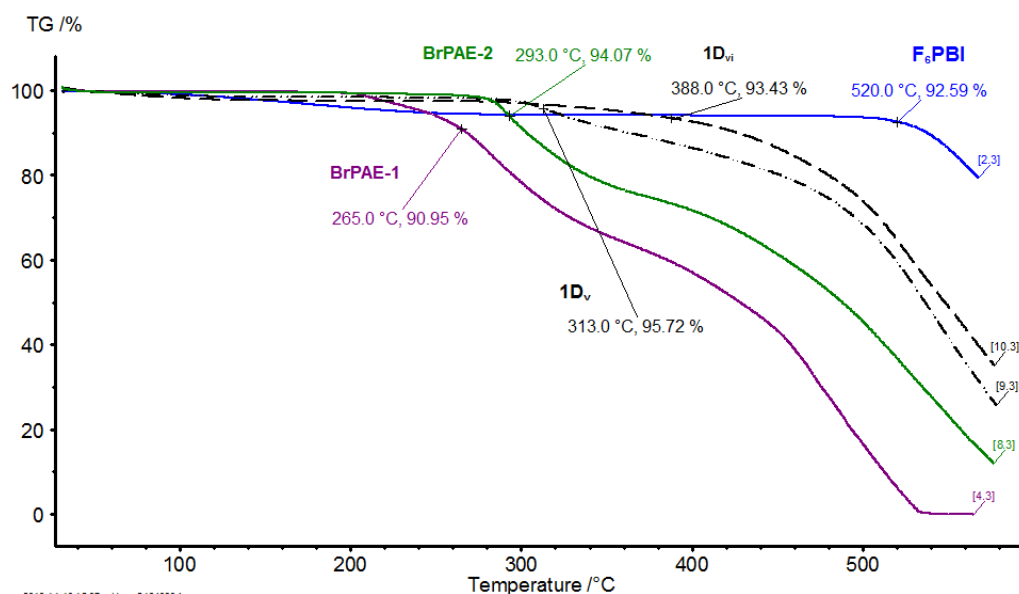
Figure 3.7: Covalently cross-linked membranes $1D_v$ and $1D_{vi}$ with polymer blend components F_6PBI and BrPAE-1/2.

51

After acid treatment, the % changes for the T_{onset} and T_{SO_2} values (Table 3.3) of the cross-linked membranes corresponded to the findings of the individual polymer behaviours after acid treatment, as discussed in the previous chapter (see Section 2.3.2 Table 2.2). The weight losses (32-43%) of cross-linked membranes $1D_{i-iv}$, associated with a decrease in T_{SO_2} values (14-22%) after treatment, correspond to the loss of low molecular fragments reported for SFS in Section 2.3.2. In the absence of these fragments (after treatment), the polymer backbone is found to be stabilised, which shows negligible changes (-3 to 6%) for the T_{onset}. It can be concluded that the F_6PBI-containing cross-linked membranes showed negligible changes (3-8.8%) after H_2SO_4 treatment in terms of the determined T_{onset} and T_{SO_2} values.

3.4 Conclusion

The investigated polymer combinations (1D and $1D_{i-vi}$) were successfully cross-linked to form homogeneous 2-component blend membranes when mixed in a 1:1 molar ratio. During subsequent stability characterisation, it was shown that the partially fluorinated BrPAE-1 combinations were slightly more favourable (smaller weight changes and water uptake) than the non-fluorinated BrPAE-2. However, while improved thermal stabilities (60-80 °C) for the cross-linked SFS and BrPAE-1/2 blends ($1D_{i-iv}$) were noted, the H_2SO_4 stability was still insufficient, with weight losses of up to 40 %. Since the results confirmed that the ionic and covalent F_6PBI-containing cross-linked membranes (1D, $1D_v$ and $1D_{vi}$) were more stable in H_2SO_4 than the only ionic cross-linked SFS and BrPAE-1/2 blends ($1D_{i-iv}$), it is proposed to combine the selected polymers from Chapter 2 and cross-link them using both ionic and covalent cross-linking to make novel 4-component PBI-blend membranes, which will hopefully have adequate chemical stability to be suitable for SO_2 electrolysis at elevated temperatures (>100 °C).

3.5 References

[1] Kerres JA. Design Concepts for Aromatic Ionomers and Ionomer Membranes to be Applied to Fuel Cells and Electrolysis. Polymer Reviews. 2015;55:273-306.

[2] Elias HG. Makromoleküle. Vol. 1, 5th Ed.; Hüthig and Wepf Basel,1990.

[3] Kerres JA. Blended and Cross-Linked Ionomer Membranes for Application in Membrane Fuel Cells. Fuel Cells. 2005;5:230-47.

[4] Kerres JA. Blended and Cross-Linked Ionimer Membrane for Appliction in Membrane Fuel Cells. Fuel Cells. 2005;2:230-47.

[5] Peighambardoust SJ, Rowshanzamir S, Amjadi M. Review of the proton exchange membranes for fuel cell applications. International Journal of Hydrogen Energy. 2010;35:9349-84.

[6] Costamagna P, Yang C, Bocarsly AB, Srinivasan S. Nafion® 115/zirconium phosphate composite membranes for operation of PEMFCs above 100 °C. Electrochimica Acta. 2002;47:1023-33.

[7] J.S. Yang, D. Aili, Q. Li, L.N. Cleemann, J.O. Jensen, Bjerrum NJ. Covalently cross-linked sulfone polybenzimidazole membranes with poly(vinylbenzyl chloride) for fuel cell applications. ChemSusChem. 2013;6:275-82.

[8] Peach R. Characterisation of proton exchange membranes in an H_2SO_4 environment. North-West University, Potchefstroom 2520, South Africa: North-West University, Potchefstroom campus; 2014.

[9] Peach R, Krieg HM, Krüger AJ, van der Westhuizen D, Bessarabov D, Kerres J. Comparison of ionically and ionical-covalently cross-linked polyaromatic membranes for SO_2 electrolysis. International Journal of Hydrogen Energy. 2014;39:28-40.

[10] Schoeman H, Krieg HM, Kruger AJ, Chromik A, Krajinovic K, Kerres J. H_2SO_4 stability of PBI-blend membranes for SO_2 electrolysis. International Journal of Hydrogen Energy. 2012;37:603-14.

[11] Schönberger F, Chromik A, Kerres J. Partially fluorinated poly(arylene ether)s: Investigation of the dependence of monomeric structures on polymerisability and degradation during sulfonation. Polymer. 2010;51:4299-313.

[12] Morandi CG, Peach R, Krieg HM, Kerres J. Novel morpholinium-functionalized anion-exchange PBI-polymer blends. Journal of Materials Chemistry A. 2015;3:1110-20.

[13] Morandi CG, Peach R, Krieg HM, Kerres J. Novel imidazolium-functionalized anion-exchange polymer PBI blend membranes. Journal of Membrane Science. 2015;476:256-63.

[14] Peach R, Krieg HM, Krüger AJ, Rossouw JJC, Bessarabov D, Kerres J. Novel cross-linked partially fluorinated and non-fluorinated polyaromatic PBI-containing blend membranes for SO_2 electrolysis. International Journal of Hydrogen Energy. 2016;41:11868-83.

[15] Kerres J, Atanasov V. Cross-linked PBI-based high-temperature membranes: Stability, conductivity and fuel cell performance. International Journal of Hydrogen Energy. 2015;40:14723-35.

[16] Banerjee S, Maier G, Burger M. Novel Poly(arylene ether)s with Pendent Trifluoromethyl Groups. Macromolecules. 1999;32:4279-89.

[17] Li Q, He R, Jensen JO, Bjerrum NJ. Approaches and Recent Development of Polymer Electrolyte Membranes for Fuel Cells Operating above 100 °C. Chemistry of Materials. 2003;15:4896-915.

[18] Chromik A, Kerres JA. Degradation studies on acid–base blends for both LT and intermediate T fuel cells. Solid State Ionics. 2013;252:140-51.

Chapter Overview

From the results of Chapter 3 it is clear that the simple acid-base interactions would have to be strengthened to increase the long-term chemical stability of PBI-blend membranes for SO_2 electrolysis at elevated temperatures (>100 °C). To attain this, both ionic and covalent cross-linking was investigated in this chapter using twelve different PBI-blended membranes. The components used included SFS as the acidic polymer, F_6PBI as the basic polymer (using acid-base ratios A, B and C), and variations of BrPAE-1/2 (anion exchange group) and TMIm/EMIm. The suitability of these membranes for SO_2 application was determined using stability studies and conductivity measurements. The stability was determined in terms of i) the H_2SO_4 stability (80 wt% H_2SO_4 at 100 °C for 120 hours), (ii) the oxidative stability (Fenton's test, FT) and (iii) the organic solvent stability (extraction in DMAc). Membranes were characterised in terms of the percentage weight changes, the ion exchange capacities (IEC) and the thermal stabilities (TGA-FTIR) before and after the various treatments. Furthermore, proton conductivity measurements were performed as a measure of their suitability of the membranes for SO_2 electrolysis. Although all blended membrane types were sufficiently stable in the H_2SO_4 stability tests, the blends containing partially fluorinated blend components ($1A_i$, $1B_i$ and $1C_i$) showed improved stability as well as conductivity. It was shown that the sulfonation of BrPAE-1 discussed in Chapter 2 actually improved the proton conductivity and thermal stability within the blend without sacrificing membrane stability. Accordingly, membranes $1A_i$, $1B_i$ and $1C_i$ were selected for the SO_2 electrolyser studies at 80, 95 (Chapter 5) and 120 °C (Chapter 6).

4.1 Introduction

The improvement of more environmentally friendly and sustainable energy systems such as the production of hydrogen and its conversion to electrical energy has become a priority in recent literature [1, 2].Specific attention has been given to the operation of electrolysers and fuel cells (FC) at elevated temperatures (above 100 °C) for improved electrode reaction kinetics, higher tolerances for impurities such as carbon monoxide (CO), and reduced costs with the opportunity of decreasing platinum (Pt) catalyst loadings or even using non-platinum catalysts [3-5].

For both fuel cells and electrolysers, the proton exchange membrane (PEM) is an important component and crucial for efficient operation. However, further research is needed to improve the chemical, mechanical and thermal stability when working at temperatures above 100 °C. Whilst maintaining high proton conductivity, the membrane is required to act as barrier, prohibiting or at least limiting the crossover and subsequent mixing of reactant gases that result in accelerated catalyst degradation.

At temperatures above 100 °C, commercial membranes such as Nafion®, which are based on perfluorinated sulfonic acid (PFSA) , become less suitable due to the dehydration of the membranes due to both the temperatures and the sulfuric acid produced during SO_2 electrolysis [6, 7]. This dehydration results in an increase in membrane resistance, ultimately decreasing the performance [8, 9]. Recently other membrane types such as those based on sulfonated polybenzimidazole (s-PBI) have been shown to be less influenced by the limited water supply at elevated temperatures, while remaining stable in the presence of the sulfuric acid produced during SO_2 electrolysis [8, 10]. In addition, these PBI-based membranes are promising due to their excellent thermal stability and good ionic conductivity reported when applied as PEMs at elevated temperatures [11-14]. The development of PBI-based membranes has included strategies to maintain the intrinsic stability with sufficient ion conductivities while preventing acid leaching and polymer dissolution during operation [15-17]. The cross-linking of various functionalised aromatic polyether backbone polymers with both acidic and pyridine moieties have been considered to increase the conductivity and stability within the membrane matrix [4, 18]. Kerres et al. have shown in previous studies that ionic cross-linking of the basic PBI polymer with suitable acidic polymers, such as sulfonated arylene main-chain ionomers, can provide intermolecular interactions resulting in membranes with increased chemical stability without sacrificing ion conductivity [19, 20].

It was shown in Chapter 3 that the simple acid-base interactions present in the polymers used in this study would have to be strengthened to increase the chemical stability of such membranes, specifically when operating in an H_2SO_4 environment at elevated temperatures (>100 °C). It was therefore proposed to combine ionic and covalent cross-linking through the mixing of acid-base (SFS-F_6PBI) blends with BrPAE-1/2 and imidazole-based (EMIm/TMIm-based) groups.

In recent studies, this type of cross-linking was successfully applied to anion exchange membranes (AEMs), and included the addition of a halo-methylated aromatic component and imidazole, as quaternisation agent, in the presence of PBI as basic polymer and a sulfonated polymer as acidic polymer [21, 22]. This allowed for the incorporation of both covalent and ionic cross-links within the polymer network and yielded a macroscopically homogeneous and mechanically and chemically stable AEM. As depicted in Figure 4.1, the interactions in the formed blend membranes included the entanglement of a sulfonated polymer (brown) in a matrix of the PBI polymer (purple) being ionic cross-linked with the bromo-methylated polymer (black), which in turn was again covalently cross-linked with the PBI polymer (purple). The addition of the imidazole (blue) leads to the quaternisation of the bromo-methylated polymer and the subsequent formation of ionic cross-links with the sulfonated polymer within the matrix [21].
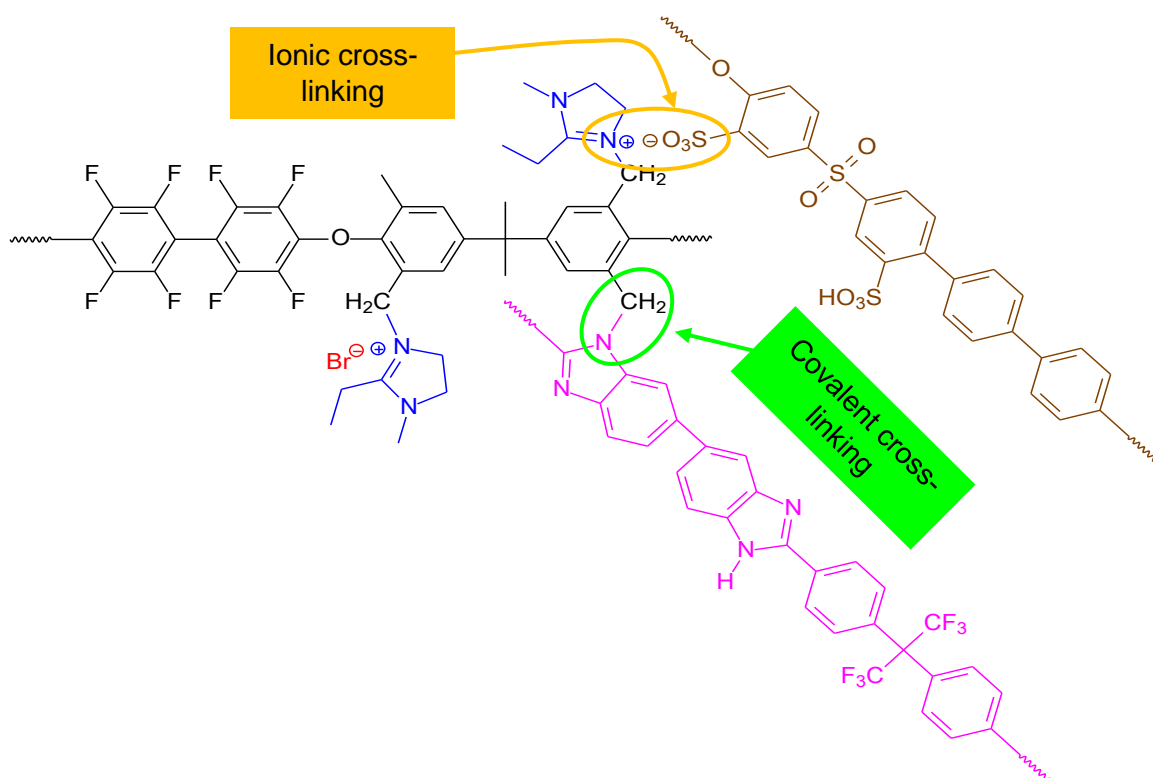
Figure 4.1: Schematic of the ionic-covalently cross-linking concept for the blend membranes (black – BrPAE, purple – F$_6$PBI, blue – EMIm, and brown - sPPSU).

In this chapter, the described acid-base blend concept was used to prepare cation exchange membranes by mixing the sulfonated arylene main-chain polymer (SFS) with F$_6$PBI at specific ratios (see Chapter 1: Table 1.2 and Figure 4.2) with a bromo-methylated arylene polymer (partially fluorinated BrPAE-1 and non-fluorinated BrPAE-2). To these combinations, either 1-ethyl-2-

methylimidazole (EMIm) or 1,2,4,5-tetramethyl-imidazole (TMIm) was added to quaternise the bromo-methyl groups.

In addition to evaluating the novel cross-linking of the acid-base PBI-containing blend membranes, the influence of the specifically partially fluorinated components on the stability of the blend membranes within an H_2SO_4 environment was investigated as it was reported previously that such partially fluorinated polymers can result in higher proton-conductivities and durabilities [23, 24], which was ascribed to the differences in bond strength energies between the C-F and C-H bonds [25-27]. However, for SO_2 electrolysis, it still needs to be determined whether the best membrane properties and compatibilities are obtained when partially fluorinated and non-fluorinated polymer components are blended, or when partially fluorinated and non-fluorinated polymers are combined. In accordance, the compatibility between a partially fluorinated and a non-fluorinated bromo-methylated polymer (BrPAE 1 and 2) and 2 different alkylated imidazoles (1-EMIm and 2-TMIm) with the partially fluorinated sulfonated arylene main-chain polymer (SFS) and fluorinated PBI (F_6PBI) was evaluated in Chapter 4 (see Table 1.1 (Chapter 1) for the structure of the various polymers).

In addition to varying the types of BrPAE and imidazoles, the ratios of the polymer components were varied such that either SFS, F_6PBI or BrPAE was the dominant polymer component yielding membranes A, B or C, respectively (see Figure 4.2). With the four variations possible when adding the two BrPAE and two imidazole components, 12 different blend membranes were obtained and evaluated.
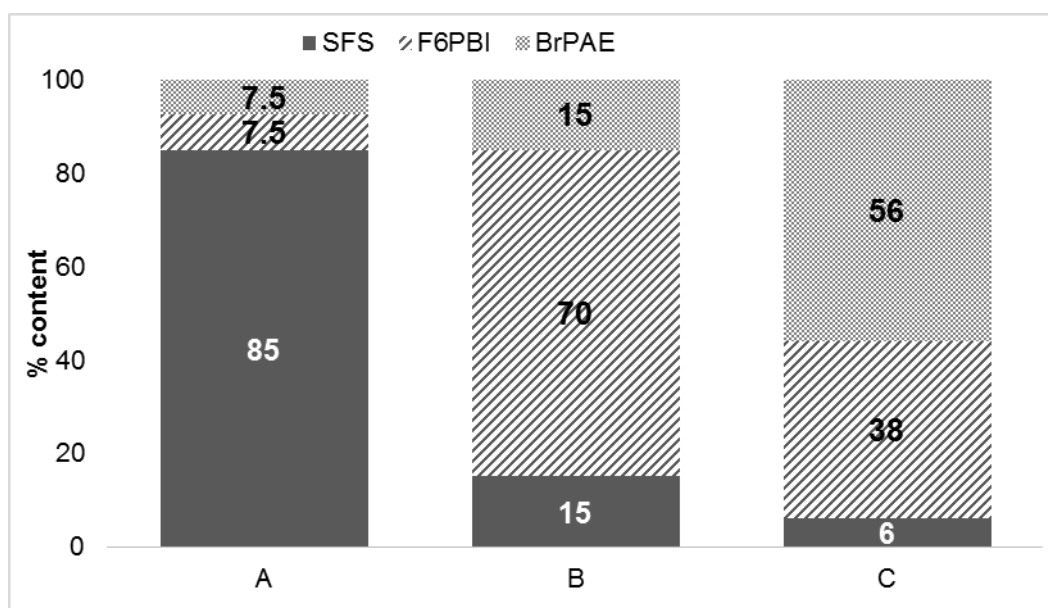

Figure 4.2: Variation of the polymer ratios of the blend membranes A, B and C.

The stability of these membranes was determined in terms of their H_2SO_4, oxidative and organic solvent stability using (i) an H_2SO_4 treatment, (ii) the Fenton's Test and (iii) an extraction with the organic solvent N,N-dimethylacetamide (DMAc). The characterisation of the blend membranes (before and after treatment) included monitoring of weight changes, ion exchange capacity (IEC) and thermogravimetric analysis (TGA). These results were used to compare the membranes similarly to what was done for the polymers discussed in Chapter 2 and 3 [28, 29]. Lastly, the proton conductivity was measured for the blend membranes. Nafion® 212 was included as reference material for the both stability assessment and the conductivity measurements.

4.2 Experimental

4.2.1 Materials

Chemicals were used as received from the manufacturers. N,N-Dimethylacetamide (DMAc, 99.5% purity) was obtained from Sigma Aldrich, while the polymer material F_6PBI was obtained from YANJIN Technology. The sulfonated polymer, SFS, and bromo-methylated polymers (BrPAE 1 and 2) were synthesised in-house as described in Chapter 3 and earlier works [21, 27, 30]. The alkylated imidazoles 2-ethyl,1-methyl-imidazole (EMIm) and 1,2,4,5-tetramethylamine (TMIm) were purchased from Ionic Liquids Technologies GmbH and TCI, respectively. The H_2SO_4 (98 wt. %), H_2O_2, methanol (CH_3OH) and $(NH_4)_2Fe(SO_4)_2.6H_2O$ that were used for the stability treatments, were obtained from Sigma Aldrich. For the IEC titrations, NaOH (ACE, SA) and HCl (0.1 M, Titrosol®) solutions were prepared using Bromothymol blue as indicator (Merck, SA).

4.2.2 Membrane preparation and post-treatment

As can be seen from Figure 4.2, three combinations of ratios for SFS:F_6PBI:BrPAE were chosen with excess of SFS, F_6PBI and BrPAE for membrane series A (SFS:F6PBI:BrPAE = 11.3:1:1), B (1:4.7:1) and C (9.3:1.5:1), respectively. In addition (see Table 1.1) two types or BrPAEs and imidazoles were included for each ratio of SFS:F_6PBI:BrPAE, resulting in four possible combinations, which were named i (BrPAE-1 + EMIm), ii (BrPAE-2 + EMIm), iii (BrPAE-1 + TMIm) and iv (BrPAE-2 + TMIm). This resulted in a total of 12 blend membranes, i.e. $1A_{i-iv}$, $1B_{i-iv}$ and $1C_{i-iv}$, that were manufactured and characterised.

The three polymers (SFS, F_6PBI and BrPAE) were dissolved in DMAc to obtain solutions of 10 wt% (SFS and BrPAE) and 5 wt% (F_6PBI), respectively. After dissolving the various polymers in DMAc, they were blended in specific ratios with the addition of the imidazoles to yield the 12 different blended membranes (see Table 1.2). The SFS polymeric solution was first neutralised with n-propylamine before mixing with the basic polymers to prevent precipitation of the poly-electrolyte complex, as discussed previously [20, 28, 31]. In each case the imidazole was added

last and in all membranes in a fourfold molar excess in terms of the -CH_2Br groups (BrPAE) to ensure adequate quarternisation and complete formation of the anion-exchange groups [22, 29].

The polymer mixtures were mixed until homogeneous and cast onto glass plates before cross-linking has set in. Extra care was taken with the higher anion exchange group content membranes (type C, BrPAE and imidazole) and more viscous polymeric solutions (type B) where quicker gellification of polymeric solutions (cross-linking already taking place at room temperature) occurred in comparison to type A membranes. This resulted in shorter handling times allowed for final blending/mixing of polymer solutions for B and C before casting of the blend membranes. Immediately after casting, the plates were placed in convection ovens at 80 °C for 2 hours before increasing the temperature to 130 °C for 6 hours to ensure a gradual and adequate evaporation of the solvent. After cooling the membranes to room temperature, they were immersed in water and removed after detaching from the glass surface (1-3 h).

The blended membranes were then post-treated by submersion in a 10% HCl solution at 90 °C for 48 h, followed by a H_2O post-treatment at 60 °C for another 48 h. The membrane materials were subsequently stored in plastic bags. Membrane samples intended for characterisation studies were dried overnight at 80 °C and weighed (Section 4.2.4).

4.2.3 Stability assessment of blended membranes

The H_2SO_4-, oxidative- and organic solvent stabilities were determined using (i) an H_2SO_4 treatment, (ii) the Fenton's Test and (iii) an extraction with the organic solvent DMAc. To determine the changes within these membranes during treatment, the membranes were characterised using weight changes, ion exchange capacities and TGA-FTIR measurements before and after the treatments (see Section 4.2.4).

4.2.3.1 H_2SO_4 treatment

The dried membrane samples were submerged in an 80 wt% H_2SO_4 solution for 5 days at 100 °C, which is higher than the temperatures used in earlier studies where membranes were treated at 80 °C [28, 29, 31]. This was based on the required higher temperature stability (see Chapter 6). After the acid treatment, the membranes were rinsed repeatedly with deionised water (approximately 3 hours at 60 °C) and dried as described in the general post-treatment discussion (Section 4.2.2) before any further characterisation was done [28].

4.2.3.2 Oxidative stability (Fenton's Test)

Dried samples (app. 100 mg) were placed in Fenton's Reagent (FR = 3 wt % aq H_2O_2 with 4 ppm Fe^{2+} salt) at 68 °C for 144 h. The FR was freshly prepared and replaced every 24 h as described in [32]. Afterwards membranes were washed thoroughly with water and dried. The residual weight of the membrane samples was determined and expressed as % weight change.

4.2.3.3 Solvent extraction stability with DMAc

The degree of cross-linking for the different blended membranes was evaluated by means of DMAc extraction (weight loss).The dry weight of the membrane samples was determined before the membranes were placed in DMAc for 96 h (4 days) at 90 °C. Thereafter, the membrane samples were thoroughly washed with methanol and dried at 80 °C overnight to determine the residual weight of the membrane fractions, which was expressed as a % weight (loss) change [32].

4.2.4 Membrane characterisation

It should be noted that the characterisation techniques (4.2.4.1-4.2.4.3) were used in support of each other, providing an evaluation of the different PBI-blend membranes in terms of their $H_2SO_4^-$, oxidative- and organic solvent stability.

4.2.4.1 Weight changes

Dried weight changes were determined for each membrane sample before and after treatment on an Adams balance (PW analytical grade 0.0001 g). The weight changes were reported as a % of the dry weight before treatment.

4.2.4.2 Ion exchange capacity (IEC)

The IEC provides an indication of the number of ion-exchange groups present per weight unit of dry membrane, which for monovalent ions is usually presented in meq/g or mmol/g. [25]. The IECs of the blend membranes were calculated using the following formula [33]:

$$IEC = 1000*(N_{group}/M_{polymer}) \qquad (meq/g) \qquad\qquad [4\text{-}1]$$

with N_{group} equivalent number of functional groups (eq/mol) and $M_{polymer}$ as molecular mass (g/mol) of polymer. For the acid-base blend membranes, all the basic groups (basic polymer) are assumed to be protonised by the protons from the SO_3H groups (acidic polymer), which then form the ionic cross-links:

$$IEC_{membrane} = ((m_{acid} \times IEC_{acid}) - (m_{base} \times IEC_{base}))/(m_{acid} + m_{base}) \quad (meq/g) \qquad [4\text{-}2]$$

with $m_{acid/base}$ the mass of the acidic/basic polymer (g), $IEC_{acid/base}$ the ion-exchange capacity of the acidic/basic polymer, and $IEC_{membrane}$ the ion-exchange capacity of the membrane.

Experimentally the IEC was determined through acid-base titrations [25, 34], providing both direct and total IEC values as was previously reported [28]. To attain this, the membrane samples were stirred in a saturated NaCl solution for 24 h before being titrated with 0.1 M NaOH from which the H$^+$ ions (acid) released and hence the direct IEC was determined. Thereafter, a back titration with 0.1 M HCl was done to determine the total IEC through the consumption of NaOH. The IEC values were calculated using the following equations:

$$IEC_{direct} = V*0.1/m \qquad\qquad\qquad [4-3]$$

$$IEC_{total} = (V+R)*0.1/m \qquad\qquad\qquad [4-4]$$

where V is the volume of titration solution used (L), R is the additional volume not needed by back titration (L), taking into account a 3 ml NaOH excess, m is the weight of the membrane (g) and 0.1 represents the molarity of the solution (mol/L).

4.2.4.3 Thermogravimetry-FTIR

Thermogravimetric analysis (TGA) with the Netzsch model STA 449C was used to evaluate the thermal stability of the blend membranes with a heating rate of 20 °C/min under an oxygen enriched atmosphere (65-70 % O_2, 35-30 % N_2). Coupling with FTIR (Fourier-Transform-Infrared spectroscopy) allowed for analysis of the released gaseous products from the TGA with the FTIR spectrometer (Nicolet Nexus). The onset splitting-off of functional groups (e.g. –SO_3H as S-O stretch vibration at 13520-1380 cm^{-1} and C-O stretch vibration around 2200 cm^{-1}) was determined as described in [28, 35].

4.2.4.4 Conductivity in SO_2 electrolyser operation environment

Ion-conductivity through-plane measurements of the blended membranes were conducted using a Membrane Test System (MTS 740) from Scribner Associates Inc., USA. Measurement conditions were chosen to resemble operation in the SO_2 electrolyser by reporting data in the temperature range of 60 to 130 °C with restricted relative humidity (RH= 50 %). Before measurements, the membrane samples were doped in a 1 M H_2SO_4 solution for 24 hrs. at 80 °C where the doping was reported as a weight % increase. A Nequist plot was recorded and the ohmic resistance, derived from the high-frequency intercept of the complex impedance with the real axis, was obtained. The conductivity was calculated using Eq. [4-5].

$$\sigma = \frac{1}{Rsp} = \frac{d}{RA}$$

[4-5]

With σ the conductivity (mS/cm); R_{sp} the resistivity (Ω cm), d the thickness of the membrane (cm), R the ohmic resistance (Ω) and A the electrode dimensions (cm^2).

4.3 Results and discussions

Firstly, the three treatments (H_2SO_4 stability, FT and DMAc extraction) used to determine the stability are discussed separately (Section 4.3.1-4.3.3) in terms of the weight changes, IEC and TGA-FTIR results of the blend membranes (where possible - some materials dissolved completely). After having discussed the influence of the three treatments, the conductivity results (Section 4.3.4) are used to support the selection of blend membranes to be used for the SO_2 electrolysis presented in Chapters 5 and 6.

Weight changes provide a simple method to evaluate the stability of blend membranes, either by degradation and dissolution (weight loss), or sulfonation and salt formation (weight gain). For comparative purposes, the % weight changes for all three treatments are summarised in Table 4.1. In the following subsections, these trends in weight changes were further clarified by IEC and TGA-FTIR analysis where possible.

Table 4.1: Weight changes of the blend membranes after the stability treatments.

Membrane	Weight changes (%)		
	H_2SO_4 treatment	FT	DMAc extraction
$1A_i$	1.88	diss.*	-63.4
$1A_{ii}$	7.34	diss.*	-64.2
$1A_{iii}$	2.16	diss.*	-63.6
$1A_{iv}$	8.05	diss.*	-63.5
$1B_i$	-1.12	-4.10	-9.66
$1B_{ii}$	0.12	-4.45	-17.9
$1B_{iii}$	-1.15	-5.37	-2.29
$1B_{iv}$	-0.83	-6.66	-24.6
$1C_i$	-10.2	-96.7	-15.0
$1C_{ii}$	-10.2	-90.7	-11.9
$1C_{iii}$	-2.85	-85.5	-8.44
$1C_{iv}$	-5.28	-76.6	-7.04

diss.* = Dissolved after 48 hours in FT.

4.3.1 H_2SO_4 stability

This section discusses the weight changes due to the H_2SO_4 treatment (Section 4.3.1.1; see also Table 4.1), followed by changes in the IEC (Section 4.3.1.2) and TGA-FTIR (Section 4.3.1.3) data. The experimental error for the H_2SO_4 stability determinations was below 10 % as has been shown in previous studies within our research group [28].

4.3.1.1 Weight changes

The weight losses reported for similar blended membranes due to H_2SO_4 treatment, determined in past studies, were ascribed to the loss of low molecular fractions (oligomers) of the sulfonated SFS polymer [26, 28, 36]. For this discussion, the sulfuric acid stability of the separate polymer components described in Chapter 2 was included in an attempt to link the weight change behaviour for the blended membranes to the individual polymer components. According to Chapter 2, weight losses of 13.6 % were reported for pure SFS due to the loss of oligomers compared to the negligible loss of 0.4 % for F_6PBI. Simultaneously, respective weight increases of 20.6 and 6.6

% were reported for the partially fluorinated and non-fluorinated BrPAE, due to sulfonation (supported by TGA-FTIR data shown in Section 4.3.1.3). It could be speculated that the more hydrophobic BrPAE-1 (partially fluorinated) has a more separated nanomorphology than the BrPAE-2 (non-fluorinated), which leads to a better accessibility of the more hydrophilic moieties of BrPAE-1 to the sulfuric acid, resulting in the higher sulfonation obtained at 100 °C.

When comparing the H_2SO_4 stability of the individual polymers presented in Section 2.3.2, the weight changes were smaller for the blend membranes (Table 4.1) showing increased stabilities, which can be ascribed to the additional cross-linking between the polymer components. It was found in earlier studies that weight changes of ±10 % were acceptable for H_2SO_4 stability [37]. It can be noted that the weight of blend membranes A (SFS-excess) increased slightly more than the weight increase of blend membranes C (BrPAE-excess), although both were within the mentioned 10 % range. The blend membranes B reported the least change (±1.2 %), confirming the stability of the F_6PBI polymer shown previously (Section 2.3.2). The decrease in weight noted for blend C can possibly be ascribed to slight sulfonation of the BrPAE polymer and subsequent splitting-off of cross-links leading to the dissolution and washing-out of polymer fragments after H_2SO_4 treatment.

Higher stability due to the improved compatibility of polymer components in specifically blend membranes $1A_i$ and $1A_{iii}$ was as expected for the fluorinated compared to the non-fluorinated polymer-containing blends, $1A_{ii}$ and $1A_{iv}$ which had a 7-8 % change in weight. Furthermore, the influence of the added imidazole only became evident in blend C with a higher BrPAE content (Figure 4.2). The mass of the blend membranes $1C_{iii}$ and $1C_{iv}$, containing the more sterically hindered amine TMIm, decreased less (2.8-5.3 %) in comparison to the EMIm-containing blend membranes ($1C_i$ and $1C_{ii}$), which decreased by 10 %.

4.3.1.2 IEC changes

The determined IEC_{total} provides information on all the available $-SO_3H$ groups and quaternised imidazolium groups contributing to the conductivity of the blend membrane, while the IEC_{direct} represents only those $-SO_3H$ groups in the ionically cross-linked membranes where the protons are able to contribute to the proton conductivity [25].

InTable 4.2, the IEC results are presented, showing the calculated IEC values (eq. 4-2, for untreated blend membranes only), the IEC_{direct} and IEC_{total} for the 12 untreated membranes, as well as the subsequent changes in the IEC_{direct} and IEC_{total} after the H_2SO_4 treatment. As can be seen, the higher BrPAE content and fourfold addition of imidazole-1 or -2 of blend C (see Figure 4.2 for ratios) generally had higher initial IEC_{total} values due to the available quaternary imidazolium groups not occupied by ionic cross-links with a minor amount of SFS added in comparison to blend A membranes (SFS-excess). No IEC measurements were measurable for the blend B membranes (F_6PBI-excess) as the sulfonic acid ($-SO_3H$) groups of the SFS polymer component are bound to

F_6PBI through acid-base bonds, resulting in negligible amounts of free $-SO_3H$ groups [37] leading to IEC values that were too low to measure (marked X in Table 4.2). These included IEC_{Direct} values for blend membranes C due to the low SFS content (6 %) of blend C membranes and restrictedly available $-SO_3H$ groups (not-cross-linked) for ion-exchange.

Table 4.2: IEC measurements before, and % changes reported after H_2SO_4 treatment for the blend membranes.

Membrane	IEC Before			IEC After	
	IEC_{Calc} [mmol/g]	IEC_{Direct} [mmol/g]	IEC_{Total} [mmol/g]	IEC_{Direct} % Change	IEC_{Total} % Change
$1A_i$	1.48	1.48	1.68	5.78	5.62
$1A_{ii}$	1.53	1.46	1.72	6.53	1.46
$1A_{iii}$	1.48	1.44	1.64	3.79	4.70
$1A_{iv}$	1.52	1.48	1.73	-1.03	-0.97
$1B_i$	X	X	X	X	X
$1B_{ii}$	X	X	X	X	X
$1B_{iii}$	X	X	X	X	X
$1B_{iv}$	X	X	X	X	X
$1C_i$	2.43	X	2.34	X	-3.75
$1C_{ii}$	2.12	X	2.15	X	-2.25
$1C_{iii}$	2.37	X	2.17	X	-8.39
$1C_{iv}$	2.09	X	2.14	X	2.46

X = IEC values that were too low to measure.

It can be seen for the blend membranes A that the calculated IEC_{Calc} and experimental ICE_{Direct} values were close to one another (variations of -1 to 6 %) after acid treatment, which was in accordance with the minimal weight changes observed. This includes the deviation in behaviour of blend membranes $1A_{iv}$ and $1C_{iv}$, considered minor and likely due to handling (washing and drying)

of materials after treatment. It is known that increases in IEC values can be attributed to the splitting-off of ionic cross-links and/or formation of imidazolium hydrogen sulfate groups within the PBI portion due to sulfonation of polymer components [28]. The same could be observed for corresponding weight and IEC decreases of blend C membranes associated with dissolution of polymer fragments from the membrane network after H_2SO_4 treatment.

4.3.1.3 TGA-FTIR changes

TGA was used to evaluate the chemical stability of the blend membranes with regards to the thermal stability before and after acid treatment, while the coupling with FTIR was used to identify the starting points of the degradation of the polymer backbone (T_{onset}) and the splitting-off of -SO_3H groups (T_{SO_2}). The T_{onset} and T_{SO_2} values determined for the blend membranes before and after acid treatment are summarised in Table 4.3. TGA-curves for the blend membranes before and after acid treatment are presented in Appendix B (Figures B-1 to B-12).

Table 4.3: T_{onset} and T_{SO_2} of blend membranes before and after H_2SO_4 treatment.

Membrane	T_{onset} [°C]		T_{SO_2} [°C]	
	Before	After	Before	After
$1A_i$	330	345	289	277
$1A_{ii}$	344	340	284	281
$1A_{iii}$	333	337	277	277
$1A_{iv}$	342	337	289	286
$1B_i$	351	355	425	423
$1B_{ii}$	353	383	418	430
$1B_{iii}$	357	364	433	420
$1B_{iv}$	353	373	418	418
$1C_i$	320	314	-	358
$1C_{ii}$	344	314	-	383
$1C_{iii}$	310	314	-	376
$1C_{iv}$	316	352	-	378

T_{onset} = onset temperature of polymer backbone degradation, T_{SO_2} = onset temperature of -SO_3H groups splitting off. (-) = no peak detected for SO_2 association (below detection limit).

The TGA-curves reported for the individual polymer components and their TGA behaviour due to the H_2SO_4 treatment discussed in Chapter 2 will be used to help explain the TGA data obtained with the different blend membranes A, B and C. From Section 2.3.2 (see Table 2.2), it is clear that F_6PBI had outstanding thermal stability with a T_{onset} of 520 °C compared to the T_{SO_2} and T_{onset} of 384 and 417 °C, respectively, reported for SFS. BrPAE-1 (partially fluorinated with an ether linkage) had a T_{onset} of 265 °C, which was lower than the 29 °C noted for BrPAE-2 with the addition of a T_{SO_2} at 355 °C associated with the polyethersulfone present in the polymer backbone. As reported in Chapter 2, the suspected higher degree of sulfonation for BrPAE-1 (% weight increase) was supported by the TGA curve measured after acid treatment (Figure 2.8). A prominent SO_2 band was identified and associated with the weight loss at 322 °C, stabilising the polymer backbone and reporting an increased T_{onset} of 314 °C compared to the 265 °C before acid treatment.

It was therefore expected that the blend membranes B (as shown in Figure 2.8) should be thermally most stable as was confirmed in Table 4.3 in terms of the T_{onset} values which only started at 351 °C, compared to the 330 °C of blend membranes A (SFS-excess) and 310 °C of blend membranes C (BrPAE-excess). The higher T_{SO_2} reported (Table 4.3) for blend membranes B (418-433 °C) in comparison to A (277-289 °C) further demonstrates the stabilising effect (increased degradation temperatures noted) of F_6PBI in base-excess blends B due to shielding of SO_3H groups (SFS) in the blend through cross-linking.
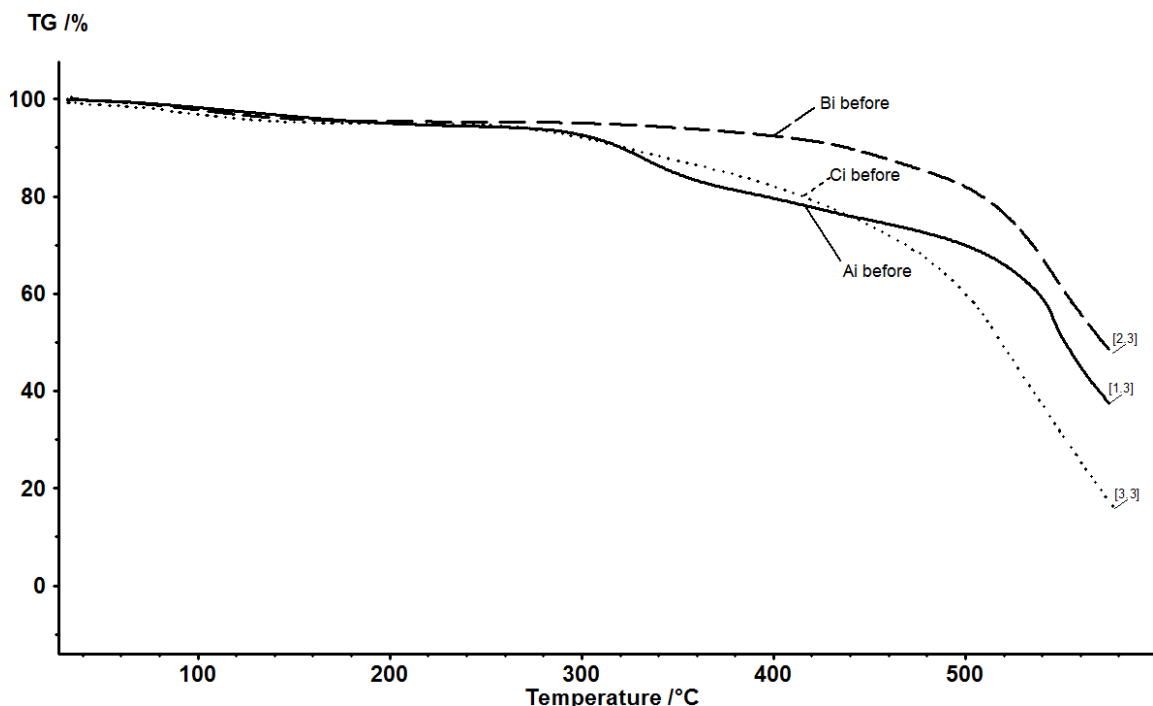

Figure 4.3: TGA curves recorded for blends 1A$_i$, 1B$_i$ and 1C$_i$ before treatments.

The average differences between the onset temperatures before and after H_2SO_4 treatment ranged between 3 and 10 °C, confirming considerable stability, being sufficient for applications up to 200 °C. The slight increases observed for the T_{onset} and T_{SO_2} after H_2SO_4 treatment for membranes $1A_i$ and $1C_{iv}$ could be ascribed to some sulfonation of polymer components and onset temperature decreases due to the splitting-off and dissolution of polymer fragments as discussed earlier for the weight and IEC changes (Sections 4.3.1.1 & 4.3.1.2).

It can be concluded that the H_2SO_4 stability of all the blend membranes investigated was satisfactory in view of the minimal weight, IEC and TGA changes reported after treatment. Before any further distinction on the suitability of the blend membranes and their possible selection for SO_2 electrolysis, the oxidative organic stability results in conjunction with the conductivity results should be considered.

4.3.2 Oxidative stability (FT)

The Fenton's test was used to evaluate the oxidative stability of the blended membranes. Weight loss data (Table 4.1, third column) and TGA-FTIR (Table 4.4) measurements were used as post-characterisation methods to compare blend membranes A, B and C. IEC measurements were not included due to the high dissolution observed for blend membranes A and C (Table 4.1) and the negligible amounts of free $-SO_3H$ groups present and measurable in blend membranes B (Section 4.3.1.2).

In Table 4.1 it can be seen that blend membranes A completely dissolved after only 48 hours in the FT due to the larger SFS content in contrast to the electron deficient F_6PBI-excess blend membranes B, where weight losses of only 4-7 % were observed. This is in agreement with studies on similar blend membranes where it was found that a too great electron-deficiency in aromatic structures, as found in the partially fluorinated SFS-excess blend membranes A, can facilitate an attack of nucleophiles [27, 32]. This was also seen for blend membranes C, where weight losses ranged between 76 and 96.7 %. The non-fluorinated BrPAE-excess blend membrane $1C_{iv}$ proved most stable due to the more alkylated imidazole, TMIm, offering better resistance against radical degradation (see also its H_2SO_4 stability, Section 4.3.1.1).

For the TGA-curves recorded after FT (see Appendix B (Figures B-1 to B-12) and Table 4.4), the greater weight losses reported specifically for $1C_i$ (Table 4.4) were in agreement with the increased loss of polymer fragments i.t.o. the higher T_{onset} reported after FT. $1C_{ii-iv}$, on the other hand, showed decreases in their T_{onset} values that could be associated with the loss of polymer fragments and the weight losses reported. Note that no T_{SO_2} values were reported for blend membranes C (marked – within table) as the $-SO_3H$ groups associated with the SFS polymer in these blends were only present in small quantities (Figure 4.1). Only negligible changes (2-14 °C) for T_{onset} and T_{SO_2} values after FT were noted for blend membranes B due to the excess of the F_6PBI polymer.

This emphasises and confirms the expected contribution of the F_6PBI polymer towards the stability of the blended membranes against radical attack [20, 32].

Table 4.4: T_{onset} and T_{SO_2} of blend membranes before and after FT treatment.

Membrane	T_{onset} [°C]		T_{SO_2} [°C]	
	Before	After	Before	After
$1A_i$	330	diss.*	289	diss.*
$1A_{ii}$	344	diss.*	284	diss.*
$1A_{iii}$	333	diss.*	277	diss.*
$1A_{iv}$	342	diss.*	289	diss.*
$1B_i$	351	348	425	425
$1B_{ii}$	353	367	418	425
$1B_{iii}$	357	359	433	430
$1B_{iv}$	353	361	418	421
$1C_i$	320	390	-	-
$1C_{ii}$	344	305	-	-
$1C_{iii}$	310	285	-	-
$1C_{iv}$	316	285	-	-

T_{onset} = onset temperature of polymer backbone degradation, T_{SO_2} = onset temperature of -SO_3H groups splitting off. diss.* = dissolved after 48 hours in FR.

4.3.3 Solvent extraction stability with DMAc

The differences in the weight before and after DMAc extraction (Table 4.1) are indicative of the degree of cross-linking [32]. Hence only the weight changes and not IEC or TGA-FTIR data was relevant to, and used, in this discussion. The influence of the cross-linking on the weight change is dependent on both the type and strength of the cross-links present within the blended membrane network, whereas the polymer components that were not cross-linked or entangled within the membrane matrix would dissolve and be washed from the matrix. This is also the case for

additives which did not fully react and were not successfully removed during polycondensation or bromination of the BrPAE polymer components, including smaller functionalised polymer chains. It may also be that some of the residual imidazole (added in excess) was washed from the membrane during the extraction with DMAc. Table 4.5 summarises the dominant types of cross-linking likely to occur between the various polymer components present in the blend membranes, as presented in Figure 4.1. It is to be expected that the dominant cross-linking type (ionic or covalent) in the blend membrane would be dependent on the polymer that was in excess (Figure 4.2). Taking into account that covalent bonds are considered stronger than ionic bonds, it was to be expected that the % weight losses reported in Table 4.1 (fourth column) for DMAc extraction, would be lower for the highest BrPAE containing blends (C>B>A). This was the case for blends B and C, reporting losses between 2 and 25 % in comparison to the average weight loss of 64 % reported for the SFS-excess blend membranes A. The deviation in weight % losses noted for blends B and C due to extraction could likely be due to a variation in the time that was allowed for mixing of the polymer solutions (until homogeneous) before casting the blended membranes. This could have resulted in a loss of polymer fragments that were not sufficiently cross-linked within the membrane matrix during extraction (as described above).

Table 4.5: Possible cross-linking types between polymer components used in the blend membranes.

Polymers	Cross-linking possibilities
SFS-F_6PBI	Ionic
SFS-BrPAE	Ionic
F_6PBI-BrPAE	Covalent

4.3.4 Conductivity

In this section, the proton conductivity of blend membranes $1A_{i-iv}$ was determined to evaluate the influence of BrPAE-1/2 and TMIm/EMIm on proton conductivity. In addition to membrane series A, the conductivity of the apparently most suited membranes from blends B ($1B_i$) and C ($1C_i$) as well as Nafion® 212 (N212, 50 μm) were also included for comparison. The selected membranes, which were doped in H_2SO_4 as described in Section 4.2.4.4, had membrane thicknesses varying in the range of 50 to 80 μm that were taken into account when discussing the conductivity data obtained. Doping levels were determined at 23.8 ± 6 wt%. The conductivity was determined under restricted humidity (RH=50 %) in the range of 60 to 130 °C (Figure 4.4).
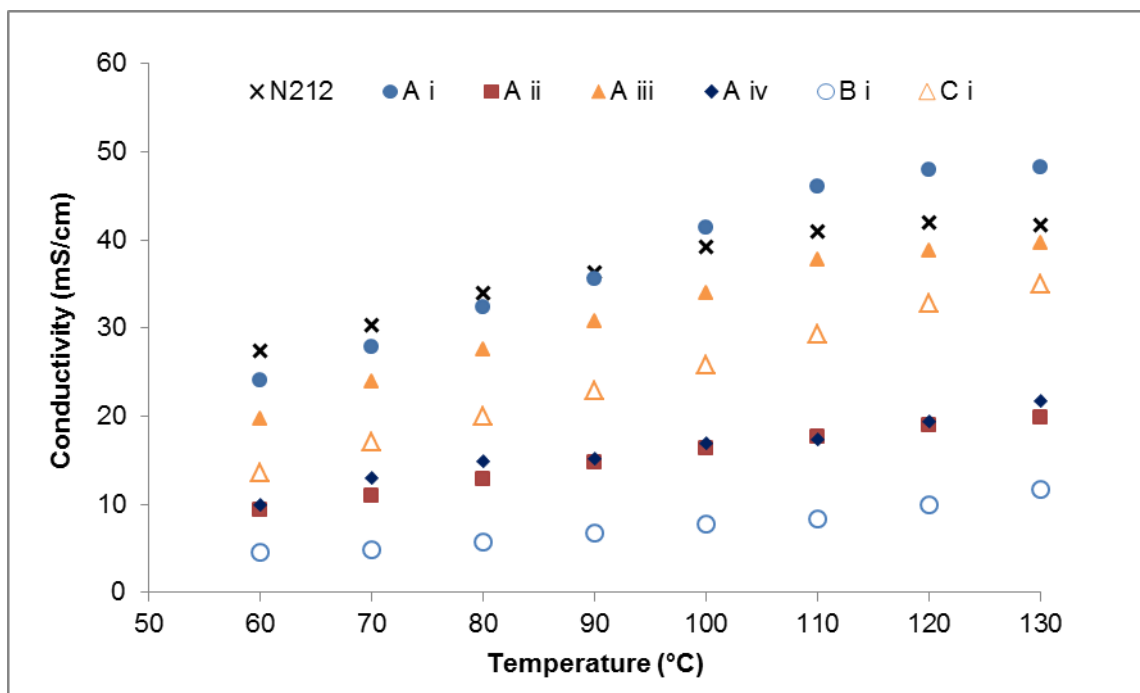
Figure 4.4: Proton conductivity measurements for blend 1A, 1B$_i$ and 1C$_i$ membranes with Nafion® 212 included as reference at RH = 50 % for temperatures at 60 to 130 °C.

From Figure 4.4 it becomes evident that the partially fluorinated BrPAE-1-containing blend membranes 1A$_i$ and 1A$_{iii}$ had a higher conductivity than the non-fluorinated BrPAE-2 blends 1A$_{ii}$ and 1A$_{iv}$. This is likely due to the sulfonation of BrPAE-1 (confirmed earlier during the H$_2$SO$_4$ stability testing (Section 4.3.1)) resulting in an increase in conductivity. Furthermore, the EMIm containing blend membrane 1A$_i$ displayed a conductivity that was closest (2-7 mS/cm) to the commercial Nafion®212 up to 100 °C. Above 100 °C, the conductivity improved further, reaching 48 mS/cm compared to the 40 mS/cm obtained for Nafion® at 120 °C. It was shown earlier that TMIm contributes more towards the stability of the investigated blends in comparison to EMIm (Sections 4.3.1.1 and 4.3.1.3). From the conductivity results it can be added that TMIm restricted the sulfonation of BrPAE-1 more effectively than EMIm when considering the results for the blend membranes 1A$_i$ and 1A$_{iii}$. It can therefore be concluded that the composition of the blend membrane 1A$_i$ allowed for improved conductivity results due to the combination of BrPAE-1 and EMIm, without sacrificing stability.

For comparison, the conductivity was measured for 1B$_i$ and 1C$_i$, again using the combination of BrPAE-1 and EMIm while only varying the main polymer combinations. It is clear that the higher SFS-containing blend membrane 1A$_i$ had the highest conductivity in comparison to the dominating F$_6$PBI blend (B) and BrPAE blend (C) membranes. This could be ascribed to the available -SO$_3$H

groups within the SFS polymer structure and likely partial sulfonation of the BrPAE component during pre-treatment, which contributed towards proton conductivity. The influence of H_2SO_4 treatment and degree of sulfonation on conductivity is further emphasised by comparison with the IEC_{total} (Table 4.3) values determined for the blend membranes (C>A>B). After considering the characterisation and conductivity data discussed earlier (Section 4.3.1 and 4.3.4), the blend membranes where BrPAE-1 and EMIm was used, i.e. $1A_i$, $1B_i$ and $1C_i$, were selected for further evaluation in SO_2 electrolysis (Chapters 5 & 6).

4.4 Conclusion

Within this study the suitability of partially and non-fluorinated blend components were evaluated in blended PEMs regarding their stability and conductivity capabilities in H_2SO_4-, oxidative- and extractive environments. Overall, the 12 blend membranes investigated proved sufficiently stable after H_2SO_4 treatment. The base excess blend membranes B showed superior stability due to the outstanding thermal and chemical stability of the F_6PBI component. The blend membranes C (BrPAE excess) reported both high stabilities and acceptable proton conductivities for possible use as PEMs during SO_2 electrolysis. Furthermore, in combination, the partially fluorinated polymer components (SFS, F_6PBI and BrPAE-1) were most stable with minimal weight losses and excellent thermal stabilities reported. It is concluded that the higher compatibility of the fluorinated blend components in membranes A, B and C contributed more to the overall stability of the blend membranes (i and iii types) than was the case for the non-partially fluorinated blend components (ii and iv types). Furthermore, it was noted that the partial sulfonation found when combining BrPAE-1 and EMIm ($1A_i$) during H_2SO_4 treatment benefitted the conductivity of blend types $1A_i$, $1B_i$ and $1C_i$ without sacrificing stability, showing the suitability of the blend types $1A_i$, $1B_i$ and $1C_i$ for SO_2 electrolyser studies. Before investigating the suitability of $1A_i$, $1B_i$ and $1C_i$ at the higher temperatures (120 °C) in Chapter 6, Chapter 5 is devoted to a more in-depth study of the larger SFS content blend membranes A since these yielded the highest proton conductivity (A>C>B). Various combinations of blend membrane A (in similar acid:base ratios, see Table 1.2) were prepared to determine how the fluorinated nature of the acidic and basic polymer components in blend $1A_i$ would influence the blend's acid stability and hence suitability for application in the SO_2 electrolyser at temperatures below 100 °C.

4.5 References

[1] Staser JA, Ramasamy RP, Sivasubramanian P, Weidner JW. Effect of water on the electrochemical oxidation of gas-phase SO_2 in a PEM electrolyzer for H_2 production. Electrochemical and Soild-state Letters. 2007;10:E17-9.

[2] Rosen MA, Scott DS. Comparative efficiency assessments for a range of hydrogen production processes. International Journal of Hydrogen Energy. 1998;23:653-9.

[3] Timothy M, Leonard B, Radenka M. Catalyst, Membrane, Free Electrolyte Challenges, and Pathways to Resolutions in High Temperature Polymer Electrolyte Membrane Fuel Cells. Catalysts, Vol 7, Iss 1, p 16 (2017). 2017:16.

[4] Shao Y, Yin G, Wang Z, Gao Y. Review: Proton exchange membrane fuel cell from low temperature to high temperature: Material challenges. Journal of Power Sources. 2007;167:235-42.

[5] Zhang J, Xie Z, Zhang J, Tang Y, Song C, Navessin T, et al. High temperature PEM fuel cells. Journal of Power Sources. 2006;160:872-91.

[6] Higashihara T, Matsumoto K, Ueda M. Sulfonated aromatic hydrocarbon polymers as proton exchange membranes for fuel cells. Polymer. 2009;50:5341-57.

[7] Staser JA, Weidner JW. Effect of Water Transport on the Production of Hydrogen and Sulfuric Acid in a PEM Electrolyzer. Journal of The Electrochemical Society. 2009;156:B16-B21.

[8] Jayakumar JV, Gulledge A, Staser JA, Kim C-H, Benicewicz BC, Weidner JW. Polybenzimidazole Membranes for Hydrogen and Sulfuric acid Production in the Hybrid Sulfur Electrolyzer. ECS Electrochemistry Letters. 2012;1:F44-F8.

[9] Weidner JW. Electrolyzer performance for producing hydrogen via a solar-driven hybrid-sulfur process. Journal of Applied Electrochemistry. 2016:1-11.

[10] T. R. Garrick, C. H. Wilkins, A. T. Pingitore, J. Mehlhoff, A. Gulledge, B. C. Benicewicz, et al. Characterizing Voltage Losses in an SO2 Depolarized Electrolyzer Using Sulfonated Polybenzimidazole Membranes. Journal of the Electrochemical Society. 2017;164:F1591-F5.

[11] Savinell R, Yeager E, Tryk D, Landau U, Wainright J, Weng D, et al. A Polymer Electrolyte for Operation at Temperatures up to 200°C. Journal of The Electrochemical Society. 1994;141:L46-8.

[12] Seland F, Berning T, Børresen B, Tunold R. Improving the performance of high-temperature PEM fuel cells based on PBI electrolyte. Journal of Power Sources. 2006;160:27-36.

[13] Lobato J, Cañizares P, Rodrigo MA, Linares JJ, Pinar FJ. Study of the influence of the amount of $PBI–H_3PO_4$ in the catalytic layer of a high temperature PEMFC. International Journal of Hydrogen Energy. 2010;35:1347-55.

[14] Li Q, Jensen JO, Savinell RF, Bjerrum NJ. High temperature proton exchange membranes based on polybenzimidazoles for fuel cells. Progress in Polymer Science. 2009;34:449-77.

[15] Jouanneau J, Mercier R, Gonon L, Gebel G. Synthesis of Sulfonated Polybenzimidazoles from Functionalized Monomers: Preparation of Ionic Conducting Membranes. Macromolecules. 2007;40:983-90.

[16] Vogel H, Marvel CS. Polybenzimidazole, new thermally stable polymers. Journal of Polymer Science. 1961;50:511–39.

[17] Glipa X, Bonnet B, Mula B, Jones DJ, Roziere J. Investigation of the conduction properties of phosphoric and sulfuric acid doped polybenzimidazole. Journal of Materials Chemistry. 1999;9:3045-9.

[18] Kalamaras I, Daletou MK, Neophytides SG, Kallitsis JK. Thermal crosslinking of aromatic polyethers bearing pyridine groups for use as high temperature polymer electrolytes. Journal of Membrane Science. 2012;415-416:42-50.

[19] Kerres JA. Blended and Cross-Linked Ionomer Membranes for Application in Membrane Fuel Cells. Fuel Cells. 2005;5:230-47.

[20] Chromik A, Kerres JA. Degradation studies on acid–base blends for both LT and intermediate T fuel cells. Solid State Ionics. 2013;252:140-51.

[21] Morandi CG, Peach R, Krieg HM, Kerres J. Novel morpholinium-functionalized anion-exchange PBI-polymer blends. Journal of Materials Chemistry A. 2015;3:1110-20.

[22] Morandi CG, Peach R, Krieg HM, Kerres J. Novel imidazolium-functionalized anion-exchange polymer PBI blend membranes. Journal of Membrane Science. 2015;476:256-63.

[23] Lee K-S, Jeong M-H, Lee J-P, Kim Y-J, Lee J-S. Synthesis and Characterization of Highly Fluorinated Cross-linked Aromatic Polyethers for Polymer Electrolytes. Chemistry of Materials. 2010;22:5500-11.

[24] Kim DS, Robertson GP, Guiver MD, Lee YM. Synthesis of highly fluorinated poly(arylene ether)s copolymers for proton exchange membrane materials. Journal of Membrane Science. 2006;281:111-20.

[25] Kerres JA, Xing D, Schönberger F. Comparative investigation of novel PBI blend ionomer membranes from nonfluorinated and partially fluorinated poly arylene ethers. Journal of Polymer Science Part B: Polymer Physics. 2006;44:2311-26.

[26] Kerres J, Schönberger F, Chromik A, Häring T, Li Q, Jensen JO, et al. Partially Fluorinated Arylene Polyethers and Their Ternary Blend Membranes with PBI and H3PO4. Part I. Synthesis and Characterisation of Polymers and Binary Blend Membranes. Fuel Cells. 2008;8:175-87.

[27] Schönberger F, Chromik A, Kerres J. Partially fluorinated poly(arylene ether)s: Investigation of the dependence of monomeric structures on polymerisability and degradation during sulfonation. Polymer. 2010;51:4299-313.

[28] Peach R, Krieg HM, Krüger AJ, van der Westhuizen D, Bessarabov D, Kerres J. Comparison of ionically and ionical-covalently cross-linked polyaromatic membranes for SO_2 electrolysis. International Journal of Hydrogen Energy. 2014;39:28-40.

[29] Peach R, Krieg HM, Krüger AJ, Rossouw JJC, Bessarabov D, Kerres J. Novel cross-linked partially fluorinated and non-fluorinated polyaromatic PBI-containing blend membranes for SO_2 electrolysis. International Journal of Hydrogen Energy. 2016;41:11868-83.

[30] Xing J, Kerres J. Improved performance of sulphonated polyarylene ethers for proton exchange membrane fuel cells. Journal of Membrane Science. 2006;17 591-7.

[31] Schoeman H, Krieg HM, Kruger AJ, Chromik A, Krajinovic K, Kerres J. H_2SO_4 stability of PBI-blend membranes for SO_2 electrolysis. International Journal of Hydrogen Energy. 2012;37:603-14.

[32] Kerres J, Atanasov V. Cross-linked PBI-based high-temperature membranes: Stability, conductivity and fuel cell performance. International Journal of Hydrogen Energy. 2015;40:14723-35.

[33] Kerres J, Ullrich A. Synthesis of novel engineering polymers containing basic side groups and their application in acid–base polymer blend membranes. Separation and Purification Technology. 2001;22-23:1-15.

[34] Kerres J, Zhang W, Jörissen L, Gogel V. Application of Different Types of Polyaryl-Blend-Membranes in DMFC. Journal of New Materials for Electrochemical Systems. 2002;5:97-107.

[35] Kerres J, Ullrich A, Hein M, Gogel V, Friedrich KA, Jörissen L. Cross-Linked Polyaryl Blend Membranes for Polymer Electrolyte Fuel Cells. Fuel Cells. 2004;4:105-12.

[36] Krüger AJ, Kerres J, Bessarabov D, Krieg HM. Evaluation of covalently and ionically cross-linked PBI-excess blends for application in SO_2 electrolysis. International Journal of Hydrogen Energy. 2015;40:8788-96.

[37] Peach R. Characterisation of proton exchange membranes in an H_2SO_4 environment. North-West University, Potchefstroom 2520, South Africa: North-West University, Potchefstroom campus; 2014.

CHAPTER 5 : PERFORMANCE OF IONIC-COVALENTLY CROSS-LINKED MEMBRANES DURING SO$_2$ ELECTROLYSIS (80-95 °C)[2]

Chapter Overview

It was concluded in Chapter 4 that the partially fluorinated polymer components of blends 1A$_i$, 1B$_i$ and 1C$_i$ were sufficiently stable (chemically and thermally), while displaying the highest conductivies. In this chapter, the blend membrane with the highest conductivity (1A$_i$) according to Chapter 4 was investigated further. To further improve this membrane, the partially fluorinated SFS and F$_6$PBI, and the non-fluorinated sPPSU and PBIOO main acidic and basic polymer components were combined (using the the same acid-base ratios that had been used for 1A$_i$ - Table 1.2) as blend components with BrPAE-1/2 and EMIm. Accordingly, three additional ionic-covalently cross-linked membranes (apart from 1A$_i$), were prepared, evaluated and compared to blend membrane 1A$_i$. These four membranes (*1*A$_i$*, 2*A$_{ii}$*, 3*A$_i$*, 4*A$_i$) were again submitted to an H$_2$SO$_4$ treatment, characterised and compared to the H$_2$SO$_4$ stability results presented in Chapter 4. The acid stability of the blend membranes was evaluated in an 80 wt% H$_2$SO$_4$ environment for 120 hours at 80 and 95 °C, respectively. From the characterisation results obtained by monitoring weight and thickness change, IEC, SEM-EDX and TGA signals before and after treatment, it was confirmed that the cross-linked blend membrane, 1A$_i$, containing only partially fluorinated polymer components (SFS-F$_6$PBI-BrPAE-1), showed exceptional stability. Membrane 1A$_i$ and Nafion®115 were selected for electrochemical evaluation by obtaining polarisation curves at 80 and 95 °C. Blend 1A$_i$ was found to perform the best at the operation temperature of 95 °C, reaching a current density of 0.63 A/cm² in comparison to the 0.42 A/cm² obtained for Nafion®115 at 1.0 V. The durability of the membranes within the electrolyser was measured by means of voltage stepping and subsequent characterisation using SEM-EDX, TEM and TGA, which confirmed the minimal degradation observed for the 250 cycles completed.

---

[2] Peach, R.; Krieg, H. M.; Krüger, A. J.; Rossouw, J. J. C.; Bessarabov, D.; Kerres, J. (2016) Novel cross-linked partially fluorinated and non-fluorinated polyaromatic PBI-containing blend membranes for SO$_2$ electrolysis. International Journal of Hydrogen Energy. 41, 11868-11883.

5.1 Introduction

In light of the increased interest in hydrogen as a cleaner alternative fuel source for energy, the demand for hydrogen is growing as research on the development and commercialisation of alternative power systems for hydrogen production is conducted [1, 2]. Of the hydrogen production technologies investigated so far, the thermo-chemical processes prove promising [3]. Of these the Hybrid Sulfur (HyS) thermo-chemical cycle, using a proton exchange membrane (PEM) based electrolyser, has received increased attention over the past years due to energy efficiency [2, 4].

Within the HyS process it is possible to produce clean hydrogen at efficiencies higher than normal water electrolysis [5]. Westinghouse Electric Corporation first developed the HyS process in the 1970s [6], which comprises a higher temperature step where H_2SO_4 is decomposed to produce SO_2, O_2 and H_2O [7]. Within the lower temperature HyS process step, the isolated SO_2 is then electrochemically oxidised to produce H_2SO_4 and H_2 in the presence of water [8, 9]. It has been determined by Gorensek et al. [10] that, for the HyS cycle to be competitive, the electrolyser should be operated at 0.6 V and 0.5 A cm $^{-2}$ while producing at least a 65 wt% H_2SO_4 product concentration.

As the membrane forms an integral part of the electrolyser system, a high chemical and thermal stability is required to withstand the harsh environment encountered during operation, while having a high conductivity and selectivity towards proton transport. One of the challenges arising is the possible degradation of the PEM due to the presence of the concentrated H_2SO_4 within the electrolyser. Furthermore, the advantages of operating at higher temperatures [11, 12] within the SO_2 electrolyser will in future require membranes that possess outstanding thermal stability along with the ability to maintain high proton conductivities in the midst of humidification requirements.

To date the commercially available and widely used Nafion® membranes, also proposed for SO_2 electrolysis [6], have demonstrated restrictions in their subsequent humidification requirements when operating at temperatures above 100 °C and dehydration of the membrane is observed [13]. This has led to the search to find suitable polymers for membrane materials to overcome the identified problems for higher temperature (HT) operation [12, 14-17], as would be appropriate for SO_2 electrolysis.

Chapter 4 describes how the acid-base blend concept was used to prepare 12 novel ionic-covalently cross-linked PEMs that were characterised to determine the suitability of the blend membranes (in terms of stability and conductivity) for application in SO_2 electrolysis. It was found that, by mixing the sulfonated arylene main-chain polymer (SFS) with F_6PBI in various ratios (see Figure 4.2) with a bromo-methylated arylene polymer (BrPAE-1/2) and EMIm/TMIm, stable and conductive blend membranes could be obtained. Furthermore, it was determined that the partially

fluorinated polymer components (SFS-F_6PBI-BrPAE-1) of blends $1A_i$, $1B_i$ and $1C_i$ showed exceptional stability.

In order to confirm the selection of SFS and F_6PBI (partially fluorinated) as main acidic and basic polymer components in blends (Chapters 3 and 4), the non-fluorinated sPPSU and PBIOO were included as blend components with BrPAE-1/2 and EMIm to obtain 3 additional ionic-covalently cross-linked membranes ($2A_{ii}$, $3A_i$ and $4A_i$) with the same acid-base ratios (Table 1.2) to compare with $1A_i$ (Chapter 4). In determining the suitability of the prepared novel blended membranes for SO_2 electrolysis, the chemical stability of the membranes was evaluated within a highly concentrated H_2SO_4 (80 wt%) environment at temperatures of 80 and 95 °C, followed by the appropriate characterisation tests for comparison of the membranes before and after the acid treatment as reported in previous works [18, 19]. This entailed the physical and chemical characterisation of membranes and included the comparison of weight and thickness changes, ion exchange capacity (IEC), Scanning Electron Microscopy (SEM) coupled with Energy-dispersive X-ray spectroscopy (EDX) (elemental analysis) and Thermo Gravimetric Analysis (TGA) measurements before and after treatment.

The prepared membranes that proved suitable were evaluated further in the SO_2 electrolyser at operation temperatures of 80 and 95 °C. This included long-term stability tests in the form of voltage stepping and characterisation of the membrane materials after electrolysis with SEM-EDS, TEM and TGA. Nafion® 115 was also included as reference material during the characterisation and electrolyser measurements.

5.2 Experimental

In order to determine the suitability of the partially- and non-fluorinated sulfonated PBI containing blend membranes for SO_2 electrolysis, the membranes were first subjected to an (ex-situ) acid treatment whereafter they were characterised using weight and thickness change, IEC measurements, SEM-EDS and TGA-FTIR. Nafion®115 was included for reference purposes both for the stability study and the SO_2 electrolyser evaluation where the most stable blend membrane was tested.

5.2.1 Materials

Chemicals were used as received from the manufacturers. N,N-Dimethylacetamide (DMAc, 99.5% purity) was obtained from Sigma Aldrich while the polymer materials PBIOO and F_6PBIOO were purchased from FuMA-Tech and YANJIN Technology, respectively. The sulfonated polymers, SFS and sPPSU, and bromo-methylated polymer were synthesised in-house as described in [20-22].

The tertiary amine, 1-ethyl-2-methylimidazole (EMIm), was purchased from Ionic Liquids Technologies GmbH. Nafion® 115 was obtained from Ion Power and used as is.

5.2.2 Membrane preparation and post-treatment

The structures of the polymers used in the synthesis of the different partially- and non-fluorinated sulfonated PBI-containing blend membranes are presented in Table 1.1. Solutions of the various polymers were prepared in DMAc. 10 wt % of the sulfonated (SFS and sPPSU) and bromo-methylated (BrPAE-1/2) polymeric solutions were prepared, while 5 wt% solutions were prepared for the PBIOO and F_6PBI polymers. After dissolving the various polymers in DMAc, the polymers were blended in a specific ratio (see Figure 4.2, blend A) to yield 4 different blended membranes (Table 1.2). The polymer solutions were mixed, cast onto glass plates and post-treated as discussed in Chapter 4 (Section 4.2.2).

The prepared membranes differed mainly regarding their sulfonated component and the fluorinated nature of the blend components (BrPAE-1/2) present within the different blend membranes (See Table 1.1 and 1.2). Accordingly, membranes *1* and *3A$_i$* contain the partially fluorinated sulfonated arylene main-chain polymer (SFS), and membranes *2A$_{ii}$* and *4A$_i$* contain the non-fluorinated sulfonated poly(phenyl sulfone) sPPSU.

5.2.3 H$_2$SO$_4$ stability

As described in Chapter 4 (Section 4.2.3.1), the sulfuric acid stability (chemical and mechanical) of the novel cross-linked blend membranes were first determined. This included an H$_2$SO$_4$ treatment at 80 and 95 °C for 120 hours, whereafter membranes were characterised physically and chemically by comparing weight and thickness changes, IECs, SEM-EDX, and TGA-FTIR measurements before and after treatment.

5.2.4 Membrane characterisation

As described in Chapter 4 (Section 4.2.4.1-4.2.4.3), weight changes, IECs and TGA measurements were performed both before and after treatment for the blend membranes. In addition the thickness change and SEM-EDX measurements for the blend membranes were included (Section 5.2.4.1 and 5.2.4.3).

5.2.4.1 Weight and thickness change

The average thickness of the membranes (one dimensional change) was determined by recording of at least 5 measurements, using a digital micrometer from Mitutoyo (293 MDC-MX), across the surface area of the membrane.

5.2.4.2 IEC

As described in Chapter 4 (see Section 4.2.4.2).

5.2.4.3 SEM and EDX

A FEI Quanta 250 FEG with ESEM capabilities was used to investigate the surface and cross-sections of membranes where necessary. An energy-dispersive X-ray spectroscopy (EDS) analysis with the Oxford system using INCA software, coupled with the SEM, provided an elemental analysis of each membrane sample before and after the acid treatment, which was used to compare the sulfur content. Before SEM, the samples were coated with an ultrathin coating of an electrically conducting gold/palladium alloy, using an EM Scope. For the recording of backscatter images, the samples investigated were coated with a carbon layer.

5.2.4.4 TGA

TGA was done as described in Section 4.2.4.3, except without the FTIR coupling of results. Instead, the start of degradation points for the membranes were compared before and after treatment [23].

5.2.5 SO$_2$ electrolysis

From the acid stability studies the most suitable blend membrane, with regard to the acid stability results (Section 5.3.1), was selected for further evaluation in the SO$_2$ electrolyser and compared to the performance of Nafion® 115 under the same operating conditions as described in previous studies [19]. The voltage was limited to 1 V as the flow fields are manufactured from carbon, which corrode electrochemically above 1 V. Membrane electrode assemblies (MEA) with an active area of 10 cm^2 were manufactured by hot pressing (Carver, Model #3912) the membranes between two pieces of GDE (purchased from Fuel Cell Etc.) with a 0.5 mg Pt C/cm^2 catalyst loading at 120 °C for 5 min under a load of 120 kg cm^{-2}.

Based on previous work showing that doping after hot pressing yielded a better overall cell performance [24], the PBI-based MEAs blend membrane was doped after hot pressing by submerging the manufactured MEA in a 1 M H$_2$SO$_4$ solution at 80 °C for 24 h before loading into the cell. The Nafion® 115 membrane was doped before hot-pressing with the same H$_2$SO$_4$ solution to facilitate comparison with earlier work [19, 25].

5.2.5.1 General procedure

After the MEAs under investigation had been assembled and doped, they were loaded into the electrolyser and kept at 80 °C for 1 hour before break-in where a current density of 0. A/cm² was applied over the cell for 20 min. Polarisation curves were then recorded by measuring the voltage while incrementally increasing the applied current density by 0.01 A/cm² every 90 s [26]. The polarisation curves were recorded in triplicate for both MEAs, thereby determining whether a conditioning step for the MEAs was required for ensuring the best performance within the electrolyser cell [24]. The electrolysis process was controlled and captured using a Labview®-

based program [24, 27, 28]. Measurements were performed at 80 and 95 °C. The H_2SO_4 produced during electrolysis at 80 °C was collected at different current densities and the concentration determined by titration with 0.1 M NaOH.

5.2.5.2 Voltage stepping

For an evaluation of the stability and durability of the membranes within the electrolyser during cell operation, voltage stepping was applied as a degradation method [26]. This method was performed at 80 and 95 °C for both MEAs by stepping between an upper 0.9 V and a lower 0.3 V limit, maintaining a constant voltage for 2 min at each limit. This was repeated for 250 cycles while recording the current density every second, of which only every 5th data point was captured in the subsequent figures.

5.2.6 MEA characterisation of membrane after electrolyser operation

To further elucidate the effect of voltage stepping on membrane stability, various membrane characterisation techniques were applied pre-and-post electrolysis on the Nafion® 115 and the selected novel blend membrane ($1A_i$). These techniques included Transmission Electron Microscopy (TEM) and SEM-EDX investigations of the micromorphology. Furthermore, TGA-FTIR measurements allowed for an evaluation of the thermal stability of the membrane after operation within the SO_2 electrolyser.

The micromorphology of the membrane material was investigated using TEM before and after SO_2 electrolysis operation to determine the degree of degradation the membrane underwent. The TEM images were obtained using a FEI TECNAI G220 S-Twin operating at 120 kV. The membrane material was removed from the GDE material after electrolysis using a scalpel, embedded in an epoxy (LR White), sectioned into thin samples with a Reichert-Jung Ultramicrotome, and loaded onto a copper grid for viewing under the microscope.

SEM was used to examine the membrane cross-sections as discussed earlier (Section 5.2.4.3). The samples were also prepared as discussed for TEM with the exception of being coated with a carbon layer prior to the recording of backscatter electron images of the samples. Cross-section images and EDX analysis of the membranes after electrolysis were done to support the observations made from the TEM images.

TGA measurements were performed on the respective membrane materials after electrolysis, as mentioned in Section 5.2.4.4.

5.3 Results and discussion

5.3.1 H$_2$SO$_4$ stability

The acid stability of the membranes under investigation serves as a measure of their suitability for application within the SO$_2$ electrolyser where a highly concentrated sulfuric acid environment is encountered at temperatures of 80 and 95 °C during operation. The physical changes (weight and thickness) observed for the membranes was used to evaluate their stability with support of the determined chemical changes (IEC and SEM-EDX) and thermal stability (TGA). As mentioned earlier, an experimental error smaller than 10 %, both in terms of the H$_2$SO$_4$ treatment and the analytical characterisation techniques used in this chapter, was considered acceptable [19, 27].

5.3.1.1 Weight and thickness change

The percentage weight and thickness changes obtained before and after the ex-situ acid treatment for the investigated membranes are presented in Table 5.1. To facilitate the discussion, the SFS acid-excess membranes, 1 and 3A$_i$, are compared with the non-fluorinated sPPSU membranes, 2A$_{ii}$ and 4A$_i$, and Nafion®115, which served as the commercial reference.

Table 5.1 – Weight and thickness changes (%) obtained for the membranes due to H$_2$SO$_4$ treatment at 80 and 95 °C.

Membrane	Weight changes (%)		Thickness change (%)	
	80 °C	95 °C	80 °C	95 °C
1A$_i$	-0.20	-1.6	-5.6	-2.7
2A$_{ii}$	X	X	X	X
3A$_i$	0.29	-0.64	-10.4	-22.4
4A$_i$	-19.4	X	X	X
N115	-0.14	1.4	-2.18	-0.16

X - weight losses were excessive due to the dissolution of the polymer components (no data could be obtained)

It is clear from Table 5.1 that, for the blend membranes 1 and 3A$_i$, where the higher content acid polymer (Figure 4.2) component contributing to the blend is the partially fluorinated SFS, a more stable blended membrane is obtained that withstands significant sulfonation and/or dissolution at

both 80 and 95 °C. This can be ascribed to the arylene rings of the SFS polymer being more electron-deficient due to the partially fluorinated components present, in comparison with the aromatic rings of the sPPSU polymer [29]. It has, however, been found that the loss of low molecular fractions (oligomers) of the sulfonated polymer (SFS) does occur [19, 20, 32], which can account for the slight weight decrease noted after treatment as established in Chapter 2. While the change in thickness, indicative of the one-dimensional changes (Section 5.2.4.1) measured for membrane $3A_i$, as indicated in Table 5.1, is still acceptable at 80 °C, the thickness change at 95 °C is considered too high for the application in an electrolyser. This change in thickness is likely due to the presence of the non-fluorinated PBIOO polymer in comparison with the F_6PBI used in membrane $1A_i$ with similar composition (Table 1.2). It has been shown that the PBIOO polymer is more likely to undergo sulfonation, while the F_6PBI blend component will remain stable due to the electron-deficiency present within this partially fluorinated polymer [26, 27].

The membranes $2A_{ii}$ and $4A_i$, containing the acidic polymer sPPSU, report large weight losses and dissolution of polymer components, respectively, as indicated by the X in Table 5.1. This is most likely due to sulfonation of the polyethersulfones [21, 30] present within the sPPSU polymer in the presence of H_2SO_4 during treatment at temperatures 80 and 95 °C. Due to this occurrence, the change in thickness could not be measured, as indicated by the X in Table 5.1, for the mentioned membranes.

For both the 80 and 95 °C acid treatments, Nafion®115 remained stable and negligible changes in weight and thickness were observed, as can be seen in Table 5.1.

In summary, the decrease in weight changes noted (Table 5.1) for the membranes $1A_i$ and $3A_i$ were insignificant (< 2%) in comparison to the membranes $2A_{ii}$ and $4A_i$ (> 20%), where dissolution of polymeric components was evident. The small discrepancies in corresponding weight and thickness changes of the membranes $1A_i$ and N115 is likely due to the treatment of the membranes during and after acid exposure (repeated washing and drying) and was also regarded as insignificant (< 5.6%). However, after treatment, the membranes $2A_{ii}$ and $4A_i$ had more significant thickness changes (> 10%), which can be related to the composition (weight changes) of the membranes and associated dissolution of less fluorinated polymer components as discussed above. The weight changes noted for membrane $1A_i$ were also found in agreement with the minimum weight change of (-1.88 %) reported in Chapter 4 after H_2SO_4 treatment at 80 °C (Section 4.3.1.1).

5.3.1.2 IEC

The IEC gives the number of accessible ion-exchange groups, in this case the number of -SO_3H groups, present per weight unit of dry membrane [meq/g] [31]. The number of -SO_3H groups, as determined by acid-base titrations [32], can be directly related to the proton conductivity of the

membrane. The determined IEC_{direct} represents only the $-SO_3H$ groups in the ionically cross-linked membranes where the protons contribute to the proton conductivity [31]. $-SO_3H$ groups present in dead-end ion-conducting channels within the membrane matrix will also not be captured by titration. It has been mentioned in a study of Kreuer et al. that sulfonated arylene main-chain type polymers (PARSA) show a higher share of dead-end ion-conducting channels than perfluorosulfonic acid polymer (PFSA) types like Nafion®. This is due to the smaller amount of separation evident between the polymeric backbone and sulfonic acid groups, since the polymeric backbone of the PARSAs is less hydrophobic than that of the PFSAs [33].

The calculated IEC is indicative of the expected cross-links between the acid and base polymer components based on the composition of the membranes, where the cross-linking yield is confirmed by the experimental IEC_{direct} values [34]. It can be noted from Table 5.2 that the direct IECs measured for the prepared membranes are slightly lower than expected due to the above-mentioned share of SO_3H groups present in dead-end channels. The IEC_{direct} values determined for the blend membranes $1A_i$ and $3A_i$ are comparable, while the membranes $2A_{ii}$ and $4A_i$ report the highest and lowest IEC_{direct} values within the series, with the exception of Nafion®115.

Table 5.2 - Direct (calculated and experimental) IEC [meq SO_3H/g] values as determined for the blend membranes and Nafion®115 before and after the acid treatments at 80 and 95 °C.

Membrane	IEC_{calc}	IEC_{direct}^{before}	$IEC_{direct}^{after\ 80\,°C}$	$IEC_{direct}^{after\ 95°C}$
$1A_i$	1.52	1.31	1.47	1.56
$2A_{ii}$	1.55	1.34	-	-
$3A_i$	1.60	1.44	1.39	1.62
$4A_i$	1.49	1.19	5.71	-
Nafion ®115	0.91[a]	0.82	0.82	0.88

[a] As adopted from Yang et al. [35]

Note that the blend membranes had acid excess (Figure 4.2), while the IECs obtained for the pure sulfonated polymers, SFS and sPPSU were 2.3 and 1.8 meq SO_3H/g, respectively. From the IECs measured after treatment, it is clear that the membranes $1A_i$ and $3A_i$ remained the most stable in the presence of the sulfonated polymer SFS, as previously discussed (Section 5.3.1.1), with slight increases noted. The unstable character of the sPPSU-blended membranes becomes evident in

view of the large increases in IEC values noted for the membrane $4A_i$ in Table 5.2, supporting the weight losses obtained earlier (Table 5.1) for the membranes $2A_{ii}$ and $4A_i$. This is in agreement with the likely sulfonation of the polyethersulfones [32, 38] within the sPPSU polymer proposed in Section 5.3.1.1, followed by their dissolution from the membranes. It is also likely that partial, albeit limited sulfonation of the BrPAE-1 polymer component has occurred at the higher temperature range of 95 °C (Section 5.3.3), contributing to the slightly increased IEC values reported (Table 5.2). Furthermore, the increase in IEC values noted after treatment could also be attributed to the splitting-off of the ionical cross-links during treatment and the subsequent formation of imidazolium hydrogen sulfate groups in the PBI portion of the blend membranes as reported in [19]. In addition, the increased IECs reported for the blended membranes ($1A_i$ and $3A_i$) after treatment indicate sulfonation and/ or splitting-off of cross-links occurring to a lesser extent for the more stable SFS blends (1 and $3A_i$, 12-19% change) than for the sPPSU blends ($2A_{ii}$ and $4A_i$, > 100% change).

Due to the dissolution of polymer fragments as noted earlier for membrane $2A_{ii}$, the IEC values could not be determined and are absent from Table 5.2. It should also be mentioned that the IEC_{direct} values obtained for Nafion®115 remained stable.

5.3.1.3 SEM-EDX

In support of the observations in Section 5.3.1.1 and 5.3.1.2, the EDX analysis performed on the surface of the blended membrane samples before and after treatment allowed for a comparison of the sulfur content (data not shown). The S-content of the membranes $1A_i$ and $3A_i$ were found comparable before and after treatment (standard deviations of 0.52 % and 0.30 % determined, respectively), supporting the membranes remained stable as no significant sulfonation took place in the acidic environment. The same can be concluded for Nafion®115, with a standard deviation of 0.09 % determined for measurements of the S content before and after treatment. However, the membrane $4A_i$ obtained a 55 % increase in the S content measured after treatment at 80 °C, supporting the dissolution of polymer fragments due to the sulfonation of the sPPSU polymer component, as had been reported in Section 5.3.1.1. SEM-EDX measurements of the membrane $2A_{ii}$ were not possible due to the dissolution of the membrane sample after treatment.

5.3.1.4 TGA

TGA analysis was performed to determine the suitability of the blend membranes for application in the SO_2 electrolyser at temperatures above 80 °C, while evaluating their chemical stability with regard to the thermal stability measured after acid treatment. The thermal degradation curves of the blend membranes as well as Nafion®115 before acid treatment are presented in Figure 5.1.
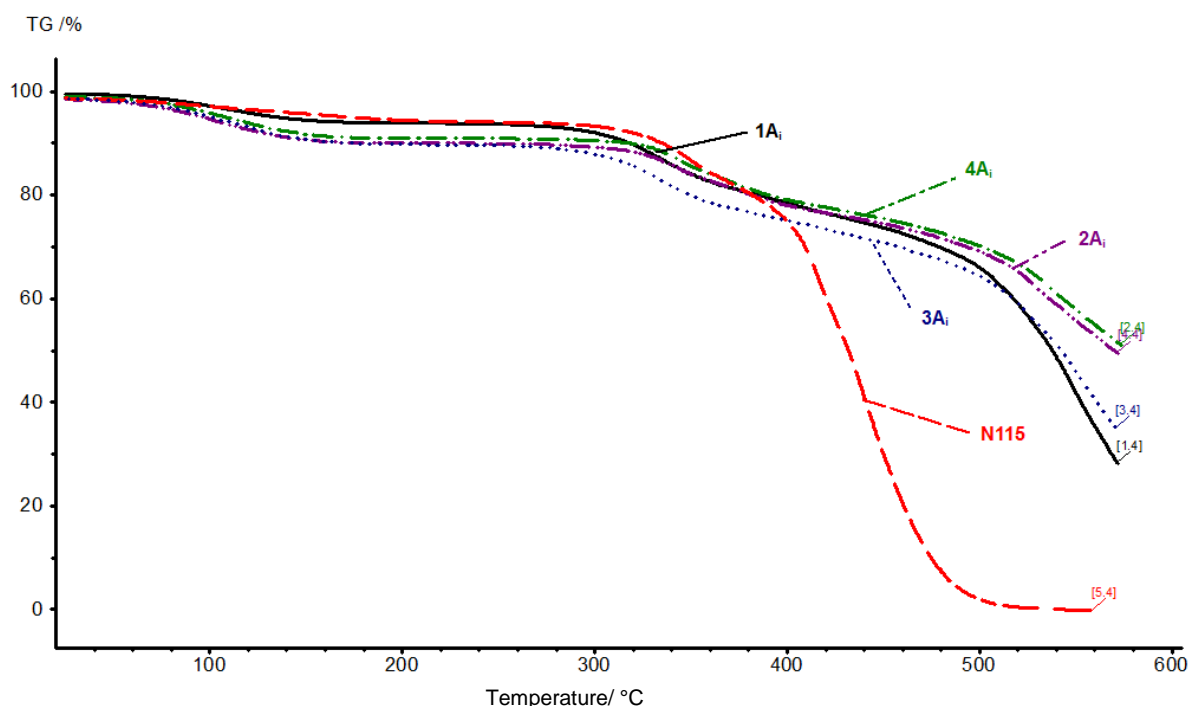
Figure 5.1: Thermal degradation of the blend membranes as well as Nafion®115 before acid treatment.

It is clear from Figure 5.1 that the TGA curves of the SFS acid-excess membranes, $1A_i$ and $3A_i$, are similar to one another when compared to the non-fluorinated sPPSU membranes, $2A_{ii}$ and $4A_i$. The membranes are considered stable up to 300 °C, from where degradation starts and weight losses increase.

Furthermore, the thermal degradation of the membranes was evaluated by comparison of the calculated first derivative of the TGA signals recorded for the membranes before and after acid treatment. From earlier studies, the weight losses obtained after 200 °C are associated with the splitting-off of the sulfonic acid groups and polymer backbone degradation [19, 36]. In this study the differential TGA signal was used to determine at what temperature degradation of the membrane started. The temperatures corresponding to these degradation starting points and the subsequent weight losses detected (from the normalised 100% residual weight before TGA analysis) for the membranes before and after the acid treatment at the specific degradation temperatures are summarised in Table 5.3.

Table 5.3 - Start of degradation temperatures and the residual weight at these degradation temperatures as determined by differential TGA for the blend membranes and Nafion ®115 before and after acid treatment.

Membrane	Start of degradation (°C)			Residual weight[a] (wt %)		
	Before	After 80 °C	After 95 °C	Before	After 80 °C	After 95 °C
1A$_i$	275	275	275	93	84	86
2A$_{ii}$	308	X	X	89	X	X
3A$_i$	275	275	275	89	85	86
4A$_i$	308	302	X	89	62	X
Nafion®115	306	305	305	91	88	89

[a]   Residual weight at start of degradation temperature

X   No analysis possible due to dissolution of material during acid treatment

The data in Table 5.3 shows that the membranes 1A$_i$ and 3A$_i$, before and after acid treatment, started to degrade after 275 °C (according to the first derivative). This is in agreement with the T$_{SO_2}$ temperatures starting from 277 °C for blend membranes 1A$_{i-iv}$ in Chapter 4 (Section 4.3.1.3, Table 4.3) and could be associated with the splitting-off of -SO$_3$H groups of either the SFS or sPPSU polymer components of the blends inspected in Chapter 5.

The small differences noted in weight losses detected after treatment (at 80 and 95 °C) in comparison to before treatment for membrane 1A$_i$ and 3A$_i$ indicates a high thermal stability, in support of the chemical stability discussed earlier (Section 5.3.1.1), for the membranes after being subjected to the H$_2$SO$_4$ treatment. Although the 2A$_{ii}$ and 4A$_i$ membranes reported a later starting point (higher temperature) of degradation, the rate of degradation thereafter was noticeably faster (increased weight loss) as detected by the residual weight of 62 wt % after treatment at 80 °C compared to the 89 wt % detected before treatment for 4A$_i$. Due to the acid instability and dissolution of polymer components noted earlier for the sPPSU-excess membranes, the TGA curves could not be recorded for all 2A$_{ii}$ and 4A$_i$ membrane materials after treatment and was therefore marked with an X. The Nafion®115 membrane proved thermally stable as insignificant changes in temperature and weight losses were detected after treatment in support of the high chemical stability noted earlier (Section 5.3.1.1).

It is clear from the TGA curves recorded for the blended membranes and Nafion®115 that degradation only started after 275 °C. Therefore, the membranes are considered to have excellent thermal and chemical stability as the temperature of operation in the SO_2 electrolyser will not exceed those within the scope of our study.

According to the characterisation data (Section 5.3.1) of the acid treated membranes, $1A_i$ was found to be most stable and was hence chosen for the further SO_2 electrolysis experiments. It becomes evident that the additional polymer components BrPAE-1 and EMIm did not contribute considerably to the stability of the blended membranes, which is understandable in view of their relatively small comparable quantities (1 and $3A_i$, Figure 4.2), but considered valuable in view of contribution toward proton conductivity of blend membranes as investigated in Chapter 4 (Section 4.3.4) However, when combined with the more stable acid-excess polymer blends SFS, their supplementary ionic cross-links and subsequent contribution to chemical stability of the membranes $1A_i$ and $3A_i$ are noticeable in comparison to similar PBI blends from previous work [19, 24, 26]. Furthermore, it is clear that the partially fluorinated membrane components (SFS, F_6PBI and BrPAE-1) of blend $1A_i$ significantly contributed to the stability of the blend membrane as minimal weight and thickness changes were detected, which was supported by the chemical stability confirmed by the IEC, SEM-EDX and TGA curves obtained after the acid treatment. Characterisation results repeated for membrane $1A_i$ (weight change, IEC_{direct} and TGA) after 80 °C were found within the 10% accepted error as stated earlier.

5.3.2 Electrolysis

Based on the acid stability tests performed in Section 5.3.1, the membranes $1A_i$ and Nafion®115 were selected for SO_2 electrolysis where Nafion®115 also served as the commercial benchmark both for the novel blend membrane $1A_i$ and for previous SO_2 electrolysis studies completed [19, 26]. For an accurate evaluation of the performance of the MEA within the SO_2 electrolyser cell, three consecutive polarisation curves were measured at 80 °C for both the membrane $1A_i$ and N115. For the triplicate experiments, the variation in voltage as a function of current densities was negligible with an average standard deviation of 0.013 V (1.7 %) determined for $1A_i$ and 0.006 V (0.64 %) for N115. This confirms the repeatability achievable for polarisation curve measurements of the membranes under investigation in the SO_2 electrolyser within our study confirming an error range below 5% that was observed for all electrolysis data presented in this study. In Figure 5.2, the average polarisation curves obtained at 80 °C and single run polarisation curves obtained at 95 °C are presented.
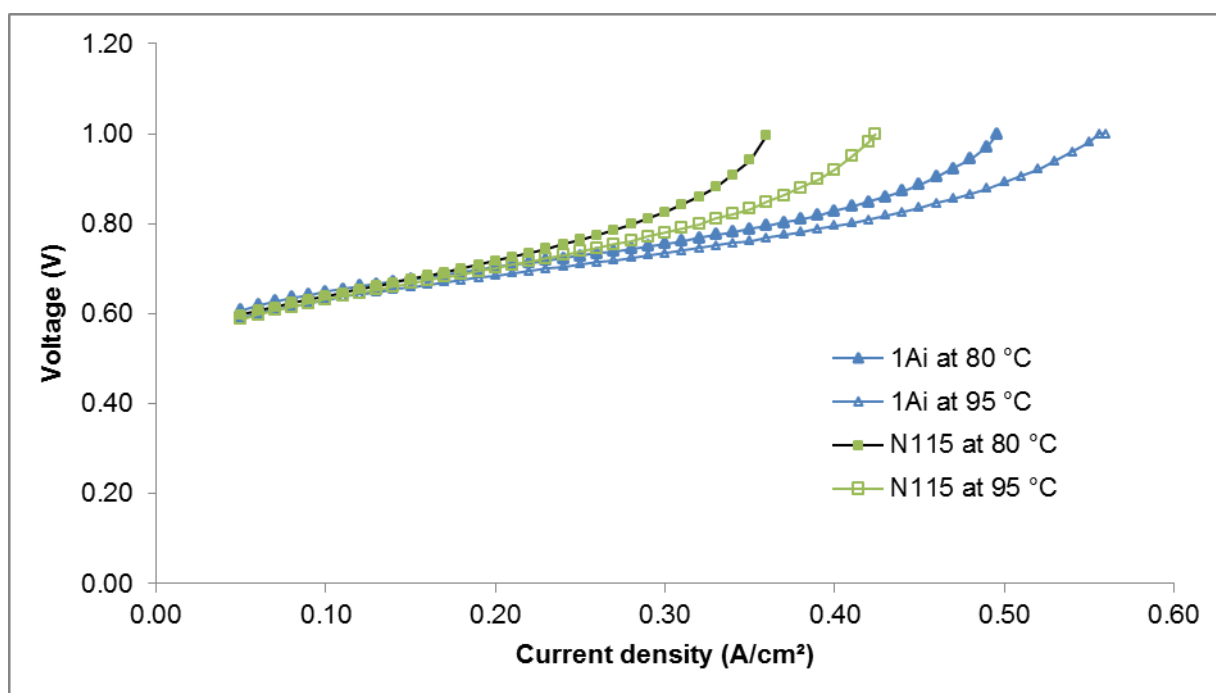
Figure 5.2: Polarisation curves obtained for the membranes blend 1A$_i$ and N115, at 80 °C and 95 °C.

It can be noted within the lower current density region of N115 (Figure 5.2) at 80 °C that a slightly lower voltage was measured in the region up to 0.16 A/cm², from where it increased to reach a maximum of 0.998 V at a current density of 0.356 A/cm², in comparison to the maximum of 0.994 V attained at 0.54 A/cm² for blend 1A$_i$.

For the electrolysis measurements conducted at 95 °C, a further increase in the current densities was observed, i.e. 0.42 and 0.63 A/cm² for N115 and blend 1A$_i$, respectively (Figure 5.2). At 95 °C, the polarisation curves obtained were comparable for N115 and 1A$_i$ within the lower current density region.

The improved performance observed for the blend membrane 1A$_i$ in comparison with N115 (Figure 5.2) is likely due to the difference in humidification needs of Nafion® within the acidic environment of the SO$_2$ electrolyser at higher operating temperatures [11, 37, 38]. It has previously been reported that the novel cross-linked membranes (SFS-F$_6$PBI blend), such as 1A$_i$, possess the ability to conduct protons from the acid produced during electrolysis which insures the continuous doping of the membrane during operation and the improved performance observed [8, 39]. From all previous evaluations of PBI-blended membranes within our group, [19, 24, 26], the blend membrane 1A$_i$ has thus far proved the most efficient (highest current density achieved) in the SO$_2$ electrolyser at operation temperatures of 80 °C.

The acid produced during SO_2 electrolysis serves as an additional measure of the efficiency of the MEA and the performance of the membranes within the electrolyser step [10], and was therefore measured at various current densities as determined from the polarisation curves obtained for the membranes at 80 °C (Figure 5.3).
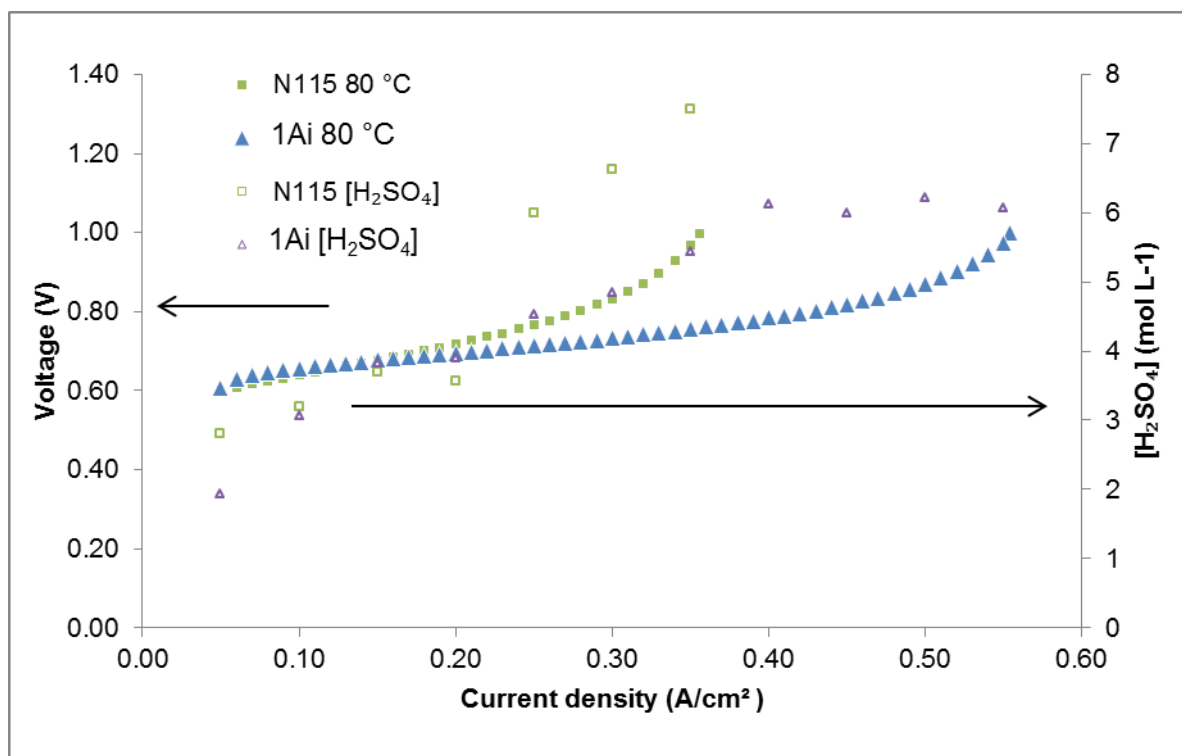
Figure 5.3: Polarisation curves recorded with the [H₂SO₄] produced for Nafion®115 and blend 1Aᵢ at 80 °C.

In previous studies it has been reported that the thickness of the membrane is known to influence the water transport and subsequent concentration of the acid produced during operation and thus affects electrolysis efficiency [24, 40]. As expected for the thinner blend membrane 1Aᵢ (55 µm), lower acid concentrations were obtained, especially at higher current densities (Figure 5.3), due to the higher H_2O cross-over and subsequent dilution in comparison with the H_2SO_4 concentrations measured for the thicker N115 membrane (127 µm).

For comparison with literature the performance of the blend membrane 1Aᵢ and N115 is summarised in Figure 5.3 at operation temperatures of 80 °C. Accordingly, blend 1Aᵢ yielded a maximum current density of 0.54 A/cm² at 1 V with 45 wt% H_2SO_4 produced compared to the 0.35 A/cm² obtained at 1 V for N115 with 52 wt% H_2SO_4 produced. It is, however, notable that, at current densities lower than 0.2 A/cm², the acid concentration produced is comparable between N115 and blend 1Aᵢ despite the thickness difference. The improved performance for the thinner

blend 1A$_i$ can be attributed to both the reduced ohmic resistance and the kinetic resistance being lower at low acid concentrations. It has been shown previously that the resistance of PFSA-based membranes increases with an increase in acid concentration due to dehydration, which limits the maximum current density obtainable [41]. For the Hybrid Sulfur cycle Gorensek *et al.* [10] determined that an optimal acid concentration produced by the electrolyser should be 65 wt % at 0.6 V and 0.5 A/cm². Although the current data is 270 mV higher than what is needed, the acid concentration is close to the target, producing in the 50 wt % acid range.

After the polarisation curves for the membranes 1A$_i$ and N115 were obtained at 80 and 95 °C, voltage stepping was performed at 80 and 95 °C to determine the MEA stability. As described in Section 5.2.5, this procedure serves to increase the stress under which the MEAs would normally operate by stepping between a low (0.3 V) and high (0.9 V) voltage for 2 minutes per step for 250 cycles, thereby accelerating the degradation of the membrane. Is has previously been shown that the catalyst is stable for at least the 250 cycles used in this study [26]. The current densities recorded as a function of the 250 voltage cycles completed for both membranes 1A$_i$ and N115 at temperatures 80 and 95 ^{0}C are shown in Figure 5.4. It should be mentioned that the current densities recorded for the investigated membranes at the lower voltage of 0.3 was measured at 0 A/cm², and are therefore not visible in Figure 5.4.
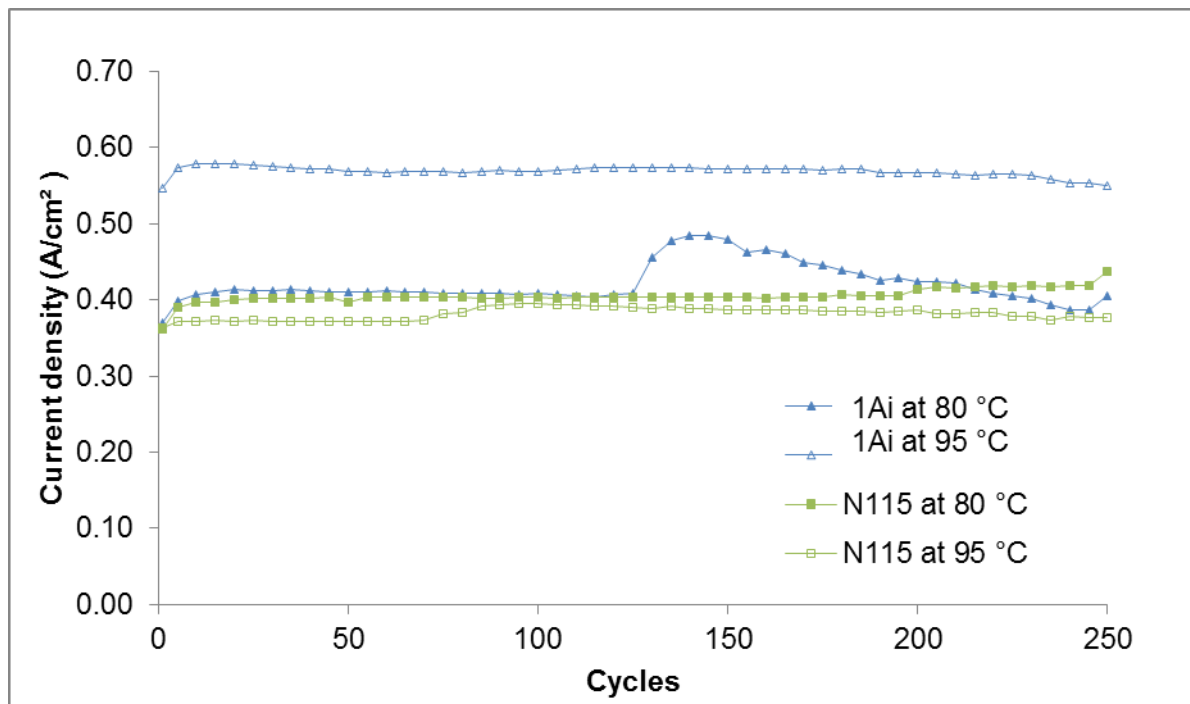
Figure 5.4: Current density (A/cm²) as a function of voltage cycling at 80 and 95 °C for the membranes 1A$_i$ and Nafion®115.

The cycles completed at 80 °C for the membranes N115 and 1A$_i$ report current densities that are comparable up to cycle 125 (Figure 5.4) from where an increase in the current density values (0.40 to 0.48 A/cm²) of membrane 1A$_i$ was noted. This could be due to the break-in procedure being insufficient, from where a conditioning effect (doping through the acid produced) from the completed cycles is noted by the increase in current densities obtained between cycles 125 and 200. However, a gradual decrease (cycle 145) is noted as membrane degradation takes effect and current densities drop from 0.48 (cycle 145) to 0.41 A/cm² (cycle 200), and membrane 1A$_i$ reports current densities just below those of N115 from cycle 220 onwards at 80 °C.

The increased performance noticed in current densities obtained for 1A$_i$ at 95 °C, initially at 0.55 A/cm² and stabilising at 0.58 A/cm² (Figure 5.4), is similar to the current densities detected in the polarisation curves, Figure 5.2 (0.55 A/cm²) and Figure 5.5 (0.54 A/cm²), at the applied potential of 0.9 V. This further emphasises the suitability and potential for higher temperature electrolyser application of the novel cross-linked membrane 1A$_i$. An improved stability with regard to previous work completed on similar blend membranes is also noted [26].

A small decrease in current densities is noted for N115 during voltage stepping at 95 °C (Figure 5.4) in comparison to the cycles completed at 80 °C, whereafter a slight increase is noted after 85 cycles. The known limitations of the Nafion® membrane at higher temperature operations [13] are also expected to affect the performance of the MEA to some extent as noted in Figure 5.4, where the signs of membrane degradation become evident, regardless of the extended hydration of the MEA before measurement. Furthermore, it can be mentioned that the initial current densities obtained for N115 in the range of 0.37 A/cm² (Figure 5.4) were comparable to the values obtained in Figure 5.2 (0.39 A/cm²) and Figure 5.6 (0.36 A/cm²) for operations at 95 °C.

When considering Figure 5.2 and Figure 5.3, a difference in the current densities obtained at the applied potential of 0.9 V in Figure 5.4, for both N115 and 1A$_i$ at 80 °C, was observed. For N115, the increase from 0.34 A/cm² (Figure 5.2) to the obtained 0.39 to 0.42 A/cm² in Figure 5.4 is likely due to the conditioning of the preliminary polarisation curves obtained at 80 and 95 °C from the MEA in the electrolyser cell before applying voltage stepping. This observation can also be ascribed to the 3h hydration of the N115 MEA within the cell before voltage stepping commenced (Figure 5.6), in comparison to the 1h break-in step (Section 5.2.5.1) before the polarisation curves of Figure 5.2 were obtained at 80 and 95 °C.

Unlike with N115, the membrane 1A$_i$ was not subjected to an extended hydration period to prevent the flushing of acid from the MEA needed for proton transport during operation [24]. The initial current density of 0.36 A/cm² reached for 1A$_i$, later stabilising at 0.41 A/cm² , at the applied 0.9 V (Figure 5.4), is slightly lower in comparison to the current density obtained in Figure 5.2 (0.52 A/cm²) at similar potential (0.9 V) for the 1A$_i$ MEA. This can be ascribed to the difference in

operating history between the 1A$_i$ MEA and Nafion®115 and the likeliness of an insufficient break-in procedure. The current densities obtained in the range of 0.41 A/cm² at 0.9 V, before and after voltage stepping (Figure 5.5), was found to support the observation regarding the blend A-MEA's performance during voltage stepping at 80 °C.

It can be summarised that both membranes 1A$_i$ and N115 showed minimal degradation during voltage stepping operations with regard to the constant current densities (steady operation) detected for the duration of the 250 cycles (Figure 5.4), with the exception of the temporary improved performance noted for 1A$_i$ at 80 °C. It can thus be concluded that both the membrane and catalyst in these instances remained relatively stable [26] for the amount of voltage cycles applied in the study. The results have also highlighted that the MEA break-in procedure should be optimised for future application in the SO$_2$ electrolyser.

Polarisation curves were recorded both before and after the voltage stepping at 80 and 95 °C as shown in Figure 5.5 and Figure 5.6. The influence of operation temperature on the performance of the membranes (current densities obtained) is clearly visible for the blend membrane 1A$_i$ (Figure 5.5), while more comparable for the N115 (Figure 5.6) in the lower current density region, below 0.25 A/cm², and in support of the observations made in Figure 5.4.
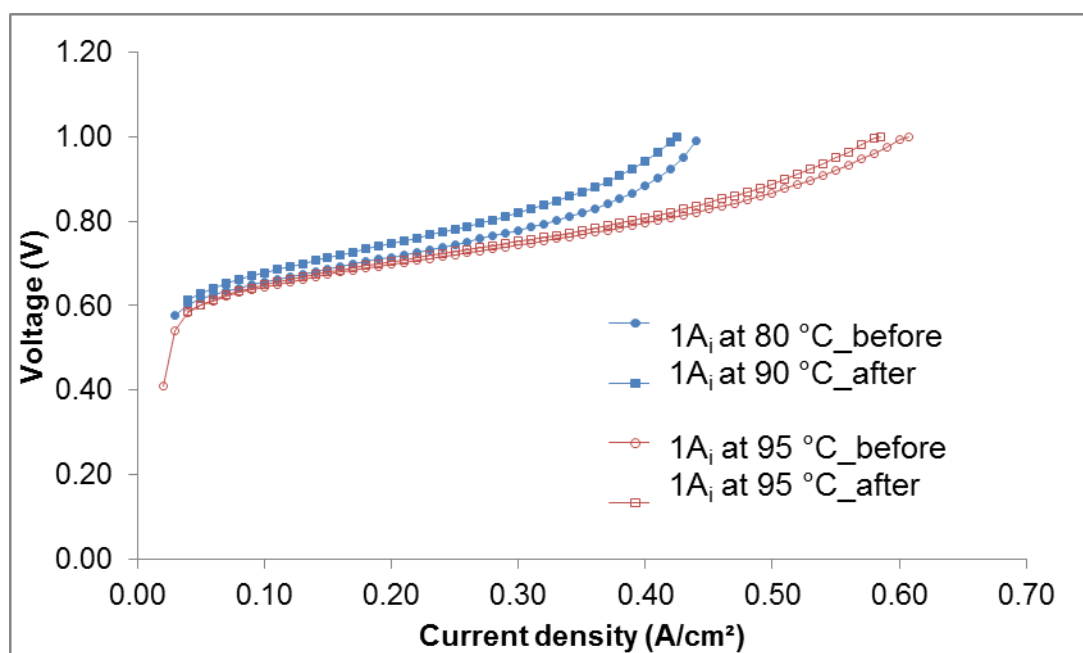
Figure 5.5: Polarisation curves recorded for membrane 1A$_i$ before and after voltage stepping at 80 and 95 °C.

In both sets (80 and 95 °C) of the polarisation curves recorded after voltage stepping for membrane 1A$_i$, a slight decrease in performance is noted for the current densities obtained (Figure 5.5). Furthermore, the noted current densities at 80 ºC after voltage stepping were obtained at higher voltage. The large increase in current densities reached before and after voltage stepping at higher operating temperatures (95 °C) is in accordance with the electrolysis data discussed earlier in the study for the blend membrane 1A$_i$. It can be summarised from Figure 5.4 and Figure 5.5 that the MEA of 1A$_i$ remained relatively stable after being subjected to increased stress at high temperatures (95 °C).
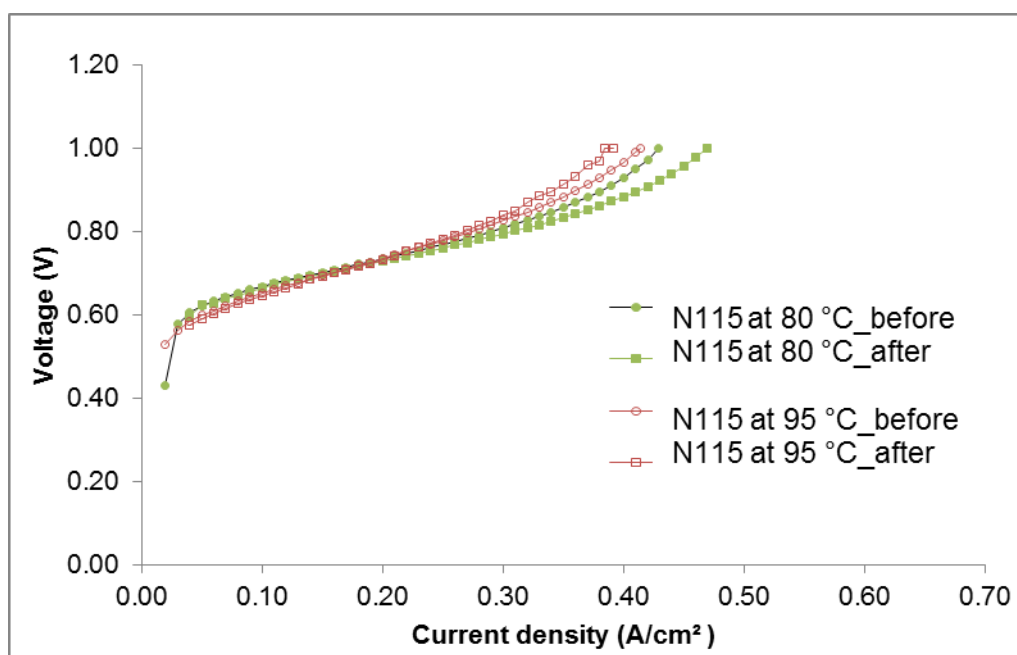
Figure 5.6: Polarisation curves recorded for Nafion®115 before and after voltage stepping at 80 and 95 °C.

In contrast to membrane 1A$_i$, the N115 membrane showed an improved performance in the current densities obtained after voltage stepping at 80 °C (Figure 5.6). As observed in earlier studies [26], this is likely due to the conditioning effect of the voltage stepping applied and the increased hydration period, as mentioned before. However, at 95 °C it is apparent that the higher temperature operation conditions within the SO$_2$ electrolyser were not ideal for N115, as discussed before, and a decreased performance was observed in the higher current density (0.25 A/cm²) region.

5.3.3 Characterisation of membrane after electrolysis

SEM-EDX and TEM micrographs were taken of the membrane cross-sections after electrolysis and voltage stepping was performed at 80 °C to compare with images obtained before electrolysis. This allows for an evaluation of the possible structural changes and sulfur deposition the membranes might have underwent during the operation of voltage stepping.

Cross-section images obtained with the use of a backscatter electron detector (BSE) in the SEM for the membranes $1A_i$ and N115 after voltage stepping are shown in Figure 5.7 and Figure 5.8, respectively. Backscattered electrons have the advantage that they are sensitive to the atomic mass of the nuclei they scatter from [42]. As a result, the heavier elements, which backscatter more efficiently, will appear brighter than the lighter elements, as observed in Figure 5.7(a) for the platinum catalyst visible as the white band between the membrane and micro-porous layer [24]. Another sample was prepared (Figure 5.7 (b, c)) from which the GDE was removed from the MEA after electrolysis for analysis of the membrane only. Upon higher magnification of the membrane $1A_i$ after electrolysis, an accumulation of elemental sulfur (white spots) was detected by EDS in the middle of the membrane (Figure 5.7(b)). The white spots in this instance were confirmed to be sulfur as the elemental analysis did not detect any platinum (data not shown) for the scanned area of the membrane as depicted in Figure 5.7(b), but instead increased sulfur content was noted. This increase in sulfur, relatively measured at 14.5 % in comparison to the 3.3 % before electrolyser operations, is visible as the white band with the formation of holes (black spots, 2-6 µm) in the membrane material (Figure 5.7(b)).
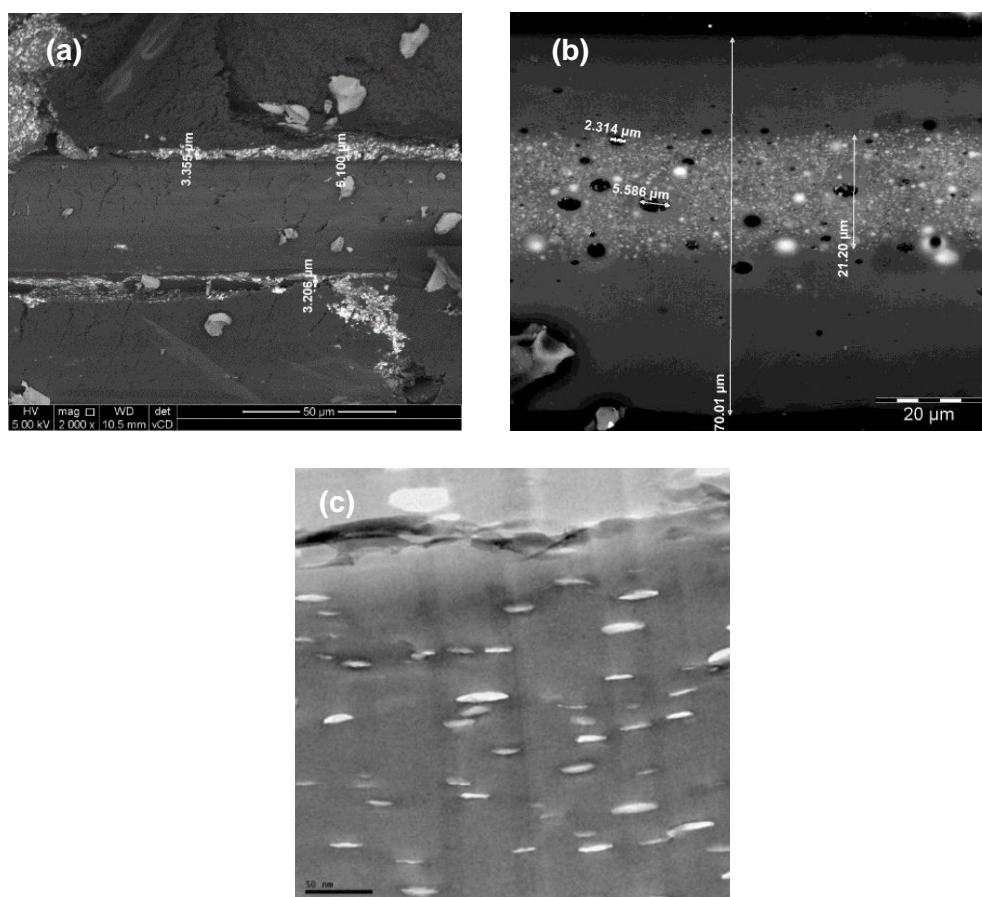
Figure 5.7: Cross-sectional images obtained for the blend membrane 1A$_i$ MEA with SEM (a) and magnified images obtained of membrane 1A$_i$ (GDE removed) with SEM (b) and using TEM micrographs (c) after voltage stepping operations in the SO$_2$ electrolyser at 80 °C.

This phenomenon is further supported by the TEM micrograph taken for the membrane 1A$_i$ (GDE removed) after electrolysis in Figure 5.7(c), indicative of the membrane's (structural) degradation. Small tears are visible (white tears) under TEM inspection (Figure 5.7(c)) of the cross-section of membrane 1A$_i$s. The same observations were made under SEM and TEM inspection for the cross-section of N115 after voltage stepping, as depicted in Figure 5.8. White and dark spots are detected in the middle of the membrane (Figure 5.8(a)), where upon higher magnification (Figure 5.8 (b)) it becomes evident that small holes (white spots/tears) are present in the membrane, also indicating structural degradation, although to a lesser extent (Figure 5.8(c)) than that detected for membrane 1A$_i$. As these holes and tears were not present in the SEM and TEM images taken of the membranes before electrolysis (images not shown, smooth surface with no holes detected), it is ascribed to electrolyser operations and were thus not due to the method of synthesis. It appears that, after voltage stepping in the electrolyser, a band of small holes (dark spots (SEM) and white tears (TEM)) accumulate in the middle of the membrane, accompanied by the measured increase in sulfur content (white spots, supported by elemental analysis). This is likely due to residual H$_2$SO$_4$

entrapped in the membrane sample after removal from the electrolyser operations, as the membranes were used as is and not rinsed before electron microscopy inspections.
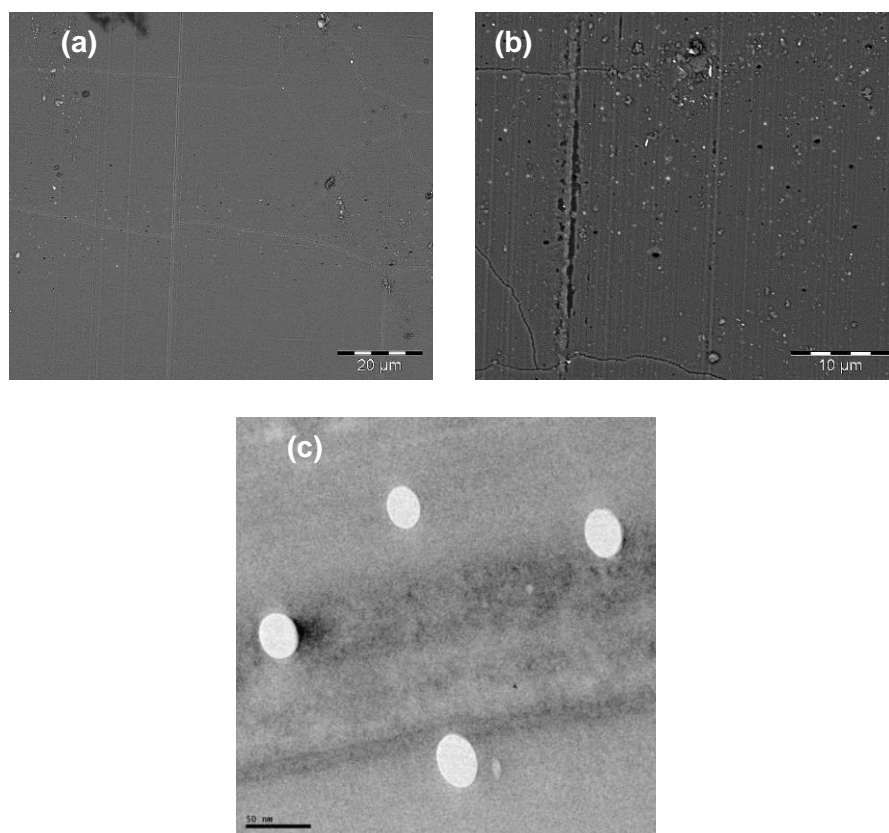
Figure 5.8: Cross-sectional SEM images obtained for the N115 membrane (a, b) and TEM micrographs (c) after voltage stepping operations in the SO$_2$ electrolyser at 80 °C.

The small holes forming after electrolysis can possibly be ascribed to the dissolution of membrane fragments during operation within the SO$_2$ electrolyser [4, 36]. However, the stability observed for 1A$_i$ and Nafion®115 during and after voltage stepping (Section 5.3.2) suggests that the structural degradation observed in TEM and SEM images (Figure 5.7 and Figure 5.8) had a negligible effect on the electrolyser performance of the membranes during the course of the study.

The thermal stabilities of the membrane 1A$_i$ and Nafion®115 were evaluated after voltage stepping operations at 80 and 95 °C and compared with the TGA curves previously obtained for the membranes, as presented in Figure 5.9 and Figure 5.10.
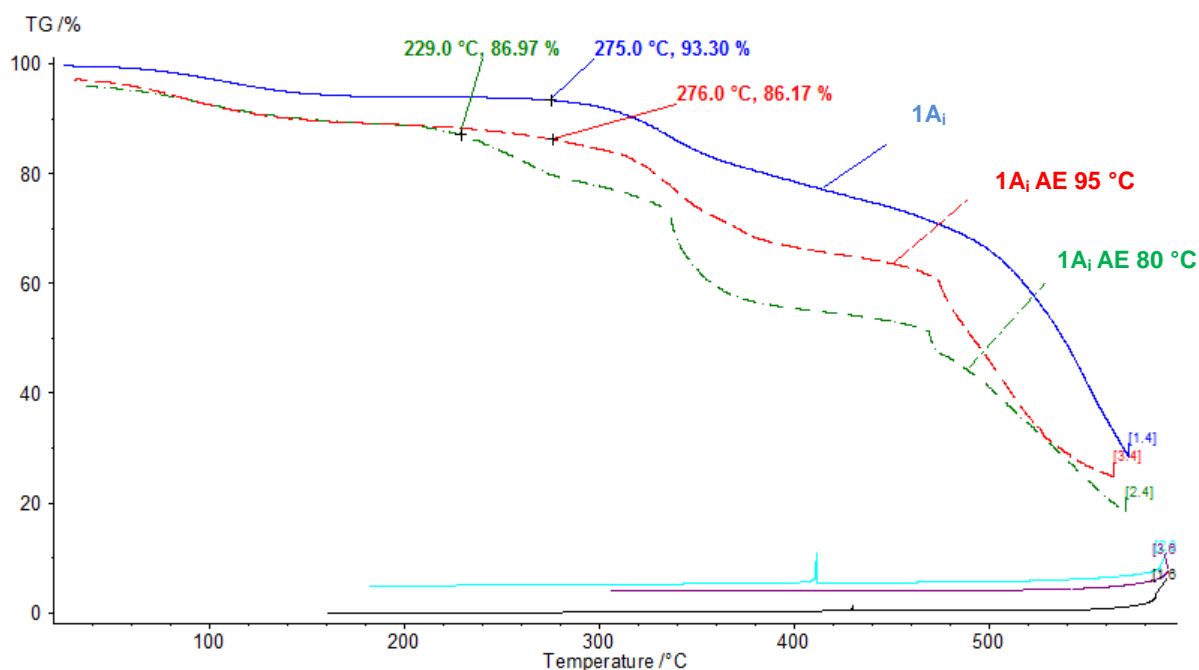
Figure 5.9: Thermal degradation of blend membrane 1Aᵢ before and after voltage stepping at 80 and 95 °C.

In Figure 5.9 one can see that the significant membrane degradation (strong weight decrease >200 °C) observed for the membrane $1A_i$ after operations in the electrolyser at 80 °C in comparison to the TGA curve recorded for the operations at 95 °C are quite different. The TGA curve after voltage stepping at 95 °C is more similar to membrane $1A_i$ before electrolysis operations, where the strong weight decrease is only noted from >300 °C. This is in support of the observations during the electrolysis experiments (Figure 5.4 and Figure 5.5) where the decrease in performance of the membrane after at 80 °C is greater than at 95 °C. It is suggested that this is likely due to the partial sulfonation of the BrPAE-1 (partially fluorinated) membrane component at 95 °C in the acidic environment of H_2SO_4 produced, which leads to an increase in the thermal stability of its backbone. This is supported by observations in Chapter 2 of sulfonation of the BrPAE-1 blend component by means of % weight gain and furthermore confirmed through TGA-FTIR measurements after an H_2SO_4 treatment (80 wt%) at 100 °C (120 hours). Subsequently, the treatment of these membranes in 80 wt% sulfuric acid at 95 °C, after membrane formation, can be considered a good membrane pre-electrolysis treatment procedure in the future.

The thermal degradation curves recorded for Nafion®115 after voltage stepping report a good thermal stability as can be seen in Figure 5.10. The differences noted after treatment for the obtained weight losses at the starting point of degradation (Figure 5.10) are considered insignificant after voltage stepping at 80 and 95 °C.
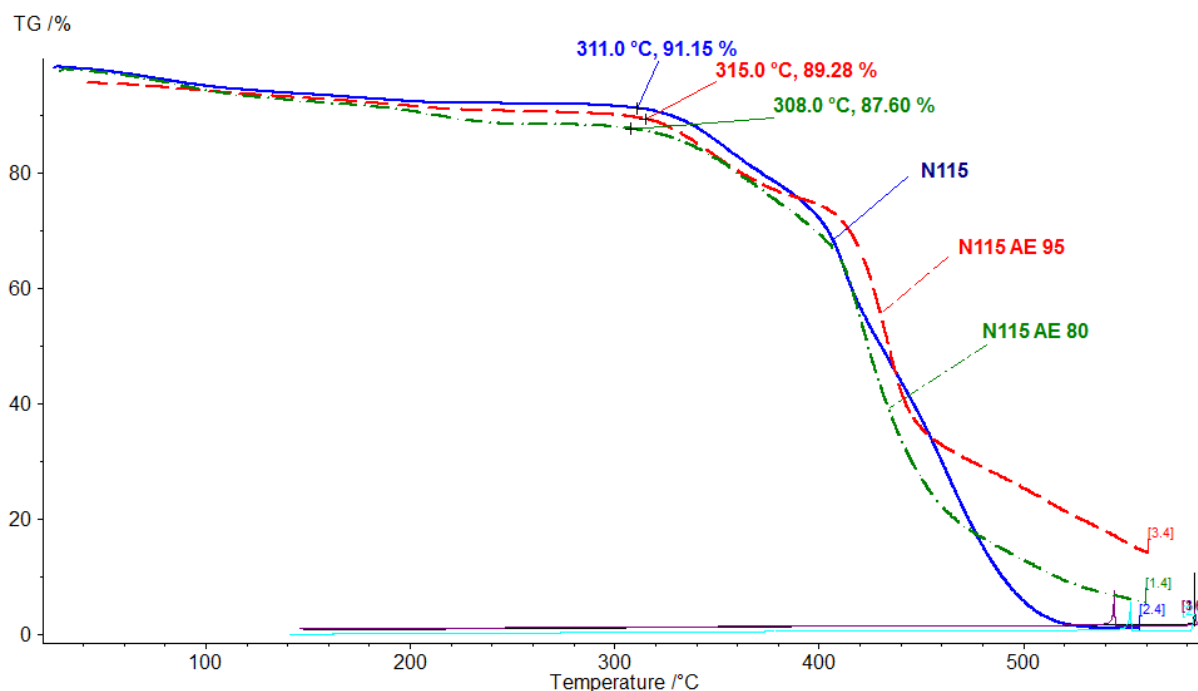
Figure 5.10: Thermal degradation of membrane Nafion®115 before and after electrolysis and voltage stepping operations at 80 and 95 °C.

It should, however, be mentioned that the start of degradation temperatures determined for the membranes $1A_i$ and Nafion®115 after electrolysis correspond with the data summarised in Table 5.3 (Figure 5.1) for the membranes after acid treatment, with the exception of $1A_i$ at 80 °C. The start of degradation temperature is noted to be 46 °C lower for $1A_i$ after electrolysis in comparison to after the acid treatment, which could be indicative of polymer degradation during electrolysis operation at 80°C. Interestingly enough, after electrolysis operation at 95°C, the membrane TGA degradation onset is at a higher temperature than after electrolysis at 80°C (Figure 5.9). An explanation for this different behaviour is partial sulfonation of the membrane in the PAE blend moiety at the higher electrolysis temperature (Chapter 2, Section 2.3.2), which protects the membrane $1A_i$ from earlier TGA degradation.

However, apart from the TGA observed temperature change, it is clear that the membrane $1A_i$ (SFS-F_6PBI-BrPAE-1) has performed better in the SO_2 electrolyser (at 80 °C), than previously studied PBI-blended membranes studied within our group (current densities of 0.54 A/cm² attained in comparison to 0.33 A cm^{-2} at 1 V for SFS-F_6PBI blend membranes) [24]. Furthermore, the blend $1A_i$ MEA's durability, measured through voltage cycling experiments, , also proves superior in terms of the current density obtained for the duration of the experiment (0.40 to the approximately 0.15 A/cm² obtained respectively, after 250 cycles), compared to similar PBI-blended membranes (base excess) from earlier studies [26]. In conclusion, the performance of membrane $1A_i$ also proved more energy efficient than the commercially available Nafion®115 at 80 and 95 °C within

our SO_2 electrolysis test station (Section 5.3.2), while proving comparable in the chemical stability aspects investigated (Section 5.3.1).

5.4 Conclusion

Lastly, the acid stability of partially- and non-fluorinated sulfonated polymer components (SFS and sPPSU) blended with basic PBI (PBIOO and F_6PBI) with d bromo-methylated polymers (BrPAE-1/2) with EMIm was included in this chapter. Characterisation of the different blend membranes confirmed the findings of Chapter 4, whereby blends containing only partially fluorinated blend components (SFS-F_6PBI-BrPAE-1), specifically blend membrane 1A$_i$, proved most stable with insignificant weight and thickness changes obtained after the 80 wt % H_2SO_4 treatment at 80 and 95 °C. Subsequently, 1A$_i$ was tested in the SO_2 electrolyser at 80 and 95 °C and compared with Nafion® 115. The polarisation curves obtained at 80 °C for the membrane 1A$_i$ indicated an improved SO_2 electrolyser performance in comparison to both similar PBI-containing blends in previous studies and the commercial Nafion® 115. At 95 °C, a further improvement in current densities achieved was detected at 0.63 A cm^{-2} for 1A$_i$ in comparison to the 0.42 A cm^{-2} reached by Nafion®115 at 1 V. This serves to support the potential for higher temperature electrolyser application of the partially fluorinated blend membrane in future studies. The membranes were also subjected to voltage stepping and both proved stable for the duration of the 250 cycles as minimal decrease in current densities was noted. To conclude, the membrane 1A$_i$ (Chapter 5) and membranes B$_i$ and C$_i$ (Chapter 4) have been confirmed both chemically and thermally stable and sufficiently conductive for further testing in SO_2 electrolysis above 100 °C and to be further investigated in Chapter 6.

5.5 References

[1] Brey JJ, Brey R, Contreras I, Carazo AF. Roll-out of hydrogen fueling stations in Spain through a procedure based on data envelopment analysis. International Journal of Hydrogen Energy. 2014;39:4116-22.

[2] Gorensek MB, Summers WA. Hybrid sulfur flowsheets using PEM electrolysis and a bayonet decomposition reactor. International Journal of Hydrogen Energy. 2009;34:4097-114.

[3] Colon-Mercado HR, Elvington MC, Hobbs DT. FY08 Membrane Characterization Report for the hybrid Sulfur Electrolyzer. Contract Number DE-AC09-08SR22470. 2008.

[4] Elvington MC, Colón-Mercado H, McCatty S, Stone SG, Hobbs DT. Evaluation of proton-conducting membranes for use in a sulfur dioxide depolarized electrolyzer. Journal of Power Sources. 2010;195:2823-9.

[5] Colón-Mercado HR, Hobbs DT. Catalyst evaluation for a sulfur dioxide-depolarized electrolyzer. Electrochemistry Communications. 2007;9:2649-53.

[6] Sivasubramanian P, Ramasamy RP, Freire FJ, Holland CE, Weidner JW. Electrochemical hydrogen production from thermochemical cycles using a proton exchange membrane electrolyzer. International Journal of Hydrogen Energy. 2007;32:463-8.

[7] Brecher LE, Spewock S, Warde CJ. The Westinghouse Sulfur Cycle for the thermochemical decomposition of water. International Journal of Hydrogen Energy. 1977;2:7-15.

[8] Jayakumar JV, Gulledge A, Staser JA, Kim C-H, Benicewicz BC, Weidner JW. Polybenzimidazole Membranes for Hydrogen and Sulfuric acid Production in the Hybrid Sulfur Electrolyzer. ECS Electrochemistry Letters. 2012;1:F44-F8.

[9] Gorensek MB, Staser JA, Stanford TG, Weidner JW. A thermodynamic analysis of the SO_2/H_2SO_4 system in SO_2-depolarized electrolysis. International Journal of Hydrogen Energy. 2009;34:6089-95.

[10] Gorensek MB. Hybrid sulfur cycle flowsheets for hydrogen production using high-temperature gas-cooled reactors. International Journal of Hydrogen Energy. 2011;36:12725-41.

[11] Asensio JA, Sanchez EM, Gomez-Romero P. Proton-conducting membranes based on benzimidazole polymers for high-temperature PEM fuel cells. A chemical quest. Chemical Society Reviews. 2010;39:3210-39.

[12] Chandan A, Hattenberger M, El-kharouf A, Du S, Dhir A, Self V, et al. High temperature (HT) polymer electrolyte membrane fuel cells (PEMFC) – A review. Journal of Power Sources. 2013;231:264-78.

[13] Higashihara T, Matsumoto K, Ueda M. Sulfonated aromatic hydrocarbon polymers as proton exchange membranes for fuel cells. Polymer. 2009;50:5341-57.

[14] Li Q, Jensen JO, Savinell RF, Bjerrum NJ. High temperature proton exchange membranes based on polybenzimidazoles for fuel cells. Progress in Polymer Science. 2009;34:449-77.

[15] Yang C, Costamagna P, Srinivasan S, Benziger J, Bocarsly AB. Approaches and technical challenges to high temperature operation of proton exchange membrane fuel cells. Journal of Power Sources. 2001;103:1-9.

[16] Kondratenko MS, Gallyamov MO, Khokhlov AR. Performance of high temperature fuel cells with different types of PBI membranes as analysed by impedance spectroscopy. International Journal of Hydrogen Energy. 2012;37:2596-602.

[17] Bose S, Kuila T, Nguyen TXH, Kim NH, Lau K-t, Lee JH. Polymer membranes for high temperature proton exchange membrane fuel cell: Recent advances and challenges. Progress in Polymer Science. 2011;36:813-43.

[18] Schoeman H, Krieg HM, Kruger AJ, Chromik A, Krajinovic K, Kerres J. H_2SO_4 stability of PBI-blend membranes for SO_2 electrolysis. International Journal of Hydrogen Energy. 2012;37:603-14.

[19] Peach R, Krieg HM, Krüger AJ, van der Westhuizen D, Bessarabov D, Kerres J. Comparison of ionically and ionical-covalently cross-linked polyaromatic membranes for SO_2 electrolysis. International Journal of Hydrogen Energy. 2014;39:28-40.

[20] Schönberger F, Chromik A, Kerres J. Partially fluorinated poly(arylene ether)s: Investigation of the dependence of monomeric structures on polymerisability and degradation during sulfonation. Polymer. 2010;51:4299-313.

[21] Xing J, Kerres J. Improved performance of sulphonated polyarylene ethers for proton exchange membrane fuel cells. Journal of Membrane Science. 2006;17 591-7.

[22] Morandi CG, Peach R, Krieg HM, Kerres J. Novel morpholinium-functionalized anion-exchange PBI-polymer blends. Journal of Materials Chemistry A. 2015;3:1110-20.

[23] Kerres J, Ullrich A, Hein M, Gogel V, Friedrich KA, Jörissen L. Cross-Linked Polyaryl Blend Membranes for Polymer Electrolyte Fuel Cells. Fuel Cells. 2004;4:105-12.

[24] Krüger AJ, Cichon P, Kerres J, Bessarabov D, Krieg HM. Characterisation of a polyaromatic PBI blend membrane for SO_2 electrolysis. International Journal of Hydrogen Energy. 2015.

[25] Kruger AJ, Krieg HM, van der Merwe J, Bessarabov D. Evalauation of MEA manufacturing parameters using EIS for SO_2 electrolysis. International Journal of Hydrogen Energy. 2014;39:18173-81.

[26] Krüger AJ, Kerres J, Bessarabov D, Krieg HM. Evaluation of covalently and ionically cross-linked PBI-excess blends for application in SO_2 electrolysis. International Journal of Hydrogen Energy. 2015;40:8788-96.

[27] Peach R. Characterisation of proton exchange membranes in an H_2SO_4 environment. North-West University, Potchefstroom 2520, South Africa: North-West University, Potchefstroom campus; 2014.

[28] Krüger AJ, Krieg HM, van der Merwe J, Bessarabov D. Evaluation of MEA manufacturing parameters using EIS for SO2 electrolysis. International Journal of Hydrogen Energy. 2014;39:18173-81.

[29] Chromik A, Kerres JA. Degradation studies on acid–base blends for both LT and intermediate T fuel cells. Solid State Ionics. 2013;252:140-51.

[30] Noshay A, Robenson LM. Sulphonatedpolysulphone. Journal of Applied Polymer Science. 1976;20:1885-903.

[31] Kerres JA, Xing D, Schönberger F. Comparative investigation of novel PBI blend ionomer membranes from nonfluorinated and partially fluorinated poly arylene ethers. Journal of Polymer Science Part B: Polymer Physics. 2006;44:2311-26.

[32] Kerres J, Zhang W, Jörissen L, Gogel V. Application of Different Types of Polyaryl-Blend-Membranes in DMFC. Journal of New Materials for Electrochemical Systems. 2002;5:97-107.

[33] Kreuer KD. On the development of proton conducting polymer membranes for hydrogen and methanol fuel cells. Journal of Membrane Science. 2001;185:29-39.

[34] Kerres JA. Development of ionomer membranes for fuel cells. Journal of Membrane Science. 2001;185:3-27.

[35] Yang B, Manthiram A. Sulfonated Poly(ether ether ketone) Membranes dor Direct Menthanol Fuel Cells. Electrochemical and Soild-state Letters. 2003;6:A229-A31.

[36] Krüger AJ, Cichon P, Kerres J, Bessarabov D, Krieg HM. Characterisation of a polyaromatic PBI blend membrane for SO_2 electrolysis. International Journal of Hydrogen Energy. 2015;40:3122-33.

[37] Jannasch P. Recent developments in high-temperature proton conducting polymer electrolyte membranes. Current Opinion in Colloid & Interface Science. 2003;8:96-102.

[38] Savinell R, Yeager E, Tryk D, Landau U, Wainright J, Weng D, et al. A Polymer Electrolyte for Operation at Temperatures up to 200°C. Journal of The Electrochemical Society. 1994;141:L46-8.

[39] Garrick RT, Gulledge A, Staser JA, Benicewicz BC, Weidner JW. Polybenzimidazole Membranes for Hydrogen Production in the Hybrid Sulfur Electrolyzer. ECS Transactions. 2015;66:31-40.

[40] Staser JA, Ramasamy RP, Sivasubramanian P, Weidner JW. Effect of water on the electrochemical oxidation of gas-phase SO_2 in a PEM electrolyzer for H_2 production. Electrochemical and Soild-state Letters. 2007;10:E17-9.

[41] Staser JA, Weidner JW. Effect of Water Transport on the Production of Hydrogen and Sulfuric Acid in a PEM Electrolyzer. Journal of The Electrochemical Society. 2009;156:B16-B21.

[42] Egerton RF. Physical Priciples of Electron Microscopy: An Introduction to TEM, SEM and AEM.: Springer; 2005.

Chapter Overview

From the respective blend membranes (1A, 1B and 1C) studied in Chapter 4, the blend membranes $1A_i$, $1B_i$ and $1C_i$ were found chemically and thermally most stable while membranes $1A_i$ and $1C_i$ displayed the highest conductivities. It was, however, decided to include $1B_i$ for a comprehensive comparison between the membrane types (A, B and C) and their suitability specifically for SO_2 electrolysis application above 100 °C. Furthermore, it was concluded in Chapter 5 that the combination of partially fluorinated polymer blend components SFS, F_6PBI and BrPAE-1 with the EMIm, yielding the blend membrane $1A_i$, displayed the highest SO_2 electrolyser performance when compared to both similar PBI-containing blends (from earlier studies) and the commercial Nafion® 115 at 80 and 95 °C. In this chapter, the blend membrane $1A_i$ was first tested at 120 °C in the SO_2 electrolyser (Section 6.3.1), comparing the modified electrolysis system running at 120 °C to the operation and performance of $1A_i$ at 80 °C (Chapter 5). This was followed (Section 6.3.2) by an evaluation of the performance of the selected blend membranes $1B_i$ and $1C_i$ at 120 °C for comparison to blend membrane $1A_i$. In Section 6.3.3, the influence of the H_2O flow rate on voltages achieved and products produced for the selected blend $1A_i$ was further determined and characterised using electrochemical impedance spectroscopy (EIS) measurements. This was followed by a study on the effect of MEA variables, such as membrane thickness and catalyst loading, on the electrolysis performance (voltages achieved and products produced) of blend $1A_i$ at 120 °C (Section 6.3.4). The study was concluded with steady state (voltage monitoring) and voltage cycling measurements for the blend $1A_i$ to establish future prospects for longer-term operations for the PBI-blend membranes at 120 °C in SO_2 electrolysis. Supplementary graphs and tables were listed under Appendix C for support of the findings of Chapter 6.

---

[3]Data was presented in the following proceeding: Peach R, Krieg HM, Krüger AJ, Bessarabov D, Kerres JA. PBI-Blended Membrane Evaluated in High Temperature SO_2 Electrolyzer. ECS Transactions. 2018; 85:21-8.

6.1 Introduction

The growing need for environmentally and economically improved energy alternatives has been driving the on-going research regarding hydrogen as energy carrier and commodity within industrial processes [1]. A well-known alternative for large scale hydrogen production the, Hybrid Sulfur (HyS) thermo-chemical cycle, using a proton exchange membrane-based (PEM) electrolyser, has received increased attention over the past years [1-7].

The Westinghouse Electric Corporation first presented the HyS process in the 1970s. It comprises a high temperature step where H_2SO_4 is decomposed to produce SO_2, O_2 and H_2O [8, 9], and a lower temperature process step where the SO_2 is fed to the anode of the electrolyser where it is oxidised to produce H_2SO_4 at the anode and H_2 at the cathode in the presence of water [10, 11]. The overall reaction for the second step, i.e. the SO_2 electrolyser can be presented as

$$SO_2 + 2\,H_2O \rightarrow H_2SO_4 + H_2 \qquad E^o = 0,158 \text{ V vs. SHE} \qquad [6\text{-}1]$$

While the HyS process is aimed at producing clean hydrogen at efficiencies higher than water electrolysis, these efficiencies can be further enhanced by operating at higher temperatures [10, 12, 13]. This holds the potential benefit of faster electrode kinetics and simplified water management, overcoming technical challenges typically encountered when operating below 100 °C [14-16].

At these elevated temperatures (>100 °C), the PEM must be able to maintain both a high proton conductivity and acid stability within the SO_2 operating environment. Perfluorinated sulfonic acid (PFSA) membranes such as Nafion® have limited suitability above 100 °C due to humidification requirements and subsequent dehydration leading to increased membrane resistance [17, 18]. For these applications, polybenzimidazole-type (PBI) membranes have been considered most promising due to their known thermal stability and high ionic conductivity even with limited water supply [19-21].

In Chapter 2, the polymers selected and synthesised were characterised and it was shown that, by and large, they are suitable for SO_2 electrolysis application (H_2SO_4 stability). While cross-linking of polymer components showed some improvement in both chemical and thermal stabilities (decreased weight losses and higher degradation temperatures, Chapter 3), further improvement with regards to conductivity (IEC) was also needed. Therefore, a combination of various polymer components and modes of cross-linking were investigated in Chapter 4 where the blend membranes (1A, 1B and 1C) proved suitable with satisfactory H_2SO_4 stability in view of the minimal weight, IEC and TGA changes reported after treatment.

It was noted that the F_6PBI-excess membranes (blend B) was more suitable when also considering the oxidative (FT) and solvent extraction stability results (Section 4.3.1-3). The BrPAE-excess membranes (C) more covalent bonds also displayed sufficient acid stability. The larger SFS-containing blend membranes (A), yielded the highest proton conductivity (A>C>B), most probably due to the presence of the larger number of free $-SO_3H$ groups. It was noted that the partial sulfonation that occured when combining BrPAE-1 and EMIm during H_2SO_4 treatment benefitted the conductivity of blend types $1A_i$, $1B_i$ and $1C_i$ without sacrificing stability (Chapter 4). This included an increase in proton conductivity for the blend membrane $1A_i$ without jeopardising the chemical and thermal stability of the membrane after H_2SO_4 treatment.

Subsequently, $1A_i$ was tested in the SO_2 electrolyser at 80 and 95 °C and compared with Nafion® 115 (Chapter 5). The polarisation curves obtained at 80 °C for the membrane $1A_i$ indicated an improved SO_2 electrolyser performance in comparison to both similar PBI-containing blends used in previous studies as well as the commercial Nafion® 115 [22]. It became evident that the cross-linked PBI-containing blend membranes possess the ability to conduct protons from the acid produced during electrolysis, insuring the continuous doping of the membrane during operation and an improved performance [10, 23].

In other studies, improvement of the SO_2-depolarised electrolyser (SDE) at operating temperatures above 100 °C has been achieved using a sulfonated PBI membrane [6, 7]. In their studies, the water vapor was fed jointly with the SO_2, either through humidification or by directly injecting the H_2O at the anode of the cell at the required flow rates (water stoichiometry), to ensure that an adequate concentration of H_2SO_4 is produced. Therefore, based on the chemical stability and conductivity results reported in Chapters 4 and 5, the ionic-covalently cross-linked and partially fluorinated blend components yielding membranes $1A_i$, $1B_i$ and $1C_i$ were selected for further SO_2 electrolysis tests at 120 °C.

When comparing the performance of $1A_i$, $1B_i$ and $1C_i$ in this chapter, it became apparent that the SFS-excess blend membrane $1A_i$ performed the best in terms of cell voltages (100-190 mV) over the applied current density range of 0.05-0.5 A/cm² at 120 °. Hence, after the initial comparison of the three membranes, it was attempted to further improve the SO_2 electrolyser performance specifically of only blend $1A_i$ at 120 °C by varying the H_2O flow rate (reactant feed), membrane thickness and catalyst loading. Polarisation curves, measurements of products (concentration and mmol/s produced) and EIS measurements facilitated the evaluation of $1A_i$'s performance by also comparing (a) the adjusted high temperature SO_2 electrolyser system with earlier work at 80 and 95 °C (Chapter 5), and (b) the available literature at temperatures above 100 °C for other PBI-type membranes [6]. Lastly, constant operations including steady state measurements at 0.3 and 0.5 A/cm² of 10-24 hours and voltage stepping (250 cycles) for the blend $1A_i$ at 120 °C were used to determine the operational stability of this novel blend membrane. Post-characterisation of the $1A_i$

MEA after voltage stepping experiments by means of TGA-FTIR and SEM-EDX was used to compare this membrane to the pre- and post-characterisation of the membrane material from Chapter 5 (SO_2 electrolysis at 80 and 95 °C).

6.2 Experimental

6.2.1 MEA preparation for SO_2

The membranes used ($1A_i$, $1B_i$ and $1C_i$) were prepared as discussed earlier (Section 4.2.2). MEAs (10 cm² active area) were prepared as described in Section 5.2.5 (Chapter 5), unless reported otherwise (1 mg Pt/cm², Section 6.3.4), to facilitate the comparison with the electrolysis results at 80 and 95 °C. For electrolysis above 100 °C, the doping procedure of the already hot-pressed MEAs was adjusted to a 5.0 M sulfuric acid solution for 2 days prior to use for comparison to literature reported for s-PBI at 110 °C [7]. The degree of doping was reported as a weight percentage increase of the prepared MEAs (Section 6.3.2 – 6.3.5).

6.2.2 SO_2 electrolyser set-up

The same basic system for SO_2 electrolyser operations at 80 and 95 °C, described in Section 5.2.5, was used for the experiments at 120 °C described in this chapter, only differing in terms of the water supply. At 80 and 95 °C (Chapter 5), pre-heated water was supplied to the cathode, while dry SO_2 was fed to the anode [24]. For electrolysis above 100 °C, the water was pumped through a coiled heater (120 °C) connected to the SO_2 supply line and fed directly to the cell anode. The flow rate of the H_2O was varied between 5, 10 and 15 mL/min (see also Section 6.3.2 - 6.3.5). An excess of SO_2 (200 mL/min) was supplied to ensure a constant voltage.

6.2.2.1 General electrolysis procedure

The cell was run for 1 hour (as was done in Chapter 5) to reach and stabilise at the operating temperature of 120 °C before measurements commenced. Polarisation curves were recorded by incrementally increasing the applied current density by 0.05-0.10 A/cm² every 90 s and measuring the corresponding cell voltage up to the limit of 1.1 V. Thereafter, the acid produced was collected at selected current densities (held for 5-10 min) while the volume H_2 produced (mL/min), was also determined as discussed in Section 6.3.2 and 0 to compare between the expected theoretical and experimental products measured (mass-balance), and to evaluate the overall efficiency of the electrolysis process. In specific cases, OCVs and EIS were reported (Section 6.3.2 and 0).

6.2.2.2 Steady State (Voltage monitoring)

To monitor the stability of the voltage for the blended membranes, the applied current density was kept constant for 10-24 hours at 0.3 and 0.5 A/cm^2. This also served to evaluate the need for pre-conditioning of the membranes by comparing the polarisation curves before and after voltage monitoring (Section 6.3.5).

6.2.2.3 Voltage stepping

The procedure for voltage stepping described in Chapter 5 (Section 5.2.5.2) was used, except that the experiments were performed at 120 °C and at a H$_2$O flow rate of 10 mL/min (Section 6.3.5).

6.2.2.4 EIS measurements

Galvanostatic electrochemical impedance spectroscopy (EIS) was used as developed earlier by van der Merwe et al. [25] to study the proton exchange during electrolysis. EIS data was obtained over the frequency range of 0.1-100 kHz by applying an AC current of 10% of the applied DC current. The equivalent circuit model (see Figure 6.1), illustrating the various SO$_2$ electrolyser components as developed by Krüger *et al.*, was used [26]. The model was used to fit the measured EIS data presented in Sections 6.3.3 and 6.3.4, providing information on the membrane resistance (Ohm), activation resistance (Charge) and mass transport limitations (Warburg), which was used to compare between various H$_2$O flow rates and other MEA variables.
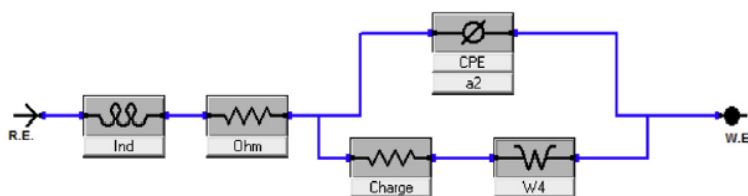
Figure 6.1: Equivalent circuit model used for SO$_2$ electrolysis modelling (Ind – Inductance, Ohm – Ohmic resistance, Charge- Charge transfer resistance, CPE – constant phase element and W – Warburg impedance) [26].

6.2.2.5 Post-characterisation

SEM-EDX and TGA-FTIR measurements were performed as mentioned in Section 5.2.5.3 to compare the stability of the membranes after the voltage stepping operations at 80 and 120 °C (Section 5.3.3).

6.3 Results and Discussion

Firstly (Section 6.3.1),the performance of the blend membrane $1A_i$s was assessed in the adjusted high temperature SO_2 electrolyser system and compared to results obtained earlier at 80 °C and 95 °C (Section 5.3.2). This was followed (Section 6.3.2) by a SO_2 electrolysis performance comparison of the selected blend membranes $1A_i$, $1B_i$ and $1C_i$, (Chapter 4) at 120 °C, before evaluating the influence of i) the H_2O flow rate in Section 6.3.3 and ii) the chosen MEA variables (membrane thickness and catalyst loading) in Section 6.3.4, on the SO_2 electrolyser performance. Lastly (Section 6.3.5), steady state measurements and voltage stepping was used to evaluate the suitability of the blend $1A_i$ for possible long-term operation at temperatures above 100 °C. Post-characterisation of the $1A_i$ MEA materials after SO_2 electrolysis at 120 °C was included (Section 6.3.5.3) and entailed SEM-EDX analysis and TGA-FTIR measurements.

6.3.1 Comparison of low and high temperature SO_2 set-ups using membrane $1A_i$

A comprehensive list of differences regarding the operations of the SO_2 electrolyser at 80 and 120 °C is presented in Table C-1 (Appendix C.1; see also the schematic representations of the electrolysis systems operated at 80 and 120 °C in Figure 1.3, Chapter 1). For an accurate evaluation of the performance of the prepared MEAs within the SO_2 electrolyser cell, three consecutive polarisation curves were measured for blend membrane $1A_i$ (thickness = ~60 µm), at both 80 and 120°C. For the triplicate experiments done at 80 and 120°C, the variation in voltage as a function of current densities was negligible with an average standard deviation of 0.013 V (1.7 %) and 0.010 V (1.4 %) at 80 and 120 °C, respectively (see Figure 6.2). This provided the repeatability achievable for polarisation curve measurements of $1A_i$ within the SO_2 electrolyser at both 80 and 120 °C. For further comparison, the results obtained from literature [6] when running an electrolyser at 110 °C using an s-PBI membrane were included (Figure 6.2).
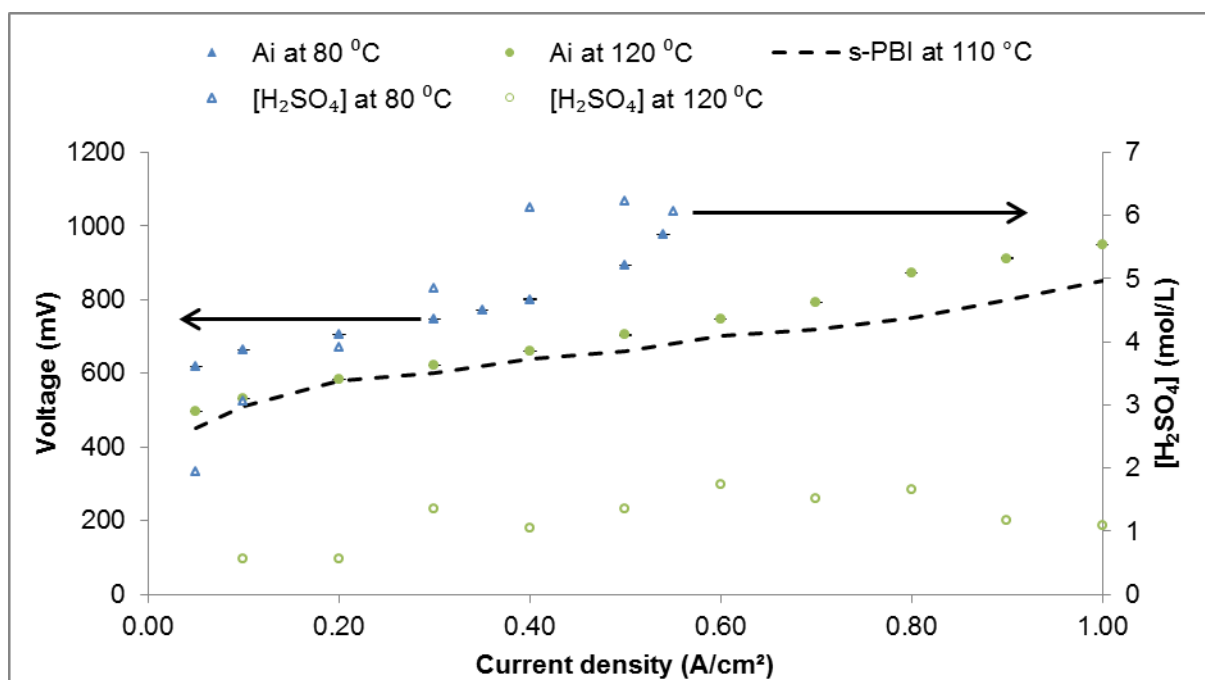
Figure 6.2: Polarisation curves recorded with the [H$_2$SO$_4$] produced for blend 1A$_i$ at 80 and 120 °C with varying SO$_2$ and H$_2$O flow rates. The literature values for a polarisation curve obtained with an s-PBI at 110 °C were included [6].

It is clear from Figure 6.2 that, by increasing the operational temperature at 0.5 A/cm^2 from 80 to 120 °C, the voltage decreased significantly from 0.89 V to 0.70 V (with 190 mV) for respective operation temperatures. This is an improvement on achieving the target operating conditions (0.6 V at 0.50 A/cm^2), determined by Gorensek et al. for efficiently producing hydrogen within the HyS process [11]. Furthermore, these results compare closely to the reported 0.66 V achieved at 0.5 A/cm^2 with an s-PBI membrane (~500 µm) at 110 °C in a similar SDE setup [6]. It should, however, be mentioned that the s-PBI MEA had a catalyst loading of 1 mg Pt/cm^2 in comparison to the 0.5 mg Pt C/cm^2 used in this section.

Furthermore, it remains to be determined whether the increase in performance noted for the membrane 1A$_i$ at 120 °C in Figure 6.2 is simply due to the increased operational temperature and subsequent faster kinetics, or due to the modified SO$_2$ electrolyser set-up and the manner in which the feed is supplied (directly to the anode). For this section of the work (Section 6.3.1), an initial flow rate of 150 mL/min SO$_2$ was maintained with 5 mL/min H$_2$O supplied, which was then increased (up to 250 mL/min for SO$_2$ and 17 mL/min for H$_2$O) with increasing current density in order to maintain a constant voltage on the system.

When considering Faraday's law, as defined by Equation [6-2] for the reaction rate in relation to the active area (A, m^2),

$$\frac{1}{A}\frac{d\,nA}{dt} = \frac{j}{n\,F}$$

[6-2]

Where j refers to the current density (A/cm^2) and n to the number of electrons, it is clear that the reagent provided or product formed, in other words the material undergoing electrochemical change, is in a rectilinear relationship with the current density achieved (N_A = It/ nF, with N_A – number of moles of reactant consumed or product formed, I – current (A), t time period (s), n – number of electrons and F = Faraday's constant = 96485.33289(59) C mol^{-1}).

Therefore, one would expect an increase in H_2O supply (directly to the anode for electrochemical reaction at 120 °C vs. diffusing across the cathode at 80 °C) to lead to an increased current at lower cell voltages as seen for blend A_i at 120 °C in Figure 6.2. It was also found that the H_2SO_4 (concentrations) produced during the polarisation curve measurement (Figure 6.2) were far lower than expected (Faraday's law), especially for the higher current density ($0.5 - 1.0$ A/cm^2) region.

6.3.2 SO_2 electrolysis of blend membranes ($1A_i$, $1B_i$ and $1C_i$) at 120 °C

To further evaluate the suitability of the selected blend compositions from Chapter 4, the blend membranes $1B_i$ and $1C_i$ were also added to $1A_i$.for SO_2 electrolyser operations at 120 °C, and compared with blend $1A_i$. The SO_2 and H_2O were supplied at flow rates of 200 and 5 mL/min, respectively. MEAs of relatively comparable membrane thicknesses and doping degrees (see Table 6.1) for the blend membranes were prepared as previously described (Section 6.2.1). The OCV and membrane resistance of the prepared MEAs are also listed in Table 6.1. The OCV was determined for each MEA (as a measure of the maximum resistance of the cell when no current is applied) before measuring the membrane resistance at 0.1 A/cm^2 to facilitate the comparison between the blend membranes. In this section, the SO_2 and H_2O feeds were kept constant at 200 and 5 mL/min, respectively, for the recording of polarisation curves.

Table 6.1: MEA properties of blend membranes for application in SO_2 electrolysis.

Membrane	Thickness	Doping	OCV	Membrane resistance
	(µm)	(wt %)	(mV)	(mOhm)
$1A_i$	45.0	150	177	7.76
$1B_i$	35.0	100	343	105
$1C_i$	30.0	120	190	16.8

Due to the comparable thicknesses, the blend membranes were doped to the same H_2SO_4 doping procedure as described in Section 6.2.1 [27]. The variation in attained doping was therefore probably due to the compositional differences of the blend membranes. As expected from the characterisation results discussed in Chapter 4, the SFS- and BrPAE-excess membranes ($1A_i$ and $1C_i$) were quicker to absorb H_2SO_4 (5 M, 2 days at room temperature) than the F_6PBI excess membrane ($1B_i$). In accordance with the conductivity data reported earlier (Chapter 4, Figure 4.4), the blend $1A_i$ showed the lowest membrane resistance and OCV corresponding to the highest doping (Table 6.1), followed by the blends $1C_i$ and $1B_i$.

The same trend could be observed for the polarisation curves recorded at 120 °C (see Figure 6.3). Starting at 0.05 A/cm², cell voltages of 385, 511 and 623 mV, respectively, were reported for membranes $1A_i$, $1C_i$ and $1B_i$.

In agreement with the conductivity results obtained for blend $1B_i$ (Figure 4.4) and the high membrane resistance (Table 6.1) measured for the doped $1B_i$ MEA, the PBI-excess blend had the worst electrolysis performance (only managing a current density maximum of 0.10 A/cm² before reaching 1 V) according to Figure 6.3. This could be ascribed to the absence of a sufficient number of proton conductive side groups ($-SO_3H$) within the blend membrane, and can likely be addressed in future by increasing the H_2SO_4 doping % (> 100 wt%).

Although similar cell voltages were achieved for blends $1A_i$ and $1C_i$ between 0.10 and 0.25 A/cm², the SFS-excess blend $1A_i$ displayed the best performance by reaching a maximum current density of 0.85 A/cm² at 1.06 V. It should also be mentioned that an overall improvement of between 100-190 mV was achieved when operating at 120 °C (vs. 80 °C) for the current density range 0.1-0.6 A/cm^2 [27]. During these polarisation studies, only between 1.5 and 2.5 M H_2SO_4 was produced. It is to be further investigated whether this is a consequence of the H_2O flow rate supplied directly to the anode (Section 6.3.3) or the membrane thickness (Section 6.3.4).
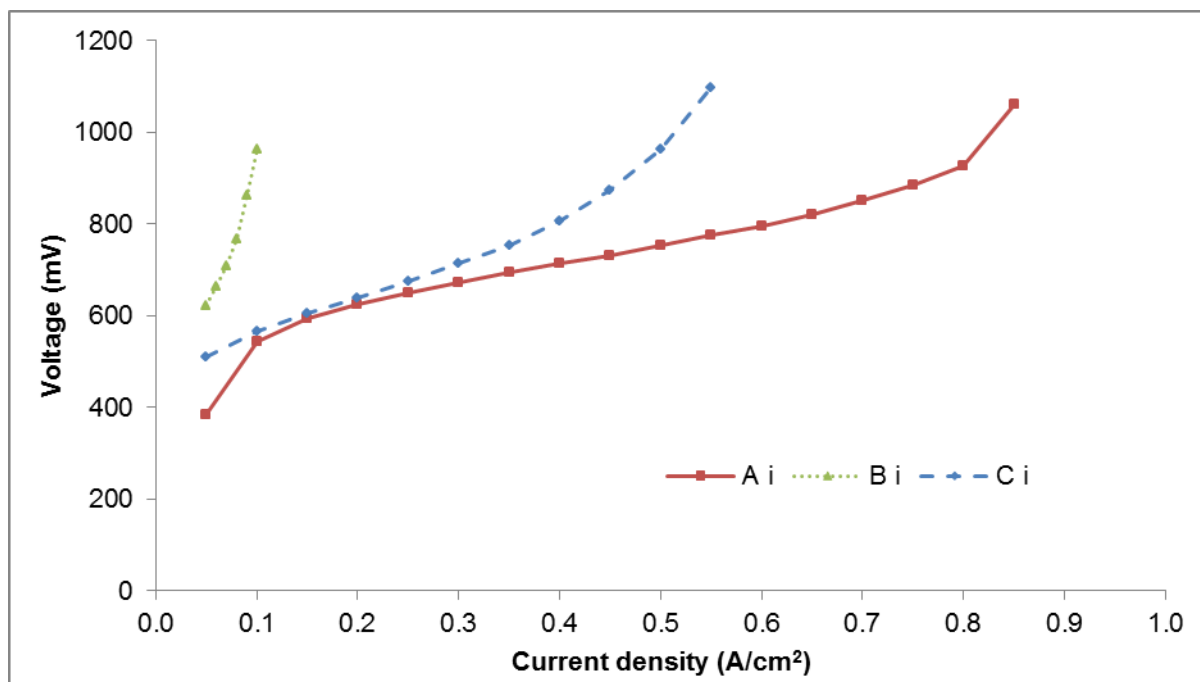
Figure 6.3: Polarisation curves recorded at 120 °C for the blends 1A$_i$, 1B$_i$ and 1C$_i$, with SO$_2$ supplied at 200 mL/min and H$_2$O at 5 mL/min directly to the anode.

After obtaining the polarisation curves, voltage monitoring was used to evaluate the steady state behaviour of the blend membranes 1A$_i$ and 1C$_i$ at the applied current density of 0.3 A/cm² for 10 hours as shown in Figure 6.4. For this experiment, 1B$_i$ was not included due to the poor electrolyser performance shown in Figure 6.3.
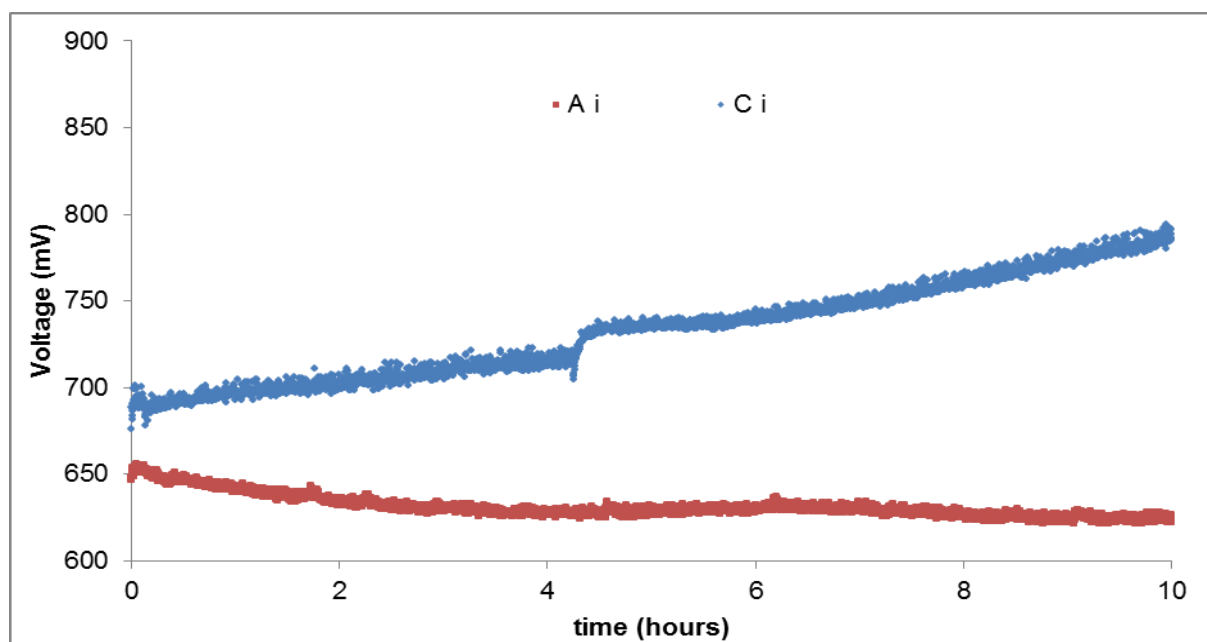
Figure 6.4: Voltage monitoring at 0.3 A/cm^2 for 10 hours for the blend membranes 1A$_i$ and 1C$_i$ at 120 °C.

During the voltage monitoring of blend 1A$_i$, a decrease of 25 mV was observed compared to the 100 mV increase noted for 1C$_i$ over the course of the 10 hour measurement. Polarisation curves recorded before and after the voltage monitoring for the blend membranes indicated that the steady state operation (constant current) served to condition the membrane to the extent where cell voltages decreased between 50-150mV for the applied current densities (Appendix C, Figure C-1). It should be added that the average [H$_2$SO$_4$] produced over this period was 2.4 and 1.8 M for MEAs 1A$_i$ and 1C$_i$, respectively. The steady state results (Figure 6.4) and the concentration of acid produced by the blends could be a result of the difference in doping of the MEAs (Table 6.1), which were 120 and 150 wt% for 1A$_i$ and 1C$_i$, respectively. The membrane resistance after voltage monitoring determined using EIS measurements, where the data was fitted with the proposed model presented in Section 6.2.2.4, yielded 6.60 and 12.8 mΩ for 1A$_i$ and 1C$_i$, respectively. In view of the significant lower resistance all further investigations of optimisation in the SO$_2$ electrolyser at 120 °C were done using only the blend membrane 1A$_i$.

6.3.3 Influence of H₂O flow rate on SO₂ electrolyser performance at 120 °C

For a clearer understanding of the effect of H_2O on cell performance, the H_2O flow rate was varied (5-15 mL/min) using the blend $1A_i$ at 120 °C. An excess of SO_2 was fed at 200 mL/min to ensure that only the influence of H_2O was observed as a reaction parameter during SO_2 electrolysis. EIS was used to differentiate between the membrane resistance, activation resistance and mass transport limitations for the varied reactant feeds and voltage stability inspections as described earlier [26]. For the experiments reported in this section, a new $1A_i$ membrane sheet was prepared with an average thickness of 60 µm. The H_2SO_4 doping resulted in an average of 90 ± 7 wt% increase for the $1A_i$ MEAs used in this section.

Initially, polarisation curves were obtained as a function of the H_2O flow rates (15, 10 and 5 mL/min) as shown in Figure 6.5. The flow rates selected were based on previous experiments (Section 6.3.1) which suggested stable voltages at current densities from 0.1 up to 1.0 A/cm² [27].
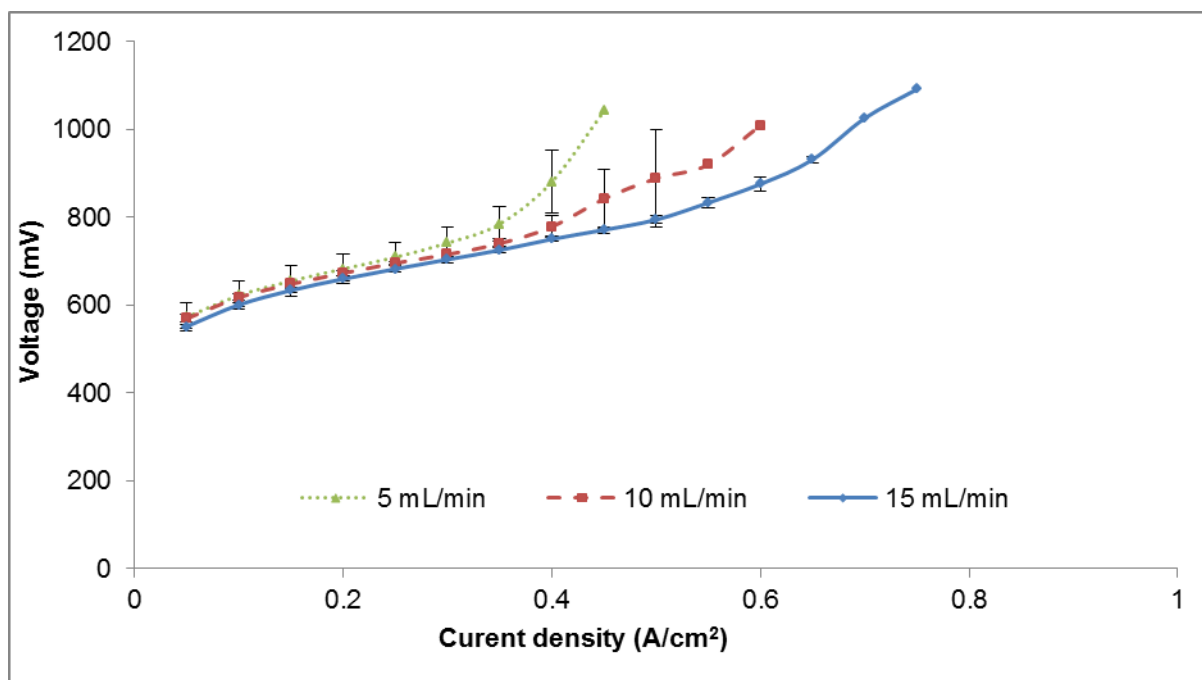
Figure 6.5: Average voltages reported for polarisation curves recorded at varying H₂O flow rates and a fixed SO₂ supply (200 mL/min) using membrane 1Aᵢ (60 µm).

For each flow rate, the repeatability (see error bars - Figure 6.5) was determined by recording three polarisation curves. It is clear that, in the lower current density region (< 0.3 A/cm²), the different flow rates of H_2O supply yielded comparable cell voltages (especially at 15 mL/min), which increased at current densities above 0.3 and 0.4 A/cm² for the 5 and 10 mL/min experiments, respectively, as confirmed by the increase in the error margin observed at the higher

current density regions (0.35-0.5 A/cm^2). At the lower flow rates (5 and 10 mL/min), higher voltages that could be ascribed to the decreased H_2O supply to the anode during the electrochemical reaction were obtained. This subsequently resulted in the production of a higher concentration sulfuric acid produced at 5 mL/min when compared to 15 mL/min as would have been expected (see Appendix C, Table C-2), which has also previously been reported to affect the cell voltage [18]. As mentioned previously, both the H_2SO_4 and H_2 produced at the different supplied H_2O flow rates were measured (mL/min) and presented in mmol/s (Table 6.2) for a comparative discussion on both the performance and products produced during SO_2 electrolysis at 120 °C.

Table 6.2: H_2SO_4 and H_2 produced (mmol/s) as a function of H_2O flow rates at various current densities.

A/cm^2	H_2SO_4 produced (mmol/s)			H_2 produced (mmol/s)		
	15 mL/min	10 mL/min	5 mL/min	15 mL/min	10 mL/min	5 mL/min
0.1	0.21	0.24	0.15	20.7	21.4	21.2
0.3	0.20	0.19	0.15	68.0	71.2	72.2
0.5	0.19	0.25	0.19	120	120	118
0.7	0.24	-	-	160	-	-
Average	0.21±0.02	0.23±0.03	0.16±0.02			

Although a more concentrated (mol/L) H_2SO_4 was measured at the H_2O flow rate of 5 mL/min, the total volume produced at 10 and 15 mL/min accounted for a higher mmol/s H_2SO_4 (Table 6.2). This was in agreement with Eq. [6-1] where it was deduced that, for every 1 mole SO_2 consumed, 2 moles of H_2O is required for the production of both H_2 and H_2SO_4 (1 mole relation). Hence it was expected that an increase in the H_2O flow rate would result in an increase in H_2SO_4 produced (at the anode), as the SO_2 supply was kept constant (200 mL/min) for the H_2O flow rates inspected. However, it was noted that the H_2 produced and measured (at the cathode) was relatively unaffected by the increase in supplied H_2O, but rather increased with applied current densities (Table 6.2). Therefore, Faraday's law (Eq. [6-2]) was applied to determine the theoretical (predicted) H_2SO_4 and H_2 mmol/s produced (Table 6.3) and compared this to the experimentally measured results for the different applied current densities.

Table 6.3: Theoretically determined H_2SO_4 and H_2 at applied current densities of 0.1, 0.3, 0.5 and 0.7 A/cm^2.

j (A/cm²)	0.1	0.3	0.5	0.7
$H_2SO_{4\,theo}$ (mmol/s)	0.31	0.93	1.55	2.18
H_2O_{theo} (mmol/s)	18.7	56.0	93.3	130

According to Table 6.3, it is clear that between 22 and 89 % less mmol/s H_2SO_4 was produced (Table 6.2) than had been predicted by Faraday's law, while 5.2-29 % mmol/s more H_2 was produced in the current density range (0.1-0.7 A/cm^2) investigated. Furthermore, a fluctuation in H_2SO_4 concentration for current densities 0.3 and 0.5 A/cm^2 was noted at 10 and 15 mL/min H_2O, respectively (Table 6.2). This was likely due to the excess H_2O fed to the anode being more than otherwise electrochemically required for the applied current density range.

Again using Faraday's law (Eq. [6-2]), the required amount (mL/min) of water that would theoretically be needed at a specific current density (A/cm^2) for a 10 cm^2 MEA could be calculated. For example, at 0.5 A/cm^2, 3.11 mol/min (18.66 mmol/s or 0.06 mL/min) water would be needed, confirming that even at 5 mL/min an excess of water should have been present. Hence, when feeding an excess of water, the decrease in acid concentration was to be expected, especially when the design of operations at temperatures above 100 °C did not make provision for the excess water vapour leaving the cell to escape, for example by means of a knock-out drum under regulated pressure (no differential pressure across membrane managed) as reported in similar works [6]. Instead, the anode exit stream was connected to a spiral cooler and the complete volume captured, both the acid produced during electrolysis and the water vapour condensed, resulting in the capture of a more diluted H_2SO_4. This was confirmed by measuring the volume exiting the anode and comparing it to the volume (mL/min) H_2O fed in the time measured, for example feeding 5 mL/min H_2O produced an amount of 25±0.6 mL/min (Appendix C, Table C-2) for 5 min measurements capturing H_2SO_4. Furthermore, the volume produced at the cathode was also captured and ranged between 0.5 and 1 mL (1 wt% H_2SO_4) for the same time period, which accounts for some SO_2 crossover, but was considered acceptable for the duration of the studies performed.

It could be added that the measured H_2 (Table 6.2) at the cathode outlet related better to Faraday's prediction for the applied current densities, although still higher (5-29%) than the theoretically determined values (Table 6.3). Since the current design did not allow for analysis of the cathode

outlet by use of a GC-MS, the total volume exiting the cathode was instead measured using an in-house designed bubble meter. This implies that the volume measured could also have included other gases apart from H_2, for example SO_2 in the event of SO_2 crossover, which is possible considering the excess feed thereof (200 mL/min). This crossover could further result in side reactions which could produce H_2S gas at the cathode [4, 18].

However, irrespective of the reasons, it is clear that,even with the reduced 5 mL/min H_2O supply, the SO_2 electrolysis process was unable to produce a H_2SO_4 concentration (20 wt%) close to the recommended 65 wt% (roughly 10 M H_2SO_4) for the HyS cycle [11]. Compared to earlier work on s-PBI at 80 and 90 °C, it was found that the production rate of H_2SO_4 varied by 25 % with regard to the predicted values (calculated) from Faraday's law [10]. In their case, it was suggested that the H_2SO_4 had either leached or absorbed from the membrane under the investigated operational conditions [10]. More recently, using a ~300 μm s-PBI at 110 °C, it was reported that, by feeding water in a stoichiometry (mol feed/ mol required) of 10:1 (0.45 mL/min), a H_2SO_4 concentration of 4 M was achieved [6]. When lowering the stoichiometry to 5:1, a concentration of 8 M was achieved. These results also confirm the possible influence of the membrane thickness on the concentration of the acid produced. This was further investigated and will be discussed in Section 6.3.4.

After determining and discussing the mmol/s H_2SO_4 and H_2 obtained, EIS was used to electrochemically characterise and evaluate the effect of H_2O supply on the MEA's performance by reporting the membrane resistance (*Ohm*), activation energy (*Charge*) and mass transport effects (Warburg term, *W*) [26, 28]. The obtained EIS data with fitted models for the various flow rates and applied current densities are presented in Appendix C.3 (see Figures C-2 to C-8).

The measured membrane resistance (*Ohm*) did not vary significantly with varying flow rates or current densities (0.1-0.7 A/cm² where applicable), averaging 9.21 ± 0.78 mΩ for the $1A_i$ MEA. This correlated with recent literature, which reported no adverse effect of membrane resistance for s-PBI [6, 10]. It should be added that the obtained average 9 mΩ was lower than the resistance of previous PBI-blended membranes (18-25 mΩ) evaluated at 80 °C [26].

As can be seen from Figure 6.6, the activation resistance (*Charge*) increased with increasing current densities for the different flow rates. It is clear that the activation resistance for the restricted H_2O feed at 5 mL/min (150-371 mΩ, 0.015-0.037 Ohm/cm^2) was generally higher than what had been obtained at 10 mL/min (with the exception of the 264 mΩ obtained at 0.5 A/cm²) and 15 mL/min (Figure 6.6). Therefore, measurements beyond 0.2 A/cm², when using 5 mL/min H_2O were discarded due to a too large deviation in reported data points from the applied model. This was likely due to the washing of acid from the doped membrane and a corresponding decrease in conductivity as recording of EIS data at 5 mL/min only commenced after the repeated recording of polarisation curves at 15 and 10 mL/min with their respective EIS measurements. It

would therefore be suggested in future to prepare separate MEAs with comparable doping degrees for the intended EIS variables to be inspected.

Both the H_2O flow rates, 10 and 15 mL/min, demonstrated parabolic-type behaviour (slightly higher at 0.1 A/cm^2 than for 0.2 and 0.3 A/cm^2) in Figure 6.6, which showed an increased charge resistance with increasing current density. This was in agreement with the increasing cell voltages and corresponding standard deviations noted for current densities above 0.35 A/cm^2 (Figure 6.5) of respective H_2O flow rates.
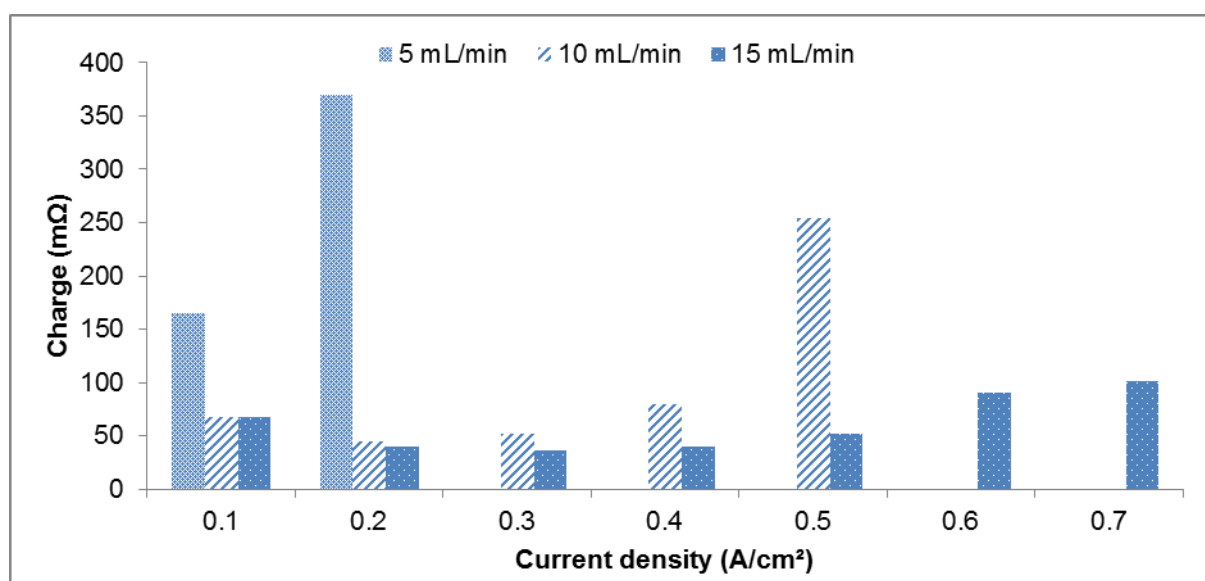
Figure 6.6: Charge resistances reported for the different applied H_2O flow rates.

In summary, the trend of charge resistance with corresponding membrane resistance and Warburg constant was illustrated in Figure 6.7 for the H_2O flow rate of 15 mL/min. Accordingly, a similar trend to that of Figure 6.6 (this was also the case for 10 ml/min H_2O – data not shown) was obtained. The slightly higher resistance measured at 0.1 A/cm^2 could likely be related to a higher initial activation resistance in the absence of sufficient conditioning of the cell, until measurement commenced and H_2SO_4 had been produced, which serves to dope the membrane and aid in proton transport. A similar pattern, albeit with a much smaller change, was observed for the membrane resistance. This was opposed to the obtained Warburg constant. Since a larger constant (S*s^(1/2)) implies a smaller limiting effect of mass transport on the reaction [28], the results were in agreement with the smaller resistances measured above 0.2-0.5 A/cm^2, while mass transport restriction in current density regions above 0.5 A/cm^2 was expected [26].
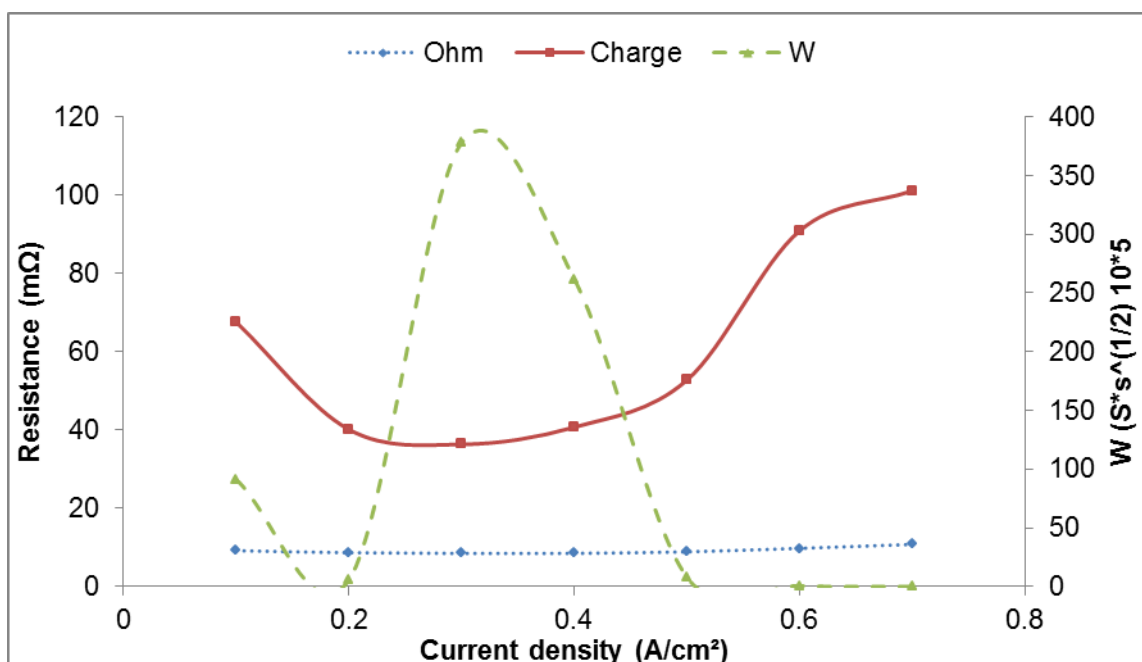
Figure 6.7: Tendency of EIS data summarised for 15 mL/min H$_2$O supplied for the measured membrane resistance (R), activation resistance (Charge) and Warburg constant (W) as plotted against applied current density (j).

Table C-3 in Appendix C summarises the average error (mΩ) and standard deviation associated with each measured constant (Ohm, charge and W) for the different H$_2$O flow rates inspected. Accordingly, the average errors determined across all EIS measurements were within 1.2 and 3.7 % for the *Ohm* and *Charge* resistances, respectively. The increase in error noted for the higher current density region measurements corresponds to the increase in standard deviation reported for the polarisation curves (Figure 6.5) due to the dependency of EIS measurements on a constant voltage during measurements.

Lastly, it should be mentioned that the current density of 1.0 A/cm^2 reached for membrane 1A$_i$ in Figure 6.2 was achieved by increasing the supplied SO$_2$ and H$_2$O flow rates to 300 and 17 mL/min, respectively, in the higher current density regions (> 0.6 A/cm^2). Furthermore, the improved performance noted for membran,e 1A$_i$ (45 μm, Figure 6.3) at the supplied 5 mL/min H$_2$O flow rate in comparison to Figure 6.5 is due to the difference in thickness (60 vs. 45 μm) and subsequent increased doping achieved (150 vs. 90 wt. % increase) for the two respective membranes.

It could be concluded for the flow rates inspected on the current SO$_2$ electrolyser set-up for measurements at 120 °C that a trade-off existed for the production of H$_2$SO$_4$ at the expense of the membrane's performance (managing lower cell voltages at a maximum current density). Since the focus of this chapter was on evaluating the PBI-blended membrane's SO$_2$ electrolyser performance at temperatures above 100 °C, and not addressing the limitations of the electrolyser's

design, it was decided to continue measurements at a H_2O flow rate of 15 mL/min. Further recommendations for adjustments to the electrolyser's design for future studies would therefore only be discussed in the Evaluations and recommendations chapter (Chapter 7).

6.3.4 MEA variables: membrane thickness and catalyst loading

After completing an initial evaluation influence of the H_2O feed on the PBI-blended membrane's SO_2 electrolyser performance by means of polarisation curves (Section 0) and H_2SO_4 concentrations produced for blend $1A_i$ (A_i_60 μm), the influence of membrane thickness and catalyst (Pt) loading was investigated. For this purpose, two different A_i MEAs were prepared, namely $1A_i$_160 μm with membrane thickness of 160 μm, and $1A_i$_1 mg Pt with a platinum loading of 1.0 mg /cm^2. These were compared to $1A_i$_45 μm (see Section 6.3.2) and $1A_i$_60 μm (see Section 0), which both had a coating of 0.5 mg Pt/cm^2. The three different H_2O feeds were again applied and the H_2SO_4 concentrations determined at selected current densities (Figure 6.9). In addition, membrane resistances for the respective prepared $1A_i$ MEAs were included for comparison (Table 6.5). In Table 6.4, the properties of the different prepared $1A_i$ MEAs are summarised for further discussion in this section.

Table 6.4: Properties of different prepared $1A_i$ MEAs for comparison in SO_2 electrolysis at 120 °C.

Membrane	Thickness	H_2SO_4 Doping	Catalyst loading
	(μm)	(wt %)	(mg Pt/cm^2)
$1A_i$_45 μm	45	150	0.5*
$1A_i$_60 μm	60	90	0.5*
$1A_i$_160 μm	160	85	0.5*
$1A_i$_1 mg Pt (60 μm)	60	80	1.0

∗ Carbon supported Pt-coated GDE.

The individual studies of H_2O flow rate influence on MEAs $1A_i$_160 μm and $1A_i$_1 mg Pt is presented in Appendix C.4 (Figure C-9 and C-10), for comparison with the already discussed performance of MEA $1A_i$ (60 μm) as $1A_i$_60 μm in Section 0. When comparing these results, it

seems that the difference in performance of the polarisation curves recorded for the different H_2O flow rates was smaller between $1A_i\_160$ µm and $1A_i\_1$ mg Pt in comparison to the thinner $1A_i\_60$ µm membrane. Cell voltages were comparable below 0.3 A/cm^2, whereafter the better performance at 15 mL/min H_2O became more evident, reaching current densities of 0.55 and 0.65 A/cm^2, respectively, just below the 1 V limit (see Appendix C, Figures C-9 and -10). Since the thinner $1A_i\_45$ µm MEA's performance at 120 °C was only investigated at the 5 mL/min H_2O feed (Section 6.3.2), comparison with the other $1A_i$ MEAs was summarised in Figure 6.8 for 5 mL/min.
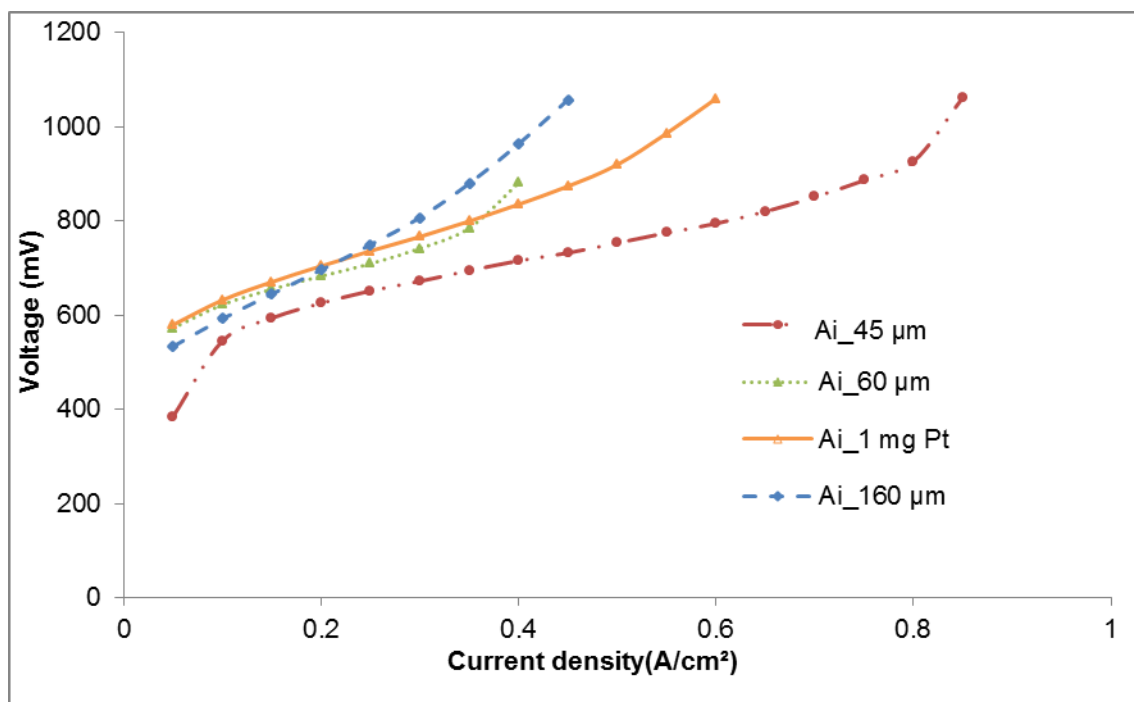
Figure 6.8: Comparison of differently prepared $1A_i$ MEAs for 5 mL/min H_2O feed.

A decrease in membrane thickness resulted in a decrease of the cell voltages achieved over the entire current density range for the $1A_i$ MEAs (Figure 6.8), allowing for a maximum current density of 0.85 A/cm^2 to be reached by the thinnest $1A_i$ _45 µm at 5 mL/min H_2O. This performance was followed by the 60 µm, 1 mg Pt/cm^2 and 0.5 mg Pt (supported C)/cm^2, and lastly the thickest 160 µm $1A_i$ MEA. This order (45 µm < 1 mg Pt < 60 µm < 160 µm) corresponds to the membrane resistances (Ohm) measured for the $1A_i$ MEAs at 0.1 A/cm^2 Figure 6.8). It should be added that the initial wt% H_2SO_4 doping reported for the prepared $1A_i$ MEAs (Table 6.4) and H_2SO_4 concentrations produced (see Appendix C, Table C-4), corresponds to the order of performance 45 µm > 60 µm > 160 µm. This emphasises the effect of MEA doping (preliminary with H_2SO_4) on the electrolyser's performance (polarisation curve, Figure 6.8) and the sulfuric acid (mol/L) produced during electrolysis.

The higher Pt loading, as expected, benefitted the performance of the 1A$_i$_60 μm MEA and allowed for higher current densities to be achieved when restricted H$_2$O feed was applied (5 mL/min). However, similar membrane resistances at 0.1 A/cm^2 indicated an insignificant improvement due to the increased Pt loading (1A$_i$_60 μm). Ideally, future studies should include EIS measurements within the higher current density region (>0.5 A/cm^2) for a broader comparison. (At the time of data collection, the EIS measurements were restricted to < 0.2 A/cm^2)

Table 6.5: Comparison of cell voltage and membrane resistance measured (EIS) at 0.1 A/cm^2 for the different prepared 1A$_i$ MEAs at 5 mL/min H$_2$O.

1A$_i$ MEA	Cell Voltage (mV)	Membrane resistance (mΩ)
1A$_i$ _45 μm	545.2	7.760
1A$_i$ _60 μm	617.6	9.187
1A$_i$ _1 mg Pt (60 μm)	592.3	8.987
1A$_i$_160 μm	632.0	28.44

Furthermore, the H$_2$SO$_4$ concentrations measured for all 1A$_i$ MEAs remained below 2.5 M (Figure 6.9). Interestingly, it was noted that the thicker 1A$_i$_160 μm MEA produced a less concentrated H$_2$SO$_4$ (1.7 mol/L) than which had been measured for the 1A$_i$_45 μm MEA (2.3 mol/L), while being more similar to the 1A$_i$_60 μm MEA with comparable H$_2$SO$_4$ doping (see Appendix C, Table C-4). Therefore, this was considered to rather be a consequence of the MEAs initial H$_2$SO$_4$ doping (Table 6.4) and not related to the thicknesses of the membranes. It should be mentioned that the 1A$_i$ MEAs were doped under similar conditions (1M H$_2$SO$_4$, 24 hours at 80 °C), but that the thinner 1A$_i$ (45 μm) membrane's wt% increased more rapidly (150 %) in comparison to the 160 μm 1A$_i$ (85%). Consequently, it was decided to monitor the produced sulfuric acid concentration of 1A$_i$_45 μm for a longer time (10 hours, Section 6.3.5.1). For the duration of the voltage monitoring experiment at 0.3 A/cm^2, which was measured every 2 hours, averaged at 2.24 ±0.20 M, which was comparable to the reported 2.34 M presented in Figure 6.9. It can be concluded for the 1A$_i$ MEAs studied in this section, that the H$_2$SO$_4$ doping of the MEAs before electrolyser operations had a greater effect on the cell voltages and H$_2$SO$_4$ produced for the respective MEAs than the increased catalyst loading or membrane thickness. This was supported by the higher maximum

current densities achieved at lower cell voltages and higher H_2SO_4 concentrations produced Figure 6.8and Figure 6.9).
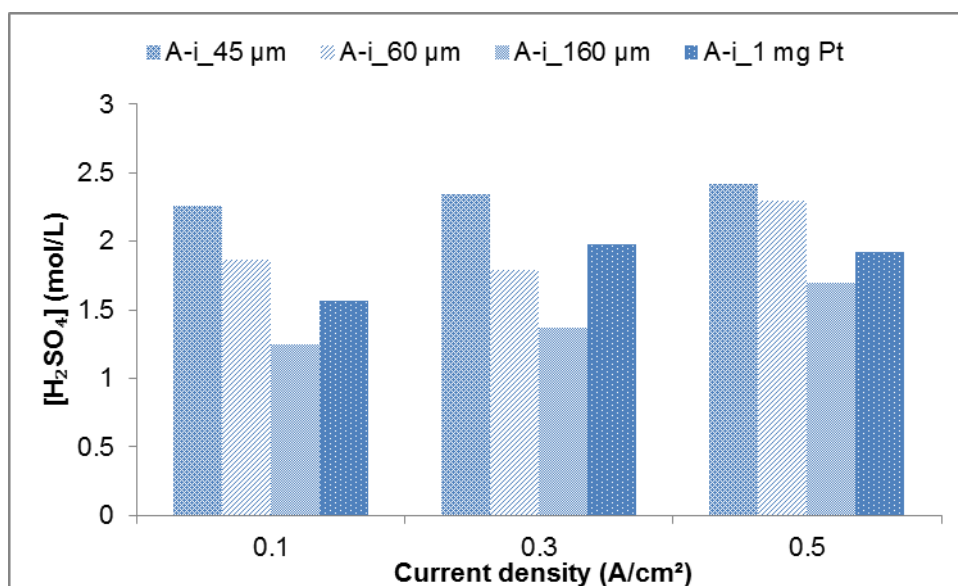
Figure 6.9: Concentration H_2SO_4 (mol/L) produced by $1A_i$ MEAs_45, 60, 160 μm and 1 mg Pt at the supplied 5 mL/min H_2O.

In conclusion, it was found that the increased membrane thickness of $1A_i$_160 μm did not lead to an increase in the sulfuric acid concentration. As mentioned earlier (Section 6.3.3), this is a likely consequence of the current SO_2 electrolyser design which does not allow for the excess H_2O (steam, fed directly to the anode) to escape from the anode exit stream, but is rather condensed with the produced H_2SO_4, leading to a diluted acid. Instead, the thinner $1A_i$ MEAs (45 and 60 μm) proved sufficient for the current SO_2 electrolyser set-up at 120 °C. It remains to be determined whether a decrease in catalyst loading of Pt would be more cost-effective on a larger scale, opposed to a limited H_2O supply needed for a more concentrated H_2SO_4 production and overall improved efficiency of the HyS cycle. It was further found that doping of the MEA greatly influenced the electrolyser performance, which is to be considered in future studies.

After recording of polarisation curves, the different $1A_i$ MEAs (45, 60 and 160 μm) were further evaluated using voltage stepping and steady state (voltage monitoring) measurements at 120 °C.

6.3.5 Stability evaluation of 1A$_i$ MEAs

The stability determinations of the 1A$_i$ MEA (catalyst loading of 0.5 mg Pt/cm^2) included voltage monitoring at 0.3 and 0.5 A/cm^2 for 10-24 hours, accompanied by the recording of polarisation curves and cell voltages achieved before and after voltage monitoring (Section 6.3.5.1). Further stability tests included voltage stepping of 1A$_i$_60 µm at 120 °C (Section 6.3.5.2).

6.3.5.1 Voltage monitoring at 120 °C

As seen in Figure 6.10, voltage monitoring for the membrane 1A$_i$_160 µm was included for 5 and 10 hours at 0.3 and 0.5 A/cm^2, respectively. The voltage monitored at 0.3 A/cm^2 remained relatively constant (759 ±7.67 mV) for the thicker (160 µm) 1A$_i$ membrane, which agreed with the 748 mV (Figure C-11) measured for the polarisation curve before voltage monitoring, decreasing to 714 mV after the 10 hour measurement. Overall decreases of 65-120 mV in cell voltages were noted across the current density region for the polarisation curves recorded after voltage monitoring was applied at 0.3 A/cm^2 (Figure C-11). The measurement at 0.5 A/cm^2 for 1A$_i$_160 µm had to be terminated after only 5.5 hours, yielding 854 ± 24.2 mV, due to a system error and directly proceeded to the recording of the polarisation curve. For the polarisation curves (Figure C-12), an improvement was noted only in the higher current density region with cell voltages decreasing between 60-175 mV, whilst reaching an improved maximum current density of 0.85 A/cm^2.
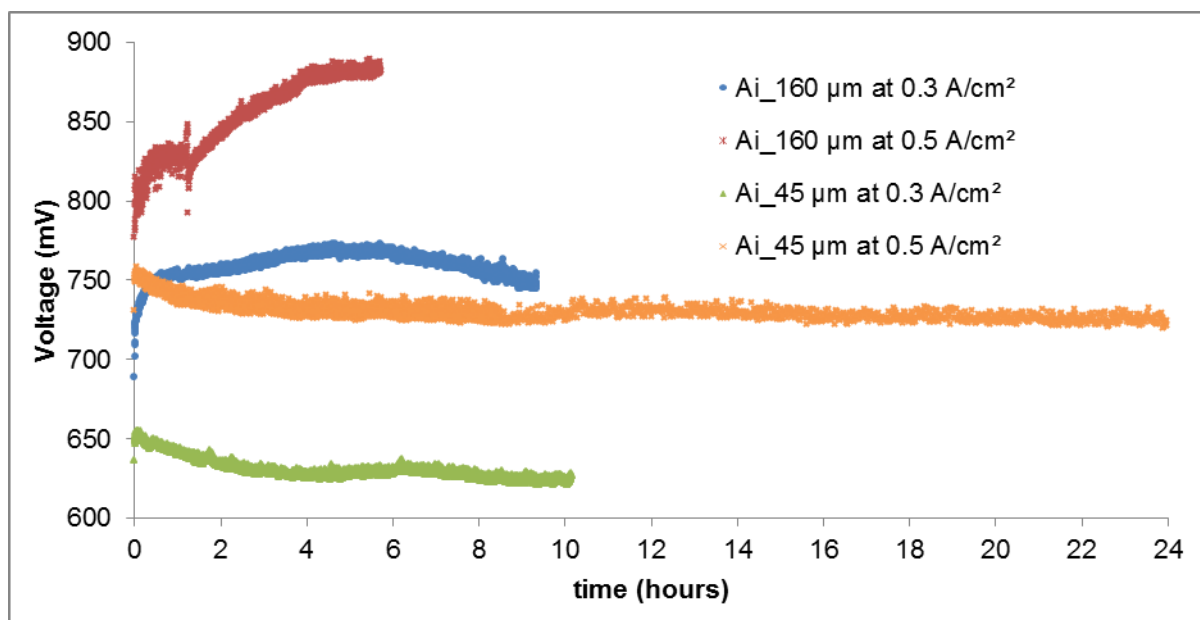
Figure 6.10: Voltage monitoring conducted on membranes 1A$_i$_45 and 160 µm at 120 °C with 5 mL/min H$_2$O supply.

For the thinner 1A$_i$_45 µm, the voltage monitoring at 0.3 A/cm^2 served to condition the membrane, reporting a steady voltage of 631 ± 6.60 mV for the 10 hours (Section 6.3.2), in agreement with the decrease of 18 mV for the applied 0.3 A/cm^2 in the polarisation curve recorded after voltage monitoring (Figure C-11). Thereafter, a measurement at 0.5 A/cm^2 was performed for 24 hours, reporting a slow but steady decrease of 732 ±6.17 mV as seen in Figure 6.10. The polarisation curves recorded after voltage monitoring showed a decrease of between 50 to 180 mV in the current density range above 0.3 A/cm^2, as shown in Figure 6.11.

The change in voltage before and after monitoring confirms the benefit of applying a constant current for a period (in this case 5-10 hours) to condition the membrane in providing an improved performance (lowered cell voltages) in the SO$_2$ electrolyser at elevated temperatures. However, longer voltage stability measurements (24-300 hrs) would in future be required to verify the accepted suitability of the PBI-blended membrane in commercial applications at elevated temperatures. To briefly investigate this, membrane 1A$_i$ -60 µm was subjected to voltage stepping at 120 °C to measure the blended membrane's suitability under stress in comparison to the observed membrane and catalyst stability at 80 °C (Section 6.3.2 and 6.3.3).
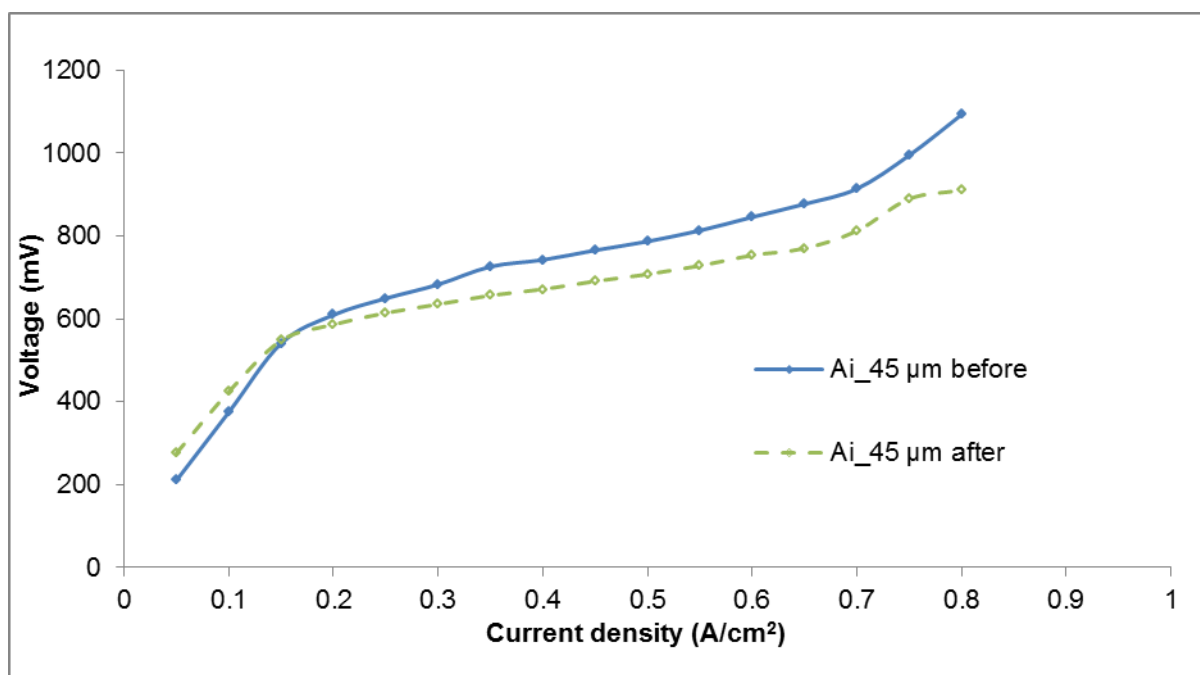
Figure 6.11: Voltage monitoring comparison of polarisation curves at 0.5 A/cm^2 recorded before and after for 1A$_i$_45 µm with H$_2$O flow rate of 5 mL/min at 120 °C.

6.3.5.2 Voltage stepping at 120 °C for 1A$_i$_60 μm

As described in Section 5.2.5.2, the stability of the blended membrane will be evaluated by applying an increased stress using voltage stepping for 250 cycles between a lower (0.3 V) and upper voltage limit (0.9 V). The H_2O flow rate was kept at 10 mL/min during voltage stepping and polarisation curves were recorded before and after. This allows for a comparison of the 1A$_i$ _60 μm MEA's stability at operation temperatures of 80 and 120 °C. Furthermore, a comparison in catalyst stability for SO_2 electrolyser operations at 80 and 120 °C could be made since similar GDEs were used in preparation of the 1A$_i$ MEAs.

Note that the current densities recorded at the lower voltage of 0.3 V measured below the OCV and was hence reported at 0 A/cm2 and are therefore not shown in the voltage stepping data presented in Figure 6.12. Initially, membrane 1Ai yielded a current density of 0.6 A/cm2 at 120 °C at the applied upper limit of 0.9 V, which corresponds to the current achieved for the polarisation curve recorded before voltage stepping (Figure 6.13). At 80 °C, the blend 1Ai remained stable, maintaining a current density of approximately 0.4 A/cm² for the first 125 cycles at the applied 0.9 V. This is in agreement with the polarisation curve recorded after voltage stepping (Figure 6.13), measuring 893 mV at 0.4 A/cm2. Interestingly, a temporary increase in current density was observed after the noted decrease of the first 130 cycles for blend 1Ai at both 80 and 120 °C (Figure 6.12) [22]. This could also likely be ascribed to the increased H2O supply and varying concentrations H2SO4 produced and an effect of insufficient doping of the membrane during voltage cycling at 120 °C. It is clear that both steady state and stepping results have highlighted the benefit of including a break-in procedure of the MEA at low and elevated operating temperatures for improved SO_2 electrolyser performance.
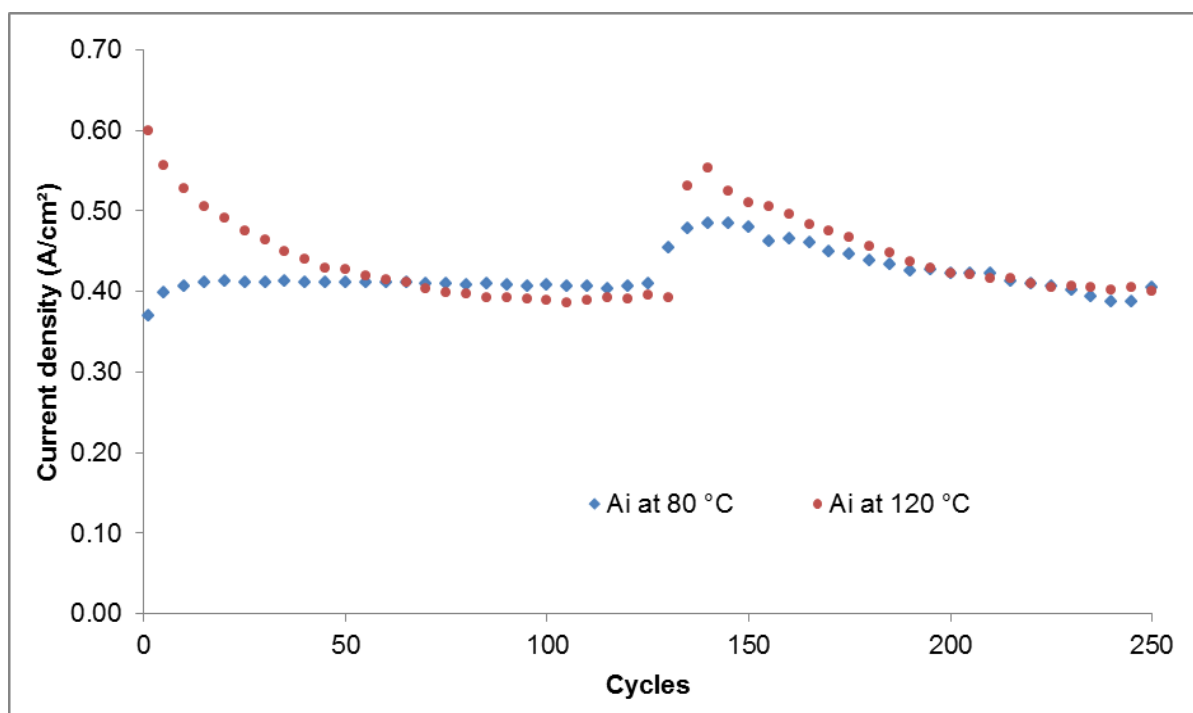
Figure 6.12: Current density (A/cm^2) as a function of voltage cycling for 1A$_i$_60 μm at 80 and 120 °C.
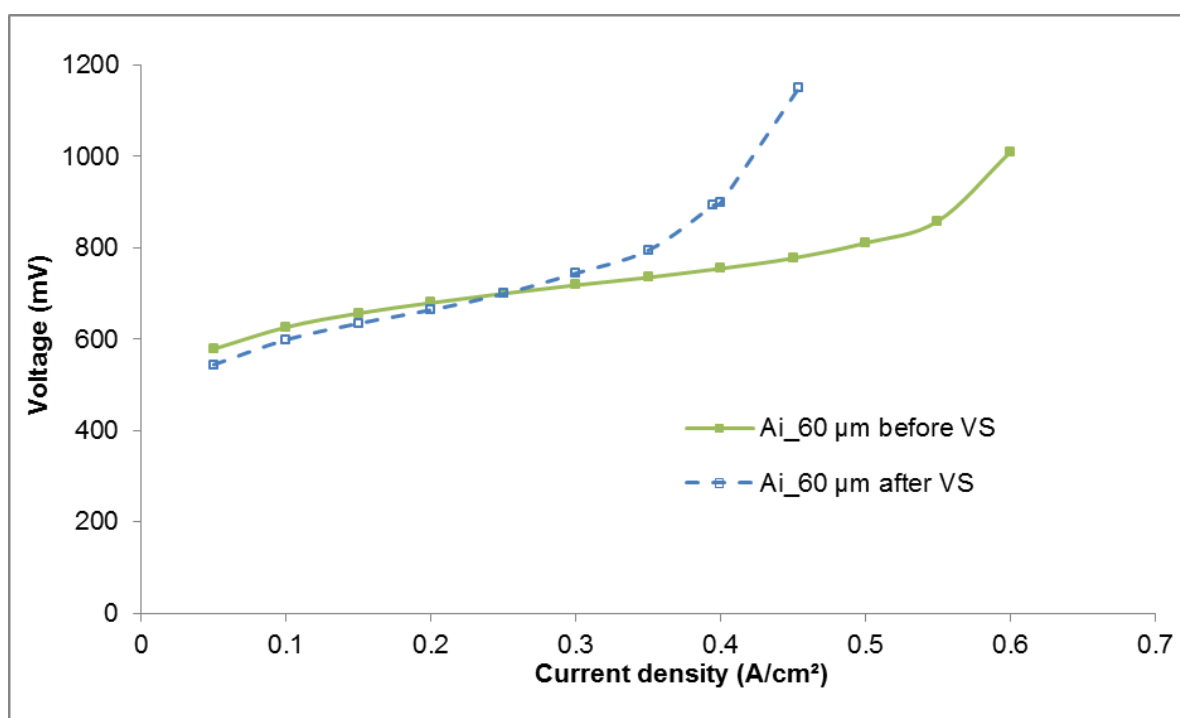
Figure 6.13: Polarisation curves recorded before and after voltage stepping at 120 °C for 1A$_i$.

Polarisation curves recorded for 1Ai_45 µm after voltage stepping displayed a slight decrease in performance as seen in Figure 6.13, which is in agreement with the behaviour observed at 80 °C for membrane 1Ai after voltage stepping (Figure 6.5). Overall, the voltage stepping conducted at 120 °C serves to support a required conditioning procedure irrespective of the temperature of operation in an SO2 electrolyser. The minimal degradation observed during voltage stepping operations for 1Ai confirmed the suitability of this membrane, and was further investigated by means of post-characterisation of MEA material using TGA-FTIR and SEM techniques for inspection of membrane stability. It could be added that, for the duration and under the conditions tested, the catalyst (Pt supported on carbon) remained sufficiently stable, as confirmed by the constant current densities attained during voltage stepping.

6.3.5.3 Post characterisation of blend A_i after SO_2 electrolysis at 120 °C

The post characterisation included SEM-EDX analysis and TGA-FTIR measurements after SO_2 electrolysis at 120 °C, which was then compared to the characterisation results obtained for the membrane material $1A_i$ before electrolysis (Chapter 4) and after electrolysis at 80 °C (Chapter 5, see Section 5.3.3).

For the SEM and EDX analysis, the GDE material was removed from the MEA (directly from electrolyser cell and analysed as is) to expose the anode surface of the membrane as seen in Figure 6.14 (b). In comparison to images taken of $1A_i$ before electrolysis (Figure 6.14 (a)), no visible structural damage (pin holes, etc.) on the membrane's surface area was noticeable using SEM (300 x magnified). However, the appearance of darker and lighter spots on the $1A_i$ membrane surface after SO_2 electrolysis at 120 °C, as seen in Figure 6.14 (b), was analysed further using EDS (Figure 6.14 (c)). The expected C-, O-, F- and S-content, associated with the $1A_i$ blend membrane, was in accordance with the analysis completed after SO_2 electrolysis at 80 °C for blend $1A_i$. The only difference between 80 °C and 120 °C, was an increase in the S-content (Section 5.3.3) from 3.3 % before electrolysis to between 12 and 14.4 % after electrolysis at 120 °C. The appearance of lighter spots on the surface merely indicated a higher Pt content, from GDE elements left behind on the membrane surface after removal.
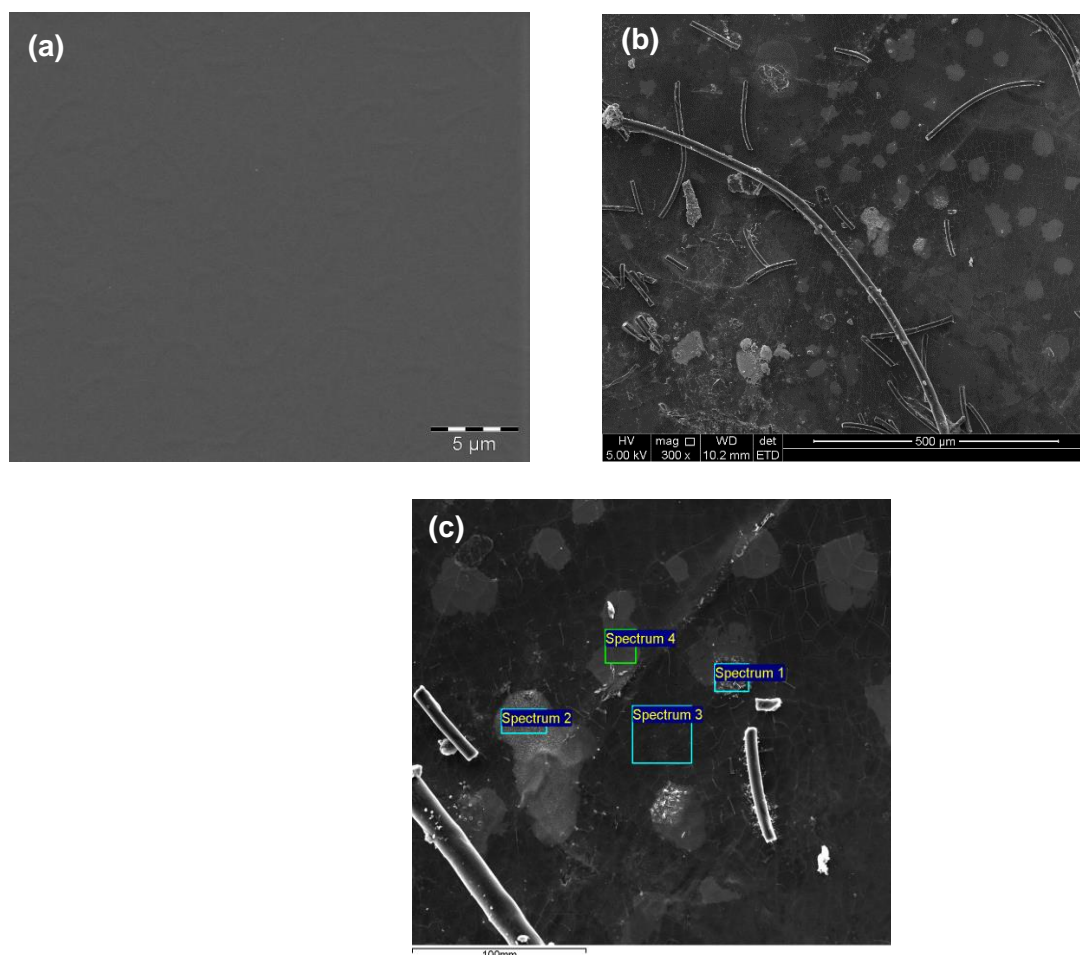
Figure 6.14: SEM images taken of the 1A$_i$ MEA before (a) and after (b and c) SO$_2$ electrolysis operations at 120 °C. Images of (b) and (c) were obtained with a back-scatter electron detector for EDS measurements of the anode surface area (GDE removed).

Considering the TGA data, a decrease in thermal stability was noted after electrolysis operations at 120 °C for the blend 1A$_i$ (Figure 6.15). However, degradation associated with the polymer backbone only started at 333 °C, with SO$_2$ splitting-off occurring at 391 °C, in comparison to the 275 °C noted for 1A$_i$ before electrolysis (Section 5.3.3). This further serves to support the observation made in Chapter 5 that, under increased operation temperatures (>95 °C) in an acidic environment (as found during electrolyser operations), sulfonation of the BrPAE-1 blend component serves to increase the thermal stability of its backbone, and hence the blend. However, the associated decrease in residual weight % (86 % after SO$_2$ electrolysis at 80 °C to 70 % after 120 °C) corresponds to the early detection of peaks in the 720-750 cm^{-1} region of the FTIR spectra. These could be identified as aromatic C-H bends (mono- and ortho-position) likely associated with the weaker benzylic bonds of the covalently cross-linked polymers [29] (BrPAE-F$_6$PBI) of the blend membrane 1A$_i$ starting to come off already at 120 °C (Figure 6.15), reporting a residual weight of 86 %.
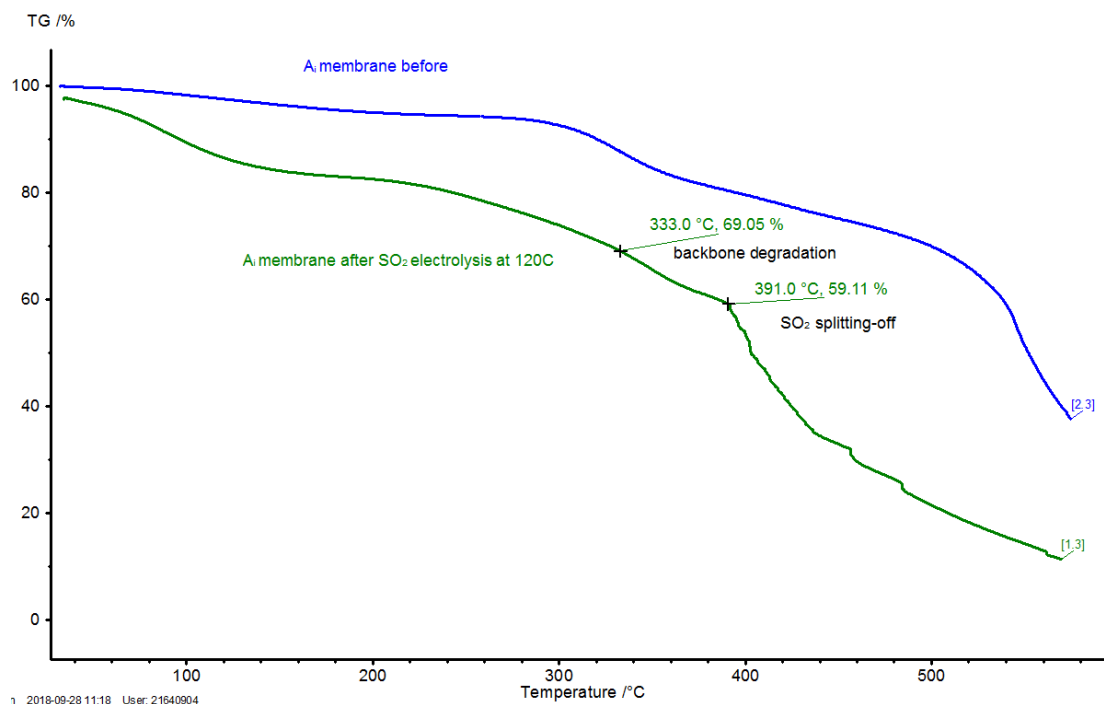
Figure 6.15: TGA measurements of membrane 1A$_i$ before and after SO$_2$ electrolysis at 120 °C with an included 1st derivative of 1A$_i$.

The conducted post-characterisation studies after electrolyser operations at 120 °C on the blend 1A$_i$ indicated no adverse effects on membrane stability in comparison to electrolyser operations at 80 °C, and serves to support further long-term testing at temperatures above 100 °C within the SO$_2$ electrolyser.

6.4 Conclusion

As proposed in earlier Chapters (4 and 5), the acid-excess partially fluorinated PBI-blended membrane, 1A$_i$, was confirmed to perform the best for the tested SO$_2$ electrolyser set-up at 120 °C (1A$_i$ > 1C$_i$ > 1B$_i$). Overall, an improved performance for membrane 1A$_i$ was attained at 120 °C through a decrease in cell voltages (up to 150 mV), achieved for the maximum current density of 1.1 A/cm^2. While the operational performance (decreased cell voltages at current densities up to 1.0 A/cm^2) was influenced more by the H$_2$O supply fed directly to the anode, the amount of H$_2$SO$_4$ produced was more influenced by the wt% doping of MEAs. The highly diluted H$_2$SO$_4$ concentrations measured during SO$_2$ electrolysis at 120 °C was ascribed to the current design not permitting the escape of excess water (steam) at the anode exit stream. However, the measured H$_2$ at the cathode was closer to the Faraday predictions. Accordingly, the 150 wt% doped 1A$_i$_45

μm MEA showed the best performance, reaching current densities up to 8.5 A/cm^2 for the 1 V voltage limit at 5 mL/min H_2O with H_2SO_4 concentrations exceeding that of the 60 and 160 μm prepared $1A_i$ MEAs (80-90 wt% H_2SO_4 doped). Furthermore, lower membrane resistances benefitted the 45 and 60 μm thin $1A_i$ MEAs above the thicker 160 μm $1A_i$ MEA. Lastly, the 1 mg Pt/cm^2 loaded $1A_i$ MEA did not show a significant improvement in electrolyser performance in comparison to the 0.5 mg Pt/cm^2 prepared MEA, which serves to further reduce costs for the SO_2 electrolyser operated at temperatures above 100 °C. Initial voltage stability and stepping experiments served to also confirm the suitability and stability of the $1A_i$ blended membrane for future long term SO_2 electrolyser operations at temperatures above 100 °C.

6.5 References

[1] Lokkiluoto A, Taskinen PA, Gasik M, Kojo IV, Peltola H, Barker MH, et al. Novel process concept for the production of H_2 and H_2SO_4 by SO_2-depolarized electrolysis. Environment, Development and Sustainability. 2012;14:529-40.

[2] Colón-Mercado H, Elvington MC, Hobbs DT. FY08 Membrane Characterization Report for the hybrid Sulfur Electrolyzer. 2008.

[3] Gorensek MB, Summers WA. Hybrid sulfur flowsheets using PEM electrolysis and a bayonet decomposition reactor. International Journal of Hydrogen Energy. 2009;34:4097-114.

[4] Elvington MC, Colón-Mercado H, McCatty S, Stone SG, Hobbs DT. Evaluation of proton-conducting membranes for use in a sulfur dioxide depolarized electrolyzer. Journal of Power Sources. 2010;195:2823-9.

[5] Corgnale C, Shimpalee S, Gorensek MB, Satjaritanun P, Weidner JW, Summers WA. Numerical modeling of a bayonet heat exchanger-based reactor for sulfuric acid decomposition in thermochemical hydrogen production processes. International Journal of Hydrogen Energy. 2017;42:20463-72.

[6] T. R. Garrick, C. H. Wilkins, A. T. Pingitore, J. Mehlhoff, A. Gulledge, B. C. Benicewicz, et al. Characterizing Voltage Losses in an SO2 Depolarized Electrolyzer Using Sulfonated Polybenzimidazole Membranes. Journal of the Electrochemical Society. 2017;164:F1591-F5.

[7] Weidner JW. Electrolyzer performance for producing hydrogen via a solar-driven hybrid-sulfur process. Journal of Applied Electrochemistry. 2016:1-11.

[8] Sivasubramanian P, Ramasamy RP, Freire FJ, Holland CE, Weidner JW. Electrochemical hydrogen production from thermochemical cycles using a proton exchange membrane electrolyzer. International Journal of Hydrogen Energy. 2007;32:463-8.

[9] Brecher LE, Spewock S, Warde CJ. The Westinghouse Sulfur Cycle for the thermochemical decomposition of water. International Journal of Hydrogen Energy. 1977;2:7-15.

[10] Jayakumar JV, Gulledge A, Staser JA, Kim C-H, Benicewicz BC, Weidner JW. Polybenzimidazole Membranes for Hydrogen and Sulfuric acid Production in the Hybrid Sulfur Electrolyzer. ECS Electrochemistry Letters. 2012;1:F44-F8.

[11] Gorensek MB, Staser JA, Stanford TG, Weidner JW. A thermodynamic analysis of the SO_2/H_2SO_4 system in SO_2-depolarized electrolysis. International Journal of Hydrogen Energy. 2009;34:6089-95.

[12] Staser JA, Gorensek MB, Weidner JW. Quantifying Individual Potential Contributions of the Hybrid Sulfur Electrolyzer. Journal of The Electrochemical Society. 2010;157:B952-B8.

[13] Colón-Mercado HR, Hobbs DT. Catalyst evaluation for a sulfur dioxide-depolarized electrolyzer. Electrochemistry Communications. 2007;9:2649-53.

[14] Zeis R. Materials and characterization techniques for high-temperature polymer electrolyte membrane fuel cells. Beilstein Journal of Nanotechnology. 2015;6:68-83.

[15] Li Q, Jensen JO, Savinell RF, Bjerrum NJ. High temperature proton exchange membranes based on polybenzimidazoles for fuel cells. Progress in Polymer Science. 2009;34:449-77.

[16] Zhang J, Xie Z, Zhang J, Tang Y, Song C, Navessin T, et al. High temperature PEM fuel cells. Journal of Power Sources. 2006;160:872-91.

[17] Higashihara T, Matsumoto K, Ueda M. Sulfonated aromatic hydrocarbon polymers as proton exchange membranes for fuel cells. Polymer. 2009;50:5341-57.

[18] Staser JA, Weidner JW. Effect of Water Transport on the Production of Hydrogen and Sulfuric Acid in a PEM Electrolyzer. Journal of The Electrochemical Society. 2009;156:B16-B21.

[19] Savinell R, Yeager E, Tryk D, Landau U, Wainright J, Weng D, et al. A Polymer Electrolyte for Operation at Temperatures up to 200°C. Journal of The Electrochemical Society. 1994;141:L46-8.

[20] Seland F, Berning T, Børresen B, Tunold R. Improving the performance of high-temperature PEM fuel cells based on PBI electrolyte. Journal of Power Sources. 2006;160:27-36.

[21] Lobato J, Cañizares P, Rodrigo MA, Linares JJ, Pinar FJ. Study of the influence of the amount of PBI–H_3PO_4 in the catalytic layer of a high temperature PEMFC. International Journal of Hydrogen Energy. 2010;35:1347-55.

[22] Peach R, Krieg HM, Krüger AJ, Rossouw JJC, Bessarabov D, Kerres J. Novel cross-linked partially fluorinated and non-fluorinated polyaromatic PBI-containing blend membranes for SO_2 electrolysis. International Journal of Hydrogen Energy. 2016;41:11868-83.

[23] Garrick RT, Gulledge A, Staser JA, Benicewicz BC, Weidner JW. Polybenzimidazole Membranes for Hydrogen Production in the Hybrid Sulfur Electrolyzer. ECS Transactions. 2015;66:31-40.

[24] Peach R, Krieg HM, Krüger AJ, van der Westhuizen D, Bessarabov D, Kerres J. Comparison of ionically and ionical-covalently cross-linked polyaromatic membranes for SO_2 electrolysis. International Journal of Hydrogen Energy. 2014;39:28-40.

[25] van der Merwe J, Uren K, van Schoor G, Bessarabov D. Characterisation tools development for PEM electrolysers. International Journal of Hydrogen Energy. 2014;39:14212-21.

[26] Kruger AJ, Krieg HM, van der Merwe J, Bessarabov D. Evalauation of MEA manufacturing parameters using EIS for SO_2 electrolysis. International Journal of Hydrogen Energy. 2014;39:18173-81.

[27] Peach R, Krieg HM, Krüger AJ, Bessarabov D, Kerres JA. PBI-Blended Membrane Evaluated in High Temperature SO_2 Electrolyzer. ECS Transactions. 2018;85:21-8.

[28] Wagner N. Characterization of membrane electrode assemblies in polymer fuel cells using A.C. impedance soectroscopy. Journal of Applied Electrochemistry. 2002;32:856-63.

[29] Kerres J, Atanasov V. Cross-linked PBI-based high-temperature membranes: Stability, conductivity and fuel cell performance. International Journal of Hydrogen Energy. 2015;40:14723-35.

7.1 Introduction

As outlined in Chapter 1, this study included a three-fold process of membrane manufacture, characterisation and application. Firstly, various polymer compositions (type of polymer, cross-linking and ratio) were cast into membranes and characterised. Subsequently, the membranes were evaluated in terms of their H_2SO_4 stability (ex situ) as well as their SO_2 electrolyser performance (in situ). It is accordingly the purpose of this chapter to summarise and evaluate whether the H_2SO_4 stability results of the 1-, 2- and 4-component blend membranes (summarised in Section 7.2.1) can be related to the observed SO_2 electrolyser performance for selected PBI-based blend membranes at 80 °C, 95 °C and 120 °C (summarised in Section 7.2.2). Subsequently (Section 7.3), the question of whether the improved electrolyser performance observed for the novel PBI-based blend membrane ($1A_i$) was a consequence of the cross-linking and type of polymers used, or simply a consequence of the improved reaction kinetics due to the higher operating temperatures (120 °C), is evaluated. Finally, this chapter concludes with recommendations (Section 7.4) based on the observations made during this study.

7.2 H_2SO_4 stability and SO_2 electrolysis performance

7.2.1 H_2SO_4 stability (Chapters 2 - 4)

The aim of *Chapter 2,* i.e. to successfully synthesise and functionalise the bromo-methylated polymers BrPAE-1 and -2 as blend components for SO_2 electrolysis, was achieved. Subsequently, the 1-component films prepared from BrPAE-1 and -2 as well as from SFS and F_6PBI, were exposed to H_2SO_4 to determine the stability of the individual polymer components. Accordingly, only the fluorinated polybenzimidazole (F_6PBI) effectively resisted sulfonation. The weight and decomposition profile (TGA-FTIR) changes due to H_2SO_4 treatment (comparison of values before and after treatment) for the SFS, BrPAE-1 and -2 polymers necessitated further studies to focus specifically on the effect of cross-linking (type and strength) on H_2SO_4 stability.

In *Chapter 3,* insight into the cross-linking contribution (strength and type) of a 2-component blend membrane system was investigated in terms of its effect on H_2SO_4 stability. Seven homogeneous, macroscopically compatible cross-linked membranes were prepared and evaluated. From these results, the tendency was observed that 2-component blend membranes containing the partially fluorinated BrPAE-1 were slightly more stable (weight changes and water uptake) than those containing the non-fluorinated BrPAE-2, irrespective of the other polymer combined with the

BrPAE. However, in spite of the slightly improved stability due to either covalent or ionic cross-linking, it became apparent that a combination of both covalent and ionic cross-linking would be required for adequate thermal- and H_2SO_4 stability as well as suitability for SO_2 electrolysis.

To attain this, 4 polymer groups (SFS, F_6PBI, BrPAE-1/-2 and E/TMIm), where combined to form novel 4-component PBI-blend membranes, as discussed in *Chapter 4*. It was found that the fluorinated nature of both the acidic (SFS) and basic (F_6PBI, BrPAE-1) polymers in the 4-component PBI-blend membranes not only resulted in improved compatibility, but also contributed to an improved H_2SO_4 stability, specifically for the A-, B- and $C_{i \& iii}$ type membranes. In fact, the inclusion of the EMIm as a quaternising imidazole, when combined with BrPAE-1, led to a partial sulfonation of the blend membrane during H_2SO_4 treatment, which actually benefitted the conductivity of blend types $1A_i$, $1B_i$ and $1C_i$ without jeopardising the chemical (H_2SO_4) and thermal stability of the membranes. Although all 12 blend membranes investigated were sufficiently stable in H_2SO_4, the larger SFS content blend membrane ($1A_i$) yielded the highest proton conductivity (48 mS/cm at 120 °C), which decreased in the order A > C > B.

7.2.2 SO_2 electrolysis (Chapters 5 & 6)

The SO_2 electrolysis performance of the most stable blend membrane A, as well as 3 combinational variations thereof using the non-fluorinated PBIOO and sPPSU (see Chapter 1, Table 1.2) instead of the partially fluorinated F_6PBI and SFS, respectively, was investigated as described in *Chapter 5*. In this case, the same acid-base ratios that had been used for $1A_i$ were combined with the blend components BrPAE-1/2 and EMIm. However, it was again the cross-linked blend membrane, $1A_i$, containing only the partially fluorinated polymer components (SFS-F_6PBI-BrPAE-1), that showed exceptional H_2SO_4 stability (%wt change < 2 %; IEC_{Direct} (% change after treatment) < 12 %, TGA degradation (T_{SO_2}) > 275 °C). The SO_2 electrolysis performance of membrane $1A_i$ was evaluated by comparing the polarisation curves obtained at 80 °C and 95 °C to those of the benchmark Nafion®115. At 80 °C, membrane $1A_i$ reached current densities of 0.5 A/cm^2 for the 1 V limit when compared to the 0.35 A/cm^2 obtained for two similar PBI cross-linked membranes presented in literature [1] as well as the commercial Nafion® 115. At 95 °C, a further improvement was noted for $1A_i$, achieving current densities of 0.63 A cm^{-2} at 1 V, compared to the 0.42 A/cm^2 attained by Nafion®115. During voltage stepping, both Nafion® and membrane $1A_i$ remained stable for the duration of 250 cycles, showing a minimal increase of less than 0.05 A/cm^2. The minimal degradation of the $1A_i$ membrane (with its hot-pressed catalyst) was confirmed by its post-characterisation (SEM-EDX, TEM and TGA).

In *Chapter 6,* the performance of the developed blend membranes $1A_i$, $1B_i$ and $1C_i$ in an electrolyser operated at 120 °C, was investigated. At 120 °C, a decrease in cell voltages (up to 150 mV) was obtained for membrane $1A_i$ for the current density range investigated. Furthermore a maximum current density of 1.0 A/cm^2 was reached by $1A_i$, in comparison to the 0.1 A/cm^2 and 0.55 A/cm^2 reached by membranes $1B_i$ and $1C_i$, respectively. According to the studied H_2O flow rates at 120 °C, a trade-off existed between the H_2SO_4 concentration produced and the performance attained for membrane $1A_i$. It was also shown that the H_2SO_4 doping influenced electrolyser operation (cell voltages and $[H_2SO_4]$ produced), more than the catalyst loading (0.5 mg Pt (supported C)/cm^2 vs. 1 mg Pt/cm^2) or the membrane thickness (60 vs.160 μm). Steady state measurements (voltage monitoring) at 0.3 A/cm^2 resulted in a further performance improvement (cell voltages decreased between 60-175 mV) after 10 hours (12-16.5 % improvement over the current density range > 0.5 A/cm^2). In agreement with the voltage stepping conducted at 80 °C (Chapter 5), the current density increased with 0.14 A/cm^2 (roughly 20 %) after 135 cycles at 0.9 V. This increase was probably due to an insufficient conditioning effect, as H_2SO_4 is produced during cycling in varying concentrations. The stability of $1A_i$ was again confirmed by post electrolyser characterisations using SEM and TGA-FTIR, showing no adverse effects.

7.3 Evaluation

In this study, various polymers were cast as membranes, both individually and in combination, whereby the effect of such polymers and their interactions on the H_2SO_4 stability and SO_2 electrolysis behaviour was determined. In terms of the envisaged aim, an ionic-covalently cross-linked PBI-based blend membrane ($1A_i$) was prepared that displayed both improved H_2SO_4 stability and increased SO_2 electrolyser performance compared to Nafion®115 and other similarly developed PBI-based membranes [2]. At 120 °C, the target operating conditions set for the HyS process (0.6 V at 0.50 A/cm^2) [3] were attained. In the following sub-sections, the influence of the operating temperature on the obtained results will be discussed, followed by an evaluation of the polymer properties in relation to their H_2SO_4 stability and SO_2 electrolyser performance.

7.3.1 Effect of temperature on electrolysis

In Appendix C (Table C-1A), a detailed description of the operational differences required of an SO_2 electrolysis run below and above 100 °C is given. When considering the effect of temperature on performance, it should be mentioned that the required H_2O and SO_2 for the runs above 100 °C were supplied directly to the anode, whereas for the runs below 100 °C the SO_2 was supplied to the anode and the water to the cathode before diffusing across the membrane to the anode. Table 7.1 provides a comparison of the most important data relating to the respective electrolyser performance parameters obtained for the best performing membrane $1A_i$ at both 80 °C and 120 °C.

Table 7.1: Electrolysis performance comparison at 80 °C and 120 °C for blend membrane 1A$_i$.

MEA 1A$_i$.	80 °C	120 °C	% Improvement
Voltage (V) measured at 0.05 A/cm^2 (initial activation barrier)	0.62 V	0.50 V	20
Voltage measured at 0.5 A/cm^2	0.89 V	0.70 V	21
Maximum current density reached (at corresponding cell voltage)	0.5 A/cm^2 (0.99 V)	1.0 A/cm^2 (0.95 V)	50
Average current density during voltage cycling at 0.9 V	0.42 ± 0.03 A/cm^2	0.43 ± 0.05 A/cm^2	-2.0

As seen in Table 7.1, an overall improved cell performance of 50% (in terms of the maximum current density) was reached at 120 °C compared to 80 °C for blend membrane 1A$_i$ (Chapter 5). It is probable that both the delayed H$_2$O supply from the cathode at 80 °C and the generally faster reaction kinetics at 120 °C contributed to the increased performance observed. This is in line with recent studies where it was found that the measured membrane resistance, as in this case of s-PBI at 110 °C, was independent of the temperature (70 °C -120 °C), when supplying the H$_2$O feed to the anode at 0.5 mL/min [2]. In other studies, it was shown that the performance of both PBI-based and Nafion® membranes was not adversely affected by the increase in H$_2$SO$_4$ concentration (2 M - 8 M) produced at higher current densities [4, 5].

It also became apparent that the SO$_2$ electrolyser design and supplied H$_2$O mainly affected the H$_2$SO$_4$ concentration produced during operations at 120 °C, and was not detrimentally influenced by the membrane thicknesses investigated. A diluted H$_2$SO$_4$ was the result, due to the excess H$_2$O (steam) fed directly to the anode, which could not escape from the anode exit stream through an appropriate gas outlet and therefore condensed and was captured with the H$_2$SO$_4$ produced at the cathode during electrolysis.

7.3.2 Membrane composition, H$_2$SO$_4$ stability and SO$_2$ electrolysis

It was shown in this study that the H$_2$SO$_4$ stability assessment for the PBI-based blend membranes at 100 °C in 80 wt% H$_2$SO$_4$ as a pre-screening of membranes correlated well with the suitability for SO$_2$ electrolyser applications. For example, F$_6$PBI was identified in Chapters 2 – 3 to contribute significantly to H$_2$SO$_4$ stability (-0.4 % wt change), which then also improved the SO$_2$ electrolysis

performance. Similarly, the larger % weight changes observed for polymers SFS and BrPAE-1/2 after H_2SO_4 treatment indicated the need for further stabilisation of polymer backbones in the presence of H_2SO_4 at elevated temperatures (>100 °C). The % weight changes of individual polymers and the effect of cross-linking type thereon is summarised in Table 7.2 for Membrane $1A_i$ as an example.

Table 7.2: Change in % weight change (H_2SO_4 stability) of individual polymers and blends.

Polymer and blends	%wt change (H_2SO_4 stability)	Cross-linking (if present)
SFS	-13.6	-
F_6PBI	-0.4	-
BrPAE-1	20.6	-
BrPAE-2	6.6	-
1D (SFS-F_6PBI)	-1.8	Ionic
$1D_i$ (SFS-BrPAE-1 & EMIm)	-35.9	Ionic
$1D_v$ (BrPAE-F_6PBI)	-3.4	Covalent
$1A_i$ (SFS- F_6PBI -BrPAE-1 & EMIm)	1.88	Ionic-covalent

Since the introduction of ionic cross-links between SFS and BrPAE-1/2 alone was not sufficient (% wt changes increased, Table 7.2), the addition of F_6PBI was required and subsequent inclusion of covalent cross-links yielded a covalent and ionic 4-component PBI-blend membrane. The characterisation studies confirmed that the cross-linked membrane type proved both stable (H_2SO_4 stability of F_6PBI) and sufficiently conductive in the presence of both covalent and ionic interactions (SFS and BrPAE-1/2).

When considering that the finally best performing membrane, in terms of SO_2 electrolysis at both 80 °C and 120 °C was $1A_i$ (F_6PBI, SFS, BrPAE-1 and EMIm), it becomes evident that the H_2SO_4 stability could be used to predict SO_2 performance. The evaluation of the H_2SO_4 stability should, however, be combined with conductivity measurements at operational conditions (RH and temperature) for a more accurate prediction of the membrane's performance during SO_2 electrolyser operations. Accordingly, the evaluation of both the H_2SO_4 stability and the conductivity of membranes $1A_i$, $1B_i$ and $1C_i$ (Chapter 4) was found to be in agreement with the electrolyser evaluation (polarisation curve trends) conducted at 120 °C, as well as their predicted order of performance (A > C > B).

It has to be kept in mind though that both the H_2SO_4 doping % of the MEA before electrolysis and the H_2O supply to the anode (Chapter 6), can adversely affect the cell voltages achieved and the corresponding $[H_2SO_4]$ produced. This was confirmed by the decrease (50-200 mV) observed for the 150 % H_2SO_4 doped $1A_i\_45$ µm, compared to the 90 % doped $1A_i\_60$ µm MEA at a controlled H_2O supply of 5 mL/min to the anode.

It was finally concluded that the combined fluorinated nature of the acidic (SFS) and basic (F_6PBI, BrPAE-1) polymers in the 4-component membrane $1A_i$ contributed to a more compatible blend with improved H_2SO_4 stability that was sufficiently conductive at temperatures below and above 100 °C. Furthermore, the improved SO_2 electrolyser performance at 120 °C could be ascribed to faster kinetics at increased temperature operations, supported by the increased conductivity and H_2SO_4 stability attained for the PBI-based blend (4-component) membrane $1A_i$ due to the combination of partially fluorinated polymer/blend components in an ionic-covalently cross-linked membrane network. This was also confirmed by the electrolyser results attained for either only ionic- or only covalently cross-linked PBI-based membrane blends investigated at 80 °C [6, 7].

7.4 Recommendations

Further improvement of the combined chemical stability and conductivity of the novel blend membrane types could perhaps be attained by investigating alternative arylene main-chain backbone chemistries for the sulfonated and the halomethylated polymeric blend components. This could be accompanied with a broader investigation on the use of more sterically hindered cyclic tertiary amines for in situ quaternisation of the halomethylated polymers by evaluating their effect both on the stability and conductivity of such cross-linked blend membranes.

Preliminary characterisation techniques could also include more elaborate small scale measurements such as the thermal conductivity and interfacial thermal conductance of individual blend membranes and composited MEAs in conditions similar to that of the operating SO_2 electrolyser. This could assist more directly (time and cost saving) with the characterisation of additional polymer components and their specific contribution towards conductivity in the blend and MEA as one unit.

While the study was conducted, various opportunities for improvement on the current SO_2 electrolyser design became apparent. Future work could, for example, include refinement to the high temperature SO_2 electrolyser system allowing for the release of excess water vapour at the anode exit. In addition, pressure regulators could be added across the cell (both anode and cathode), which will allow for better control and subsequent study of the effect of the H_2O supply on electrolyser performance and the H_2SO_4 concentration produced.

By expanding a study on the doping effect of H_2SO_4 on an MEA's SO_2 electrolyser performance, improved cell voltages at higher maximum current densities and $[H_2SO_4]$ produced could be attained.

More prolonged voltage monitoring measurements (24-300 hrs and longer) could be conducted for a more accurate long-term prediction of for example the $1A_i$ membrane's stability at elevated temperatures.

Finally, future optimisation could also include a more in-depth study on the MEA fabrication while also focussing on improving the catalyst layer with regards to loading and binder types (PBI) for elevated temperature use.

7.5 References

[1] Peach R, Krieg HM, Krüger AJ, Rossouw JJC, Bessarabov D, Kerres J. Novel cross-linked partially fluorinated and non-fluorinated polyaromatic PBI-containing blend membranes for SO_2 electrolysis. International Journal of Hydrogen Energy. 2016;41:11868-83.

[2] T. R. Garrick, C. H. Wilkins, A. T. Pingitore, J. Mehlhoff, A. Gulledge, B. C. Benicewicz, et al. Characterizing Voltage Losses in an SO2 Depolarized Electrolyzer Using Sulfonated Polybenzimidazole Membranes. Journal of the Electrochemical Society. 2017;164:F1591-F5.

[3] Gorensek MB, Staser JA, Stanford TG, Weidner JW. A thermodynamic analysis of the SO_2/H_2SO_4 system in SO_2-depolarized electrolysis. International Journal of Hydrogen Energy. 2009;34:6089-95.

[4] Weidner JW. Electrolyzer performance for producing hydrogen via a solar-driven hybrid-sulfur process. Journal of Applied Electrochemistry. 2016:1-11.

[5] Jayakumar JV, Gulledge A, Staser JA, Kim C-H, Benicewicz BC, Weidner JW. Polybenzimidazole Membranes for Hydrogen and Sulfuric acid Production in the Hybrid Sulfur Electrolyzer. ECS Electrochemistry Letters. 2012;1:F44-F8.

[6] Krüger AJ, Kerres J, Bessarabov D, Krieg HM. Evaluation of covalently and ionically cross-linked PBI-excess blends for application in SO_2 electrolysis. International Journal of Hydrogen Energy. 2015;40:8788-96.

[7] Peach R, Krieg HM, Krüger AJ, van der Westhuizen D, Bessarabov D, Kerres J. Comparison of ionically and ionical-covalently cross-linked polyaromatic membranes for SO_2 electrolysis. International Journal of Hydrogen Energy. 2014;39:28-40.

APPENDIX A: (CHAPTER 2)

A-1: NMR (^{1}H, ^{13}C and ^{19}F) spectra for polymer PAE-1
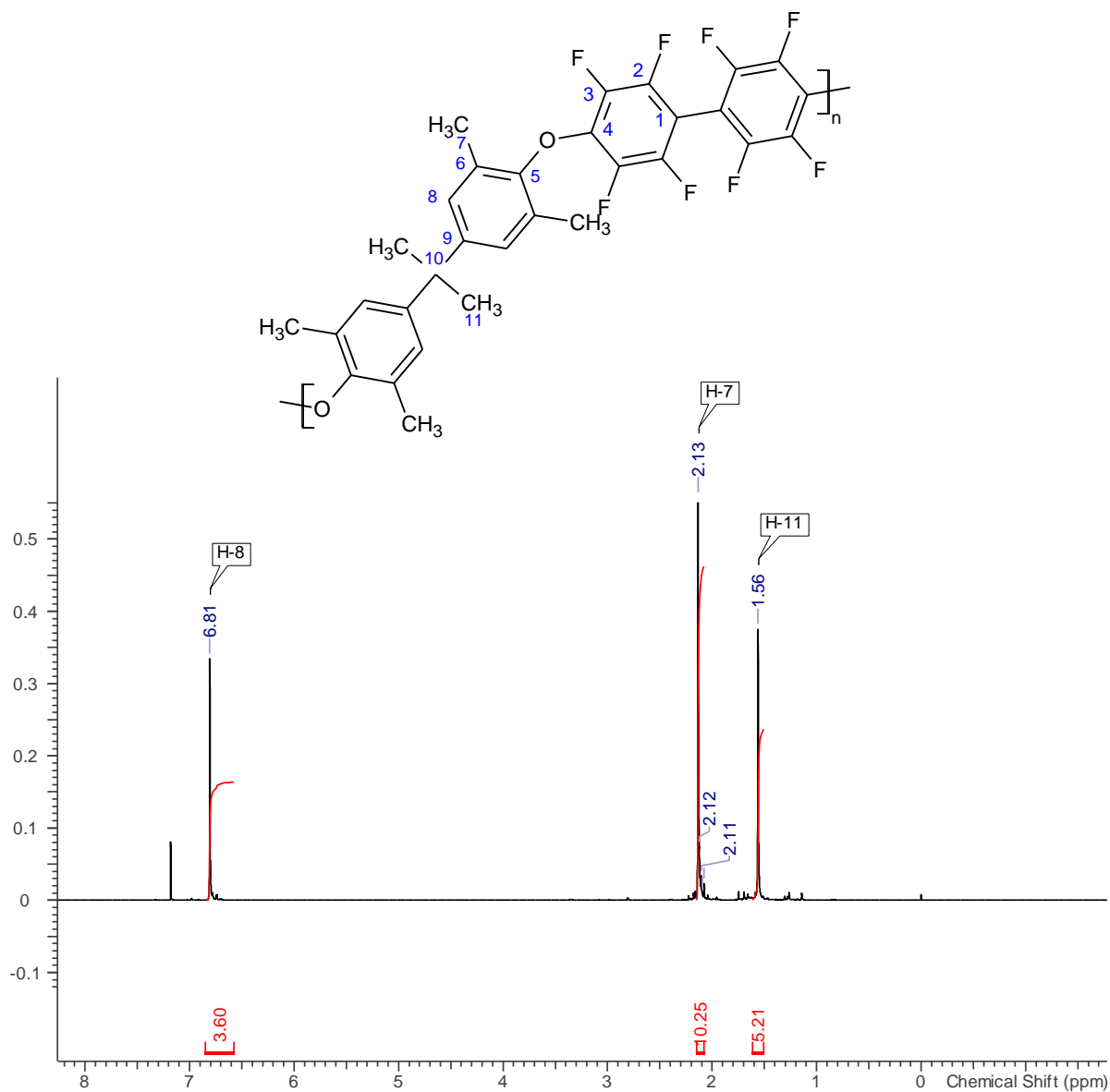
Figure A - 1: ^{1}H-NMR spectrum of PAE-1.

^{1}H-NMR (700 MHz, Chloroform-*d*) δ ppm : 6.81 (H-8), 2.13 (H-7), 1.56 (H-11)
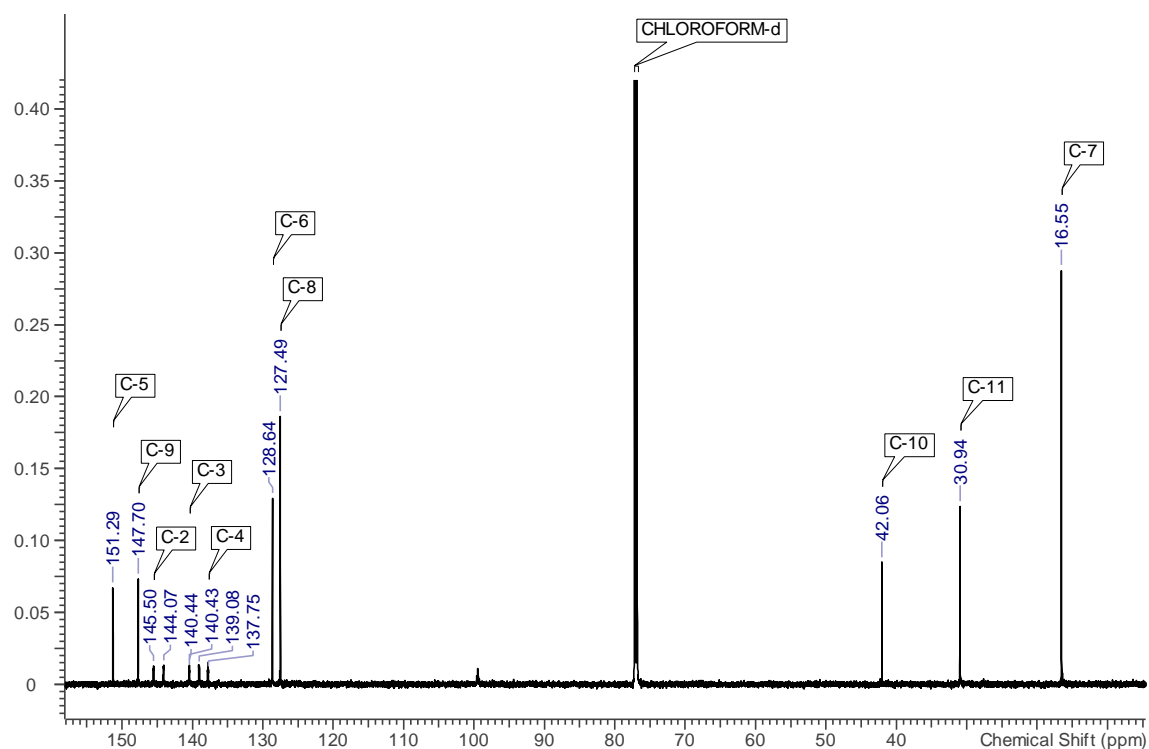
Figure A - 2: ¹³C-NMR spectrum of PAE-1.

¹³C NMR(176 MHz, Chloroform-*d*) δ ppm: 151.29 (C-5); 147.70 (C-9); 145.50 (d, *J* = 245.4 Hz, C-2); 140.44 (d, *J* = 253.04 Hz, C-3); 137.75 (C-4); 128.65 (C-6); 127.49 (C-8), 99.4 (C-1); 42.06 (C-10); 30.94 (C-11); 16.55 (C-7).
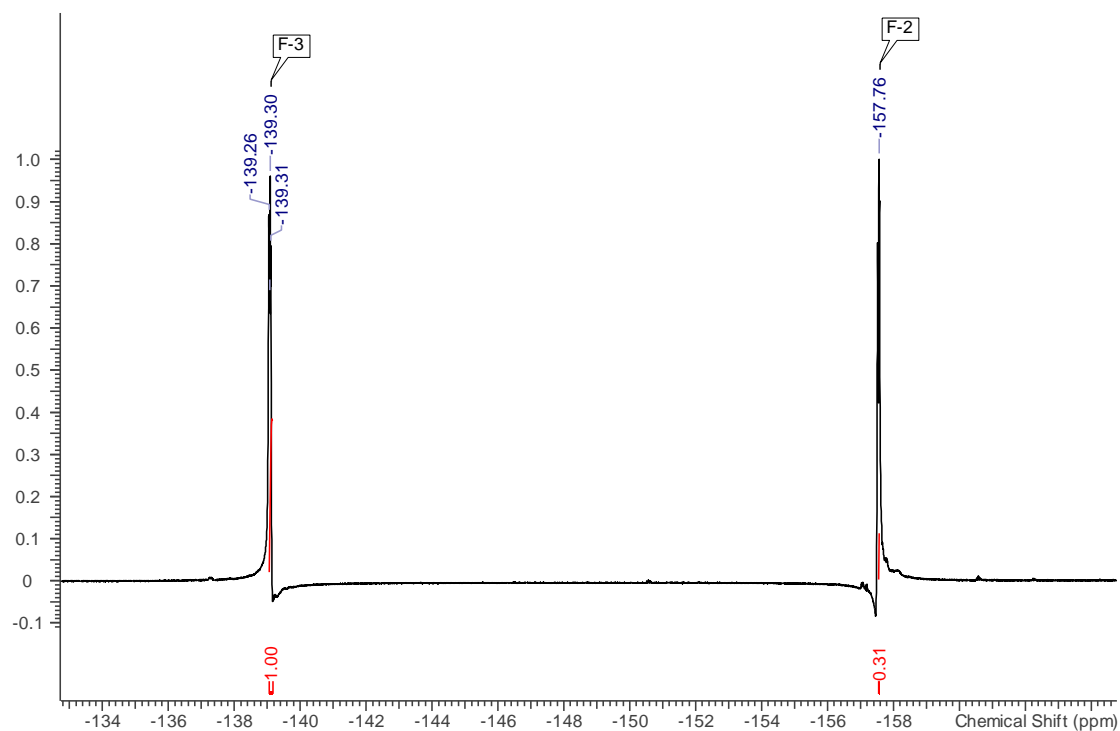
Figure A - 3: ¹⁹F-NMR spectrum of PAE-1.

¹⁹F-NMR (376 MHz, Chloroform-*d*) δ ppm: -157.76 (F-2); -139.3 (F-3).

A-2: NMR (^{13}C and ^{19}F) spectra of brominated PAE-1 (BrPAE-1)

See Chapter 2 (Figure 2.6) for the ^{1}H spectrum.
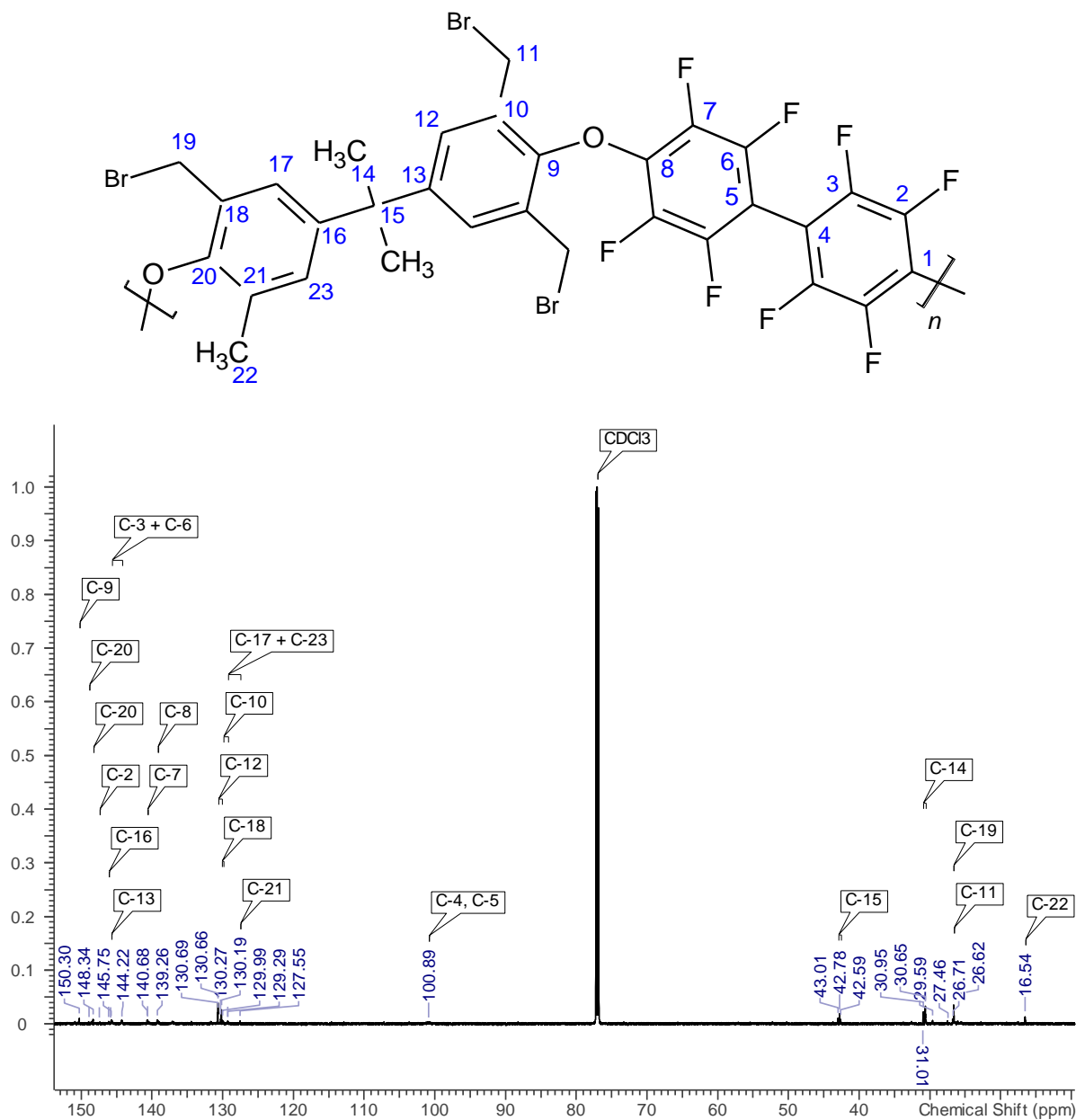
Figure A - 4: ^{13}C-NMR spectrum of BrPAE-1 (full spectrum).
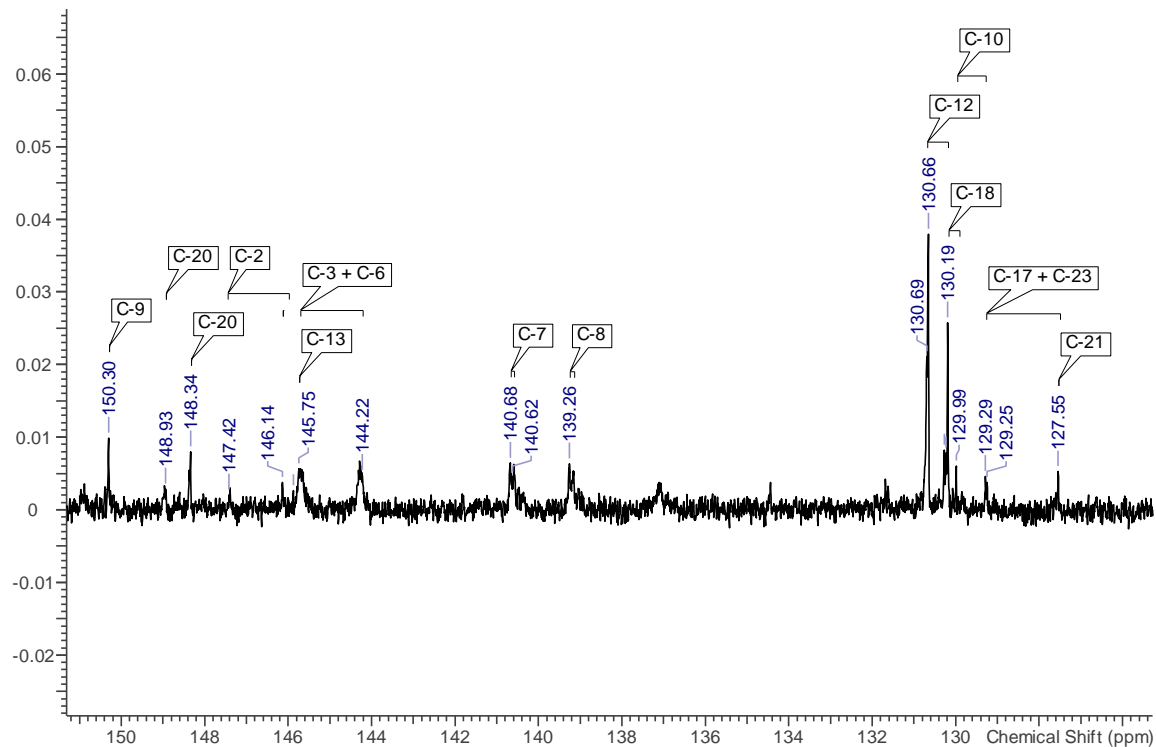
Figure A - 5: ^{13}C-NMR spectrum of BrPAE-1 (magnified for 150-130 ppm spectrum).

^{13}C NMR(176 MHz, Chloroform-*d*) δ ppm: 150.30 (C-9); 148.93 (C-20, X= H); 148.34 (C-20, X = Br); 147.42 (C-2); 146.14 (C-16); 145.75 (C-13); 145.75-144.22 (C-3 + C-6); 140.64 (d, *J* = 30.52 Hz, C-7); 139.26 (C-8); 130.66 (C-12); 130.19 (C-18, X= H); 129.99 (C-18, X =Br); 129.29 (C-10); 129.25 (C-17 + C-23); 127.55 (C-21); 100.89 (C-4, C-5); 42,78 (C-15, X=Br); 42,59 (C-15, X=H); 30.958 (C-14, X=Br); 30.65 (C-14, X=H); 26.71 (C-19, X=Br); 26.62 (C-11); 16.54 (C-22).
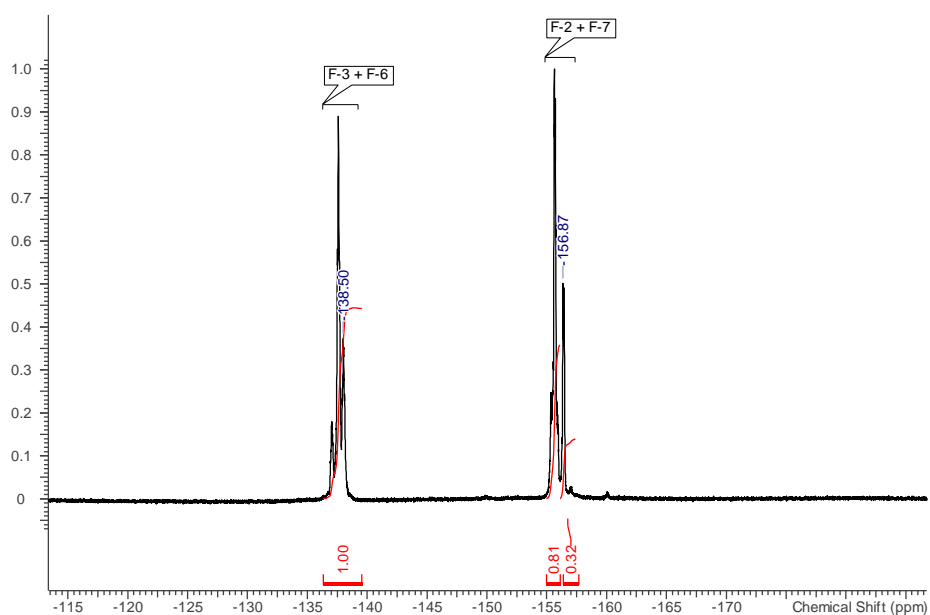
Figure A - 6: ^{19}F-NMR spectrum of BrPAE-1.

^{19}F-NMR (235 MHz, Chloroform-*d*) δ ppm: -138.50 (F-3 + F-6)-156.87 (F-2 + F-7).

A-3: NMR (^{1}H and ^{13}C) spectra of PAE-2
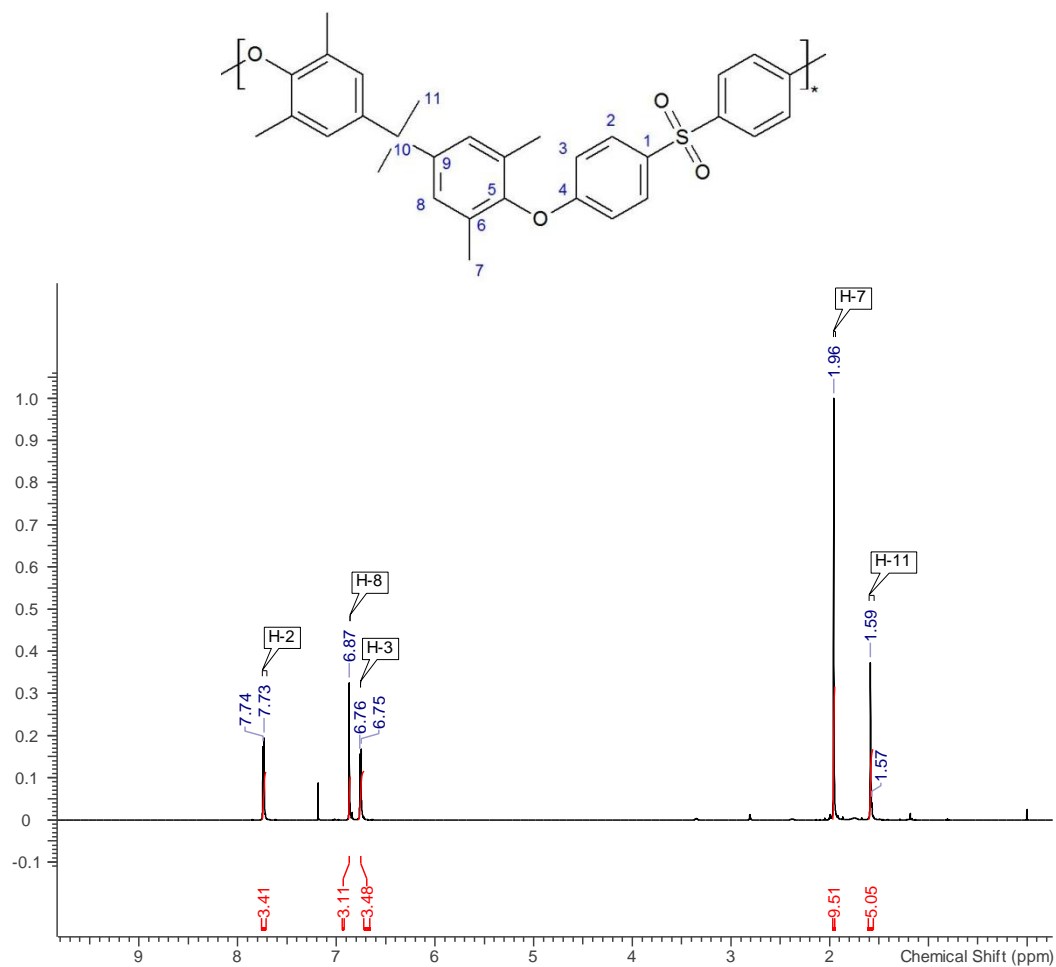
Figure A - 7: ^{1}H-NMR spectrum of PAE-2.

^{1}H-NMR (700 MHz, Chloroform-*d*) δ ppm : 7,74 (d, J=9.03 Hz, H-2); 6.87 (s, H-8); 6.75 (d, J=8.82 Hz, H-3); 1.96 (s, H-7); 1.56-1.56 (m, H-11).

Figure A - 8: ¹³C-NMR spectrum of PAE-2.

¹³C NMR(176 MHz, Chloroform-*d*) δ ppm: 161.59 (C-4); 148.17 (C-5); 147.97 (C-9); 134.51 (C-1); 130.14 (C-2); 129.85 (C-6); 127.58 (C-8); 115.25 (C-3); 41.89 (C-10); 31.17 (C-11); 16.54 (C-7).

A-4: NMR (¹H and ¹³C) spectra of brominated PAE-2 (BrPAE-2)

Figure A - 9: ¹H-NMR spectrum of BrPAE-2 (full spectrum).

Figure A - 10: ¹H-NMR spectrum of BrPAE-2 (magnified for ranges 7.9 – 6.9 ppm).

¹H-NMR (700 MHz, Chloroform-*d*) δ ppm: 7.80-7.74 (m, H-3 + H-6); 7.24 (H-17, X=H); 7.10 (H-17, X=Br); 7.00 (H-23); 6.89-6.86 (H-7); 6. 86 (s, H-12); 6.82 (d, H-2, X=Br); 6.77 (d, H-2, X=H); 4.23 (s, H-19), 4.18 (s, H-11); 2.10 (s, H-22, X=H); 1.95 (H-22, X=Br); 1.63 (m, H-14).
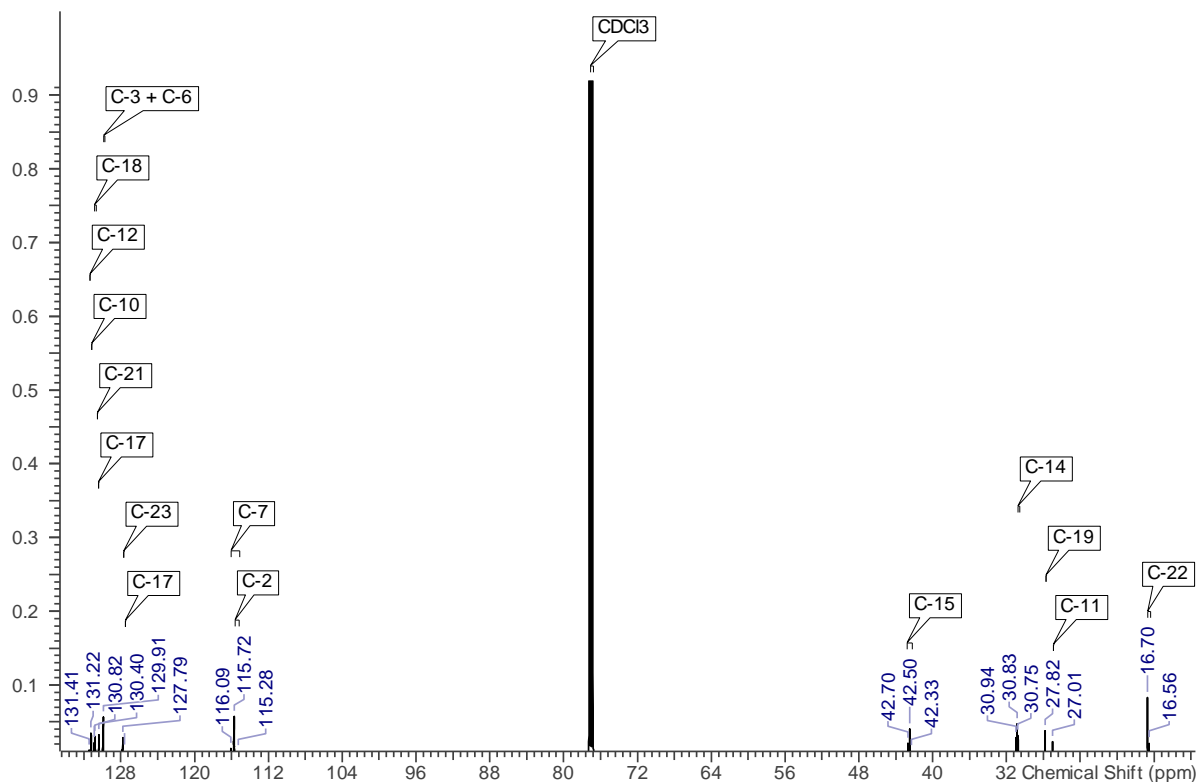
Figure A - 11: ¹³C-NMR spectrum of BrPAE-2 (full spectrum).

¹³C NMR(176 MHz, Chloroform-*d*) δ ppm: 161.34 (tr, C-1, X=Br); 161.19 (C-1, X=H, C-8); 149.07 (C-9); 148.72 (C-20, X=H); 148.30 (C-20, X=Br); 148.15 (C-16, X=H); 148.03 (C-16, X=Br); 147.64 (C-13, X=H); 147.58 (C-13, X=Br); 135,11 (C-4 + C-5); 131.41 (C-12); 131.22 (C-10); 130.90 (C-18, X=H); 130.82 (C-18, X=Br); 130. 61 (C-21); 130.51 (C-17); 129.91 (C-3 + C-6); 127.79 (C-23); 127.60 (C-17); 116.09 (C-7); 115.72 (C-2, X=H); 115.28 (C-2, X=Br); 42.50 (d, C-15); 30.83 (q, C-14); 27.82 (d, C-19); 27.01 (d, C-11); 16.70 (C-22, X=H); 16.56 (C-22, X= Br).
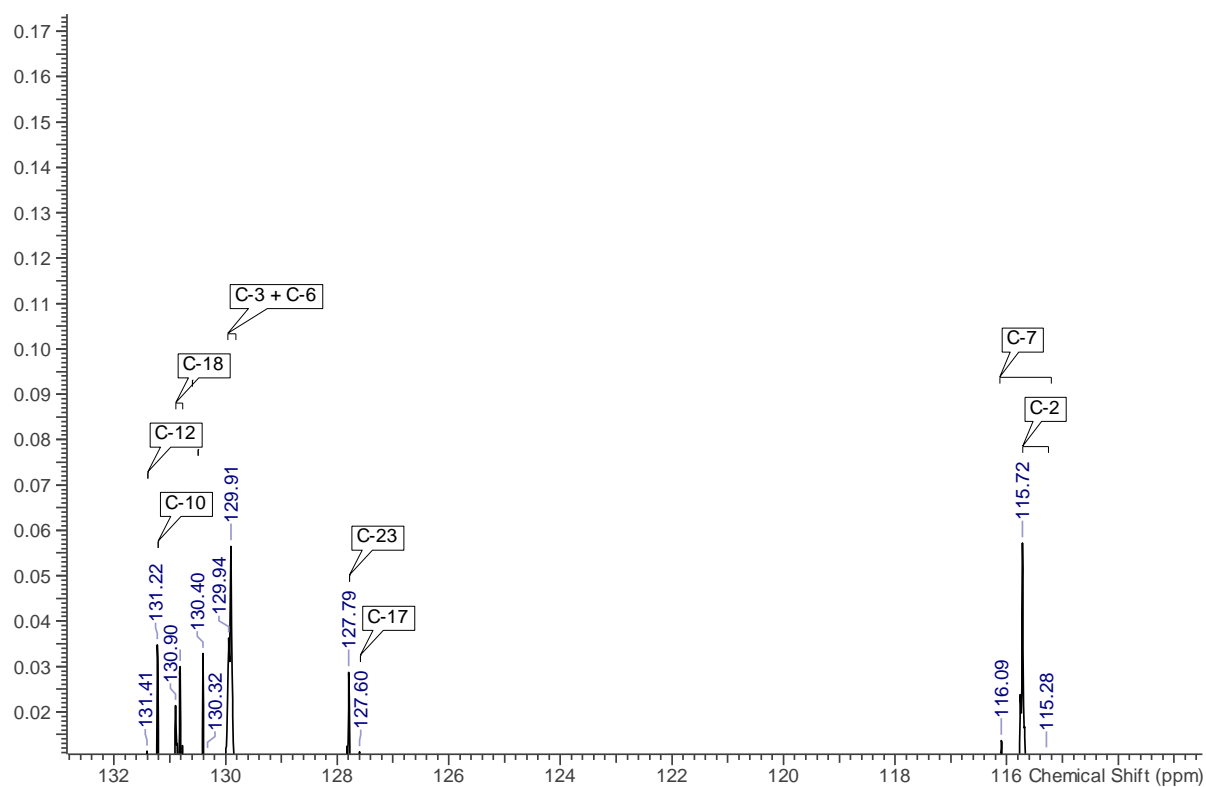
Figure A - 12: ¹³C-NMR spectrum of BrPAE-2 (magnified for ranges 132-116 ppm).
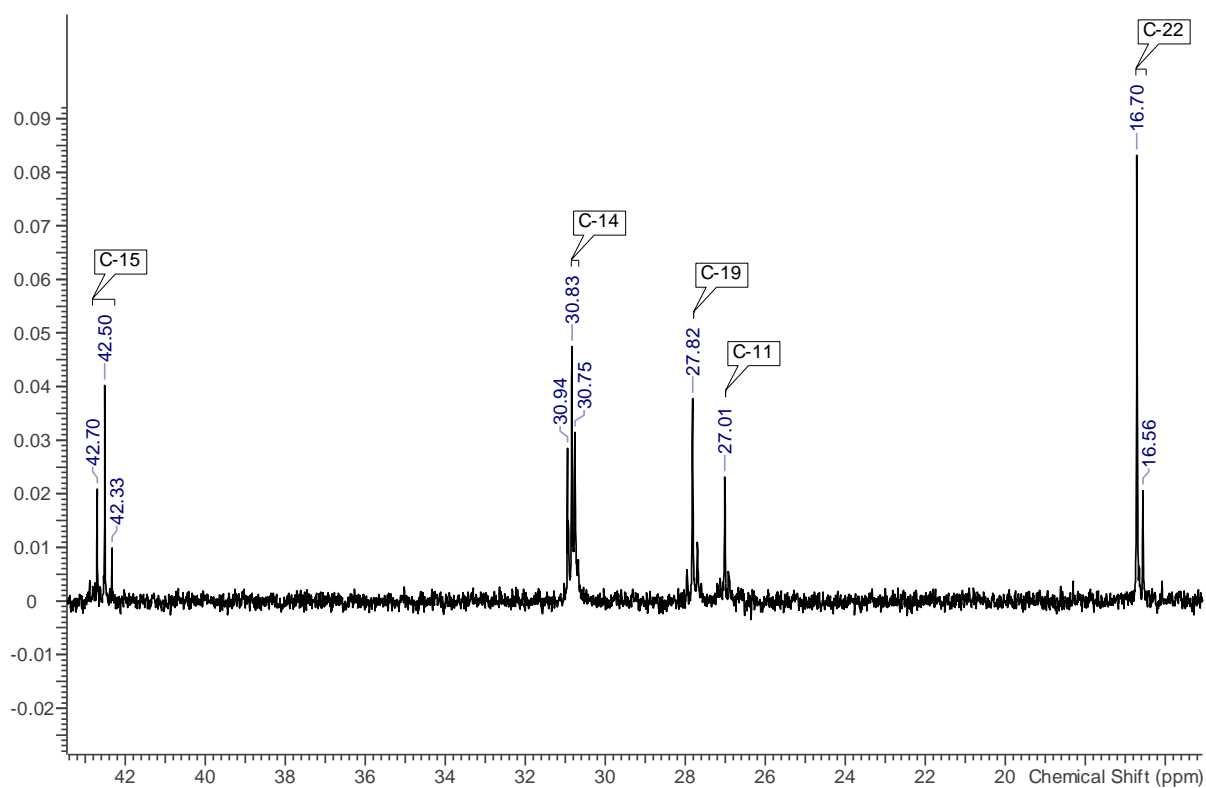
Figure A - 13: ¹³C-NMR spectrum of BrPAE-2 (magnified for ranges 42-10 ppm).

A-5: Polymer characterisation (supplementary data)

Table A - 1: Elemental analysis of PAE polymers

Element	PAE-1 Calc. (%)	PAE-1 Exp. (% diff)	BrPAE-1 Calc. (%)	BrPAE-1 Exp. (% diff)	PAE-2 Calc. (%)	PAE-2 Exp. (% diff)	BrPAE-2 Calc. (%)	BrPAE-2 Exp. (% diff)
C	64.4	-0.7	45.8	-8.3	74.4	-0.6	56.7	-2.6
H	3.8	0.8	2.1	1.0	6.0	-0.2	4.3	-3.3
O	5.5	*	3.9	*	12.8	6.9	9.0	8.0
S	-	-	0.0	-	6.4	-5.9	4.9	-6.6
Br	-	-	29.5	8.5	-	-	24.3	7.8
F	26.3	x	18.7	X	-	-	-	-

Calc. = % element present in PAE polymer as determined from NMR estimation of bromination degree (Section 2.3.1), * = oxygen estimated from the difference between 100% and the sum of other elements present in the sample, x = not measurable (F sensitive), - = relevant element not present within sample.

A-6: H_2SO_4 stability and characterisation of blend components

See Figure 2.8, Chapter 2 for the TGA data of BrPAE-1.
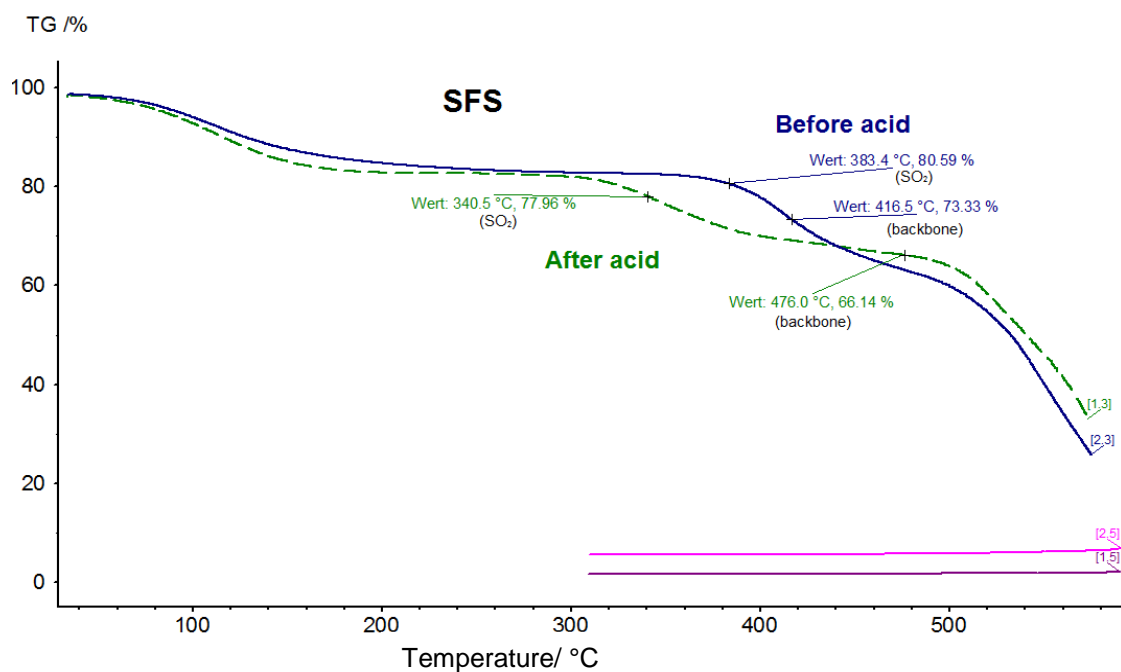
Figure A - 14: TGA curves recorded for SFS before and after acid treatment.
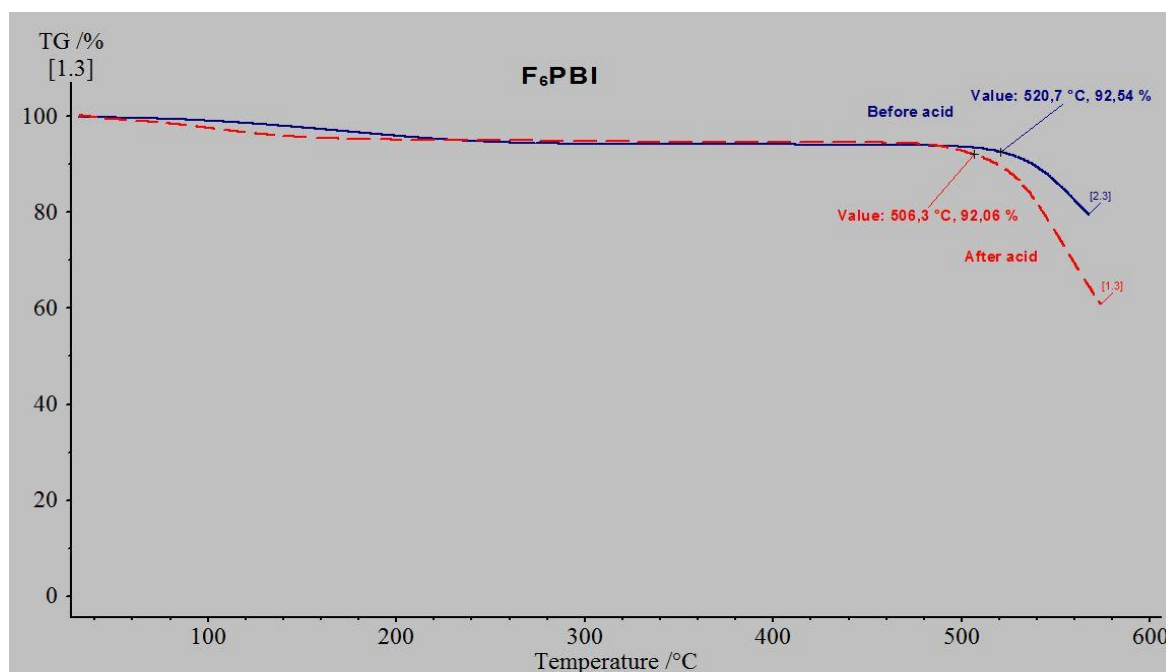
Figure A - 15: TGA curves recorded for F$_6$PBI before and after acid treatment.

156
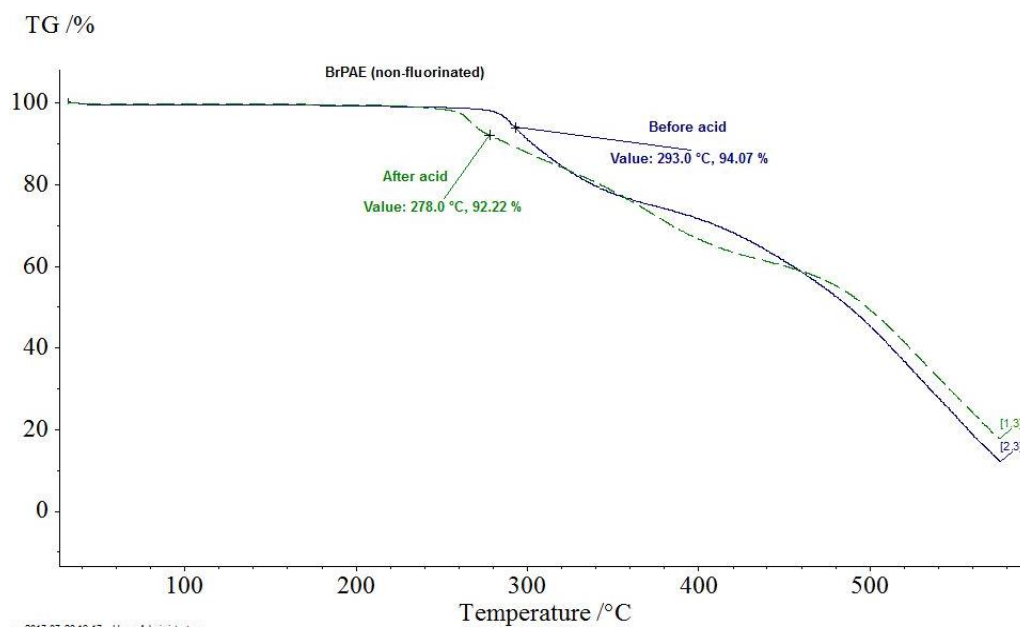
Figure A - 16: TGA curves recorded for BrPAE-2 before and after acid treatment.

B-1:TGA-data of blend membranes before and after treatments (acid and FT)
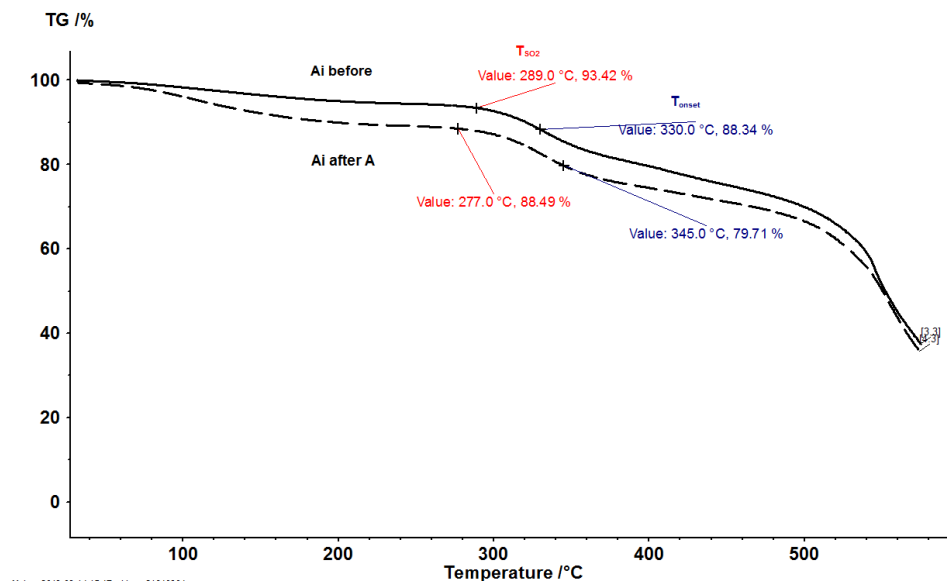
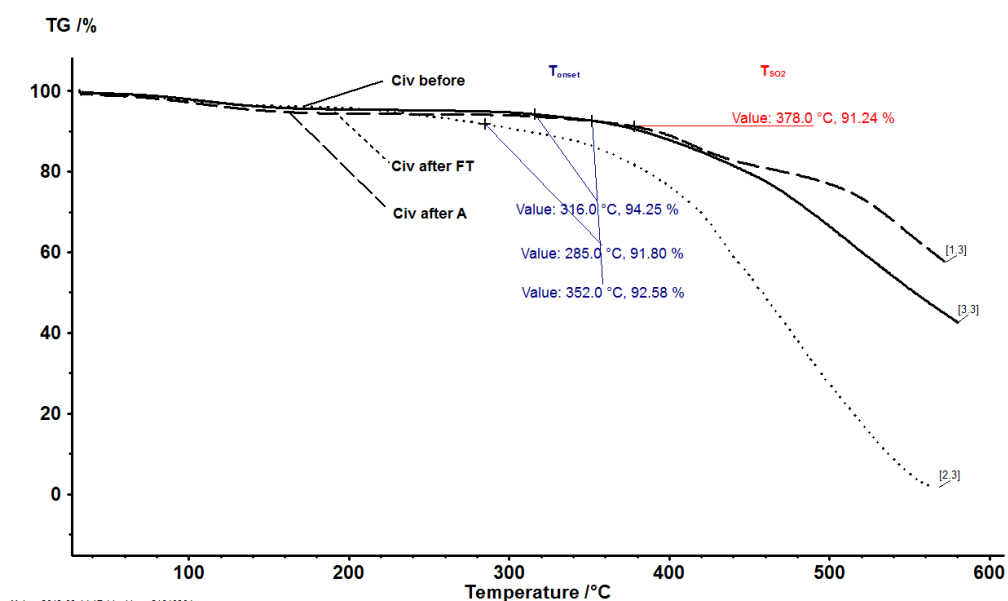**Figure B - 1: Blend membrane 1A$_i$ before and after treatments (only acid).**
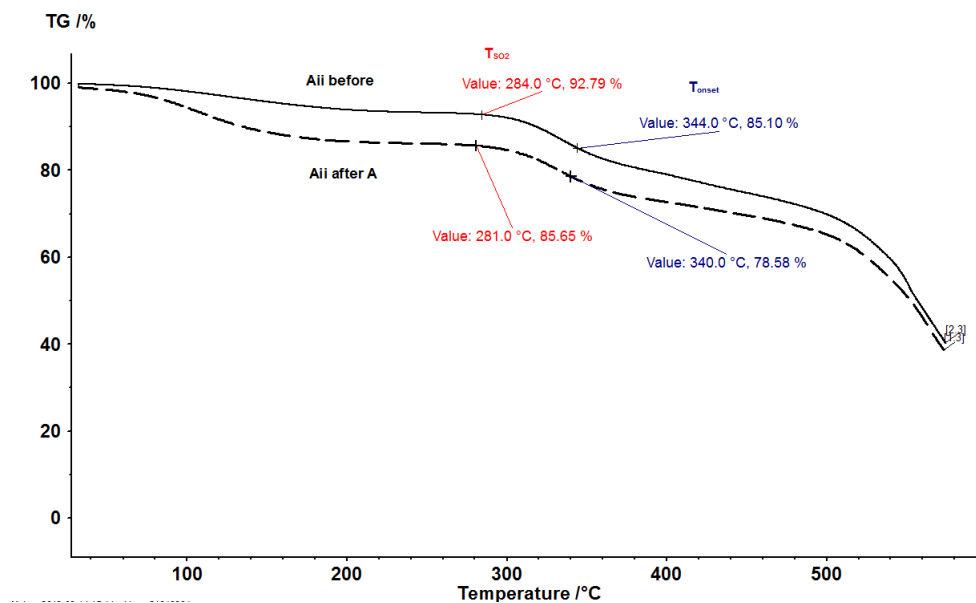
Figure B - 2: Blend membrane 1A$_{ii}$ before and after treatments (only acid).
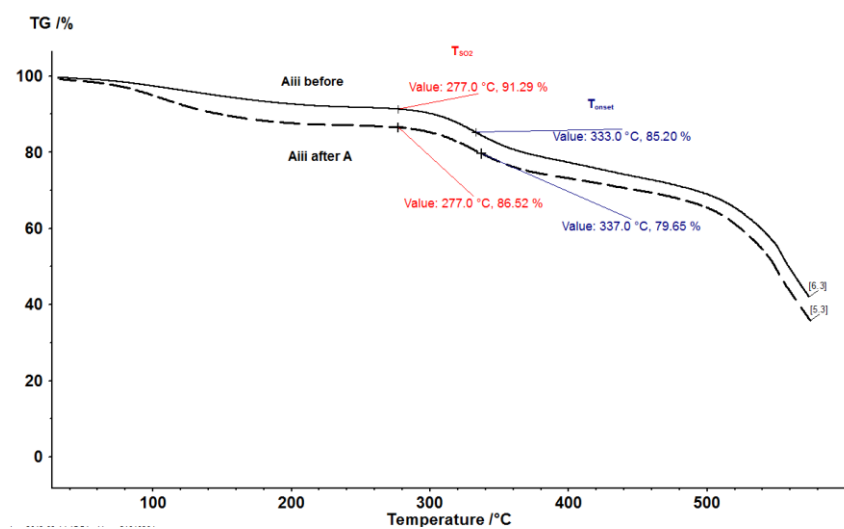
Figure B - 3: Blend membrane 1A$_{iii}$ before and after treatments (only acid).
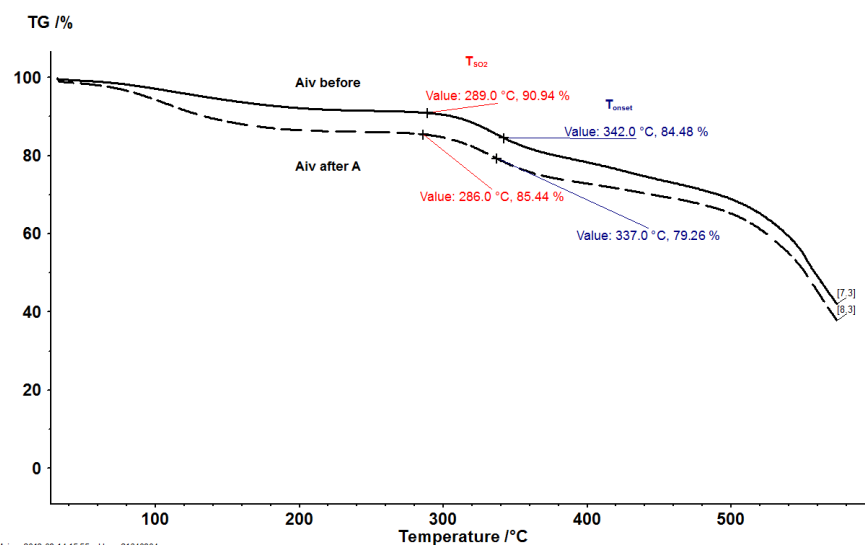
Figure B - 4: Blend membrane 1A$_{iv}$ before and after treatments (only acid).

159
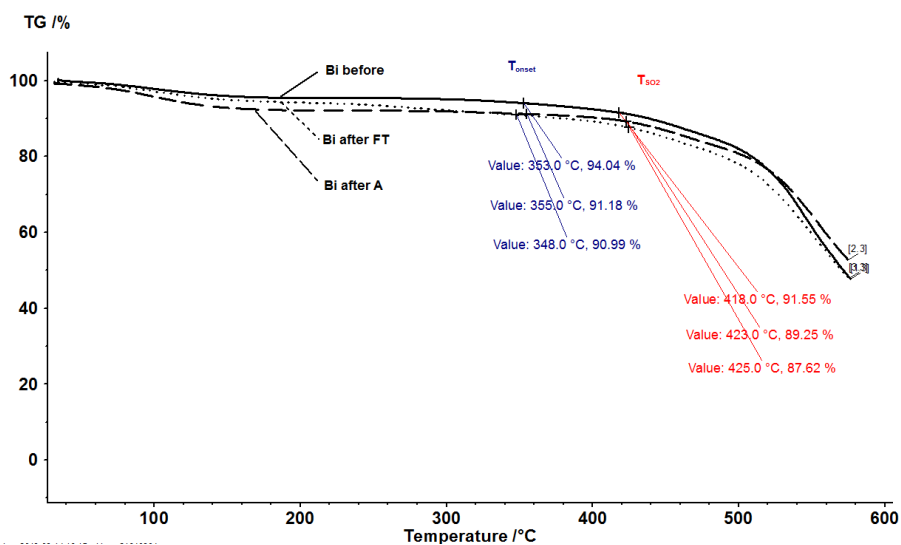
Figure B - 5: Blend membrane 1B$_i$ before and after treatments (acid and FT).
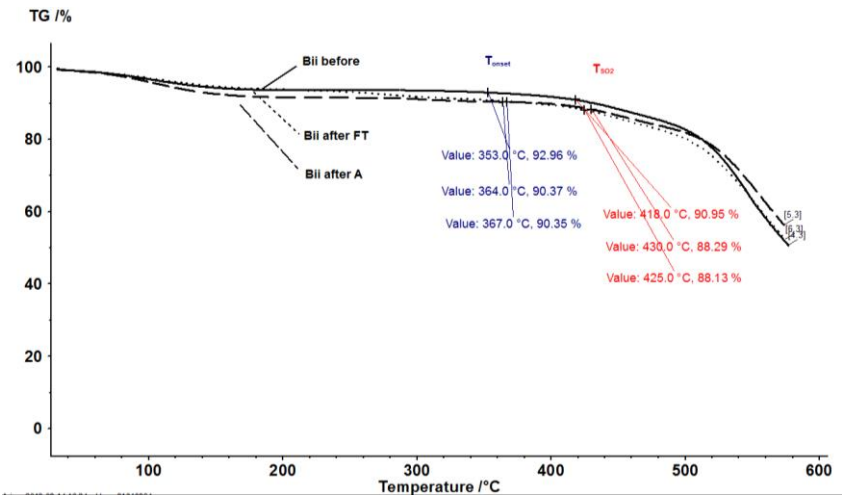
Figure B - 6: Blend membrane 1B$_{ii}$ before and after treatments (acid and FT).
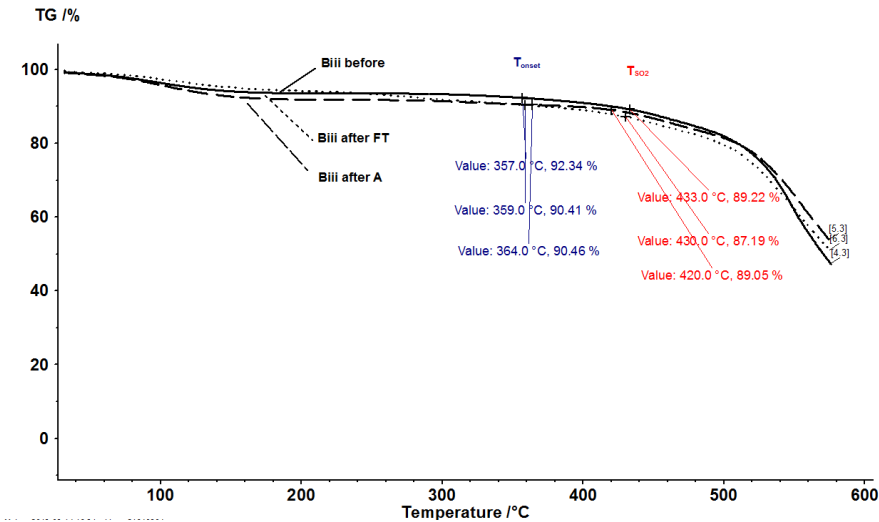
Figure B - 7: Blend membrane 1B$_{iii}$ before and after treatments (acid and FT).
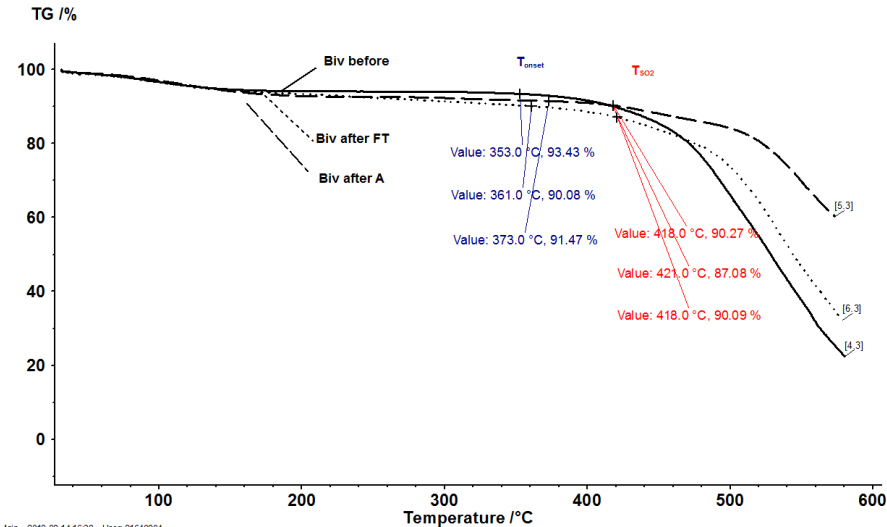
Figure B - 8: Blend membrane 1B_{iv} before and after treatments (acid and FT).
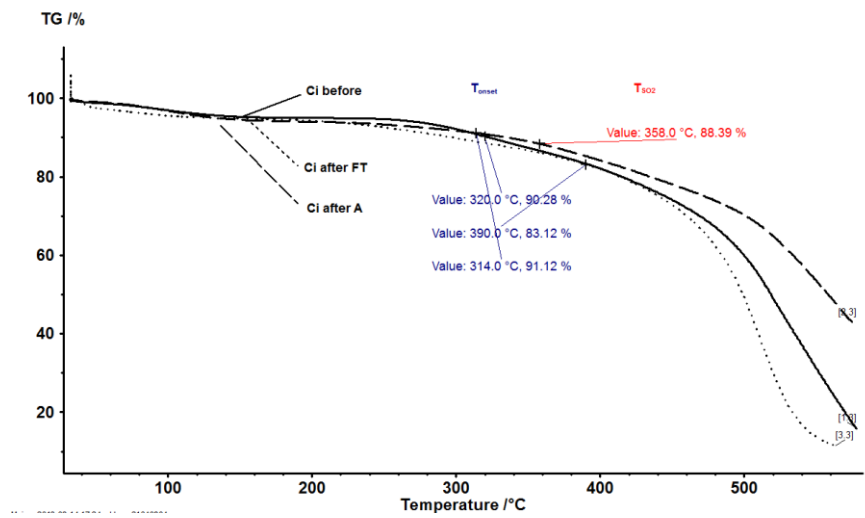
Figure B - 9: Blend membrane 1C_i before and after treatments (acid and FT).
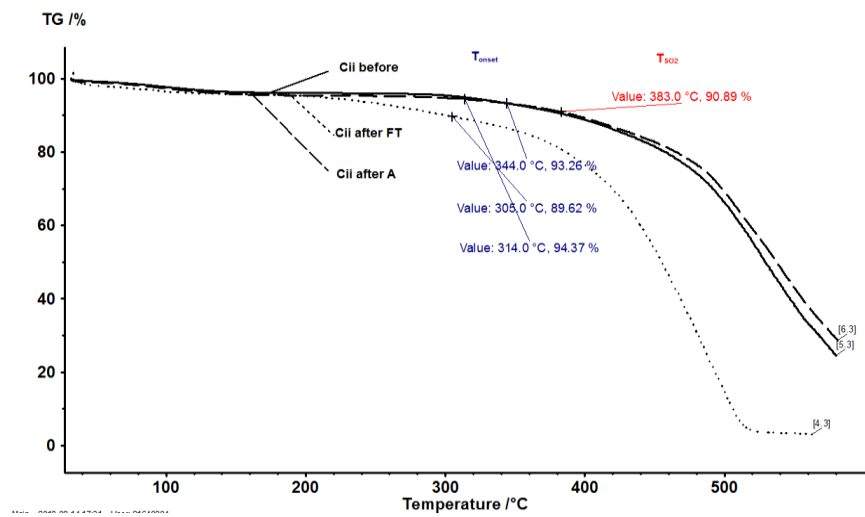
Figure B - 10: Blend membrane 1C_{ii} before and after treatments (acid and FT).
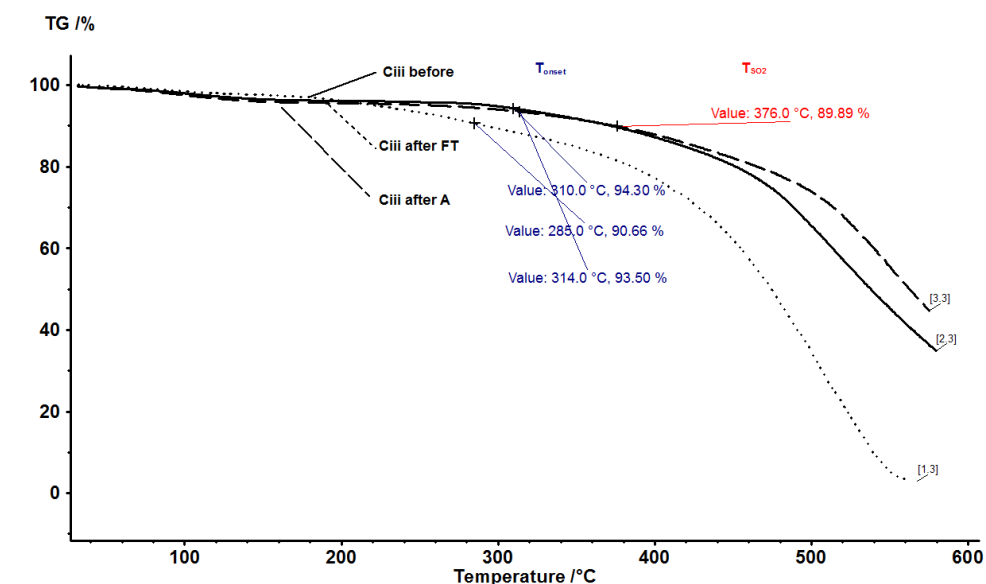
Figure B - 11: Blend membrane 1C$_{iii}$ before and after treatments (acid and FT).

Figure B - 12: Blend membrane 1C$_{iv}$ before and after treatments (acid and FT).

162

APPENDIX C (CHAPTER 6)

C-1 Comparison of SO$_2$ set-up variables at 80 and 120 °C

Table C - 1: Summary of differences for SO$_2$ electrolyser operations at 80 and 120 °C.

Variable	80 °C	120 °C
H$_2$O (DI)	Pre-heated and supplied (50 mL/min) to the cathode, allowing for H$_2$O to diffuse across MEA to the anode during operation.	H$_2$O passes through a coiled heater before merging with the SO$_2$ supply and entering the cell at the anode (supplying humidified SO$_2$). Varying flow rates (5, 10 and 15 mL/min) were applied.
SO$_2$	Supplied dry (150 mL/min) to anode using a mass flow controller.	Excess of 200 mL/min supplied with varying H$_2$O content to the anode using a (thermal) mass flow controller.
Products	The H$_2$SO$_4$ concentration was determined by collecting the H$_2$SO$_4$ produced at the anode. No H$_2$ measurements were recorded.	H$_2$SO$_4$ was collected as described for 80 °C, while the H$_2$ produced was measured (mL/min) at the cathode using an in-house flow bubble meter.
MEA preparation	MEAs with an active area of 10 cm^2 were manufactured by hot pressing (Carver, Model #3912) the membranes between two GDEs (Fuel Cells Etc.) with a 0.5 mg Pt C/cm^2 catalyst loading at 120 °C for 5 min under a load of 120 kg cm^{-2}.	As described for 80 °C, with addition of either 0.5 or 1.0 mg Pt/cm² (Section 6.3.4).
Doping	1 M H$_2$SO$_4$ solution at 80 °C for 24 h before loading into the cell [1].	5 M H$_2$SO$_4$ solution at room temperature (RT) for 2 days [2].
Before starting measurements	MEA was loaded into the electrolyser and kept at 80 and 120 °C, respectively, for 1 hour before break-in commenced.	

Break-in	Electrolyser was run at a current density of 0.1 A cm^{-2} for 20 min.	A preliminary polarisation curve was recorded at a constant current density of 0.1 A/cm^2 for 10 minutes before incrementally increasing by 0.1 A/cm^2 until the voltage limit of 1.1 V had been reached.
Measurement procedure	Polarisation curves were recorded (repeatedly) by measuring the voltage while incrementally increasing the applied current density by 0.01 A cm^{-2} every 90 s . System was controlled using Labview® [1].	Polarisation curves were recorded (repeatedly) by measuring the voltage while incrementally increasing the applied current density by 0.05 A/cm^2 every 90, 180 or 300 s as specified. System was controlled using Labview®.

C-2 PBI-blended membranes compared at 120 °C
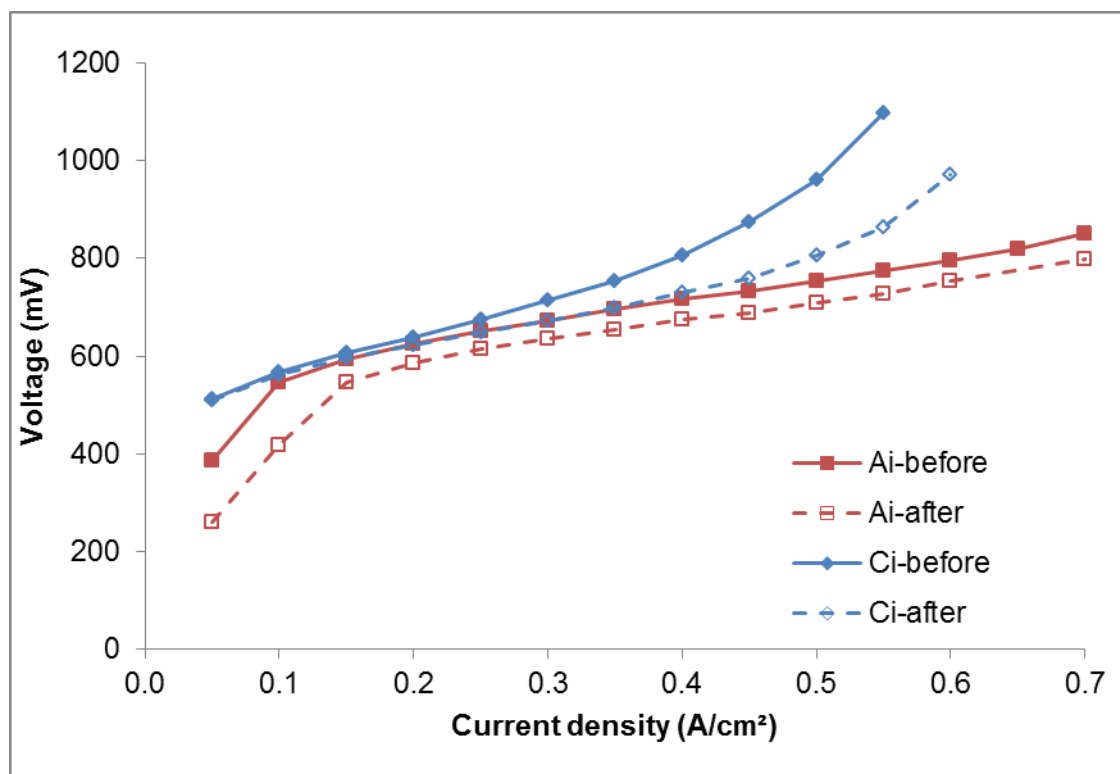
Figure C - 1: Polarisation curves recorded for blend membranes 1A$_i$ and 1C$_i$ after voltage monitoring at 0.3 A/cm^2 for 10 hours at 120 °C and 5 mL/min H$_2$O supply.

164

C-3 Products (H_2SO_4 and H_2) produced and EIS data obtained at different H_2O feeds (15, 10 and 5 ml/min) as a function of current density

C.3.1 H_2SO_4 and H_2 measured for different flow rates (15, 10 and 5 mL/min) at applied current densities (0.1, 0.3, 0.5 and 0.7 A/cm^2)

Table C - 2: Concentration H_2SO_4 (mol/L) and volume (mL/min) H_2 produced for current densities 0.1, 0.3, 0.5 and 0.7 A/cm^2.

A/cm^2	[H_2SO_4] produced (mol/L)			H_2 produced (mL/min)		
	15 mL/min	10 mL/min	5 mL/min	15 mL/min	10 mL/min	5 mL/min
0.1	0.83	1.44	1.78	7.95	8.00	7.77
0.3	0.81	1.11	1.79	27.0	26.7	25.4
0.5	0.78	1.47	2.30	36.8	44.8	45.1
0.7	0.96	-	-	-	-	60.0
Total Vol collected (5 min)	75.0 ± 1.85	45.0 ± 2.84	25.0 ± 0.58	-	-	-

C.3.2 EIS obtained at 15 mL/min H_2O
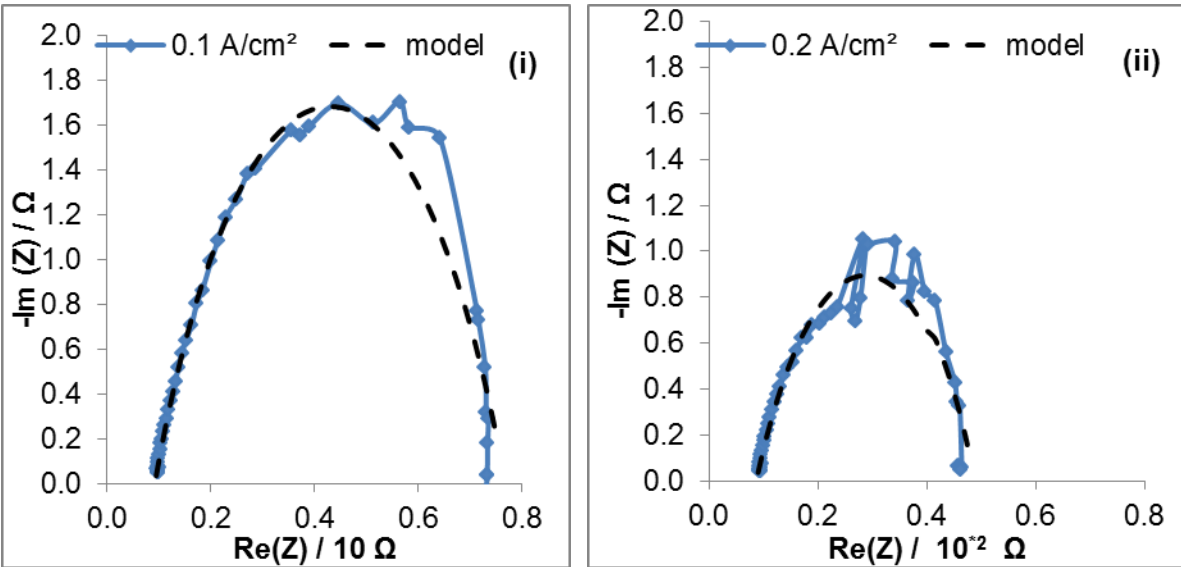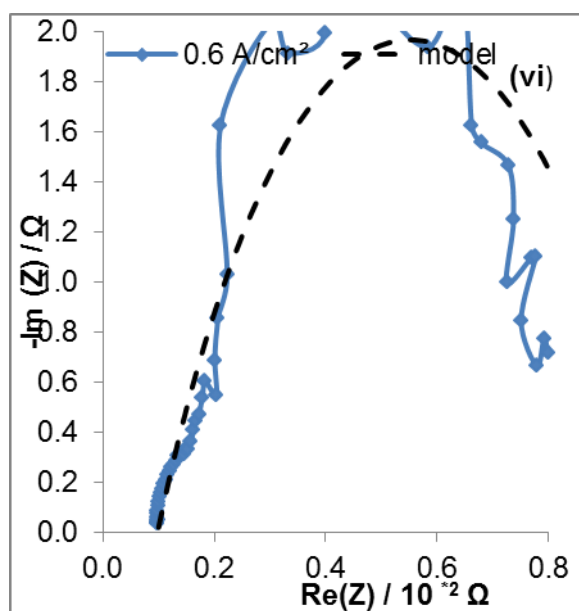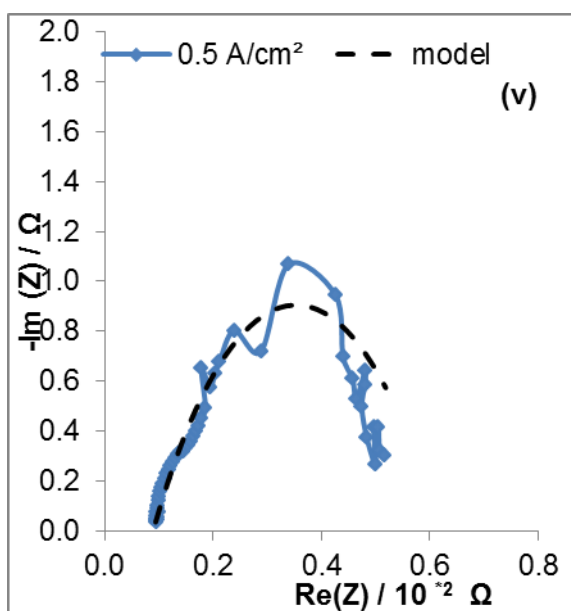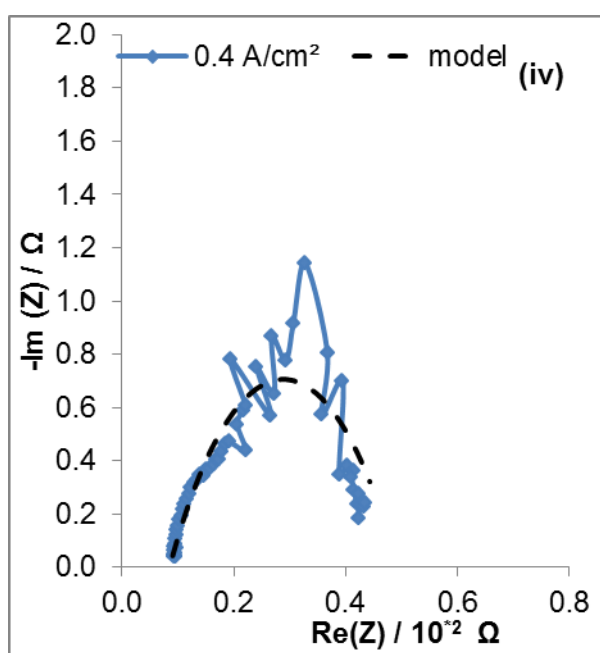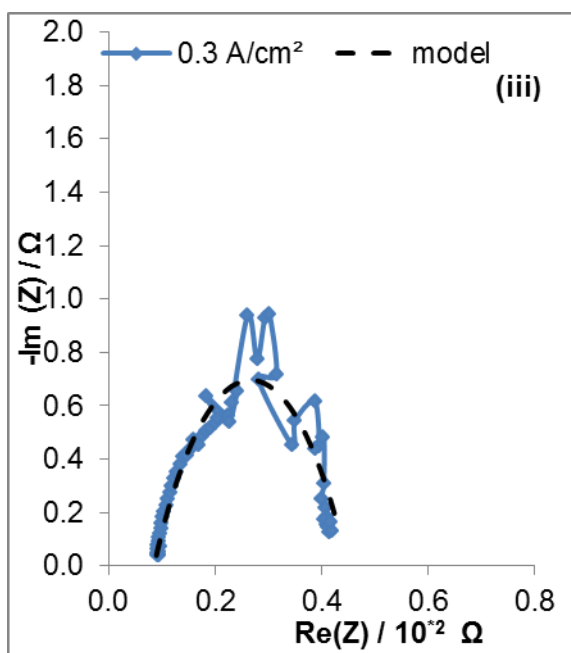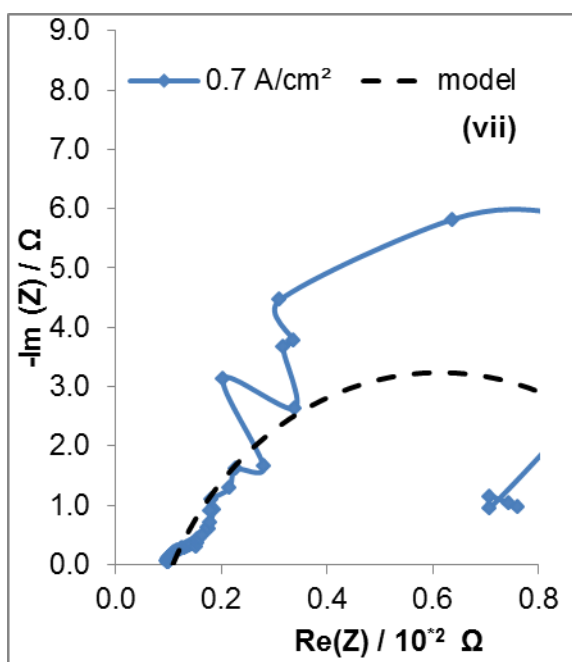
Figure C- 2: EIS spectra at 0.1 – 0.7 A/cm^2 (i-vii) at 15 ml/min H$_2$O (-lim (Z) = 0.0 – 9.0 Ω and Re(Z) = 0.0 – 0.8 x 10^{-2} Ω)
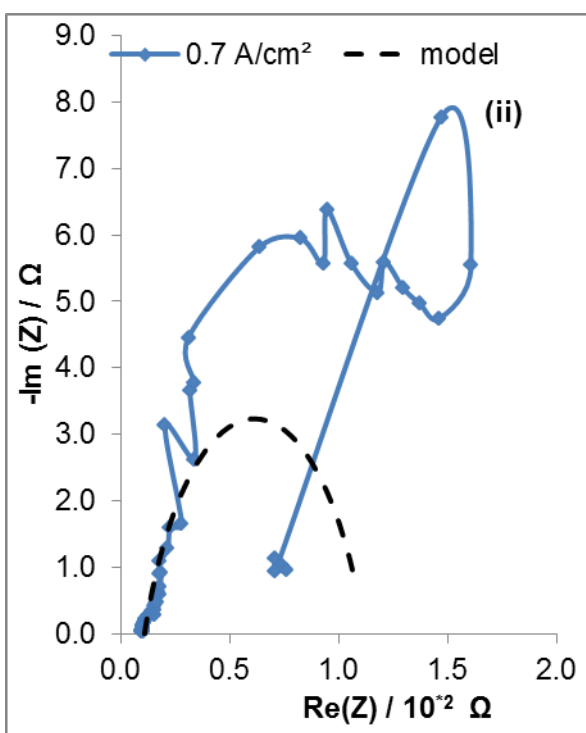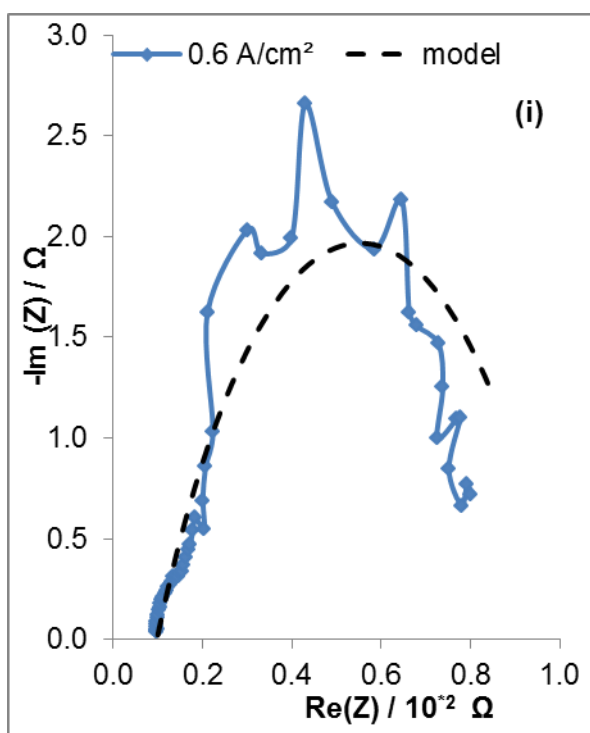
Figure C- 3: EIS spectra at 0.6 and 0.7 A/cm^2 (i-ii) at 15 ml/min H$_2$O (-lim (Z) = 0.0 – 9.0 Ω and Re(Z) = 0.0 – 2.0 x 10^{-2}Ω)
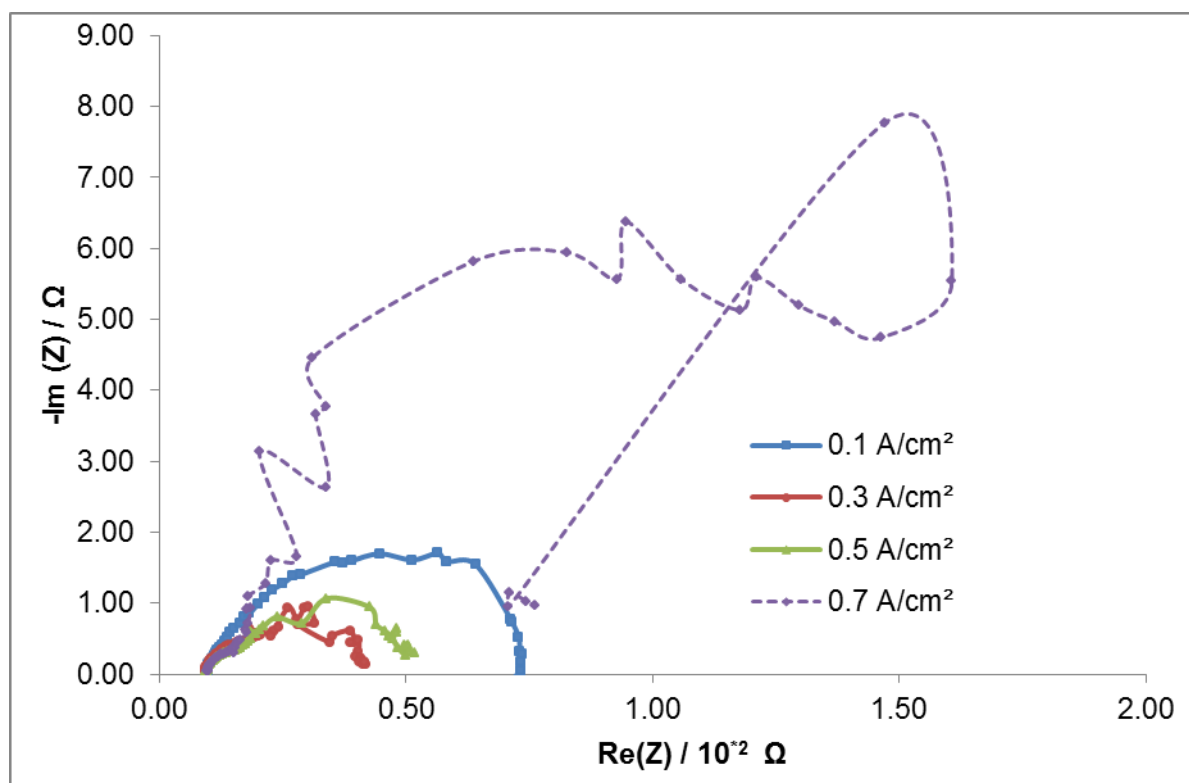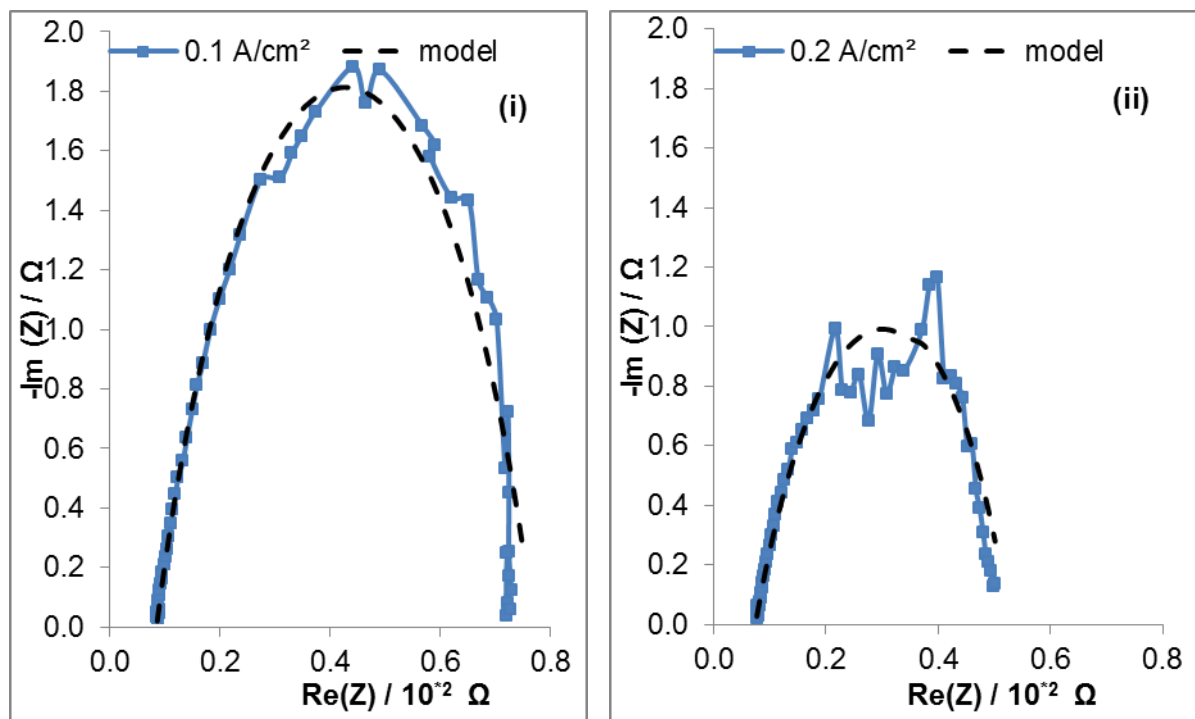
Figure C- 4: EIS spectra comparison at current densities 0.1, 0.3, 0.5 and 0.7 A/cm^2 for 15 ml/min H$_2$O.
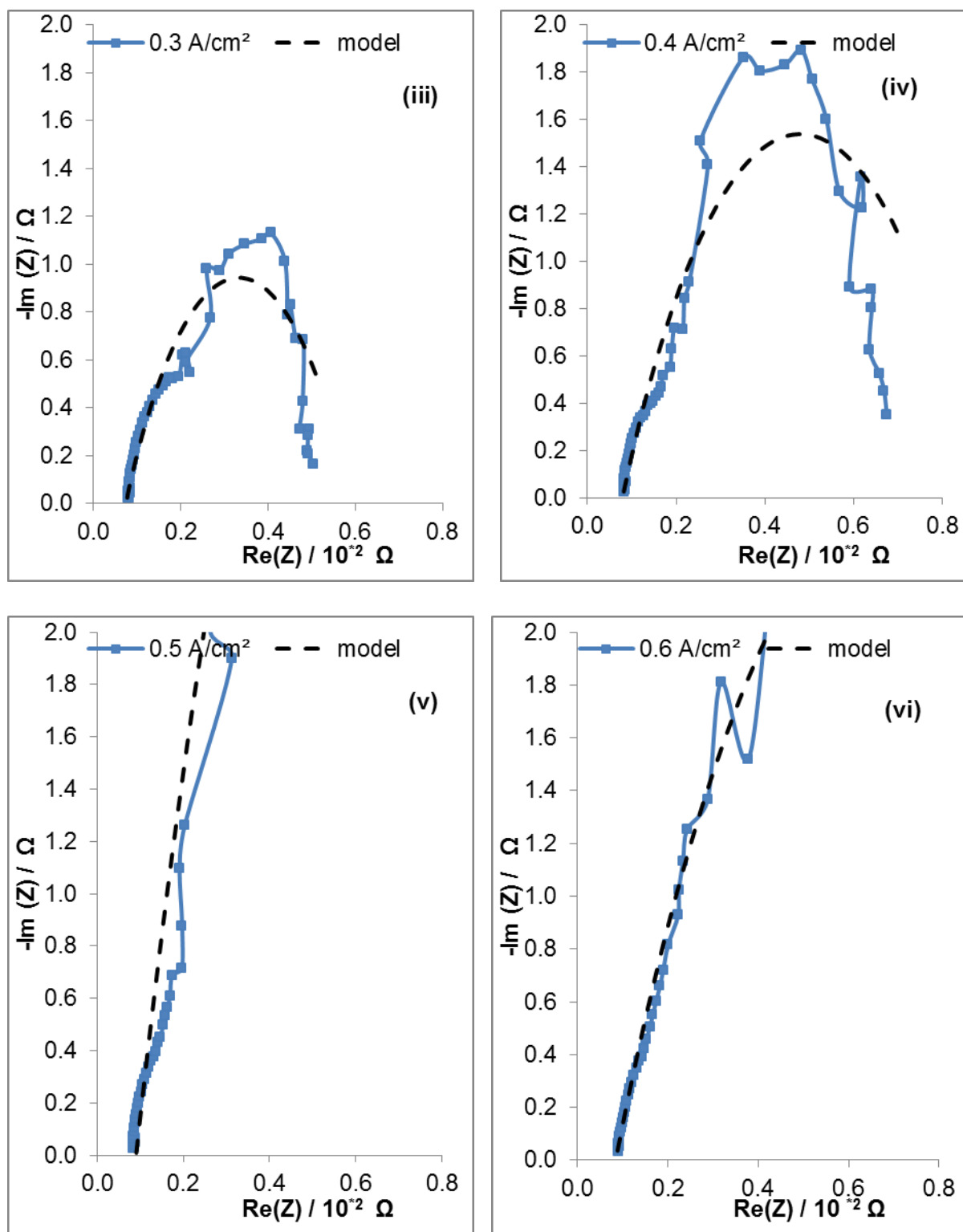
C.3.3 EIS obtained at 10 mL/min H$_2$O

Figure C- 5: EIS spectra at 0.1 – 0.6 A/cm² (i-vi) at 10 ml/min H₂O (-lim (Z) = 0.0 – 2.0 Ω and Re(Z) = 0.0 – 0.8 x 10⁻² Ω).
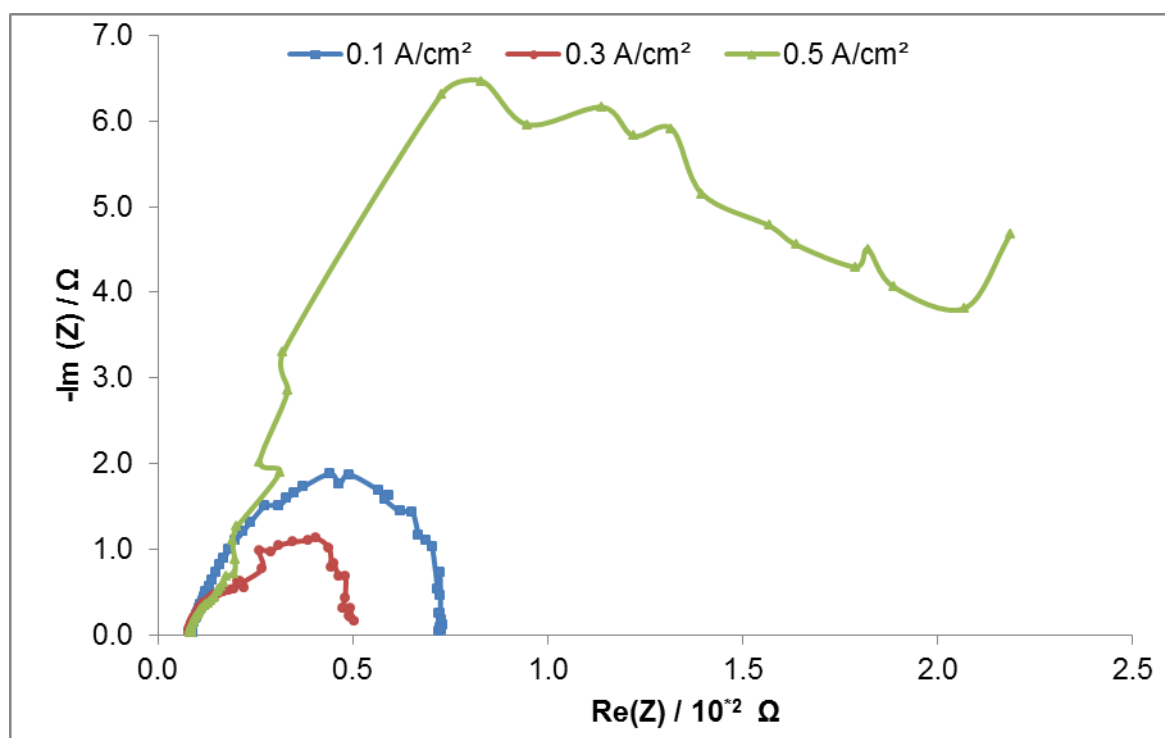
Figure C- 6: EIS spectra comparison at current densities 0.1, 0.3 and 0.5 A/cm^2 for 10 ml/min H$_2$O.
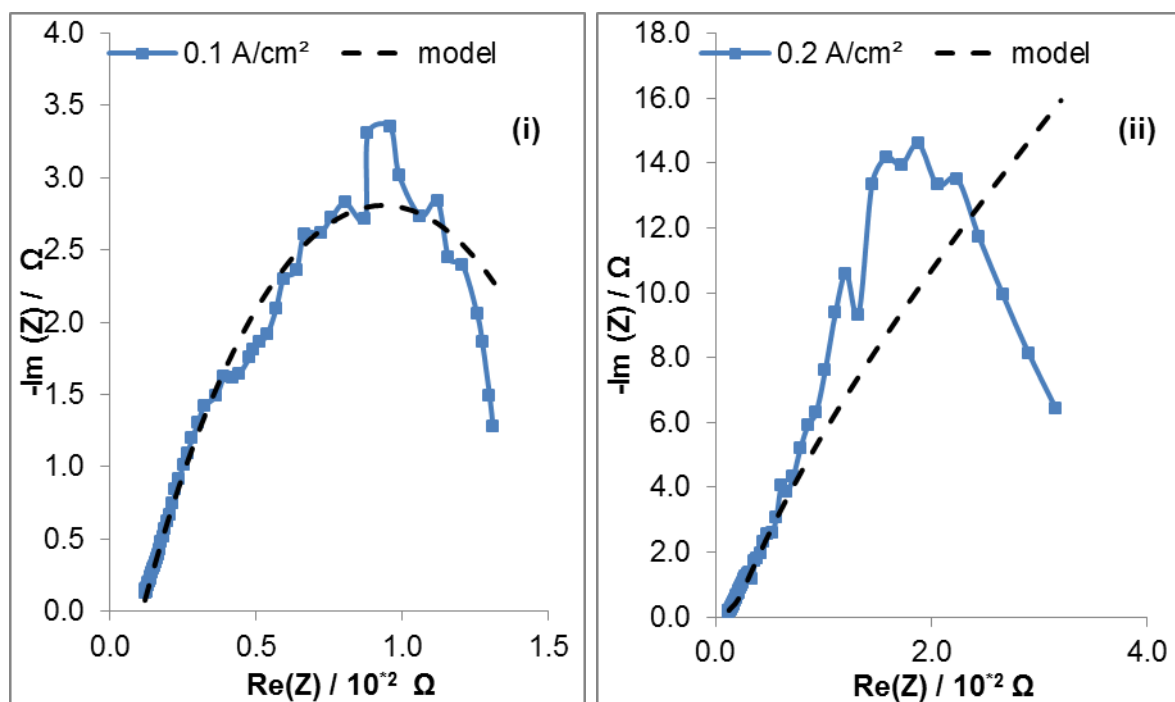
C.3.4 EIS obtained at 5 mL/min H₂O

Figure C- 7: EIS spectra at 0.1 and 0.2 A/cm² (i and ii) at 5 ml/min H₂O (-lim (Z) = 0.0 – 18 Ω and Re(Z) = 0.0 – 4.0 x 10⁻² Ω).
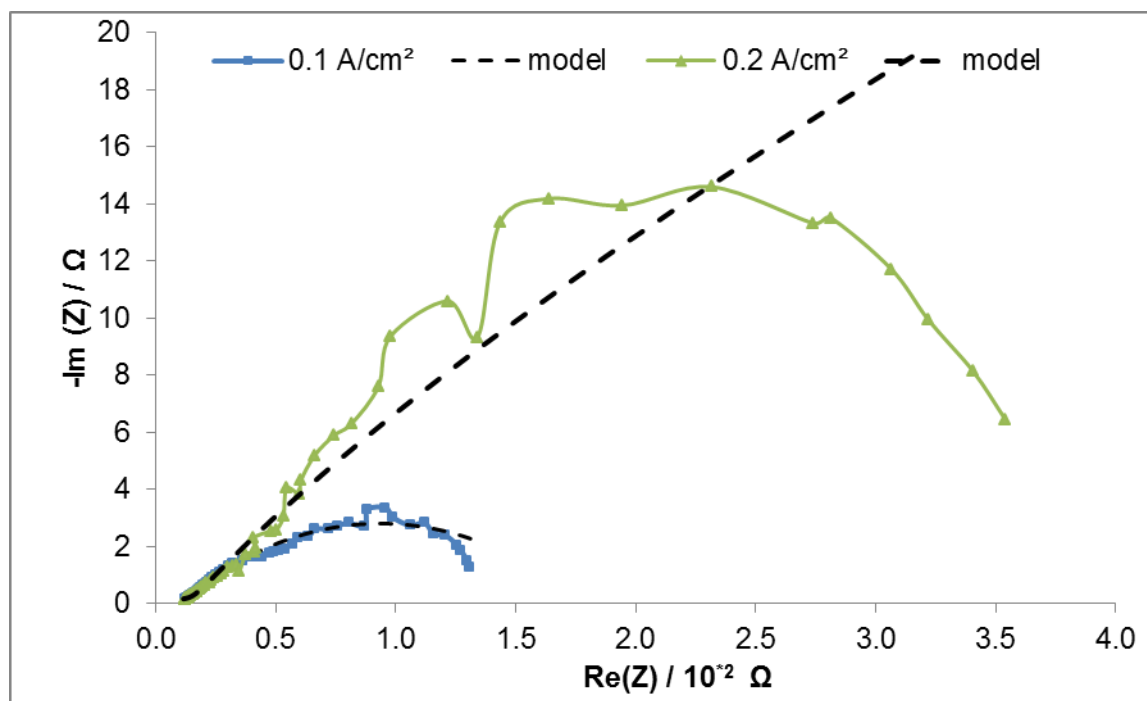

Figure C- 8: EIS spectra comparison at current densities 0.1 and 0.2 A/cm² for 5 ml/min H₂O.

Table C - 3: Average error and standard deviation determined for EIS data over the applied current densities for $1A_i$ (0.1-0.7 A/cm^2, for the different H_2O flow rates inspected).

EIS data	15 mL/min		10 mL/min		5 mL/min	
	mOhm error average	STDEV	mOhm error average	STDEV	mOhm error average	STDEV
Ohm	8.77E-02	1.51E-02	1.14E-01	2.37E-02	1.34E+00	1.59E+00
W	2.86E+06	5.11E+06	1.94E+05	3.85E+05	3.83E+02	4.48E+02
Charge	3.72E+00	3.89E+00	1.86E+00	1.00E+00	1.68E+01	2.40E+01

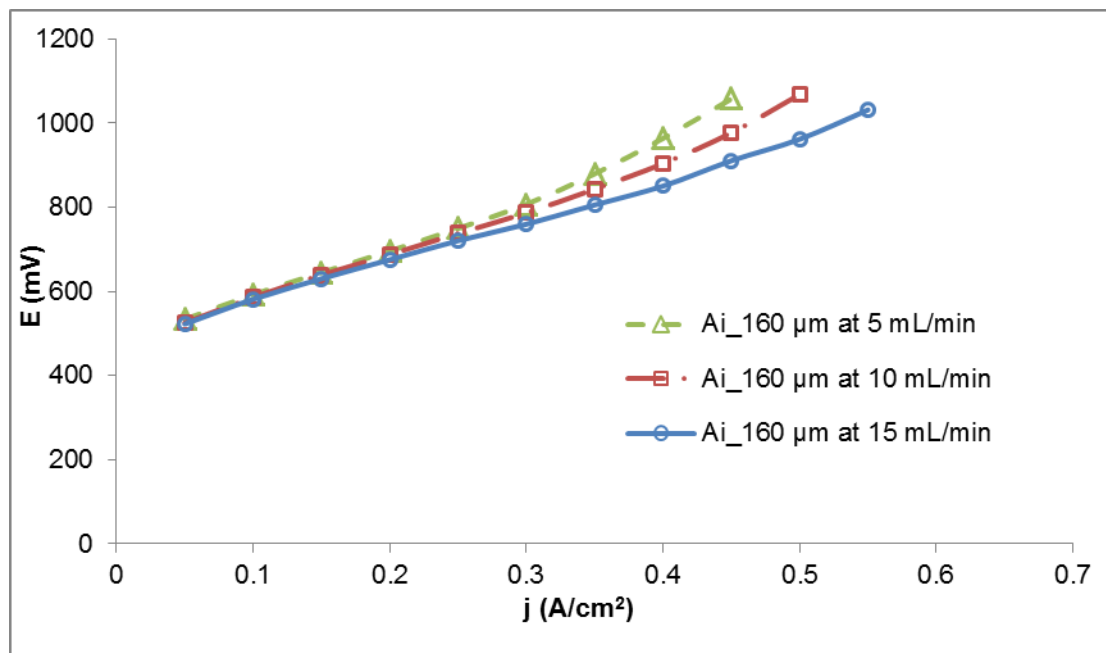## C-4 MEA variables: Membrane thickness and catalyst loading

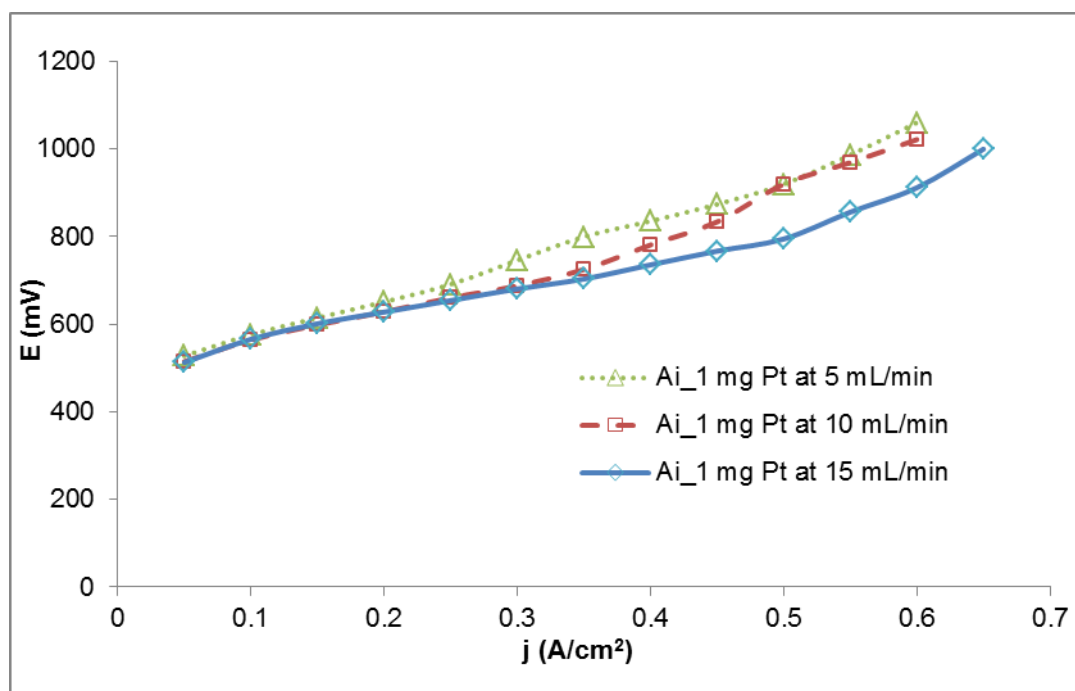**Figure C- 9: Polarisation curves recorded for the thicker $1A_i\_160$ µm at flow rates 5, 10 and 15 mL/min H_2O.**

Figure C- 10: Polarisation curves recorded for 1A$_i$ with 1 mg Pt/cm^2 (60 μm) at flow rates 5, 10 and 15 mL/min H$_2$O.

Table C - 4: Concentration (mol/L) H$_2$SO$_4$ produced by different prepared 1A$_i$ MEAs for current densities 0.1, 0.3, 0.5 and 0.7 A/cm^2 at 5 mL/min H$_2$O feed.

A$_i$ MEA's	[H$_2$SO$_4$] at 5mL/min H$_2$O				Initial H$_2$SO$_4$ doping
	0.1 A/cm²	0.3 A/cm²	0.5 A/cm²	0.7 A/cm²	wt %
1A$_i$ _45 μm	2.26	2.34	2.42	2.57	150
1A$_i$_60 μm	1.87	1.79	2.30	-	90.0
1A$_i$_160 μm	1.65	1.72	-	-	85.0
1A$_i$_1 mg Pt	1.57	1.98	1.92	-	80.0

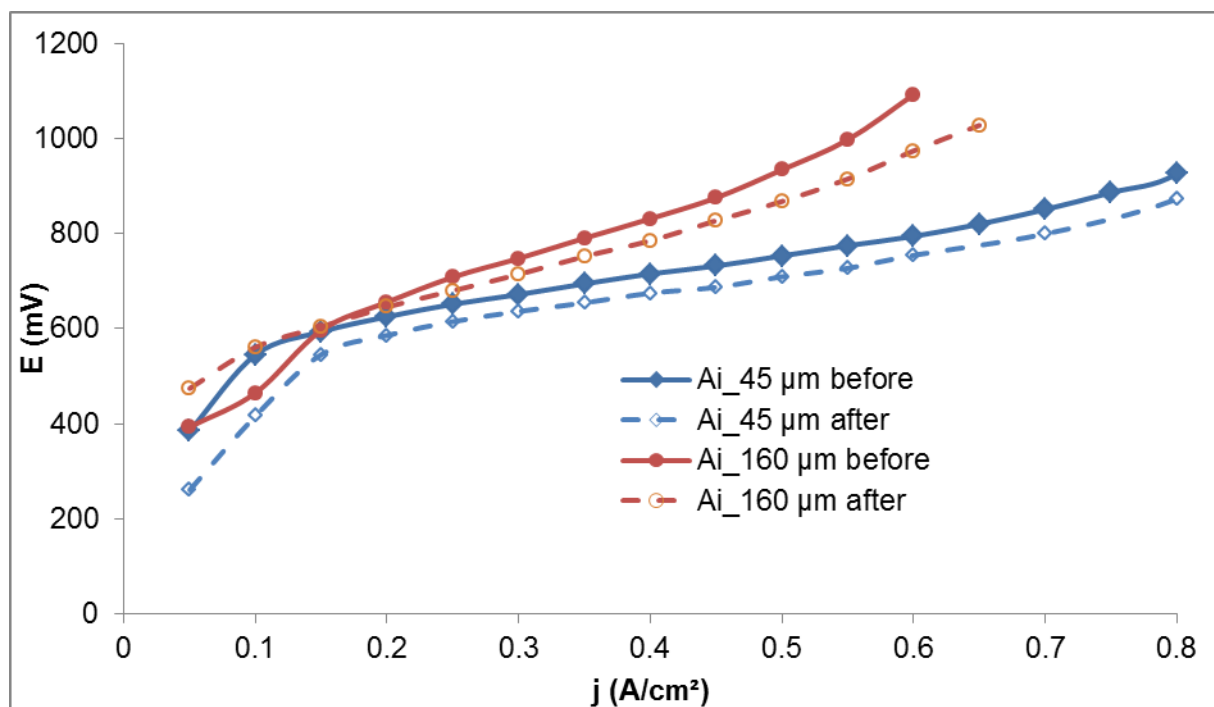## C-5 Stability evaluation of 1A$_i$ MEAs

**Figure C- 11: Polarisation curves recorded before and after voltage monitoring at 0.3 A/cm²
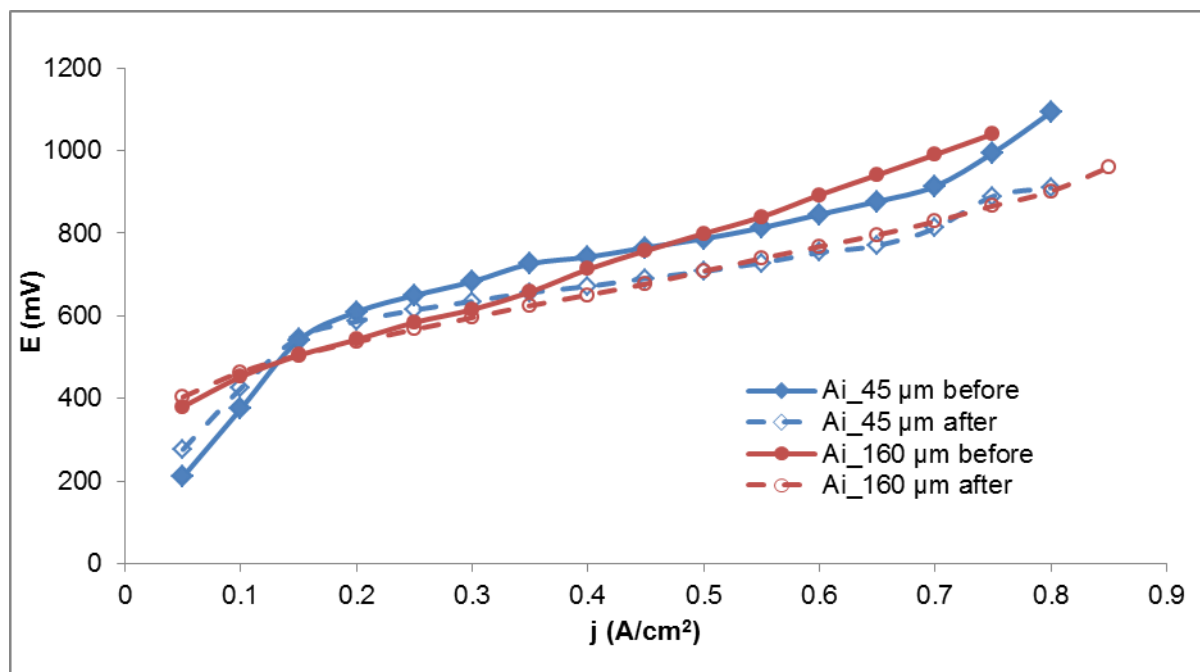for the membranes 1A$_i$_45 and 60 μm at 120 °C with 5 mL/min H$_2$O supply.**

**Figure C- 12: Voltage monitoring comparison at 0.5 A/cm^2 of polarisation curves recorded
before and after for 1A$_i$_45 and 160 μm with H$_2$O flow rate of 5 mL/min managed at 120 °C.**

C-6 REFERENCES:

1.   Peach, R., et al., Novel cross-linked partially fluorinated and non-fluorinated polyaromatic PBI-containing blend membranes for SO2 electrolysis. International Journal of Hydrogen Energy, 2016. 41(28): p. 11868-11883.

2.   Weidner, J.W., Electrolyzer performance for producing hydrogen via a solar-driven hybrid-sulfur process. Journal of Applied Electrochemistry, 2016: p. 1-11.